

5-6-2019

Development of Organic Carbon Monoxide prodrugs

Zhixiang Pan

Follow this and additional works at: https://scholarworks.gsu.edu/chemistry_diss

Recommended Citation

Pan, Zhixiang, "Development of Organic Carbon Monoxide prodrugs." Dissertation, Georgia State University, 2019.
https://scholarworks.gsu.edu/chemistry_diss/165

This Dissertation is brought to you for free and open access by the Department of Chemistry at ScholarWorks @ Georgia State University. It has been accepted for inclusion in Chemistry Dissertations by an authorized administrator of ScholarWorks @ Georgia State University. For more information, please contact scholarworks@gsu.edu.

DEVELOPMENT OF ORGANIC CARBON MONOXIDE PRODRUGS

by

ZHIXIANG PAN

Under the Direction of Binghe Wang, PhD

ABSTRACT

Carbon monoxide (CO) is an endogenously produced gasotransmitter in mammals and may have signaling roles in bacteria as well. It has many recognized therapeutic effects. A significant challenge in this field is the development of pharmaceutically acceptable forms of CO delivery with controllable and tunable release rates. Our lab has designed a series of organic CO prodrugs as prototypes of “carbon monoxide in a pill.” In the first project, a series of such CO prodrugs was synthesized to examine the structure-release rate in aqueous solution at neutral pH.

CO prodrugs with triggered release mechanisms are highly desirable for targeted delivery. In the second project, we focused on the development of reactive oxygen species ROS-sensitive CO prodrugs, which selectively deliver CO to cells with elevated ROS levels and sensitize cancer cells to chemotherapy. CO prodrugs as such could serve as powerful tools for targeted delivery to disease sites with elevated ROS levels and for exploring the therapeutic applications of CO.

In the third project, we focused on metal-free CO prodrugs with dual-responsive endogenous triggers, which have the advantage of controlled activation at the desired site of action. These CO prodrugs afford highly selective release profiles as compared to others with no or a single trigger. In addition, one representative CO prodrug showed significant anti-inflammatory effects both *in vitro* and in an LPS-simulated systemic inflammation models, suggesting its possible application in treating systemic inflammatory conditions. The prodrug also conferred very pronounced protective effects against LPS-induced acute liver injury. These results firmly established such CO prodrugs as either research tools or candidate compounds for the treatment of systemic inflammation or other inflammation-related organ injuries.

INDEX WORDS: Organic CO prodrugs, Metal free, Tunable release rates, Click and release, ROS sensitive, Esterase-sensitive

DEVELOPMENT OF ORGANIC CARBON MONOXIDE PRODRUGS

by

ZHIXIANG PAN

A Dissertation Submitted in Partial Fulfillment of the Requirements for the Degree of

Doctor of Philosophy

in the College of Arts and Sciences

Georgia State University

2019

Copyright by
Zhixiang Pan
2019

DEVELOPMENT OF ORGANIC CARBON MONOXIDE PRODRUGS

by

ZHIXIANG PAN

Committee Chair: Binghe Wang

Committee: Gangli Wang

Suri S. Iyer

Electronic Version Approved:

Office of Graduate Studies

College of Arts and Sciences

Georgia State University

May 2019

DEDICATION

The dissertation is dedicated to my parents (Xiaozhu Pan and Daohua Xue), who had instilled in me the strength of character that navigates me through each challenge. Without your unconditional love, encouragement and support, I would not be where I am today.

I also want to dedicate this dissertation to my beloved fiancée (Sihui Tan), who has accompanied me on this journey. It is your support made it possible for me to accomplish many things.

ACKNOWLEDGEMENTS

I would like to express my deep gratitude to my advisor Dr. Binghe Wang, for his advice, patience, encouragement and support throughout the whole work. He is not only a supervisor for my research work, but also a mentor for my life, who benefits me a lot in personality development.

I would like to extend a special thank you to Dr. Gangli Wang and Dr. Suri S. Iyer for their time and patience in helping me throughout my PhD program. In addition to the professional knowledge I gained from their courses, their enthusiasm and passion in research have inspired me.

Besides, I would like to sincerely thank my colleagues, who have helped me a lot in the past five years. I would especially thank Dr. Xingyue Ji and Dr. Yueqin Zheng for their hand-on teaching and training of my professional skills. I would also thank Dr. Kaili Ji for her help on biochemistry-related work. Technical support from Dr. Siming Wang and Dr. Zhenming Du should be also acknowledged. In addition, I would like to express my appreciation to Dr. Xiaoxiao Yang, Dr. Wen Lu, Dr. Ke Wang, Dr. Wenyi Wang, Dr. Jalisa Holmes, Mengyuan Zhu, Dr. Bingchen Yu, Lingyun Yang, Vayou Chittavong, Ravi Tripathi, Ce Yang, Abiodun Anifowose, Manjusha Roy Choudhury, Zhengnan Yuan, Ladie Kimberly De La Cruz and other group members for their help and discussions. Financial support from Molecular Basis of Disease program is gratefully acknowledged.

TABLE OF CONTENTS

ACKNOWLEDGEMENTS	V
LIST OF TABLES	XI
LIST OF FIGURES	XII
LIST OF ABBREVIATIONS	XIV
1 ORGANIC CO-PRODRUGS: STRUCTURE CO-RELEASE RATE	
RELATIONSHIP STUDIES.....	1
1.1 Introduction	1
<i>1.1.1 Inhalation</i>	<i>2</i>
<i>1.1.2 Metal-based carbon monoxide releasing molecules (CO-RMs).....</i>	<i>3</i>
<i>1.1.3 Esterase and protease sensitive CO-RMs</i>	<i>5</i>
<i>1.1.4 CO delivery in encapsulated form.....</i>	<i>7</i>
<i>1.1.5 Photosensitive organic CO-RMs.....</i>	<i>8</i>
<i>1.1.6 Organic CO prodrugs.....</i>	<i>9</i>
1.2 Results and discussion	12
<i>1.2.1 Design of CO prodrugs.....</i>	<i>12</i>
<i>1.2.2 Synthesis of CO prodrugs.....</i>	<i>14</i>
<i>1.2.3 CO release kinetics and structure CO release rate relationships</i>	<i>18</i>
<i>1.2.4 Cytotoxicity study.....</i>	<i>22</i>
<i>1.2.5 Intracellular CO release.....</i>	<i>23</i>

1.3	Experimental Section	24
1.3.1	<i>General information</i>	24
1.3.2	<i>Experimental procedure for the synthesis of CO prodrugs</i>	25
1.3.3	<i>Experimental procedure for the CO detecting using a house-hold CO detector</i> .	44
1.3.4	<i>Experimental procedure for Myoglobin-CO assay</i>	44
1.3.5	<i>Experimental procedure for the CO release rate study of BW-CO-108-121</i>	46
1.3.6	<i>Experimental procedure for cytotoxicity study of CO prodrugs and corresponding products</i>	46
1.3.7	<i>Experimental procedure for intracellular CO release study of BW-CO-109, 117 and 119</i>	47
1.3.8	<i>Experimental procedure for computation of electron density distributions</i>	48
1.4	Conclusion	48
1.5	Statements	49
2	ORGANIC CO PRODRUGS ACTIVATED BY ENDOGENOUS ROS	50
2.1	Introduction	50
2.2	Results and discussion	52
2.2.1	<i>Design of reactive oxygen species (ROS) sensitive CO prodrugs</i>	52
2.2.2	<i>Synthesis of ROS sensitive CO prodrugs</i>	53
2.2.3	<i>Kinetics study of ROS sensitive CO prodrugs</i>	53
2.2.4	<i>Detection of intracellular CO release</i>	55

2.2.5	<i>Synergistic effects of CO and doxorubicin (Dox)</i>	56
2.3	Experimental Section	57
2.3.1	<i>General information</i>	57
2.3.2	<i>Experimental procedure for the synthesis of ROS-activated CO prodrugs</i>	58
2.3.3	<i>Experimental procedure for Myoglobin-CO assay</i>	62
2.3.4	<i>Experimental procedure for the study of sensitivity of BW-OTCO-102 to various ROS</i>	62
2.3.5	<i>Experimental procedure for study of stability of BW-OTCO-101/102 in the absence of ROS</i>	63
2.3.6	<i>Experimental procedure for CO release kinetics of BW-OTCO-101/102 in response to hypochlorite</i>	64
2.3.7	<i>Experimental procedure for synergetic effect study of CO prodrugs with Dox in killing cancer cells</i>	66
2.3.8	<i>Experimental procedure for cytotoxicity study of CO prodrugs and their respective products to H9C2 cells</i>	68
2.4	Conclusion	69
2.5	Statements	69
3	ESTERASE-SENSITIVE AND PH-CONTROLLED CARBON MONOXIDE PRODRUGS FOR TREATING SYSTEMIC INFLAMMATION	70
3.1	Introduction	70
3.2	Results and discussion	72

3.2.1	<i>Design of esterase-sensitive and pH-controlled CO prodrugs</i>	72
3.2.2	<i>Synthesis of esterase-sensitive and pH-controlled CO prodrugs</i>	73
3.2.3	<i>CO release kinetics study</i>	73
3.2.4	<i>Cell imaging study</i>	75
3.2.5	<i>Anti-inflammatory study of CO prodrugs</i>	76
3.3	Experimental Section	78
3.3.1	<i>General information</i>	78
3.3.2	<i>Experimental procedure for the synthesis of Esterase-sensitive and pH-controlled CO prodrugs</i>	79
3.3.3	<i>Experimental procedure for cell imaging study</i>	82
3.3.4	<i>Experimental procedure for anti-inflammatory effects study</i>	82
3.3.5	<i>Experimental procedure for the study of 6a's Anti-inflammatory and liver protective effects in an LPS-simulated mouse model</i>	83
3.4	Conclusion	83
3.5	Statements	83
	REFERENCES	85
	APPENDICES	94
	Appendix A Spectra of compounds in the study of structure CO-release rate relationship	94
	Appendix B Spectra of compounds in the study of ROS-activated CO prodrugs	147

Appendix C Spectra of compounds in the study of esterase-sensitive and pH-controlled CO prodrugs	154
---	------------

LIST OF TABLES

Table 1.1 Reported metal-containing CO-RMs Structures and CO-Release properties.....	4
Table 1.2 Reported photo-sensitive organic CO-RMs structures and CO-release properties	9
Table 1.3 CO release kinetics for CO prodrugs with scaffold I	20
Table 1.4 CO release kinetics for CO prodrugs with scaffold II	21
Table 1.5 CO release kinetics for CO prodrugs with scaffold III	22
Table 2.1 The HPLC condition used for analysis	64

LIST OF FIGURES

Figure 1.1. Heme degradation releases bioactive products including CO.....	1
Figure 1.2 Mechanism of esterase-activated ET-CO-RMs.....	6
Figure 1.3 Mechanism of protease-activated ET-CO-RMs.....	7
Figure 1.4 The photo-release mechanism for fluorescein analogue.....	8
Figure 1.5 A bimolecular click and release prodrug system.....	11
Figure 1.6 A unimolecular click and release prodrug system.....	12
Figure 1.7 General structures of CO prodrugs and their CO release mechanism.....	13
Figure 1.8 Fluorescence imaging of fixed Raw 264.7 cells.....	24
Figure 1.9 UV–Vis spectra demonstrating the conversion of deoxy-Mb to carbon monoxide myoglobin (MbCO) (BW-CO-113).	45
Figure 1.10 UV–Vis spectra demonstrating the conversion of deoxy-Mb to carbon monoxide myoglobin (MbCO) (BW-CO-117).	45
Figure 1.11 UV–Vis spectra demonstrating the conversion of deoxy-Mb to carbon monoxide myoglobin (MbCO) (BW-CO-119).	45
Figure 1.12 The cytotoxicity of CO prodrugs to RAW264.7 after 24h incubation.	46
Figure 1.13 The cytotoxicity of inactive products of CO prodrugs to RAW264.7 after 24h incubation.....	47
Figure 1.14 Computational studies of charge distributions.	48
Figure 1.15 A summary of the relationship between structure and CO release rate.	49
Figure 2.1 A schematic illustration of the general strategy for stimulus-triggered CO prodrugs. 51	
Figure 2.2 The CO release kinetics of BW-OTCO-101 (A) and 102 (B) in response to ClO ⁻ at 37 °C.....	54

Figure 2.3 Fluorescent imaging of CO release of BW-OTCO-102 in different type of cells.....	56
Figure 2.4 CO myoglobin assay.....	62
Figure 2.5 The sensitivity of BW-OTCO-102 to various ROS at 37 °C	63
Figure 2.6 The stability of BW-OTCO-101 and BW-OTCO-102 in the absence of ROS.	64
Figure 2.7 HPLC chromatogram of BW-OTCO-101 in the presence of 40 μM ClO^-	65
Figure 2.8 HPLC chromatogram of BW-OTCO-102 in the presence of 40 μM ClO^-	65
Figure 2.9 HPLC chromatogram of BW-OTCO-102 in the presence of 500 μM O_2^-	66
Figure 2.10 HPLC chromatogram of BW-OTCO-102 in the presence of 500 μM $^1\text{O}_2$	66
Figure 2.11 The lack of synergistic effects of control compounds with Dox.....	67
Figure 2.12 The lack of synergistic effects of BW-OTCO-102 with Dox in H9C2 cells.....	67
Figure 2.13 The cytotoxicity of BW-OTCO/OTCP-102 to H9C2 cells	68
Figure 3.1 The schematic illustration of the CO prodrugs with two triggers.	72
Figure 3.2 Release kinetics of CO from prodrugs 6a-c in the presence of PLE (3 U/mL) in 5% of DMSO in PBS at 37 °C.....	74
Figure 3.3 Cell imaging studies of CO release from 6a	76
Figure 3.4 The anti-inflammatory effects of 6a in LPS-challenged Raw264.7 cells.....	76
Figure 3.5 The protective effects of prodrug 6a against LPS-induced liver injuries	77

LIST OF ABBREVIATIONS

Carbon monoxide (CO)

Lipopolysaccharide (LPS)

Acute Respiratory Distress Syndrome (ARDS)

CO releasing molecules (CO-RMs)

Carboxyhemoglobin (COHb)

Cystathionine β -synthase (CBS)

Enzyme triggered CO-RMs (ET-CO-RMs)

Doxorubicin (Dox)

Reactive oxygen species (ROS)

Leaving group (LG)

Cytokine release syndrome (CRS)

Electron donating group (EDG)

Electron withdrawing group (EWG)

Porcine liver esterase (PLE)

Boron-dipyrromethene (BODIPY)

Bicyclo-[6.1.0]nonyne (BCN)

Tetraphenylcyclopentadienone (TPCPD)

This dissertation is partially based on materials described in the following papers

1. Ji, X.*; **Pan, Z.***; Ke, B.; Wang, B. “Dual stimuli-responsive Metal-free Carbon Monoxide prodrugs for the treatment of sepsis” *J. Med. Chem.*, **2019**, 62, 3163-3168. (*co-first author)
2. **Pan, Z.**; Zhang, J.; Ji, K.; Chittavong, V.; Ji, X.; Wang, B. “Organic CO prodrugs activated by endogenous ROS” *Org. Lett.* **2018**, 20, 8-11.
3. **Pan, Z. ***; Chittavong, V. *; Li, W.; Ji, K.; Zhu, M.; Ji, X.; Wang, B. “Organic CO-prodrugs: Structure CO-release rate relationship Studies” *Chem. Eur. J.* **2017**, 23, 9838-9845. (*co-first author)

1 ORGANIC CO-PRODRUGS: STRUCTURE CO-RELEASE RATE RELATIONSHIP STUDIES

1.1 Introduction

Carbon monoxide (CO) has long been recognized as a toxic gas and regarded as a “silent killer” mainly due to its high affinity for hemoglobin and the fact that many people die from CO poisoning every year. Beyond this perception is the fact that CO is also generated endogenously in mammals at a rate of about $500 \mu\text{mol day}^{-1}$ through the degradation of heme by heme oxygenase (Figure 1.1).^{1,2} Further, the safe use of therapeutic doses of CO has also been well demonstrated.³ Now, CO is recognized as an important gasotransmitter with importance on par with that of hydrogen sulfide (H₂S) and nitric oxide (NO).⁴ Moreover, past decades have witnessed the demonstration of a myriad of therapeutic indications for CO, including cytoprotection,⁵ anti-inflammation,⁶ antibacteria⁷⁻⁹ and anticancer,¹⁰ among many others. However, work in taking CO into clinical applications is still in its infancy mainly because of the difficulty in CO delivery in pharmaceutically acceptable forms.

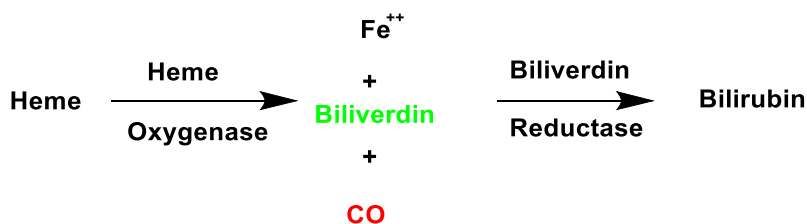


Figure 1.1. Heme degradation releases bioactive products including CO.

1.1.1 Inhalation

Inhalation of CO gas has been the most widely used CO-delivery form in the past decades in animal model studies and in human clinical trials. For example, in 1999, Otterbein and co-workers reported that CO could provide protection against oxidation stress.¹¹ In this study, it was found that CO could significantly attenuate hypoxia-induced lung injury in rats and improve the survival rate. Rats exposed to 250 parts/million (ppm) or 500 ppm had a survival rate of 100% after 72 h while in contrast rats exposed to hypoxia alone all died. CO has been well recognized as an anti-inflammatory agent by inhibiting expression of the pro-inflammatory cytokine TNF- α and augmenting expression of anti-inflammatory cytokine IL-10. In 2004, CO was reported to show strong anti-inflammatory effects in a lipopolysaccharide (LPS)-induced multiorgan failure rat model at a dose of 250 ppm for 1 h.¹² Also, CO was reported to be able to selectively sensitize cancer cells to anticancer drugs (e.g., doxorubicin) by 1000-fold due to its anti-Warburg effect, which would lead to metabolic exhaustion of cancer cells.¹³ Another utility of CO's cytoprotective effect is in its attenuation of doxorubicin's cardiotoxicity. Specifically, CO inhalation was found to promote and restore mitochondria biogenesis, and avert the myocardial pathology of Dox.¹⁴ Besides, in 2007 Mota and co-workers reported that exposure to CO gas (250 ppm, at a flow rate of ~12 liter/min, starting on day 3 after infection and continuing for 72 h) was able to greatly reduce experimental cerebral malaria (ECM) incidence in C57BL/6 mice.¹⁵ In this study, accumulation of free heme in the infected mice was demonstrated as a key component in the pathogenesis of ECM and CO was found to be able to suppress the accumulation and oxidation of hemoglobin.

As inhaled CO has shown these promising therapeutic effects in preclinical animal studies, several clinical trials had been initiated to test its safety and therapeutic efficacy in humans. For

example, a very recent Phase II clinical trial in 2019 was set up by Brigham and Women's Hospital to test the role of CO in the treatment of acute respiratory distress syndrome (Clinicaltrials.gov identifier: NCT03799874).

Though inhaled CO has been widely applied in animal or clinical studies, it is not an ideal delivery form for wide-spread applications due to difficulties in safe administration and in controlling doses, lack of portability, and the dependence on individual patient's respiratory function to deliver precise amounts. Safety issues in case of device malfunction are not trivial either. Therefore, a number of labs have been working on developing alternative delivery forms of CO for administration through oral or parenteral routes.

1.1.2 Metal-based carbon monoxide releasing molecules (CO-RMs)

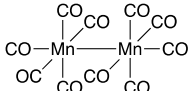
Much of the earlier work was focused on building molecules with CO immobilized on transition metals. These earlier compounds were called CO-releasing molecules, or CO-RMs. Since CO is chemically inert and it mainly coordinates with transition metals, most of the CO-RMs reported so far are transition metal based (Table 1.1).¹⁶ For example, the reactivity of CO toward metal was demonstrated by its strong interaction with reduced iron in hemoglobin to form an iron carbonyl. In 2002, Motterlini and co-workers reported a series of transition-metal based CO-RMs: dimanganese decacarbonyl (CO-RM-1) and tricarbonyldichlororuthenium (II) dimer (CO-RM-2), both of which release CO in a concentration-dependent manner.¹⁷ CO-RM-1 was shown to release CO only when it exposed to light while CO-RM-2 was shown to release CO spontaneously in DMSO. In 2003, Motterlini and co-workers also reported a new water-soluble CO-RM, tricarbonylchloro(glycinato)ruthenium(II) (CO-RM-3), which readily releases CO in buffer under near physiological conditions.¹⁸ It was found that CO-RM-3 (10 $\mu\text{mol/L}$) attenuated cell injury in a concentration-dependent manner at reoxygenation. Specially, H9c2 cells showed

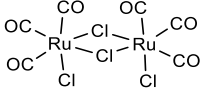
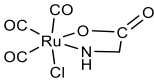
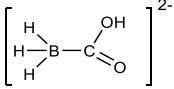
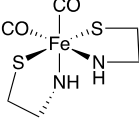
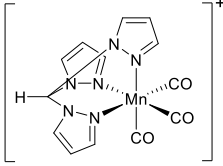
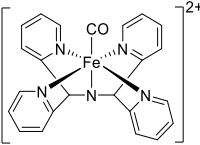
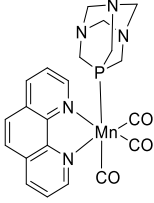
approximately 70% loss in cell viability when exposed to hypoxia for 24 hours and reoxygenated for 6 hours while cells treated with 25 $\mu\text{mol/L}$ didn't show any loss in cell viability.

In 2004, Green and Motterlini developed a transition-metal free CORM, $\text{Na}_2[\text{H}_3\text{BCO}_2]$ (CO-RM-A1) (CO-RM-A1), which has a slower half-life (~ 21 min at 37 $^\circ\text{C}$ and pH 7.4) than previous CO-RMs and thus offer the advantage of sustained duration of CO exposure.¹⁹ Further, administration of CO-RM-A1 led to a similar vasorelaxation effect in isolated aortic rings as the metal-based CO-RMs. Though CO-RM-A1 does not have transition metal, it does lead to the release of one equivalent of BH_3 , the health effect of which needs to be further examined.

Subsequently, other labs also reported many metal-based CO-RMs, which are able to release CO either spontaneously or upon light irradiation.²⁰⁻²² For example, Mascharak and co-workers reported a number of photo-sensitive CO-RMs²³ including $[\text{Mn}(\text{CO})_3(\text{phen})(\text{PTA})]\text{CF}_3\text{SO}_3$, which was shown to release CO upon exposure to visible light.²⁴ Interestingly, CO delivered by this CO-RM was found to sensitize cancer cells to doxorubicin by disrupting the redox homeostasis in breast cancer cells (MCF-7, MDA-MB-468, and Hs 578T). It was found that CO was able to inhibit cystathionine β -synthase (CBS) and further attenuate the ratio of reduced to oxidized glutathione (GSG/GSSG) which is frequently used as an indication of intracellular antioxidant capacity and redox homeostasis. A subsequent study in 2019 also showed sensitization effect on cisplatin-resistant ovarian cancer cells toward cisplatin via the same mechanism.²⁵

Table 1.1 Reported metal-containing CO-RMs Structures and CO-Release properties

Compounds	Chemical structure	Half-life ($t_{1/2}$)
$\text{Mn}_2[\text{CO}]_{10}$ (CO-RM-1)		< 1 min

$(\text{Ru}[\text{CO}]_3\text{Cl}_2)_2(\text{CO-RM-2})$		≈ 1 min
$\text{Ru}[\text{CO}]_3\text{Cl-glycinate}(\text{CO-RM-3})$		≈ 1 min (37°C, pH = 7.4)
$\text{Na}_2[\text{H}_3\text{BCO}_2] (\text{CO-RM-A1})$		≈ 21 min (37°C, pH = 7.4)
$\text{Mn}[\text{CO}]_4[\text{S}_2\text{CR}] (\text{CORM-S1})$		< 4 min
$[\text{Mn}(\text{CO})_3(\text{tpm})]\text{PF}_6$		NA
$[\text{Fe}^{\text{II}}(\text{CO})(\text{N}_4\text{Py})]^{2+}$		> 1 day in aerobic water or phosphate buffer
$[\text{Mn}(\text{CO})_3(\text{phen})(\text{PTA})]\text{CF}_3\text{SO}_3$		≈ 1.3 min

1.1.3 Esterase and protease sensitive CO-RMs

All metal-based CO-RMs discussed above have clearly demonstrated the feasibility of using CO-RMs as CO donors as research tools and for potential pharmacological applications. However, for many metal-based CO-RMs, CO release was relying on the reactions with water, pH changes or the presence of oxygen. Thus, it is very hard to control the amount of CO to be released or to delivery CO to the desired site. One way to overcome such limitations is to use stable

molecules as precursors, which could be triggered to release CO. Enzyme triggered CO-RMs (ET-CO-RMs) seems to be a good option to meet this need. In 2011, Schmalz and co-workers proposed acyloxybutadiene-iron tricarbonyl complexes as esterase-activated ET-CO-RMs (Figure 1.2).²⁶ The rationale behind this design is that stable dienyl ester complexes could be cleaved by intracellular esterase and the ensuing enolization would lead to iron dissociation and oxidation to Fe^{3+} and subsequent CO release. In this study, the CO release triggered by esterase was confirmed by a myoglobin (Mb) assay. The author confirmed that ET-CO-RMs could present potent anti-inflammatory effect by inhibition of NO production in LPS-stimulated RAW267.4 cells. In 2012, the same group reported a series of (phosphoryloxy diene) $\text{Fe}(\text{CO})_3$ complexes as water-soluble ET-CO-RMs for future application.²⁷

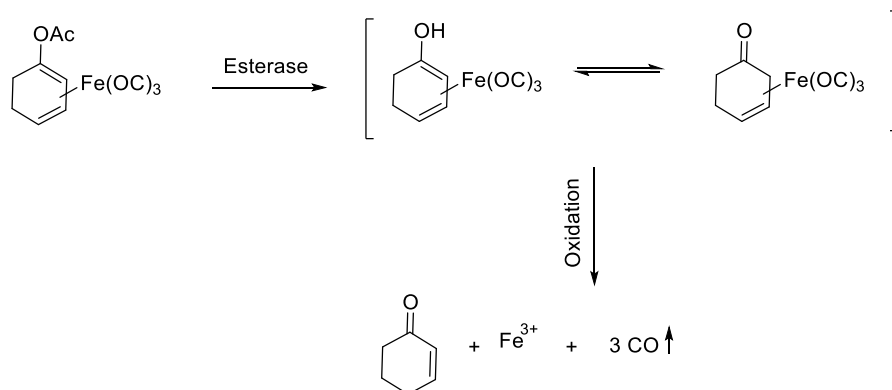


Figure 1.2 Mechanism of esterase-activated ET-CO-RMs

Beside esterase-activated ET-CO-RMs, Dr. Schmalz's group has also designed a series of protease-activated ET-CO-RMs by connecting an oxydiene- $\text{Fe}(\text{CO})_3$ complexes with a Penicillin G Amidase (PGA) cleavable side chain in 2015 (Figure 1.3).²⁸ It was demonstrated that after cleavage of the amide bond by amidase, the following residue would undergo decay and release of CO which is similar to the case in esterase-activated CO-RMs.

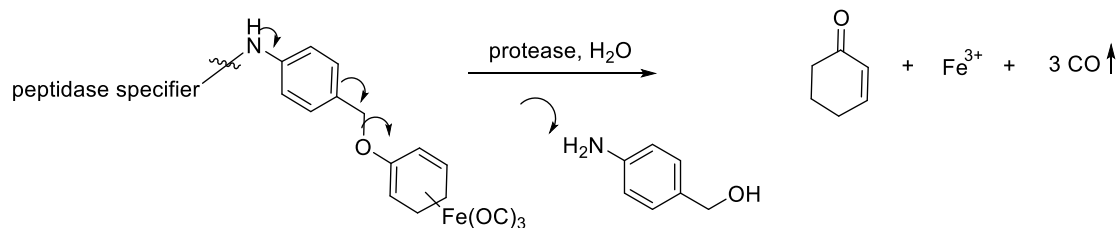


Figure 1.3 Mechanism of protease-activated ET-CO-RMs

ET-CO-RMs are clever designs for controlled release of CO. However, such design was mainly relying on the modification of metal-based CO-RMs. Undoubtedly, metal-based CO-RMs have made substantial contributions to the understanding of CO's biological effects. However, their clinical applications as therapeutic agents are somewhat hampered due to possible or may even just perceived metal toxicity issues. Consequently, encapsulated CO-RMs and photosensitive organic CO-RMs have been developed, aimed at addressing metal toxicity and targeted delivery issues.

1.1.4 CO delivery in encapsulated form

To achieve better targeting efficiency and reduce potential metal toxicity, many groups have worked on encapsulating CO-RMs in micelles, nanoparticles, and other capsules.²⁸⁻³¹ For example, in 2010 Hubbell and co-workers reported a CO delivery system using micelles.²⁹ Basically, the micelles contain three blocks: a hydrophilic poly(ethylene glycol) block, a poly(Ru(CO)₃Cl (ornithinate acrylamide) block capable of releasing CO, and a hydrophobic poly(*n*-butylacrylamide) block. These micelles were found to be stable under physiological conditions in buffer or serum, and release CO in response to thiol species such as cysteine.

In addition to CO-RM containing micelles, other new encapsulated forms of CO donors have also been developed. For example, in 2016 Maruyama and co-workers reported a type of CO

donor named CO-bound HbV (CO-HbV), in which the highly concentrated COHb solution was encapsulated inside a phospholipid bilayer membrane (liposome).³² Also, this CO-HbV was reported to possess strong anti-inflammatory and antioxidative effects in the progression of idiopathic pulmonary fibrosis and inflammatory bowel disease.

The encapsulated of CO delivery is a clever design in terms of addressing metal toxicity. However, the metabolism of remaining encapsulating materials is still a concern for the application of such a strategy.

1.1.5 Photosensitive organic CO-RMs

To avoid any metal-related toxicity issues as discussed above, organic forms of CO-RMs were sought by many groups. In 2013, Klán and co-workers reported a water-soluble fluorescein analogue as the first metal-free photo-sensitive CO-RM which releases CO when exposed to visible light (Figure 1.4).³³ The half-life of decomposition of this fluorescein analogue in phosphate buffer saline buffer (PBS) was determined to be around 4.5 h when irradiated at 500 nm. However, this fluorescein analog is hard to synthesize, and thus the chromophore was modified leading to a series of boron-dipyrromethenes (BODIPY) as photosensitive CO-RMs in 2016. These CO-RMs respond to visible-to-near IR(NIR) light (up to 730 nm), leading to activation and CO release.³⁴ The longer wavelength of absorption would allow better penetration of the light in the tissue and thus enhance their compatibility with biological applications.

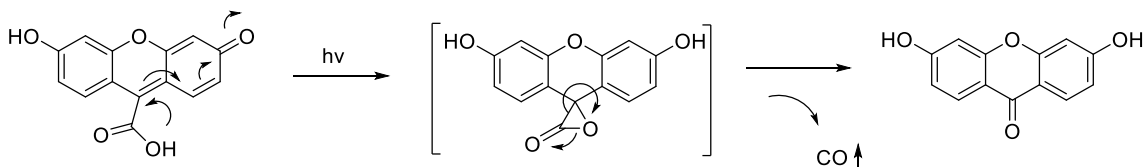
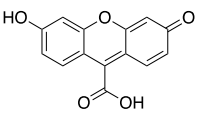
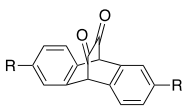
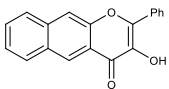
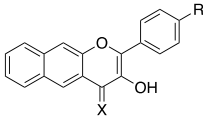
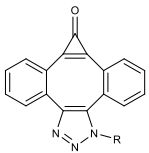


Figure 1.4 The photo-release mechanism for fluorescein analogue

Other researchers including Dr. Berreau's and Dr. Popik's group have also made extensive efforts in this area.^{35, 36} Undoubtedly, organic photosensitive CO-RMs with spatiotemporal control and minimized offsite effects have made substantial contributions to the development of organic CO prodrugs. However, there are more efforts needed to solve remaining concerns. For example, the penetration of light into deep tissue needs to be improved and structure modifications toward tunable release rates are also needed for future application.

Table 1.2 Reported photo-sensitive organic CO-RMs structures and CO-release properties

CO-RMs	Wavelength (nm)	Release rate
	500	$t_{1/2} = 270$ min
	470	Finish in 10 min
	419	Finish in 8 min
	419 or > 546	Finish in 10 min
	300	Finish in 5 min

1.1.6 Organic CO prodrugs

We strongly believe the potential of using CO for treatment of human diseases. However as with any drug discovery and development program, developability issues occupy a special place in determining the likelihood of success.³⁷⁻³⁹ As a result, we are interested in compounds that do more than releasing CO. Instead, we are very interested in the pharmaceutical developability of

such CO donors and their properties in the context of drug developability. For all these, we believe the need to take the CO donor work one step further in designing CO prodrugs, which take into consideration of developability issues as defining distinctions from CO-RMs. Therefore, the Wang lab is interested in the development of organic CO-prodrugs, which do not require light activation, can release CO under physiological conditions with tunable release rates, and are amenable to structural optimizations with regard to ADMET properties.

Ideal CO-prodrugs should have following desired properties: (1) CO release under physiological conditions; (2) devoid of any reactive functional groups or toxic ingredient; (3) amenable to optimization to tune the release rate; (4) triggered release of CO; and (5) suitable pharmaceutical properties for eventual human application.

In 2014, our lab reported the very first “click and release” CO prodrug system.⁴⁰ Specifically, the initial design takes advantage of a bimolecular inverse-electron-demand Diels Alder reaction (DA_{inv}) between a strained alkyne (bicyclo-[6.1.0]nonyne (BCN) and tetraphenylcyclopentadienone (TPCPD) to form a very strained intermediate, which undergoes a spontaneous chelotropic reaction to release CO under physiological conditions. The second order rate constant of such reactions was determined to be $0.61 \text{ M}^{-1}\text{S}^{-1}$ in aqueous solution or methanol at room temperature. Co-treatment of Raw 264.7 cells with both two compounds (1 mM) led to a 50% decrease of the LPS-induced production of TNF- α , while treatment of either compound alone had no such effect. Thus, this experiment successfully demonstrated the anti-inflammatory effect of CO and the chemical feasibility of using Diels-Alder reactions to design “click and release” CO prodrug systems.

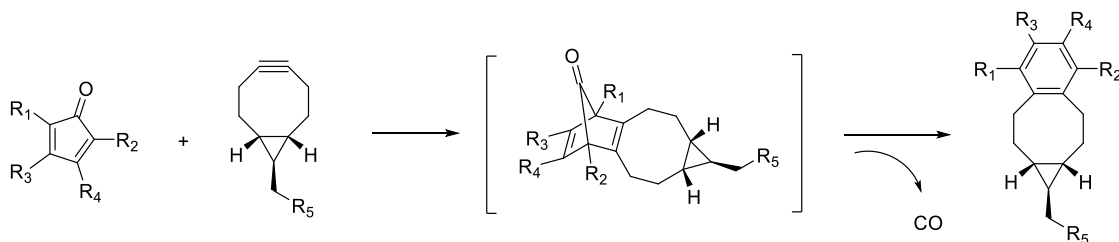


Figure 1.5 A bimolecular click and release prodrug system

To achieve better targeting efficiency and reduce potential metal toxicity, many groups have worked on encapsulating CO-RMs in micelles, nanoparticles, and other capsules.²⁸⁻³¹ For example, in 2010 Hubbell and co-workers reported a CO delivery system using micelles.²⁹ Basically, the micelles contain three blocks: a hydrophilic poly(ethylene glycol) block, a poly(Ru(CO)₃Cl (ornithinate acrylamide) block capable of releasing CO, and a hydrophobic poly(*n*-butylacrylamide) block. These micelles were found to be stable under physiological conditions in buffer or serum, and release CO in response to thiol species such as cysteine.

In addition to CO-RM containing micelles, other new encapsulated forms of CO donors have also been developed. For example, in 2016 Maruyama and co-workers reported a type of CO donor named CO-bound HbV (CO-HbV), in which the highly concentrated COHb solution was encapsulated inside a phospholipid bilayer membrane (liposome).³² Also, this CO-HbV was reported to possess strong anti-inflammatory and antioxidative effects in the progression of idiopathic pulmonary fibrosis and inflammatory bowel disease.

The encapsulated of CO delivery is a clever design in terms of addressing metal toxicity. However, the metabolism of remaining encapsulating materials is still a concern for the application of such a strategy.

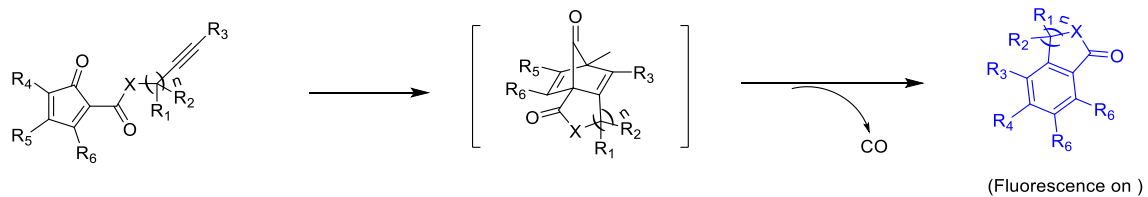


Figure 1.6 A unimolecular click and release prodrug system

1.2 Results and discussion

1.2.1 Design of CO prodrugs

Among the various features that we are interested in working on, we view the tunability of release rates being a critical one. Because of the volatile nature of CO, the release half-life plays a determining role in the effective CO concentration and duration of action. Moreover, we believe that CO prodrugs with different releasing profiles are required for different applications. Herein, we describe the first comprehensive study of the relationship between structure and CO release rate for three classes of CO prodrugs. Among them, scaffold I was reported in our previous unimolecular prodrug work as shown in Figure 1.6.⁴¹ Meanwhile, two other new structural scaffolds (Figure 1.7, Scaffolds II and III) for the same purpose are also introduced here.⁴²

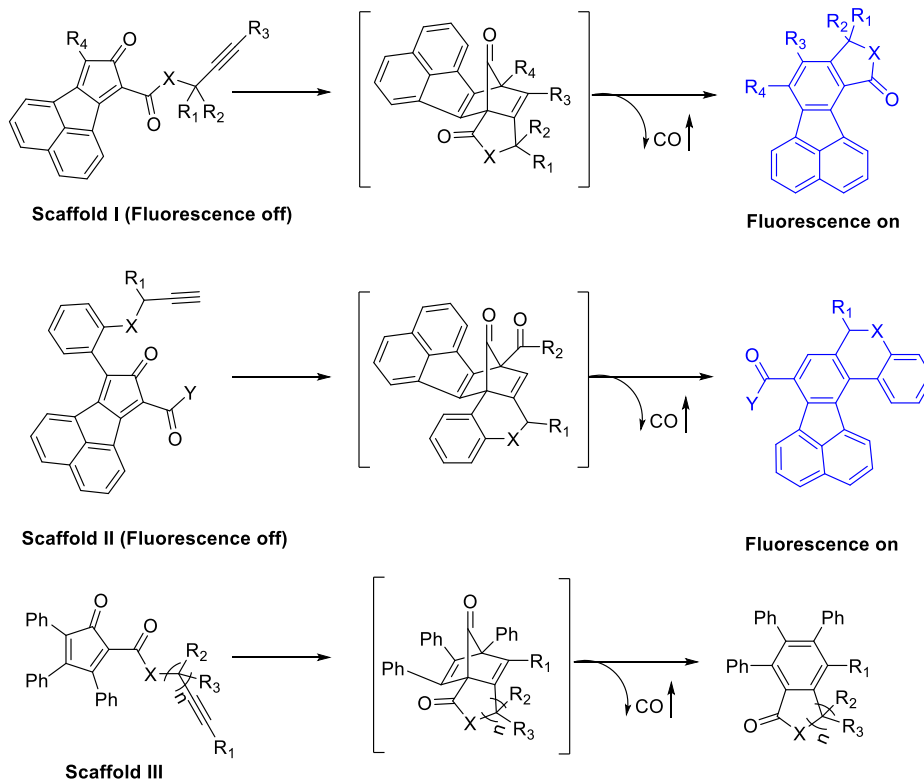


Figure 1.7 General structures of CO prodrugs and their CO release mechanism

The general design of this class of CO prodrugs cages a CO molecule in the form of a ketone carbonyl group in a substituted cyclopentadienone and relies on a Diels-Alder reaction with an alkyne for the release of CO under physiological conditions. In designing new analogs, we separate these CO prodrugs into three types. Type I represent an extension of our earlier work on fusing a cyclopentadienone ring with a naphthalene ring, which forms a fluorescent product after CO release, and thus allow for the real-time monitoring of CO formation.⁴¹ In this scaffold, the alkyne group is tethered to the cyclopentadienone moiety through a linear linker containing either an ester or amide functional group. The structural modifications to scaffold I were primarily made to the substituent on the cyclopentadienone ring (R4, Figure 1.7), the nature of the tethering linker (X, Figure 1.7), and the substituents on the tethering linker (R1-R3, Figure 1.7). In type II, the linker has a phenyl ring structure, providing additional conformational constraints. In addition, a carboxyl

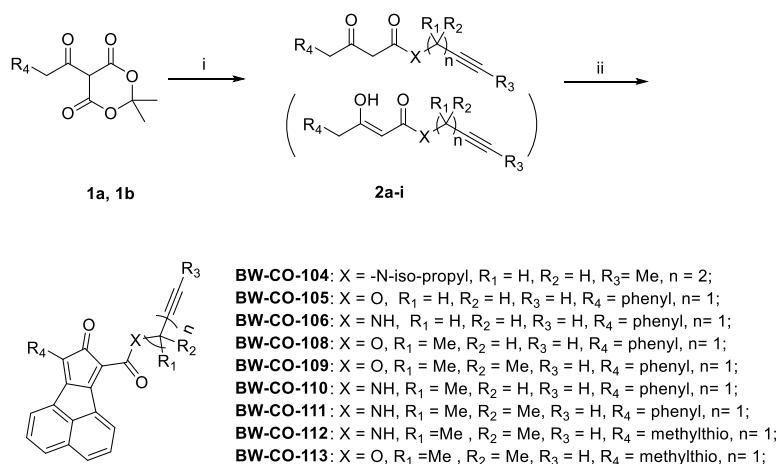
group in scaffold II can be used for structural optimization or for tethering additional structures for targeting and other applications. Similar structural modifications were also made to Scaffold II (X, Y and R₁) to probe the structure-release rate relationship. CO prodrugs with Scaffolds I and II both possess a naphthalene group fused with the dienone ring. However, the introduction of naphthalene ring is also accompanied with decreased water solubility due to its rigid and flat structural nature. Moreover, the fluorescent reporter is not necessarily needed for eventual clinical applications. Therefore, CO prodrugs with Scaffold III were also designed. In this class, each of the 3, 4 positions of the cyclopentadienone moiety is substituted with an individual aryl ring. This affords additional structural diversity and flexibility. Further modifications followed a similar approach as for Scaffolds I and II.

In considering the design, one critical factor is the balance of the reactivity needed for cycloaddition in aqueous solution at neutral pH, and stability in organic solvent and during storage. It has been reported that water and protein binding accelerate Diels-Alder reactions by thousands of folds, largely driven by hydrophobic forces.⁴³⁻⁴⁷ This allows the possibility for CO-prodrugs to be prepared in organic solvents, remain stable during storage, and yet readily undergo cycloaddition in an aqueous solution to release CO.

1.2.2 Synthesis of CO prodrugs

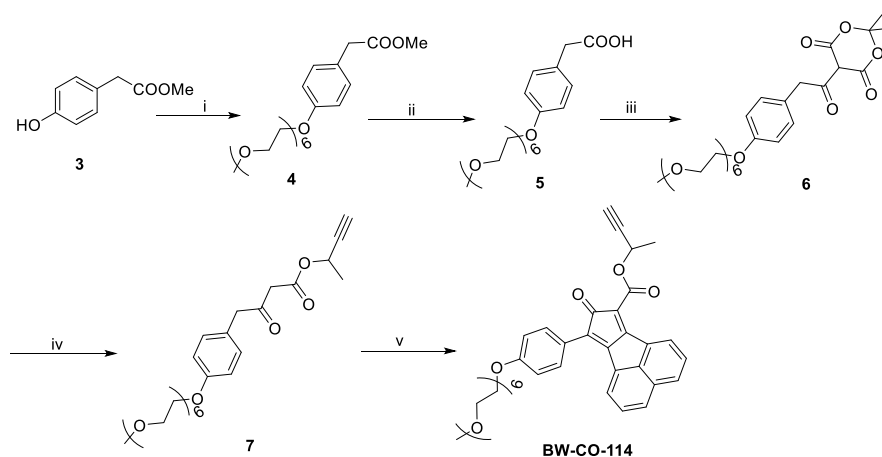
CO prodrugs **BW-CO-104-106, 108-113** with different tethering linkers and substituents were synthesized according to our previous procedures.⁴¹ Briefly, compound **1a-b** were condensed with a variety of alcohol or amine to afford compounds **2a-i**, which were found to exist as a mixture of keto-enol tautomers (Scheme 1). Compounds **2a-i** were then reacted with acenaphthylene-1,2-dione, followed by treatment with an acid for dehydration to yield the desired CO prodrugs **BW-CO-104-106, and 108-113** in 20-77% yield. CO prodrug **BW-CO-114** with a (2,5,8,11,14,17-

hexaoxonadecan-19-yl)oxyl group was also synthesized in order to improve water solubility and biocompatibility (Scheme 1.2). Briefly, compound **4** was synthesized by alkylation of compound **3**, and was subsequently hydrolyzed to afford compound **5** in 98% yield. Compound **5** was then condensed with 2, 2-dimethyl-1,3-dioxane-4,6-dione using EDC as the coupling reagent to afford compound **6**. **BW-CO-114** was then obtained by a similar dehydration method used for the synthesis of **BW-CO-104-106, 108 – 113** as shown in Scheme 1.1.



*Scheme 1.1 Synthesis of CO prodrugs **BW-CO-104-106, 108 – 113** with scaffold I.*

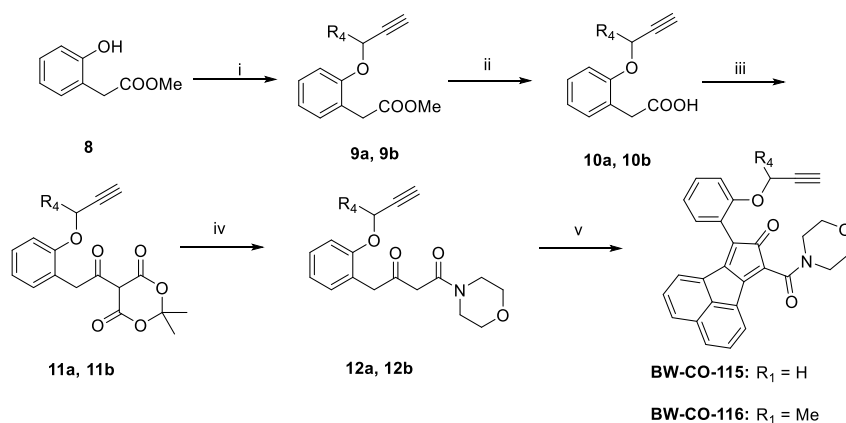
Reagents and conditions: i) toluene, substituted alcohol or amine, reflux, 1-2 h; ii) 1) acenaphthylene-1,2-dione, Et₃N, MeOH/THF (1:2), r.t, 1-3 h, 2). H₂SO₄, Ac₂O, 0 °C to r.t, 1- 2 h



*Scheme 1.2 Scheme 2. Synthesis of CO prodrugs **BW-CO-114** with scaffold I.*

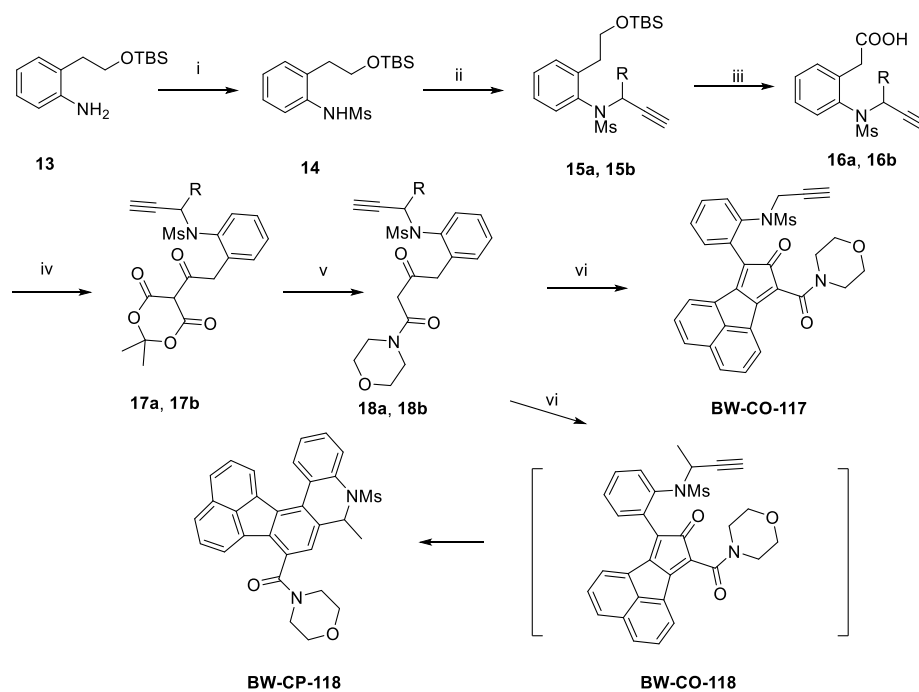
Reagents and conditions: i) 2,5,8,11,14,17-hexaoxonadecan-19-yl 4-methylbenzenesulfonate, NaH, THF, 0 °C - r.t, 24 h; ii) LiOH, MeOH/H₂O, r.t, 24h; iii) 2,2-dimethyl-1,3-dioxane-4,6-dione, Et₃N, MeOH/THF (1:2), r.t, 1-3 h, 2). H₂SO₄, Ac₂O, 0 °C to r.t, 1- 2 h

Next, we synthesized CO prodrugs with Scaffold II. As shown in Scheme 1.3, compound **8** was alkylated under basic condition to afford compounds **9a/b**. CO prodrugs **BW-CO-115-116** were then readily synthesized by a series of reactions similar to those used for the synthesis of **BW-CO-114** (Scheme 1.2). Meanwhile, in order to probe the effects of substituent on the linker for the CO release rate, CO prodrugs **BW-CO-117/118** were also synthesized as shown in Scheme 1.4. Initially, we tried to employ methyl 2-(2-aminophenyl)acetate as the starting material to make **BW-CO-117/118**, by following similar approaches used for **BW-CO-115/116**. However, unlike its phenol counterpart (**8**), methyl 2-(2-aminophenyl)acetate is unstable, and is prone to intramolecular lactamization to form a five-membered lactam ring. Consequently, compound **13** was used as the starting material, which was sulfonated and alkylated to afford compounds **15a/b**. The deprotection of the TBS group and subsequent oxidation of the alcohol to acid **16a/b** was accomplished in one pot by using KF and Jones reagent in acetone at room temperature. With compounds **16a/b** in hand, the synthesis of **BW-CO-117 /118** was straightforward by a series of similar reactions used for **BW-CO-114**. However, in the case of **BW-CO-118**, **BW-CP-118** was afforded as the major product at the dehydration step, presumably due to the fast cycloaddition of **BW-CO-118** under such conditions. The synthesis of CO-prodrugs of Type **III** is depicted in Scheme 1.5. Intermediate **2a**, **2e** and **2f** described in Scheme 1.1 were further reacted with benzil in the presence of KOH to yield the aldol intermediates, which were used directly for the dehydration step without purifications to afford **BW-CO-119 - 121** as red solid.



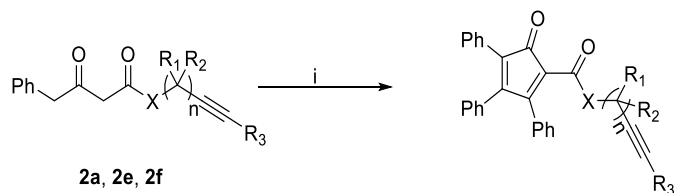
*Scheme 1.3 Synthesis route of **BW-CO-115 - 116** with scaffold II.*

Reagents and conditions: (i) propargyl bromide or 3-butyn-2-yl 4-methylbenzenesulfonate, K_2CO_3 , ACN, reflux, 4 h; (ii) KOH, H_2O /methanol (1:1), r.t., 1 h; (iii) 2,2-dimethyl-1,3-dioxane-4,6-dione, DMAP, EDC, DCM, r.t., 12 h; (iv) morpholine, trimethylsilyl chloride (TMSCl), chlorobenzene, reflux, 3 h; (v) acenaphthylene-1,2-dione, Et_3N , MeOH/THF (1:2), rt, 3 h, then H_2SO_4 , Ac_2O , 0 °C to r.t., 1 h.



*Scheme 1.4 Synthesis route of **BW-CO-117 - 118** with scaffold II.*

Reagents and conditions: (i) MsCl, pyridine, DCM, 0 °C to r.t., 20 h; (ii) propargyl bromide or 3-butyn-2-yl 4-methylbenzenesulfonate, K_2CO_3 , ACN, reflux, 4 h; (iii) KF, Jones reagent, acetone, rt, 20 h; (iv) 2,2-dimethyl-1,3-dioxane-4,6-dione, DMAP, EDC, DCM, rt, 12 h; (v) morpholine, TMSCl, chlorobenzene, reflux, 3 h; (vi) 1). acenaphthylene-1,2-dione, Et_3N , MeOH/THF (1:2), r.t., 3 h; 2). H_2SO_4 , Ac_2O , 0 °C to rt, 1 h.



BW-CO-119: X = O, R₁ = H, R₂ = H, R₃ = H, n = 1;
BW-CO-120: X = O, R₁ = Me, R₂ = H, R₃ = H, n = 1;
BW-CO-121: X = -N-iso-propyl, R₁ = H, R₂ = H, R₃ = Me, n = 2;

Scheme 1.5 Synthesis of the CO prodrugs BW-CO-119 - 121 with scaffold III.
 Reagents and conditions: i) 1).benzil, KOH, rt, 15 h; 2). H₂SO₄, Ac₂O, 0 °C to r.t, 15 min.

1.2.3 CO release kinetics and structure CO release rate relationships

With all the CO prodrugs in hand, we next studied their CO release rates in a mixed aqueous solution (DMSO/PBS = 4/1, 37 °C). For CO prodrugs of Scaffolds **I** and **II**, their CO release kinetics were easily determined by monitoring the increase of the fluorescent intensity at different time points. For CO prodrugs of Scaffold **III**, since the CO prodrugs have a UV absorbance peak at around 360 nm, and yet the cyclized product has no absorbance at this wavelength, the CO release rate was indirectly determined by monitoring the decrease of UV absorbance at 360 nm. The CO release kinetics for the CO prodrugs are summarized in Tables 1.2, 1.3 and 1.4.

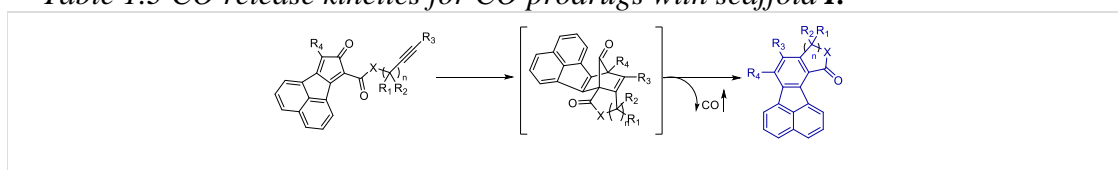
As shown in Table 1.3, all the CO prodrugs of Type **I** can readily undergo intramolecular cycloaddition to release CO. The CO release was confirmed by the structural elucidation of the fluorescent cycloaddition products **BW-CP-104 - 106, 108 – 114**, a commercial CO detector and a CO myoglobin assay. Three major factors are important in influencing the reaction rates: (1) the nature of the X, which determines whether it is an ester or amide, (2) additional substituents on the linear linker, which may impose additional conformational constraints favoring the cycloaddition reaction and thus CO release rates, and (3) the linker length, which determines

whether cycloaddition would lead to a five- or six-membered ring formation. Generally, CO-prodrugs with an amide linker lead to faster CO release as compared to those with an ester linker. For example, the half-lives of **BW-CO-108/109** ($t_{1/2} = 55.6$ or 0.55 h) with an ester linker were much longer than **BW-CO-110/111** ($t_{1/2} = 12$ or 0.2 h) with an amide linker. This is understandable because amide bond is not as freely rotatable as an ester bond, and thus provides an entropic advantage in such cycloaddition reactions. It is well known that “gem-dialkyl” effect can greatly accelerate ring-closure reaction.⁴⁸ Indeed, we find that the introduction of a gem-dimethyl group accelerates the cycloaddition rate significantly. For example, the half-lives for **BW-CO-109** and **BW-CO-111** are only around 0.55 and 0.20 h, respectively, which represent a more than 1000-fold difference as compared to **BW-CO-105/106** ($t_{1/2} > 10$ days), which do not have this gem-dimethyl group. By the same token, the introduction of one methyl group on the tethering linker also enhances the cycloaddition rate. For example, **BW-CO-106** has a half-life of more than 10 days while **BW-CO-110** has a much shorter half-life of 12.0 h after introducing a methyl group.

An additional observation related to water solubility and CO-release rate is also very interesting. The introduction of a PEG linker to the phenyl ring in **BW-CO-114** slightly decreases the CO release rate ($t_{1/2} = 97$ h vs $t_{1/2} = 56$ h of **BW-CO-108**). It is possible that the introduction of a hydrophilic unit close to the reaction site disfavors a process that is partially driven by hydrophobic forces. Unexpectedly, substituting the phenyl (**BW-CO-109/111**) on the dienone moiety with a methylthio group (**BW-CO-112/113**) does not make much of a difference in terms of CO release rate. Compared to a phenyl group, the methylthiol group is, albeit weak, an electron donating group, and should increase the LUMO energy level of the dienone compound, resulting in a decrease in the cycloaddition rate. Indeed, computational calculations of the partial charge distribution show that the electron density of dienone ring with a methylthiol group (**BW-CO-**

112/113) is higher than that of **BW-CO-109/112**. However, the results show that there is no significant difference in CO release rate between these two types of analogues, indicating that entropy factors dominated in rate acceleration instead of electron density on the dienone ring in such cases. This also opens a door for introducing substituents of varying electronic properties on the phenyl ring for structural diversity.

Table 1.3 CO release kinetics for CO prodrugs with scaffold I.



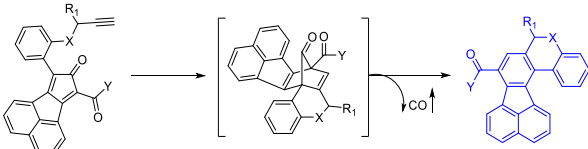
Compounds	k (h ⁻¹) [a]	t _{1/2} (h) [b]
BW-CO-104: X = -N-iso-propyl, R ₁ = H, R ₂ = H, R ₃ = Me, n = 2	0.11±0.03	6.2±0.2
BW-CO-105: X = O, R ₁ = H, R ₂ = H, R ₃ = H, R ₄ = phenyl, n = 1	-	> 10 days
BW-CO-106: X = NH, R ₁ = H, R ₂ = H, R ₃ = H, R ₄ = phenyl, n = 1	-	>10 days
BW-CO-108: X = O, R ₁ = Me, R ₂ = H, R ₃ = H, R ₄ = phenyl, n = 1	0.012±0.0003	55.6±1.5
BW-CO-109: X = O, R ₁ = Me, R ₂ = Me, R ₃ = H, R ₄ = phenyl, n = 1	1.28±0.18	0.55±0.08
BW-CO-110: X = NH, R ₁ = Me, R ₂ = H, R ₃ = H, R ₄ = phenyl, n = 1	0.058±0.003	12.0±0.74
BW-CO-111: X = NH, R ₁ = Me, R ₂ = Me, R ₃ = H, R ₄ = phenyl, n = 1	3.31 ±0.28	0.20±0.02
BW-CO-112: X = NH, R ₁ = Me, R ₂ = Me, R ₃ = H, R ₄ = methylthio, n = 1	4.63±0.28	0.15±0.009
BW-CO-113: X = O, R ₁ = Me, R ₂ = Me, R ₃ = H, R ₄ = methylthio, n = 1	1.29±0.07	0.53±0.04
BW-CO-114: X = O, R ₁ = Me, R ₂ = H, R ₃ = H, R ₄ = PEG substituted phenyl group, n = 1	0.0072±0.0003	96.85±4.45

[a] CO release rate was determined by monitoring the increase of fluorescence intensity in DMSO/PBS (pH = 7.4) 4:1 at 37 °C. [b] Half-life for CO release;

As shown in Table 1.4, all the synthesized CO prodrugs with scaffold II can release CO and generate a fluorescent reporter in DMSO/PBS (4:1) at 37 °C as well. The CO release was verified by structural elucidation of the cyclized products, a commercial CO detector and a CO myoglobin assay. As for the CO release rate, the introduction of a ring structure on the linker did not seem to afford general rate enhancement. The CO release rates are in the same general range

as that of Type **I**. Among the three analogs studied in Table 1.4, the N-methanesulfonyl aniline linker seems to provide faster CO release rates. For example, **BW-CO-117** with an N-methanesulfonyl group as “X” has a release half-life of 0.78 h. In comparison, compound **BW-CO-115**, which has an oxygen as the “X” group has a release half-life of 6.74 h. Such results are in agreement with the conformational constraints imposed by the N-methanesulfonyl aniline structure as compared to a phenol oxygen in the same place. The introduction of one methyl group into the tethering linker also enhanced the CO release. For example, **BW-CO-115** has a half-life of 6.74 h while **BW-CO-116**, which has a methyl group on the linker, has a half-life of only 2.25 h. This is the same trend as observed in the CO prodrugs of scaffold **I**.

*Table 1.4 CO release kinetics for CO prodrugs with scaffold **II**.*



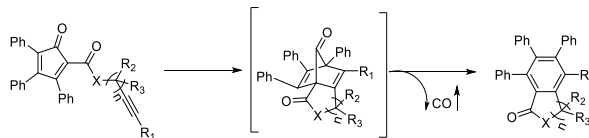
Compounds	k (h ⁻¹) [a]	t _{1/2} (h) [b]
BW-CO-115 : X = O, R ₁ = H, Y = morpholine	0.10±0.003	6.74±0.21
BW-CO-116 : X = O, R ₁ = Me, Y = morpholine	0.308±0.003	2.25±0.03
BW-CO-117 : X = NMs, R ₁ = H, Y = morpholine	0.882±0.012	0.78±0.01

[a] CO release rate was determined by monitoring the increase of fluorescence intensity in DMSO/PBS (pH = 7.4) 4:1 at 37 °C. [b] Half-life for CO release;

As shown in Table 1.5, the CO prodrugs with Scaffold **III** also readily release CO in DMSO/PBS (4:1) at 37 °C. Intriguingly, the CO release rates for prodrugs of Scaffold **III** are much faster than that of the corresponding CO prodrugs of Scaffold **I**. For example, the half-life for **BW-CO-104**, **105** and **108** of Scaffold **I** is more than 6 h, 10 days and 55 h, respectively, and yet the half-life for their Scaffold **III** counterparts is only 1h, 4 min, and 7 min, respectively. Interestingly, results from computational studies indicate that conjugation of phenyl ring would lower the

electron density of the dienone ring especially at the C4 position. It is possible that the conjugation afforded by the phenyl ring in Scaffold III prodrugs increases the reactivity of the cyclopentadienone structure in a Diels-Alder reaction by lowering the LUMO energy level of the dienone ring. In addition, **BW-CO-121** ($t_{1/2} = 0.97$ h) with an amide linker is found to release CO at a slower rate than **BW-CO-119** ($t_{1/2} = 0.12$ h), despite the fact that it has an amide group, while **BW-CO-119** has an ester linker. Such results further indicate that the size of the ring formed from the tether plays an important role as well. It is clear that lactam/lactones of five-membered rings formed by **BW-CO-119** is favored over six-membered ring formed by **BW-CO-121**, leading to enhanced CO release rates. Besides, introduction of one methyl group on the tethering linker increases the CO release rate ($t_{1/2} = 0.073$ h of **BW-CO-120** vs $t_{1/2} = 0.12$ h of **BW-CO-119**), which is similar to our previous findings in Scaffold I.

Table 1.5 CO release kinetics for CO prodrugs with scaffold III.



Compounds	k (h^{-1}) ^[a]	$t_{1/2}$ (h) ^[b]
BW-CO-119 : X = O, R ₁ = H, R ₂ = H, R ₃ = H, n = 1	5.89±0.91	0.12±0.02
BW-CO-120 : X = O, R ₁ = H, R ₂ = Me, R ₃ = H, n = 1	9.39±1.07	0.073±0.013
BW-CO-121 : X = -N-iso-propyl, R ₁ = Me, R ₂ = H, R ₃ = H, n = 2	0.72±0.08	0.97±0.11

[a] CO release rate was determined by monitoring the decrease of absorbance at 360 nm in DMSO/PBS (pH = 7.4) 4:1 at 37 °C. [b] Half-life for CO release.

1.2.4 Cytotoxicity study

The cytotoxicity of **BW-CO/CP-104** has been tested in our previous work and these compounds showed no cytotoxicity at up to 100 μM .⁴¹ Cytotoxicity of the rest CO prodrugs along

with their corresponding products after CO release was studied in Raw 264.7 cells with a drug exposure time of 24 h. The results revealed that most of the compounds tested did not present obvious cytotoxicity at 100 μ M, and only a few CO prodrugs (**BW-CO-112**, **113**, **115**, **116**, **120**, **121**) and inactive products (**BW-CP-111/115/120**) showed cytotoxicity with IC₅₀ values in the range of 50-100 μ M. Clearly, there is no general intrinsic toxicity issues related to this class of compounds, but idiosyncratic toxicity may occur with individual compounds, which can also be addressed by structural optimizations.

1.2.5 Intracellular CO release

Having confirmed that all the prodrugs readily undergo intramolecular cycloaddition to release CO in a mixed aqueous solution, we next probed whether they would release CO in a biological milieu. To this end, prodrugs **BW-CO-109** (Scaffold **I**), **117** (Scaffold **II**), and **119** (Scaffold **III**) were chosen as representatives to study intracellular CO release in Raw 264.7 cells. For **BW-CO-109/117**, the intracellular CO release was monitored by the blue fluorescence of the cyclized product. For **BW-CO-119**, the CO release was verified by using a reported CO fluorescent probe COP-1.⁴⁹ As shown in Figure 1.8, the cells treated with BW-CO-109 and 117 showed dose-dependent blue fluorescence formation, which indicated CO release intracellularly. For **BW-CO-119**, the cells treated with prodrug and COP-1 showed strong green fluorescence in a dose dependent fashion, and the cells treated with COP-1 alone showed only negligible green fluorescence. Altogether, these results indicated that all the CO prodrugs would release CO in a biological matrix.

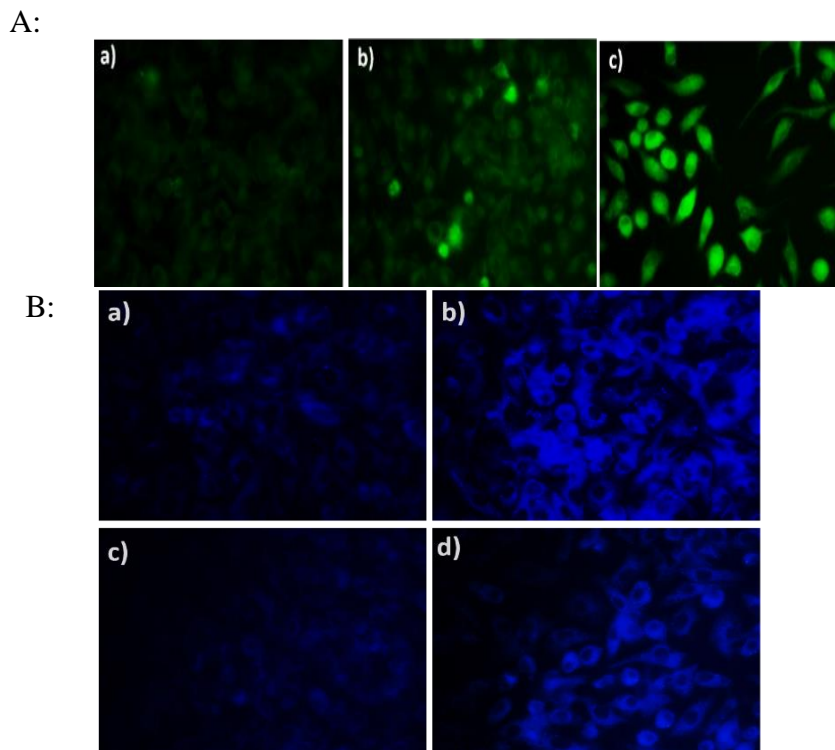


Figure 1.8 Fluorescence imaging of fixed Raw 264.7 cells

A: Fluorescence imaging of fixed Raw264.7 cells treated with **COP-1**. (a: 1 μ M) only, or **COP-1** (1 μ M) + **BW-CO-119** (b: 25 μ M, c: 50 μ M) under FITC channel. B: Fluorescence imaging of fixed Raw264.7 cells treated with BW-CO-109.

1.3 Experimental Section

1.3.1 General information

All reagents and solvents were of reagent grade and were purchased from Aldrich. ^1H -NMR (400 MHz) and ^{13}C -NMR (100 MHz) spectra were recorded on a Bruker Avance 400 MHz NMR spectrometer. Mass spectral analyses were performed on an ABI API 3200 (ESI-Triple Quadruple). Fluorescence spectra were recorded on a Shimadzu RF-5301PC fluorometer and UV absorption spectra were obtained with Shimadzu UV-1700. Compound **1a**, **2a-c**, **BW-CO-104** – **106**, 2,5,8,11,14,17-hexaoxonadecan-19-yl 4-methylbenzenesulfonate and **COP-1** were synthesized following literature procedures.^{49,50}

1.3.2 Experimental procedure for the synthesis of CO prodrugs

Synthesis of compound 1b: To a solution of 2-(methylthio)acetic acid (6.0 mmol) in anhydrous DCM (3 ml), Meldrum's acid (0.9 mmol, 1.5 equiv.) and DMAP (9.0 mmol, 1.5 equiv.) were added. The solution was cooled to 0 °C and EDC (9.0 mmol, 1.5 equiv.) was added slowly under protection of argon. After stirring at 0 °C for 1 h, the reaction mixture was allowed to warm to room temperature and then stirring continued for another 6 h. Then the reaction was quenched by aqueous HCl solution (1M, 30 mL) and extracted with EtOAc (3 × 25 ml). The combined organic phase was dried over anhydrous Na₂SO₄, evaporated under reduced pressure to afford the crude product, which was further purified by silica gel column chromatography to afford the pure product as a white solid (83%). ¹H NMR (CDCl₃) δ 15.28 (s, 1H), 3.94 (s, 2H), 2.26 (s, 3H), 1.75 (s, 6H). ¹³C NMR (CDCl₃) δ 193.1, 170.7, 160.1, 105.2, 90.4, 35.8, 26.9, 16.6.

General procedure A for the synthesis of compound 2: To a solution of **1a** or **1b** (1.5 mmol) in toluene (4 mL), the corresponding alcohol or amine (2.3 mmol, 1.5 equiv.) were added. The solution was heated at reflux for 1-2 h, after which the reaction mixture was concentrated under vacuum, and the residue was directly purified by column chromatography to afford the desired product.

2d: colorless oil, yield, 90%. ¹H NMR (CDCl₃) δ 7.38 – 7.27 (m, 3H), 7.24 (d, *J* = 6.8 Hz, 2H), 5.51 – 5.45 (m, 1H), 3.85 (s, 2H), 3.49 (s, 2H), 2.50 (d, *J* = 2.0 Hz, 1H), 1.53 (d, *J* = 6.8 Hz, 3H). ¹³C NMR (CDCl₃) δ 199.9, 165.9, 133.1, 129.6, 128.9, 127.4, 81.4, 73.4, 61.1, 50.0, 48.1, 21.1. HRMS (ESI)⁺ calculated for C₁₄H₁₄O₃ [M+Na]⁺ m/z 253.0835, found 253.0836.

2e: Colorless oil, yield, 70% ¹H NMR (CDCl₃) δ 7.36 (t, *J* = 7.2 Hz, 2H), 7.31 (t, *J* = 6.7 Hz, 1H), 7.23 (d, *J* = 7.4 Hz, 2H), 3.86 (s, 2H), 3.44 (s, 2H), 2.59 (s, 1H), 1.70 (s, 6H). ¹³C NMR

(CDCl₃) δ 200.3, 165.4, 133.3, 129.6, 129.4, 128.8, 127.3, 84.1, 73.1, 72.9, 49.9, 48.9, 28.8. HRMS (ESI)⁺ calculated for C₁₅H₁₆O₃ [M+Na]⁺: m/z 267.0997, found 267.0984.

2f: colorless oil, yield 59%. ¹H NMR (CDCl₃) δ 7.40 – 7.30 (m, 3H), 7.23 – 7.18 (m, 2H), 4.85 – 4.70 (m, 1H), 3.81 (s, 2H), 3.44 (d, *J* = 2.1 Hz, 2H), 2.26 (d, *J* = 2.3 Hz, 1H), 1.41 (d, *J* = 6.9 Hz, 3H). ¹³C NMR (CDCl₃) δ 204.3, 164.5, 132.9, 129.6, 129.0, 127.6, 83.9, 70.6, 50.8, 47.8, 37.0, 22.1. HRMS (ESI)⁺ calcd for C₁₄H₁₅NO₂ [M+H]⁺ m/z 230.1176, found 230.1171.

2g: ¹H NMR (CDCl₃) δ 7.41 – 7.31 (m, 3H), 7.25 – 7.10 (m, 3H), 3.82 (s, 2H), 3.44 (s, 2H), 2.35 (s, 1H), 1.63 (s, 7H). ¹³C NMR (CDCl₃) δ 204.7, 164.2, 132.8, 129.6, 128.9, 127.5, 86.8, 69.2, 50.8, 48.6, 47.4, 28.9. HRMS (ESI)⁺ calculated for C₁₅H₁₇NO₂ [M+Na]⁺: m/z 266.1157, found 266.1151.

2h: colorless oil, yield, 63%. ¹H NMR (CDCl₃) δ 6.97 (s, 1H), 3.56 (s, 2H), 3.30 (s, 2H), 2.34 (s, 1H), 2.07 (s, 3H), 1.64 (s, 6H). ¹³C NMR (CDCl₃) δ 200.8, 164.4, 86.7, 69.3, 47.5, 47.4, 43.9, 28.9, 15.7. HRMS (ESI)⁺ calculated for C₁₀H₁₅NO₂S [M+H]⁺ 214.0896, found 214.0899.

2i: colorless oil, 87%. ¹H NMR (CDCl₃) δ 3.61 (s, 2H), 3.31 (s, 2H), 2.56 (s, 1H), 2.04 (s, 3H), 1.66 (d, *J* = 13.6 Hz, 6H). ¹³C NMR (CDCl₃) δ 197.2, 165.3, 90.8, 73.1, 46.7, 43.0, 29.1, 15.9. HRMS (ESI)⁺ calculated for C₁₀H₁₄O₃S [M+Na]⁺ 237.0561, found: 237.0553

General procedure B for the synthesis of BW-CO-108 – 113: To a solution of compound **2** (1.0 mmol) in THF/MeOH (3:1, v/v, 1.6 mL), acenaphthylene-1,2-dione (1.0 mmol, 1.0 equiv.) and Et₃N (1.5 mmol, 1.5 equiv.) were added. The mixture was stirred at room temperature for 1 – 2 h, after which it was concentrated under vacuum and the resulting residue was dissolved in acetic anhydride (2 mL). The resulting solution was cooled to 0 °C and 2-5 drops of H₂SO₄ was then added. After stirring at room temperature for 1 h, the solution was diluted with EtOAc (40 mL), and washed with water (20 mL) and brine (20 mL). The combined organic phase was dried over

anhydrous Na₂SO₄, and evaporated under reduced pressure. The resulting crude product was purified by silica gel column chromatography. The obtained crude product was dissolved in MeOH, and the resulting purple solution was put in a freezer overnight, leading to the formation of dark needle crystals, which were filtered and dried under vacuum to yield the title compound.

BW-CO-108: purple solid, yield 77%. ¹H NMR (CDCl₃) δ 8.77 (d, *J* = 7.2 Hz, 1H), 8.02 (dd, *J* = 16.2, 7.6 Hz, 2H), 7.90 (d, *J* = 8.2 Hz, 1H), 7.85 – 7.68 (m, 3H), 7.67 – 7.39 (m, 4H), 5.76 (qd, *J* = 6.7, 2.1 Hz, 1H), 2.57 (d, *J* = 2.1 Hz, 1H), 1.73 (d, *J* = 6.7 Hz, 3H). ¹³C NMR (CDCl₃) δ 196.8, 170.2, 161.2, 150.8, 145.1, 131.6, 131.1, 130.5, 130.3, 130.0, 129.6, 129.1, 129.0, 128.6, 128.6, 128.4, 127.8, 124.4, 121.3, 109.3, 82.3, 73.3, 60.3, 21.5. HRMS (ESI)⁺ calculated for C₂₆H₁₆O₃ [M+H]⁺ m/z 377.1172, found 377.1170.

BW-CO-109: purple solid, yield 70% ¹H NMR (CDCl₃) δ 8.90 (d, *J* = 7.3 Hz, 1H), 8.06 (dd, *J* = 10.3, 7.8 Hz, 2H), 7.94 (d, *J* = 8.2 Hz, 1H), 7.86 – 7.74 (m, 3H), 7.63 (t, *J* = 7.6 Hz, 1H), 7.54 (t, *J* = 7.5 Hz, 2H), 7.46 (t, *J* = 7.4 Hz, 1H), 2.67 (s, 1H), 1.93 (s, 6H). ¹³C NMR (CDCl₃) δ 196.9, 170.3, 161.1, 150.8, 145.1, 131.6, 130.9, 130.7, 130.4, 130.1, 129.6, 129.0, 128.9, 128.7, 128.6, 128.4, 127.8, 124.1, 121.3, 110.8, 85.0, 72.8, 72.5, 29.2. HRMS (ESI)⁺ calculated for C₂₇H₁₈O₃ Na [M+Na]⁺: m/z 413.1154, found 413.1146.

BW-CO-110: purple solid, yield 59%. ¹H NMR (CDCl₃) δ 9.03 (d, *J* = 7.1 Hz, 1H), 8.04 (t, *J* = 6.9 Hz, 2H), 7.94 (d, *J* = 8.1 Hz, 1H), 7.79 (dd, *J* = 14.9, 7.6 Hz, 2H), 7.59 (dt, *J* = 24.4, *J* = 7.5 Hz, 3H), 7.47 (t, *J* = 7.5 Hz, 1H), 5.18 – 4.97 (m, 1H), 2.33 (s, 1H), 1.59 (d, *J* = 7.0 Hz, 3H). ¹³C NMR (CDCl₃) δ 202.3, 160.7, 152.5, 146.1, 131.6, 130.6, 130.4, 130.3, 130.2, 129.3, 129.2, 129.1, 128.7, 128.2, 128.1, 121.3, 111.7, 84.2, 70.2, 36.3, 22.2. HRMS (ESI)⁺ calculated for C₂₆H₁₇NO₂ [M+H]⁺ 376.1332, found 376.1329

BW-CO-111: purple solid, yield 59% ^1H NMR (CDCl_3) δ 9.06 (d, $J = 6.5$ Hz, 1H), 8.08 – 7.92 (m, 3H), 7.90 (d, $J = 7.7$ Hz, 1H), 7.76 (t, $J = 9.6$ Hz, 3H), 7.62 – 7.38 (m, 4H), 2.45 (s, 1H), 1.81 (s, 6H). ^{13}C NMR (CDCl_3) δ 202.5, 168.2, 160.8, 152.7, 146.1, 131.6, 130.4, 129.6, 129.3, 129.0, 128.7, 128.1, 122.9, 121.2, 112.7, 87.2, 69.2, 46.9, 29.5. HRMS (ESI) $^+$ calculated for $\text{C}_{27}\text{H}_{19}\text{NO}_2$ $[\text{M}+\text{Na}]^+$: m/z 412.1313, found 412.1318.

BW-CO-112: dark green solid, yield, 20%. ^1H NMR (CDCl_3) δ 8.96 (d, $J = 6.8$ Hz, 1H), 7.97 (d, $J = 8.4$ Hz, 1H), 7.83 – 7.76 (m, 3H), 7.71 (q, $J = 7.2$ Hz, 1H), 7.62 (q, $J = 7.2$ Hz, 1H), 2.73 (s, 3H), 2.42 (s, 1H), 1.77 (s, 6H). ^{13}C NMR (CDCl_3) δ 199.3, 168.3, 160.3, 151.2, 145.4, 131.4, 130.6, 130.3, 130.0, 129.7, 129.1, 128.4, 126.9, 121.8, 121.4, 113.6, 87.2, 69.2, 46.9, 29.5, 14.9. HRMS (ESI) $^+$ calculated for $[\text{M}+\text{H}]^+$ 360.1053, found: 360.1050.

BW-CO-113: dark green solid, yield, 35%. ^1H NMR (CDCl_3) δ 8.65 (d, $J = 7.2$ Hz, 1H), 7.96 (d, $J = 8.1$ Hz, 1H), 7.77 (d, $J = 8.1$ Hz, 1H), 7.68 – 7.53 (m, 3H), 2.80 (s, 3H), 2.68 (s, 1H), 1.91 (s, 6H). ^{13}C NMR (CDCl_3) δ 193.56, 169.90, 160.34, 147.84, 144.19, 131.28, 131.05, 130.17, 129.85, 128.87, 128.78, 128.59, 126.43, 123.78, 121.57, 110.89, 85.05, 72.79, 72.36, 29.25, 14.36. HRMS (ESI) $^+$ calculated for $\text{C}_{22}\text{H}_{16}\text{O}_3\text{S}$ $[\text{M}+\text{Na}]^+$ 383.0718, found: 383.0728

General procedure C for the intramolecular DA reactions: A solution of compound **BW-CO-108 – 113** (0.1 mM) in DMSO/PBS (5:1, v/v, 2mL) was incubated at 37 °C for indicated time. Then the reaction mixture was diluted with water, and extracted with EtOAc (25 mL). The combined organic layer was dried over anhydrous Na_2SO_4 , concentrated under vacuum to afford the crude product, which was purified by silica gel column to afford the cyclized product **BW-CP-108 - 113**.

BW-CP-108: yellow solid, yield 90%, ^1H NMR ($\text{DMSO}-d_6$) δ 9.09 (d, $J = 7.1$ Hz, 1H), 8.14 (d, $J = 8.1$ Hz, 1H), 8.03 (d, $J = 8.1$ Hz, 1H), 7.87 (t, $J = 7.6$ Hz, 1H), 7.69 – 7.43 (m, 7H),

7.15 (d, $J = 7.1$ Hz, 1H), 5.89 (d, $J = 6.6$ Hz, 1H), 1.70 (d, $J = 6.6$ Hz, 3H). ^{13}C NMR (CDCl_3) δ 170.6, 150.6, 144.2, 140.0, 138.3, 138.0, 135.1, 133.7, 132.6, 129.6, 128.9, 128.8, 128.6, 128.6, 128.3, 127.6, 127.5, 124.0, 121.2, 120.1, 78.3, 20.9. HRMS (ESI)⁺ calculated for $\text{C}_{25}\text{H}_{16}\text{O}_2$ $[\text{M}+\text{H}]^+$ m/z 349.1223, found 349.1222.

BW-CP-109: yellow solid, yield 90%. ^1H NMR (CDCl_3) δ 9.27 (d, $J = 7.0$ Hz, 1H), 7.99 (d, $J = 8.1$ Hz, 1H), 7.88 (d, $J = 8.1$ Hz, 1H), 7.84 – 7.72 (m, 1H), 7.68 – 7.55 (m, 5H), 7.47 – 7.38 (m, 1H), 7.25 – 7.19 (m, 2H), 1.80 (s, 6H). ^{13}C NMR (CDCl_3) δ 169.9, 154.5, 144.2, 140.1, 138.4, 137.9, 135.1, 133.8, 132.6, 129.6, 128.8, 128.8, 128.6, 128.2, 127.6, 127.5, 123.9, 120.4, 119.7, 85.8, 27.8. HRMS (ESI)⁺ calculated for $\text{C}_{26}\text{H}_{18}\text{O}_2$ $[\text{M}+\text{Na}]^+$: m/z 385.1204, found 385.1213.

BW-CP-110: yellow oil, yield, 93%. ^1H NMR ($\text{DMSO}-d_6$) δ 9.29 (d, $J = 6.9$ Hz, 1H), 8.88 (s, 1H), 8.05 (d, $J = 8.2$ Hz, 1H), 7.95 (d, $J = 8.2$ Hz, 1H), 7.81 (t, $J = 7.6$ Hz, 1H), 7.62 (s, 4H), 7.52 – 7.38 (m, 2H), 7.09 (d, $J = 7.1$ Hz, 1H), 4.81 (d, $J = 6.6$ Hz, 1H), 1.49 (d, $J = 6.5$ Hz, 3H). ^{13}C NMR ($\text{DMSO}-d_6$) δ 169.9, 149.8, 141.7, 140.4, 136.3, 136.1, 135.7, 134.6, 132.1, 129.8, 129.3, 129.1, 128.9, 128.8, 128.6, 128.2, 128.1, 127.7, 127.6, 123.4, 123.3, 52.8, 21.0. HRMS (ESI)⁺ calculated for $\text{C}_{25}\text{H}_{17}\text{NO}$ $[\text{M}^+\text{H}]^+$ 348.1383, Found 348.1371.

BW-CP-111: ^1H NMR (CDCl_3) δ 9.37 (d, $J = 6.7$ Hz, 1H), 7.94 (d, $J = 8.1$ Hz, 1H), 7.84 (d, $J = 8.3$ Hz, 1H), 7.78 (d, $J = 7.0$ Hz, 1H), 7.61 (m, 5H), 7.39 (t, $J = 7.2$ Hz, 1H), 7.24 (s, 1H), 7.18 (d, $J = 6.5$ Hz, 1H), 6.22 (s, 1H), 1.68 (s, 6H). ^{13}C NMR ($\text{DMSO}-d_6$) δ 168.7, 154.0, 141.9, 140.4, 136.3, 135.7, 134.6, 132.3, 129.8, 129.3, 129.2, 128.8, 128.6, 128.1, 127.7, 126.7, 123.3, 122.3, 59.3, 28.3. HRMS (ESI)⁺ calculated for $\text{C}_{26}\text{H}_{19}\text{NO}$ $[\text{M}+\text{Na}]^+$: m/z 384.1364, found 384.1378.

BW-CP-112: yellow solid, yield, 96%. ^1H NMR (CDCl_3) δ 9.33 (d, $J = 7.0$ Hz, 1H), 8.50 (d, $J = 7.1$ Hz, 1H), 7.94 (dd, $J = 16.1, 8.1$ Hz, 2H), 7.68-7.77 (m, 2H), 7.20 (s, 1H), 6.16 (s, 1H),

2.75 (s, 3H), 1.65 (s, 6H). ^{13}C NMR (CDCl_3) δ 169.6, 153.2, 140.2, 137.4, 135.8, 134.4, 132.4, 129.4, 128.6, 128.5, 128.3, 127.6, 127.1, 125.2, 115.2, 59.1, 28.5, 15.3. HRMS (ESI)+ calculated for $\text{C}_{21}\text{H}_{17}\text{NOS}$ $[\text{M}+\text{H}]^+$ 332.1104, found: 332.1102.

BW-CP-113: yellow oil, yield, 95%. ^1H NMR (CDCl_3) δ 9.21 (d, $J = 7.0$ Hz, 1H), 8.50 (d, $J = 7.1$ Hz, 1H), 7.97 (dd, $J = 21.8, 8.1$ Hz, 2H), 7.70-7.79 (m, 2H), 7.14 (s, 1H), 2.77 (s, 3H), 1.77 (s, 6H). ^{13}C NMR (CDCl_3) δ 169.7, 154.9, 143.3, 138.0, 136.1, 135.3, 133.6, 132.2, 129.4, 129.0, 128.5, 128.5, 127.8, 127.5, 125.7, 117.2, 113.8, 85.5, 27.9, 15.0. HRMS (ESI)+ calculated for $\text{C}_{21}\text{H}_{16}\text{O}_2\text{S}$ $[\text{M}+\text{H}]^+$ 333.0944, found 333.0938.

Synthesis of compound 4: To a solution of *2,5,8,11,14,17-hexaoxonadecan-19-yl 4-methylbenzenesulfonate* (4.5 mmol) in anhydrous THF (25 mL), NaH (6.8 mmol, 1.5 equiv.) was added. The mixture was then stirred at room temperature for 1 h, followed by addition of a solution of *methyl 2-(4-hydroxyphenyl)acetate* (**3**, 5.9 mmol, 1.3 equiv) in THF (10 mL). The mixture was stirred at room temperature for another 48 h, then quenched with MeOH (10 mL) and evaporated under reduced pressure. The resulting residue was suspended in EtOAc (150 mL) and filtered. The filtrate was dried under reduced pressure and purified by silica gel column chromatography to afford the pure product as a yellow oil (55%). ^1H NMR (CDCl_3) δ 7.16 (d, $J = 8.8$ Hz, 2H), 6.85 (d, $J = 8.4$ Hz, 2H), 4.09 (t, $J = 4.8$ Hz, 2H), 3.83 – 3.51 (m, 27H), 3.36 (s, 3H). ^{13}C NMR (CDCl_3) δ 172.3, 157.9, 130.2, 126.2, 114.7, 71.9, 70.8, 70.6, 69.7, 67.5, 59.0, 52.0, 40.3. HRMS (ESI)+ calculated for $\text{C}_{22}\text{H}_{36}\text{O}_9$ $[\text{M}+\text{Na}]^+$ 467.2257, found 467.2252

Synthesis of compound 5: To a solution of compound **4** (0.86 mmol) in THF/MeOH (4:1, v/v, 5 mL), LiOH (1.2 mmol, 1.4 equiv.) was added and the mixture was stirred at room temperature for 24 h. Then the reaction mixture was quenched with aqueous HCl solution (2M, 2 mL) and directly evaporated under reduced pressure. The resulting residue was purified via silica

gel column chromatography to afford the pure product as a yellow oil (98%). ^1H NMR (MeOD) δ 7.21 (d, $J = 8.3$ Hz, 2H), 6.90 (d, $J = 8.3$ Hz, 2H), 4.18 – 4.07 (m, 2H), 3.95 – 3.83 (m, 2H), 3.77 – 3.48 (m, 22H), 3.36 (s, 3H). ^{13}C NMR (MeOD) δ 157.9, 130.0, 127.0, 114.3, 71.6, 70.4, 70.2, 70.1, 70.0, 69.5, 67.2, 57.7. HRMS (ESI) $^+$ calculated for $\text{C}_{21}\text{H}_{36}\text{O}_9$ $[\text{M}+\text{H}]^+$ 432.2348, found 432.2334

Synthesis of compound 6: To a solution of compound **5** (1.5 mmol) in anhydrous DCM (5 mL), Meldrum's acid (1.8 mmol, 1.5 equiv.) and DMAP (1.8 mmol, 1.5 equiv.) were added. The solution was cooled to 0 °C and EDC (1.8 mmol, 1.5 equiv.) was added under protection of argon. After stirred at 0 °C for 1 h, the solution was allowed to warm to room temperature and was stirred for another 6h. Then the reaction was quenched by aqueous HCl solution (1M, 10 mL) and extracted with EtOAc (3 \times 25 ml). The combined organic phase was then dried over anhydrous Na_2SO_4 , evaporated under reduced pressure. The resulting residue was purified by silica gel column chromatography to afford the pure product as a white solid (81%). ^1H NMR (MeOD) δ 7.31 (d, $J = 8.4$ Hz, 2H), 6.88 (d, $J = 8.0$ Hz, 2H), 4.35 (s, 2H), 4.11 (d, $J = 2.4$ Hz, 2H), 3.85 (s, 2H), 3.71 – 3.55 (m, 20H), 3.38 (s, 3H), 1.72 (s, 6H). ^{13}C NMR (MeOD) δ 195.0, 158.2, 130.7, 130.3, 126.2, 114.8, 114.7, 104.9, 91.2, 71.9, 70.8, 70.6, 70.5, 70.4, 69.6, 67.4, 59.0, 40.0, 26.9. HRMS (ESI) $^+$ calculated for $\text{C}_{27}\text{H}_{40}\text{O}_{12}$ $[\text{M}+\text{Na}]^+$ m/z 579.2417, found 579.2423.

Synthesis of compound 7: To a solution of compound **6** (0.43 mmol) in chlorobenzene (5 mL), *but-3-yn-2-ol* (0.85 mmol, 2 equiv.) was added. After refluxed for 45 minutes, the reaction mixture was directly evaporated under reduced pressure to afford the crude product which was further purified by silica gel column chromatography to afford the pure product as a pale yellow oil (84%). ^1H NMR (CDCl_3) δ 7.08 (d, $J = 8.4$ Hz, 2H), 6.85 (d, $J = 8.0$ Hz, 2H), 5.43 – 5.39 (m, 1H), 4.08 (t, $J = 4.8$, 2H), 3.82 – 3.33 (m, 30H), 2.49 (s, 1H), 1.22 (d, $J = 4.8$ Hz, 3H). ^{13}C NMR

(CDCl₃) δ 206.8, 157.9, 130.6, 130.4, 130.2, 126.5, 115.0, 114.9, 114.7, 71.9, 70.8, 70.6, 70.6, 70.6, 70.5, 69.7, 67.5, 59.0, 50.1, 29.1. HRMS (ESI)⁺ calculated for C₂₇H₄₀O₁₀ [M+H]⁺ m/z 526.2767, found 526.2749.

Synthesis of compound BW-CO-114: To a solution of compound **7** (0.43 mmol) in THF/MeOH (3:1, v/v, 5 mL), *acenaphthylene-1,2-dione* (1.1 mmol, 1.0 equiv.) and Et₃N (1.4 mmol, 1.5 equiv.) were added. The mixture was stirred at room temperature for 1 h, after which it was concentrated under vacuum and the resulting residue was dissolved in acetic anhydride (2 mL). The resulting solution was cooled to 0 °C and 2-5 drops of H₂SO₄ was then added. After stirring at room temperature for 1h, the solution was diluted with EtOAc (40 mL), and washed with water (20 mL) and brine (20 mL). The combined organic phase was dried over anhydrous Na₂SO₄, and evaporated under reduced pressure to afford the crude product, which was purified by silica gel column chromatography to afford the title compound. ¹H NMR (CDCl₃) δ 8.78 (d, *J* = 7.2 Hz, 1H), 8.01 (dd, *J* = 22.4, 7.7 Hz, 2H), 7.89 (s, 1H), 7.75 (dd, *J* = 18.6, 8.2 Hz, 3H), 7.59 (t, *J* = 7.7 Hz, 1H), 7.07 (t, *J* = 12.5 Hz, 2H), 5.75 (q, *J* = 6.4 Hz, 1H), 4.22 (t, *J* = 4.7 Hz, 2H), 3.91 (d, *J* = 4.7 Hz, 1H), 3.79 – 3.48 (m, 21H), 3.37 (s, 3H), 2.56 (s, 1H), 1.72 (d, *J* = 6.7 Hz, 3H). ¹³C NMR (CDCl₃) δ 197.2, 170.9, 161.3, 159.7, 148.8, 144.9, 131.6, 131.3, 131.1, 130.6, 130.2, 128.9, 128.6, 128.4, 127.4, 124.4, 123.2, 121.0, 114.9, 109.0, 82.4, 73.4, 72.0, 70.9, 70.7, 70.6, 70.6, 70.6, 70.5, 69.7, 67.6, 60.3, 59.0, 21.6. HRMS (ESI)⁺ calculated for C₃₉H₄₂O₁₀ [M+H]⁺ 671.2851, found 671.2852.

The cyclized product BW-CP-114 was obtained according to general procedure C.

BW-CP-114. yellow oil, yield, 62%. ¹H NMR (CDCl₃) δ 9.24 (d, *J* = 6.9 Hz, 1H), 8.00 (d, *J* = 8.1 Hz, 1H), 7.89 (d, *J* = 8.2 Hz, 1H), 7.80 (t, *J* = 7.7 Hz, 1H), 7.54 (d, *J* = 7.5 Hz, 2H), 7.45 (t, *J* = 7.7 Hz, 1H), 7.32 (s, 1H), 7.24 (s, 1H), 7.14 (d, *J* = 8.0 Hz, 2H), 5.75 (dd, *J* = 13.2, 6.9 Hz,

1H), 4.30 (t, $J = 4.5$ Hz, 2H), 3.98 (t, $J = 4.4$ Hz, 2H), 3.88 – 3.50 (m, 16H), 3.39 (s, 3H), 1.76 (d, $J = 6.5$ Hz, 3H). ^{13}C NMR (CDCl_3) δ 170.5, 159.1, 150.7, 143.9, 138.2, 135.3, 133.9, 132.5, 132.3, 130.2, 129.7, 128.7, 128.4, 128.0, 127.6, 127.3, 124.1, 121.5, 119.8, 115.1, 78.4, 72.1, 71.2, 70.3, 69.6, 67.4, 58.9, 20.8. HRMS (ESI)+ calculated for $\text{C}_{38}\text{H}_{42}\text{O}_9$ $[\text{M}+\text{H}]^+$ 643.2902, found 643.2910.

General procedure D to synthesis of compound 9: To a solution of *methyl 2-(2-hydroxyphenyl)acetate* (**8**, 20 mmol) in ACN (10 mL), K_2CO_3 (60 mmol, 3.0 equiv.), and *propargyl bromide* or *3-Butyn-2-yl 4-methylbenzenesulfonate* (60 mmol, 2.0 equiv.) were added. The mixture was then heated at reflux for 4 h and allowed to recover to room temperature. The reaction was then quenched with aqueous HCl solution (1M, 30 mL) and extracted with DCM (3 \times 30 mL). The combined organic phase was dried over anhydrous Na_2SO_4 , and evaporated under reduced pressure to give the crude product which was further purified by silica gel column chromatography to give the title compound.

9a: yellow oil, yield, 91%. ^1H NMR (CDCl_3) δ 7.26 (t, $J = 7.8$ Hz, 1H), 7.21 (d, $J = 7.2$ Hz, 1H), 7.03 – 6.91 (m, 2H), 4.69 (d, $J = 2.3$ Hz, 2H), 3.68 (s, 3H), 3.66 (s, 2H), 2.50 (s, 1H). ^{13}C NMR (CDCl_3) δ 172.1, 155.6, 131.1, 128.5, 123.8, 121.6, 112.2, 78.6, 75.5, 56.1, 51.9, 35.8. HRMS (ESI)+ calculated for $\text{C}_{12}\text{H}_{12}\text{O}_3$ $[\text{M}+\text{H}]^+$ 205.0859, found: 205.0858.

9b: yellow oil, yield, 87%. ^1H NMR (CDCl_3) δ 7.34 (t, $J = 7.8$ Hz, 1H), 7.28 (d, $J = 7.4$ Hz, 1H), 7.17 (d, $J = 8.2$ Hz, 1H), 7.04 (t, $J = 7.4$ Hz, 1H), 4.94 (q, $J = 6.5$ Hz, 1H), 3.64-3.90(m, 5H), 2.55 (s, 1H), 1.73 (d, $J = 6.5$ Hz, 3H). ^{13}C NMR (CDCl_3) δ 172.3, 155.5, 131.1, 128.4, 124.0, 121.4, 113.3, 83.0, 73.9, 63.9, 51.9, 36.2, 22.2. HRMS (ESI)+ calculated for $\text{C}_{13}\text{H}_{14}\text{O}_3$ $[\text{M}+\text{H}]^+$ 219.1016, found: 219.1015.

General procedure E for the synthesis of compound 10: To a solution of **9a** or **9b** (10.5 mmol) in MeOH/ H_2O (1:1, 20 mL), KOH (12 mmol, 1.14 equiv.) was added. The reaction was

stirred at room temperature for 1 h, then quenched with aqueous HCl solution (1 M, 30 mL) and extracted with DCM (2 x 100 mL). The combined organic phase was dried over anhydrous Na₂SO₄ and the solvent was removed in the vacuum to give the crude product, which was purified by silica gel column chromatography to give the title compound.

10a: white solid, yield, 65%. ¹H NMR (CDCl₃) δ 7.32 – 7.24 (m, 1H), 7.22 (d, *J* = 7.4 Hz, 1H), 6.96-7.03 (m, 2H), 4.72 (d, *J* = 2.3 Hz, 2H), 3.69 (s, 2H), 2.49 (s, 1H). ¹³C NMR (CDCl₃) δ 178.0, 155.8, 131.3, 128.9, 123.2, 121.7, 112.4, 78.6, 75.7, 56.3, 35.8. HRMS (ESI)⁺ calculated for C₁₁H₁₀O₃ [M+Na]⁺ 213.0522, found: 213.0519.

10b: white solid, 79%. ¹H NMR (CDCl₃) δ 11.66(s, 1H), 7.31 (t, *J* = 7.8 Hz, 1H), 7.24 (d, *J* = 7.4 Hz, 1H), 7.14 (d, *J* = 8.2 Hz, 1H), 7.00 (t, *J* = 7.4 Hz, 1H), 4.90 (d, *J* = 6.5 Hz, 1H), 3.60-3.84(m, 2H), 2.50 (s, 1H), 1.68 (d, *J* = 6.5 Hz, 3H). ¹³C NMR (CDCl₃) δ 178.5, 155.6, 131.2, 128.8, 123.3, 121.5, 113.3, 82.9, 74.1, 64.1, 36.1, 22.2. HRMS (ESI)⁺ calculated for C₁₂H₁₂O₃ [M+H]⁺ 227.0679, found: 227.0676.

General procedure F for the synthesis of compound 11: To a solution of **10a** or **10b** (6.3 mmol) in DCM (30 mL), DMAP (6.3 mmol, 1.0 equiv.), EDC (6.9 mmol, 1.1 equiv.) and 2,2-dimethyl-1,3-dioxane-4,6-dione (6.9 mmol, 1.1 equiv.) were added. The reaction was allowed to stir at room temperature for 12 h and then filtered. The filtrate was washed HCl aqueous solution (1 M, 10 mL) and brine (10 mL). Then the combined organic phase was dried over anhydrous Na₂SO₄ and the solvent was removed in the vacuum to give the crude product, which was purified by silica gel column chromatography to give the title compound.

11a: yellow solid, yield, 56%. The tautomers make the NMR spectrum very complicated thus only the major peaks of enol form are reported here. ¹H NMR (CDCl₃) δ 15.38 (s, 1H), 7.32 – 7.27 (m, 1H), 7.22 (d, *J* = 7.2 Hz, 1H), 6.97-7.01 (m, 2H), 4.68 (d, *J* = 2.3 Hz, 2H), 4.48 (s, 2H),

2.47 (s, 1H), 1.76 (s, 6H). ^{13}C NMR (CDCl_3) δ 195.8, 170.8, 160.6, 155.8, 131.5, 129.0, 123.5, 121.8, 112.3, 105.1, 91.7, 78.5, 75.7, 56.4, 37.1, 27.0. HRMS (ESI)⁺ calculated for $\text{C}_{17}\text{H}_{16}\text{O}_6$ $[\text{M}+\text{Na}]^+$ 339.0839, found: 339.0851.

11b: yellow solid, yield, 65%. The tautomers make the NMR spectrum very complicated thus only the major peaks of enol form are reported here. ^1H NMR (CDCl_3) δ 15.38 (s, 1H), 7.16-7.30 (m, 2H), 7.09 (d, $J = 8.2$ Hz, 1H), 6.97 (t, $J = 7.3$ Hz, 1H), 4.92 – 4.78 (m, 1H), 4.47 (d, $J = 5.1$ Hz, 2H), 2.45 (s, 1H), 1.75 (d, $J = 3.3$ Hz, 6H). ^{13}C NMR (CDCl_3) δ 196.2, 170.8, 160.5, 155.6, 131.5, 128.9, 123.6, 121.6, 113.3, 105.1, 91.6, 82.9, 74.1, 64.1, 37.2, 27.0, 22.3.

General procedure G for the synthesis of compound 12: To a solution of **11a** or **11b** (2.6 mmol) in chlorobenzene (20 ml), morpholine (5.2 mmol, 2.0 equiv.) and TMSCl (7.3 mmol, 2.8 equiv.) were added. The reaction was heated at reflux for 3 h and was allowed to warm to room temperature. After filtration, the solvent of the filtrate was removed in the vacuum to give the crude product, which was purified by silica gel column chromatography to afford the title compound.

12a: yellow solid, yield, 60%. ^1H NMR (CDCl_3) δ 7.29 – 7.19 (m, 1H), 7.15 (d, $J = 7.0$ Hz, 1H), 6.94-6.97 (m, 2H), 4.68 (t, $J = 3.7$ Hz, 2H), 3.76 (s, 2H), 3.66 – 3.56 (m, 8H), 3.31 – 3.25 (m, 2H), 2.50 (t, $J = 2.2$ Hz, 1H). ^{13}C NMR (CDCl_3) δ 202.1, 165.5, 155.3, 131.8, 128.9, 123.4, 121.9, 112.0, 78.4, 75.9, 66.7, 66.6, 56.0, 48.2, 46.8, 45.0, 42.1. HRMS (ESI)⁺ calculated for $\text{C}_{17}\text{H}_{19}\text{NO}_4$ $[\text{M}+\text{Na}]^+$ 302.1387, found: 302.1384.

12b: yellow solid, yield, 59%. ^1H NMR (CDCl_3) 7.18 (t, $J = 7.3$ Hz, 1H), 7.08 (d, $J = 8.2$ Hz, 1H), 6.98 (s, 1H), 4.87-4.91 (m, 1H), 3.76 (q, $J = 16.0$ Hz, 2H), 3.69 – 3.54 (m, 8H), 3.26-3.29 (m, 2H), 2.46 (s, 1H), 1.64 (d, $J = 6.5$ Hz, 3H). ^{13}C NMR (CDCl_3) δ 202.4, 165.6, 155.2, 131.8,

129.0, 123.6, 113.2, 82.8, 74.3, 66.9, 66.7, 63.8, 48.0, 46.9, 45.5, 42.2, 22.3. HRMS (ESI)+ calculated for $C_{18}H_{21}NO_4$ $[M+H]^+$ 316.1543, found: 316.1541.

The prodrug BW-CO-115 - 116 were obtained according to general procedure B.

BW-CO-115: purple solid, yield, 36%. 1H NMR ($CDCl_3$) δ 8.08 (d, $J = 7.1$ Hz, 1H), 7.95 (d, $J = 8.2$ Hz, 1H), 7.85 (dd, $J = 7.1, 1.7$ Hz, 1H), 7.62 – 7.70 (m, 1H), 7.56-7.61(m, 2H), 7.41-7.50 (m, 2H), 7.20 (d, $J = 8.3$ Hz, 1H), 7.14 (t, $J = 7.5$ Hz, 1H), 4.69 (d, $J = 2.3$ Hz, 2H), 3.83 (s, 4H), 3.74 (d, $J = 4.3$ Hz, 2H), 3.57 (s, 2H), 2.50 (s, 1H). ^{13}C NMR ($CDCl_3$) δ 199.0, 164.4, 163.1, 156.1, 153.7, 145.5, 131.8, 131.7, 131.4, 130.1, 129.5, 128.7, 128.7, 127.4, 125.0, 123.8, 121.6, 120.3, 118.8, 115.5, 112.8, 78.5, 76.0, 67.5, 67.0, 56.3, 48.2, 42.9. HRMS (ESI)+ calcd for $C_{29}H_{21}NO_4$ $[M+H]^+$ 448.1543, found: 448.1545.

BW-CO-116: purple solid, yield, 45%. 1H NMR ($CDCl_3$) δ 8.09 (d, $J = 7.1$ Hz, 1H), 7.95 (d, $J = 8.1$ Hz, 1H), 7.85 (d, $J = 8.7$ Hz, 1H), 7.67 (dd, $J = 8.2, 7.2$ Hz, 2H), 7.58 (t, $J = 7.6$ Hz, 1H), 7.48 (dd, $J = 7.6, 1.5$ Hz, 1H), 7.45 – 7.37 (m, 1H), 7.28 (s, 1H), 7.12 (td, $J = 7.5, 0.9$ Hz, 1H), 4.87 (s, 1H), 3.75-3.83 (m, 6H), 3.57 (s, 2H), 2.60 (s, 1H), 1.35 (d, $J = 6.5$ Hz, 3H). ^{13}C NMR ($CDCl_3$) δ 199.1, 163.1, 155.8, 153.5, 145.4, 131.8, 131.7, 131.4, 130.1, 130.0, 129.5, 128.6, 127.3, 124.9, 121.3, 115.4, 74.6, 67.5, 67.0, 64.0, 48.2, 42.8, 22.1. HRMS (ESI)+ calcd for $C_{30}H_{23}NO_4$ $[M+H]^+$ 462.1700, found: 462.1701.

The cyclized product BW-CP-115 and BW-CP-116 were obtained according to general procedure C.

BW-CP-115: yellow solid, yield, 95%. 1H NMR ($CDCl_3$) δ 8.49 (d, $J = 7.2$ Hz, 1H), 8.39 (dd, $J = 7.6, 1.5$ Hz, 1H), 7.94 – 7.78 (m, 3H), 7.64 (dd, $J = 8.2, 7.1$ Hz, 1H), 7.61 – 7.52 (m, 1H), 7.36-7.41 (m, 1H), 7.18-7.22 (m, 2H), 7.09 (s, 1H), 5.16 – 4.92 (m, 2H), 4.07 – 3.77 (m, 4H), 3.62 – 3.16 (m, 4H). ^{13}C NMR ($CDCl_3$) δ 169.1, 156.9, 136.9, 136.3, 135.7, 135.4, 134.4, 133.0, 130.4,

130.3, 129.6, 129.0, 128.1, 128.0, 127.9, 127.8, 127.7, 123.9, 123.6, 122.3, 121.8, 121.1, 69.9, 67.2, 66.9, 47.5, 42.2. HRMS (ESI)⁺ calcd for C₂₈H₂₂NO₃ [M+H]⁺ 420.1594, found: 420.1592.

BW-CP-116: yellow oil, yield, 93%. ¹H NMR (CDCl₃) δ 8.48 (d, *J* = 7.2 Hz, 1H), 8.37 (d, *J* = 7.7 Hz, 1H), 7.89 (t, *J* = 7.3 Hz, 3H), 7.64 (t, *J* = 7.6 Hz, 1H), 7.56 (t, *J* = 7.7 Hz, 1H), 7.38 (t, *J* = 7.7 Hz, 1H), 7.14-7.21 (m, 2H), 7.08 (d, *J* = 8.9 Hz, 1H), 5.20-5.25 (m, 1H), 5.06-5.13 (m, 0.5H), 3.89-4.04 (m, 4H), 3.60 – 3.28 (m, 4H), 1.73 (d, *J* = 6.5 Hz, 1.32H), 1.62 (d, *J* = 6.5 Hz, 1.62H). ¹³C NMR (CDCl₃) δ 169.3, 155.9, 155.2, 140.4, 136.5, 135.9, 135.3, 134.3, 134.3, 133.1, 133.0, 130.4, 130.3, 129.6, 128.1, 127.9, 127.8, 127.7, 123.9, 123.8, 123.3, 123.2, 122.2, 122.1, 121.5, 120.6, 120.4, 118.8, 118.4, 77.5, 77.2, 76.8, 75.1, 74.8, 67.2, 66.9, 47.5, 42.2, 19.6, 19.4, 14.3. HRMS (ESI)⁺ calcd for C₂₉H₂₃NO₃ [M+H]⁺ 434.1751, found: 434.1751.

Synthesis of compound 14: To a solution of 2-(2-((*tert*-Butyldimethylsilyl)oxy)ethyl)aniline (**13**, 8.4 mmol) and pyridine (13 mmol, 1.5 equiv.) in anhydrous DCM (25 mL), MsCl (13 mmol, 1.5 equiv.) was added dropwisely at 0 °C under the protection of argon. The reaction mixture was stirred at room temperature for 12 h, after which it was quenched with aqueous HCl solution (1 M, 10 mL) and extracted with EtOAc (3 × 50 ml). The combined organic phase was washed with brine (10 mL), dried over anhydrous Na₂SO₄ and evaporated under reduced pressure. The resulting crude product was purified by silica gel column chromatography to afford the final product as pale yellow solid (yield: 88%). ¹H NMR (CDCl₃) δ 8.50 (s, 1H), 7.52 (d, *J* = 8.0 Hz, 1H), 7.29 – 7.21 (m, 1H), 7.18 – 7.10 (m, 2H), 4.01 – 3.83 (m, 2H), 2.96 (s, 3H), 2.93 – 2.80 (m, 2H), 0.86 (s, 9H), 0.01 (s, 6H). ¹³C NMR (CDCl₃) δ 133.4, 130.9, 128.0, 126.0, 123.7, 66.2, 40.4, 35.9, 26.1, 18.6, 5.5. HRMS (ESI)⁺ calcd for C₁₅H₂₇NO₃SSi [M+H]⁺ 330.1554, found: 330.1552.

General procedure H for the synthesis of compound 15: To a solution of **14** (15 mmol) in ACN (30 mL), K₂CO₃ (23 mmol, 1.5 equiv.) and *propargyl bromide* or *3-butyn-2-yl 4-methylbenzenesulfonate* (30 mmol, 2.0 equiv.) were added. The mixture was then heated at reflux for 4 h and recovered to room temperature. The reaction mixture then was quenched with aqueous solution (1 M, 30mL) and extracted with DCM (3 x 100 mL). The combined organic phase was dried over anhydrous Na₂SO₄, and evaporated under reduced pressure. The resulting residue was purified by silica gel column chromatography to afford the title compound.

15a: colorless oil, yield, 78%. ¹H NMR (CDCl₃) δ 7.52 (d, *J* = 7.8 Hz, 1H), 7.44 – 7.39 (m, 1H), 7.38 – 7.31 (m, 1H), 7.29 – 7.22 (m, 1H), 4.73 (d, *J* = 17.6 Hz, 1H), 4.07 (d, *J* = 17.8 Hz, 1H), 3.96 – 3.75 (m, 2H), 3.13 (d, *J* = 5.6 Hz, 3H), 3.13 – 3.00 (m, 1H), 2.86 (s, 1H), 2.43 (s, 1H), 0.84 (s, 9H), -0.01 (s, 6H). ¹³C NMR (CDCl₃) δ 140.6, 138.5, 131.4, 129.2, 128.6, 127.2, 78.9, 74.3, 63.7, 41.5, 39.8, 34.3, 26.0, 18.5, -5.3. HRMS (ESI)+ calcd for C₁₈H₂₉NO₃SSi [M+H]⁺ 368.1710, found: 368.1708.

15b: colorless oil, yield, 85%. ¹H NMR (CDCl₃) δ 7.72 (dd, *J* = 7.9, 1.2 Hz, 1H), 7.50 (dd, *J* = 7.8, 1.4 Hz, 1H), 7.33-7.36 (m, 1H), 7.25-7.27 (m, 1H), 5.15-5.17 (m, 1H), 4.01 – 3.78 (m, 2H), 3.11 (s, 3H), 3.11 – 2.88 (m, 3H), 2.55 (d, *J* = 2.3 Hz, 1H), 1.22 (d, *J* = 7.2 Hz, 3H), 0.88 (s, 9H), 0.04 (d, *J* = 3.6 Hz, 6H). ¹³C NMR (CDCl₃) δ 142.4, 134.9, 130.9, 129.1, 128.8, 126.9, 83.7, 74.1, 63.2, 46.7, 38.2, 33.9, 26.1, 20.1, 18.4, -5.2, -5.3. HRMS (ESI)+ calcd for C₁₉H₃₁NO₃SSi [M+H]⁺ 382.1867, found: 382.1848.

General procedure I for the synthesis of compound 16: To a solution of **15a** or **15b** (4.5 mmol) in acetone (20 mL), KF (9 mmol, 2.0 equiv.) and Jones reagent (9 mmol, 2.0 equiv.) were added and the reaction was stirred at room temperature for 20 h. The reaction mixture was then quenched with water (20 mL) and extracted with DCM (3 × 50 ml). The combined organic phase

was dried over anhydrous Na₂SO₄, and evaporated under reduced pressure. The resulting residue was purified by silica gel column chromatography to afford the title compound.

16a: white solid, yield, 75%. ¹H NMR (CDCl₃) δ 7.74 – 7.66 (m, 1H), 7.48 – 7.33 (m, 3H), 4.69 (d, *J* = 18.0 Hz, 1H), 4.11-4.21 (m, 2H), 3.65 (d, *J* = 16.5 Hz, 1H), 3.15 (s, 3H), 2.48 (s, 1H). ¹³C NMR (CDCl₃) δ 176.2, 139.0, 135.3, 132.2, 129.8, 128.9, 128.5, 78.9, 74.7, 41.4, 39.2, 37.3. HRMS (ESI)+ calcd for C₁₂H₁₃NO₄S [M+H]⁺ 268.0638, found: 368.0637.

16b: white solid, yield, 65%. The rotamers make the NMR spectrum very complicated thus only the major peaks are reported here. white solid. ¹H NMR (CDCl₃) δ 7.82 (dd, *J* = 7.9, 1.3 Hz, 1H), 7.54 (dd, *J* = 7.7, 1.6 Hz, 1H), 7.33-7.45 (m, 2H), 5.14-5.21 (m, 1H), 3.87 (s, 2H), 3.12 (s, 3H), 2.60 (d, *J* = 2.4 Hz, 1H), 1.20 (d, *J* = 7.2 Hz, 3H). ¹³C NMR (MeOD) δ 174.9, 139.0, 136.4, 133.0, 130.2, 130.1, 128.8, 84.3, 76.1, 54.8, 47.9, 38.4, 37.4, 20.6. HRMS calcd for C₁₃H₁₅NO₄S [M+H]⁺ 304.0614, found: 304.0600.

General procedure J for the synthesis of compounds 17: To a solution of **16a** or **16b** (3.2 mmol) in DCM (10 mL), DMAP (3.5 mmol, 1.1 equiv.), EDC (3.5 mmol, 1.1 equiv.) and 2,2-dimethyl-1,3-dioxane-4,6-dione (3.5 mmol 1.1 equiv.) were added. The reaction was stirred at room temperature for 12 h and then filtered. The filtrate was further diluted with DCM (30 mL), washed with aqueous HCl solution (1 M, 15 mL) and brine (10 mL). The combined organic phase was dried over anhydrous Na₂SO₄ and the solvent was removed in the vacuum to give the crude product, which was purified by silica gel column chromatography to give the title compound.

17a: white solid, yield, 78%. The tautomers made the NMR spectrum very complicated. Thus only the major peaks of the enol form are reported here. ¹H NMR (CDCl₃) δ 15.43 (s, 1H), 7.60-7.70 (m, 1H), 7.38-7.35 (m, 3H), 4.49-4.88(m, 2H), 3.41 (s, 2H), 3.08 (s, 3H), 2.50 (s, 1H), 1.70 (s, 6H). ¹³C NMR (CDCl₃) δ 194.5, 170.7, 160.2, 139.1, 135.9, 131.2, 129.5, 128.6, 128.3,

105.3, 92.0, 78.9, 74.7, 41.2, 39.0, 37.8, 26.8. HRMS (ESI)⁺ calcd for C₁₈H₁₉NO₇S [M+H]⁺ 394.0955, found: 394.0970.

17b: white solid, yield, 53%. The tautomers made the NMR spectrum very complicated. Thus only the major peaks of the enol form are reported here. ¹H NMR (CDCl₃) δ 15.46 (s, 1H), 7.87 (d, *J* = 7.6 Hz, 1H), 7.49 – 7.36 (m, 3H), 5.16-5.22 (m, 1H), 5.10 (d, *J* = 17.2 Hz, 1H), 4.18 (d, *J* = 17.2 Hz, 1H), 3.11 (s, 3H), 2.61 (d, *J* = 2.4 Hz, 1H), 1.77 (s, 6H), 1.31 (d, *J* = 7.2 Hz, 3H). ¹³C NMR (CDCl₃) δ 194.5, 136.9, 135.4, 132.4, 129.3, 128.7, 128.3, 105.3, 92.3, 83.5, 74.3, 46.7, 37.8, 37.3, 19.9.

General procedure K for the synthesis of compounds 18: To a solution of **17a** or **17b** (1.6 mmol) in chlorobenzene (20 mL), morpholine (3.2 mmol, 2.0 equiv.) and TMSCl (4.8 mmol, 3.0 equiv.) were added and the reaction was heated at reflux for 3 h. The mixture temperature was then brought to room temperature before filtration. The solvent of filtrate was concentrated in vacuum to give the crude product, which was purified by silica gel column chromatography to give the title compound.

18a: yellow solid, yield, 62%. The tautomers made the NMR spectrum very complicated. Thus only the major peaks of the enol form are reported here. ¹H NMR (CDCl₃) δ 7.65 (d, *J* = 7.4 Hz, 1H), 7.32-7.38 (m, 3H), 4.57 (d, *J* = 18.3 Hz, 1H), 4.11 (d, *J* = 17.4 Hz, 1H), 3.97-4.33 (m, 2H), 3.62-3.65 (m, 6H), 3.36-3.40 (m, 2H), 3.09 (s, 3H), 2.48 (s, 1H). ¹³C NMR (CDCl₃) δ 201.3, 165.3, 138.7, 135.4, 132.7, 129.4, 128.5, 127.9, 78.7, 74.7, 66.6, 48.5, 46.7, 45.8, 42.1, 41.3, 38.8. HRMS (ESI)⁺ calcd for C₁₈H₂₂N₂O₅S [M+H]⁺ 379.1322, found: 379.1317.

18b: yellow solid, yield, 65%. ¹H NMR (CDCl₃) δ 7.76 (t, *J* = 9.5 Hz, 1H), 7.44 – 7.28 (m, 3H), 5.09-5.13 (m, 1H), 4.22 (d, *J* = 17.1 Hz, 1H), 3.69 – 3.43 (m, 8H), 3.34 (d, *J* = 4.3 Hz, 2H), 3.04 (d, *J* = 8.0 Hz, 3H), 2.59 (d, *J* = 2.3 Hz, 1H), 1.13 (d, *J* = 7.2 Hz, 3H). ¹³C NMR (CDCl₃) δ

200.5, 165.6, 136.5, 134.6, 132.8, 129.2, 128.4, 128.1, 83.3, 74.4, 66.8, 66.7, 48.7, 46.7, 46.6, 44.6, 42.1, 37.9, 19.9. HRMS (ESI)⁺ calcd for C₁₉H₂₄N₂O₅S [M+H]⁺ 415.1298, found: 415.1323.

The prodrug BW-CO-117 - 118 were obtained according to general procedure B.

BW-CO-117: purple solid, yield, 54%. ¹H NMR (CDCl₃) δ 8.05 (d, *J* = 7.1 Hz, 1H), 7.99 – 7.90 (m, 2H), 7.84 (d, *J* = 8.2 Hz, 1H), 7.74 – 7.60 (m, 3H), 7.52 (7.49-7.54, m, 3H), 4.48 (s, 2H), 3.82 (s, 4H), 3.73 (s, 2H), 3.58 (s, 2H), 3.07 (s, 3H), 2.56 (s, 1H). ¹³C NMR (CDCl₃) δ 199.0, 162.8, 162.5, 145.6, 139.5, 132.0, 131.4, 130.7, 130.2, 130.1, 129.5, 129.4, 128.9, 128.7, 128.5, 128.0, 124.8, 121.4, 116.2, 78.0, 74.7, 67.4, 66.9, 48.3, 42.7, 41.6, 39.1. HRMS (ESI)⁺ calcd for C₃₀H₂₄N₂O₅S [M+H]⁺ 525.1479, found: 525.1483.

BW-CP-118: yellow solid, yield, 35%. ¹H NMR (CDCl₃) δ 8.58 – 8.40 (m, 2H), 7.96 (dd, *J* = 10.7, 5.7 Hz, 3H), 7.88 – 7.44 (m, 5H), 7.19 (d, *J* = 34.5 Hz, 1H), 5.43 (q, *J* = 6.9 Hz, 1H), 4.29 – 3.87 (m, 4H), 3.62 – 3.23 (m, 4H), 2.42 (d, *J* = 19.3 Hz, 3H), 1.29-1.34 (m, 3H). ¹³C NMR (CDCl₃) δ 168.8, 168.7, 141.12, 141.0, 137.0, 136.6, 136.6, 135.9, 135.5, 135.4, 134.8, 134.5, 134.0, 134.0, 132.9, 130.6, 130.4, 130.4, 130.3, 130.2, 130.0, 128.8, 128.7, 128.6, 128.5, 128.4, 128.3, 128.2, 128.1, 127.8, 126.9, 126.7, 123.9, 122.8, 122.5, 122.5, 121.7, 67.2, 67.0, 66.9, 55.8, 55.5, 47.6, 47.5, 42.3, 38.0, 37.8, 21.6, 21.1. HRMS (ESI)⁺ calcd for C₃₀H₂₆N₂O₄S [M+H]⁺ 511.1686, found: 511.1711.

The cyclized product BW-CP-117 was obtained according to general procedure C.

BW-CP-117: yellow oil, yield, 93%. ¹H NMR (CDCl₃) δ 8.47 (dd, *J* = 7.6, 1.5 Hz, 1H), 8.42 (d, *J* = 7.2 Hz, 1H), 7.93 (d, *J* = 7.3 Hz, 3H), 7.81 (dd, *J* = 7.9, 1.2 Hz, 1H), 7.72 – 7.64 (m, 1H), 7.62 – 7.44 (m, 3H), 7.23 (s, 1H), 5.05 – 4.66 (m, 2H), 4.04 (t, *J* = 4.7 Hz, 2H), 3.96 – 3.82 (m, 2H), 3.37-3.58 (m, 4H), 2.42 (s, 3H). ¹³C NMR (CDCl₃) δ 168.7, 137.7, 137.1, 136.2, 136.1, 135.3, 134.0, 132.9, 130.4, 130.4, 130.2, 129.9, 129.5, 128.6, 128.5, 128.4, 128.4, 128.3, 127.8,

126.8, 123.9, 122.8, 122.4, 67.1, 66.9, 50.4, 47.5, 42.3, 38.6. HRMS (ESI)⁺ calcd for C₂₉H₂₄N₂O₄S [M+H]⁺ 497.1530, found: 497.1531.

General procedure L for the synthesis of BW-CO-108 – 113: To a solution of compound **2** (0.5 mmol) in N-Methyl-2-Pyrrolidone (5 mL), benzil (0.5 mmol, 1 equiv.), and KOH (0.15 mmol, 0.3 equiv.) was stirred at room temperature for 16 h. The mixture was stirred at room temperature for 16 h, after which it was diluted with H₂O (15 mL) and extracted with EtOAc (2 x 30 mL). The combined organic phase was dried over anhydrous Na₂SO₄ and concentrated under vacuum. The resulting residue was dissolved in acetic anhydride (5 mL). The resulting solution was cooled to 0 °C and 2-5 drops of H₂SO₄ was then added. After stirring at room temperature for 15 min, the solution was diluted with EtOAc (40 mL), and washed with water (20 mL) and brine (20 mL). The combined organic phase was dried over anhydrous Na₂SO₄, and evaporated under reduced pressure. The resulting crude product was purified by silica gel column chromatography. The obtained crude product was dissolved in MeOH, and the resulting purple solution was put in a freezer overnight, leading to the formation of dark needle crystals, which were filtered and dried under vacuum to yield the title compound.

BW-CO-119: red solid, yield, 40%. ¹H NMR (CDCl₃): 7.40-7.38 (m, 1H), 7.30-7.25 (m, 4H), 7.20-7.17 (m, 4H), 7.16 (m, 2H), 7.12(d, *J* = 7.6 Hz, 2H), 6.88 (d, *J* = 8.0 Hz, 2H), 4.76 (s, 2H), 2.45 (s, 1H). ¹³C NMR (CDCl₃) δ 195.2, 168.1, 161.6, 152.0, 132.2, 131.6, 130.3, 130.0, 129.4, 128.9, 128.9, 128.3, 128.2, 128.2, 127.6, 116.3, 75.0, 52.1. HRMS (ESI)⁺ calculated for C₂₈H₂₀O₃ [M+Na]⁺: m/z 427.1310, found 427.1315.

BW-CO-120: red solid, yield, 42%. ¹H NMR (CDCl₃): 7.35-7.37 (m, 1H), 7.35-7.30 (m, 4H), 7.26-7.20 (m, 4H), 7.20-7.18 (m, 2H), 7.12 (m, 2H), 6.89 (d, *J* = 8.0 Hz, 2H), 5.49-5.54 (m, 1H), 2.42 (s, 1H), 1.41 (d, *J* = 6.4 Hz, 3H). ¹³C NMR (CDCl₃) δ 195.2, 167.2, 161.3, 152.0, 132.2,

131.7, 130.3, 129.9, 129.9, 129.4, 128.9, 128.8, 128.3, 128.2, 128.2, 127.9, 127.6, 116.8, 81.8, 73.1, 60.4, 21.0. HRMS (ESI)⁺ calculated for C₂₇H₁₈O₃ [M+H]⁺: m/z 391.1329, found 391.1328.

BW-CO-121: red solid, yield, 35%. ¹H NMR (CDCl₃): 7.35-7.21 (m, 11H), 7.04 (d, *J* = 7.2 Hz, 2H), 6.93 (d, *J* = 7.6 Hz, 2H), 3.92-3.95 (m, 1H), 3.00-3.60 (m, 2H), 2.30-2.60 (m, 2H), 1.79 (s, 3H), 1.29-0.86 (m, 6H). ¹³C NMR (CDCl₃) δ 196.9, 164.4, 155.8, 152.6, 132.5, 131.9, 130.3, 130.0, 129.7, 129.4, 128.9, 128.8, 128.6, 128.1, 128.0, 127.8, 126.6, 124.1, 76.6, 50.4, 40.4, 21.1, 20.2, 18.4, 3.5. HRMS (ESI)⁺ calculated for C₃₂H₂₉NO₂ [M+H]⁺: m/z 460.2271, found 460.2270.

The cyclized products BW-CP-119 - 121 were obtained according to general procedure C.

BW-CP-119: yellow solid, yield, 85%. ¹H NMR (CDCl₃): 7.56 (s, 1H), 7.20-7.22 (m, 6H), 7.10 – 7.13 (m, 4H), 6.97-6.99 (m, 3H), 6.79-6.81 (m, 2H), 5.39 (s, 2H). ¹³C NMR (Acetone-d₆) δ 168.8, 147.6, 147.1, 141.4, 141.4, 141.2, 138.4, 136.0, 131.5, 130.3, 129.6, 127.7, 127.0, 127.0, 126.9, 126.7, 126.1, 123.3, 122.0, 67.9. HRMS (ESI)⁺ calculated for C₂₆H₁₈O₂ [M+H]⁺: m/z 363.1380, found 363.1376

BW-CP-120: white solid, yield, 95%. ¹H NMR (CDCl₃): 7.49 (s, 1H), 7.20 (br s, 6H), 7.12-7.11 (m, 4H), 7.07-7.12 (m, 3H), 6.81-6.77 (m, 2H), 5.59-5.64 (m, 1H), 1.76 (d, *J* = 6.4 Hz, 1H). ¹³C NMR (CDCl₃) δ 169.0, 150.9, 147.9, 141.9, 141.7, 140.9, 137.9, 135.4, 131.5, 130.2, 129.6, 127.9, 127.3, 127.2, 126.3, 122.3, 122.1, 75.8, 20.7. HRMS (ESI)⁺ calculated for C₂₇H₂₀O₂ [M+Na]⁺: m/z 399.1361, found 399.1374.

BW-CP-121: yellow solid, yield, 95%. ¹H NMR (CDCl₃) δ 7.21 – 6.89 (m, 10H), 6.81 (dd, *J* = 7.2, 4.5 Hz, 3H), 6.70 – 6.60 (m, 2H), 4.90 (dt, *J* = 13.6, 6.8 Hz, 1H), 3.61 – 3.47 (m, 2H), 3.07 – 2.89 (m, 2H), 2.10 (s, 3H), 1.16 (d, *J* = 6.8 Hz, 6H). ¹³C NMR (CDCl₃): 163.4, 144.2, 141.7,

141.0, 140.7, 140.3, 139.8, 137.5, 131.7, 131.1, 129.9, 129.6, 129.0, 127.5, 126.6, 126.4, 126.2, 125.5, 125.1, 43.3, 38.3, 27.6, 19.9, 17.3. HRMS (ESI)⁺ calculated for C₃₁H₂₉NO [M+H]⁺: m/z 432.2322, found 432.2319.

1.3.3 Experimental procedure for the CO detecting using a house-hold CO detector

BW-CO-113, 117 or **121** (~10 mg) were prepared in a solution of DMSO/PBS (4:1, 10 mL) and the solution was kept in a sealed 250 mL desiccator together with the CO detector (Drager Pac 7000). After 30 minutes, the detector began to beep because of CO levels exceeding the alarm threshold (35 ppm).

1.3.4 Experimental procedure for Myoglobin-CO assay

CO release from compounds **BW-CO-113, BW-CO-117** and **BW-CO-121** was confirmed by the myoglobin-CO assay. The reported “Two compartment” myoglobin-CO assay system was employed here.⁵¹ A myoglobin solution in PBS (0.01 M, pH = 7.4) (1.7 mg/mL, 2.9 mL) was degassed by bubbling with nitrogen for at least 20 min and a freshly prepared solution of sodium dithionite (17mg/mL, 300 μL) was added to the myoglobin solution. Then the CO prodrug (1 mM) was added to the inner vial. After incubation for 1 h (**BW-CO-113**), 2 h (**BW-CO-117**) and 30 min (**BW-CO-119**) at 37 °C, respectively, the solution was cooled in an ice bath for 10 min to increase the solubility of CO in water and the UV absorption spectra was recorded (Figure 1.10-1.12).

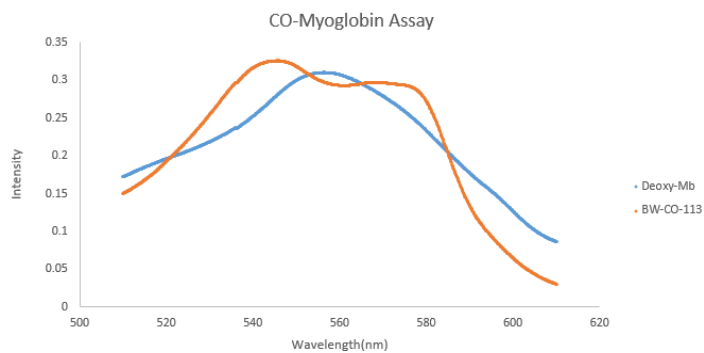


Figure 1.9 UV-Vis spectra demonstrating the conversion of deoxy-Mb to carbon monoxide myoglobin (MbCO) (BW-CO-113).

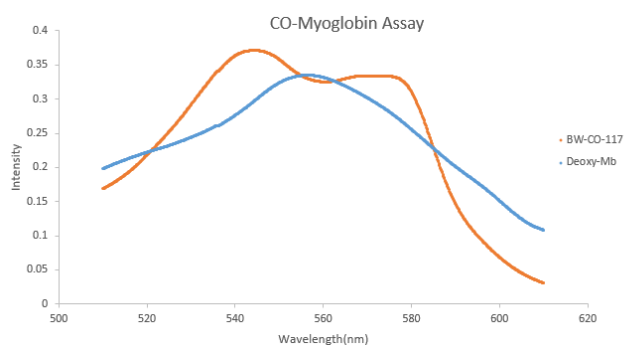


Figure 1.10 UV-Vis spectra demonstrating the conversion of deoxy-Mb to carbon monoxide myoglobin (MbCO) (BW-CO-117).

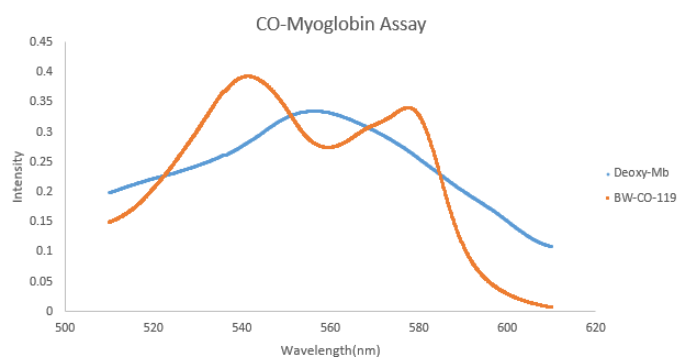


Figure 1.11 UV-Vis spectra demonstrating the conversion of deoxy-Mb to carbon monoxide myoglobin (MbCO) (BW-CO-119).

1.3.5 Experimental procedure for the CO release rate study of BW-CO-108-121

All the CO prodrugs were dissolved in in DMSO/PBS (pH 7.4, 4:1) to a final concentration of 100 μM . The CO release was monitored by fluorescent intensity at 450 nm for **BW-CO-108-117**. For CO prodrugs with scaffold **III**, the CO release was determined by the decrease of UV absorbance at 360 nm. Each experiment was repeated three times independently.

1.3.6 Experimental procedure for cytotoxicity study of CO prodrugs and corresponding products

Raw 264.7 cells were seeded in 96-well plates and cultured in Dulbecco's modified Eagle's medium (DMEM) supplemented with 10% fetal bovine serum (FBS) and 1% penicillin/streptomycin at 37 °C under 5% CO₂ for 24 h. Then RAW 264.7 cells were incubated in DMEM containing vehicle (1% DMSO) and compounds (0 – 100 μM) for 24 hours. After removal of the median, 150 μL of DMEM containing 10 μL CCK-8 was added to each well and then the cells were incubated for another three hours at 37 °C. The absorbance at 450 nm was then measured by using a Perkin Elmer 1420 multi-label counter. The cell viability was measured, and the results were normalized to the vehicle group. The experiment was triplicated, and the results are expressed as mean \pm SEM (n = 3).

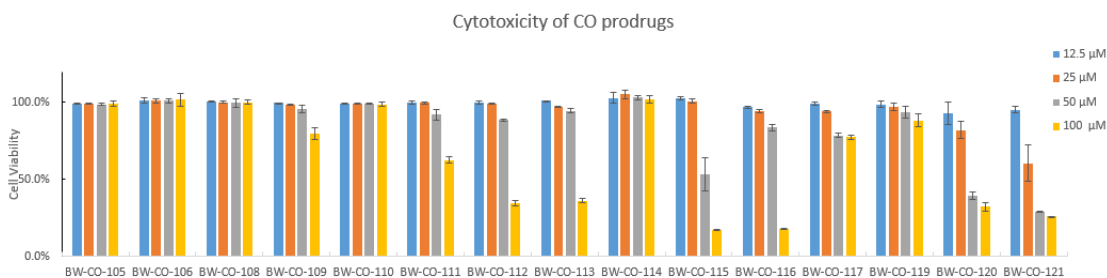


Figure 1.12 The cytotoxicity of CO prodrugs to RAW264.7 after 24h incubation.

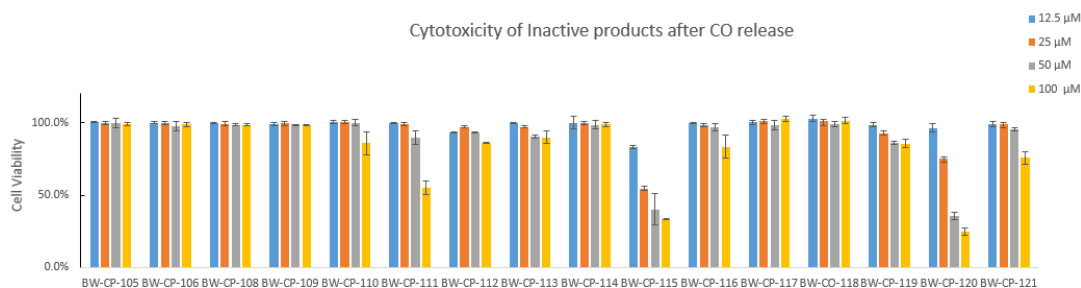


Figure 1.13 The cytotoxicity of inactive products of CO prodrugs to RAW264.7 after 24h incubation.

1.3.7 Experimental procedure for intracellular CO release study of BW-CO-109, 117 and 119

All the experiments were duplicated to confirm the CO release in the cell environment. Raw 264.7 cells were seeded on coverslips in 6-well plates one day before the experiment. CO prodrug was dissolved in DMSO and added into the cell culture media to give different final concentrations (25, 50 μM) with 1% DMSO. For **BW-CO-119**, the cells were co-treated with **BW-CO-119** and COP-1 (CO fluorescent probe). The cells were incubated with the compound for 4 h at 37 °C. After that, the cells were washed with PBS twice and fixed with 4% paraformaldehyde for 30 minutes at room temperature. The cells were then washed with PBS again twice and the coverslips with cells were immersed in DI water. The coverslips were mounted onto glass slides using the mounting media without DAPI (ProLong® Live Antifade Reagent; P36974). The fluorescent imaging was performed on a Zeiss fluorescent microscope, using DAPI (**BW-CO-109/117**)/FITC (**BW-CO-119**) imaging channel. The concentration-dependent images were taken using the oil objective.

1.3.8 Experimental procedure for computation of electron density distributions

All calculations were performed using the Gaussian 09 program.^{52, 53} Initial geometry optimizations were carried out by DFT calculations with the use of B3LYP⁵⁴ and the standard 6-31G* basis set. HF/6-31G* calculation was used to generate the electrostatic potential. Partial charges were produced fitting to the electrostatic potential at points selected according to the Merz-Singh-Kollman scheme.^{55, 56} All calculations were conducted on Georgia State University cluster Orion with 4 CPU cores.⁵⁷

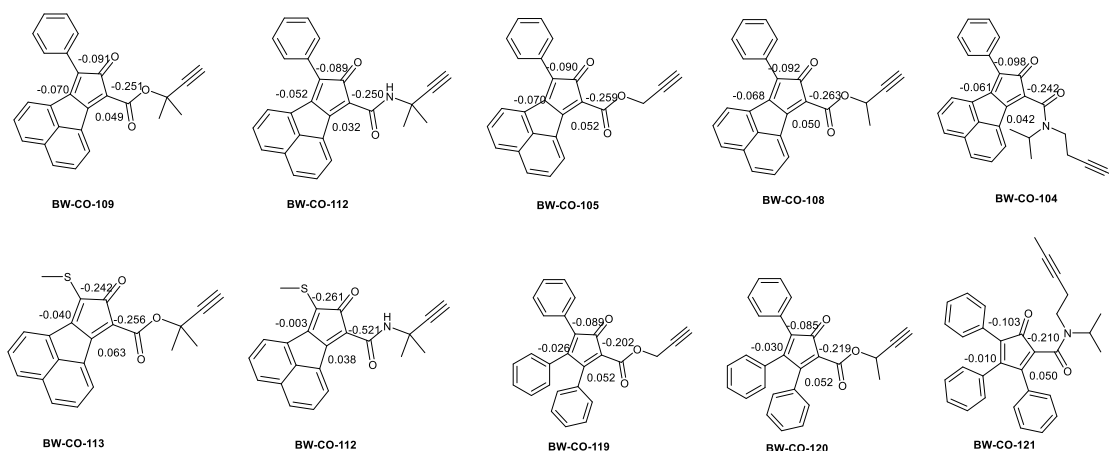


Figure 1.14 Computational studies of charge distributions.

1.4 Conclusion

In conclusion, CO prodrugs of different structural scaffolds were designed and synthesized, and their CO release rates were also determined. The CO release rate of these prodrugs is readily tunable with half-lives ranging from minutes to hours and even days. The structure-CO release rate relationships are summarized in Figure 1.10. Generally, entropic factors that each tethering linker imposes on the system seem to play very critical roles in determining the CO release rate. The more rigid tethering linkers, gem-dimethyl group and 5-membered ring formation favor the cycloaddition reaction, and hence increase CO release rate. Apart from entropic factors, other

factors could also be used to tune the CO release rate. For example, the presence of two phenyl rings at R₂ positions also substantially increased CO release rate. The understanding of the structure-CO release rate relationships achieved should allow us to further tune CO release rate and optimize our CO prodrugs. This study also provides a diverse group of CO-prodrugs for biology studies to examine the relationship among release rates, CO concentration, and efficacy and biological responses.

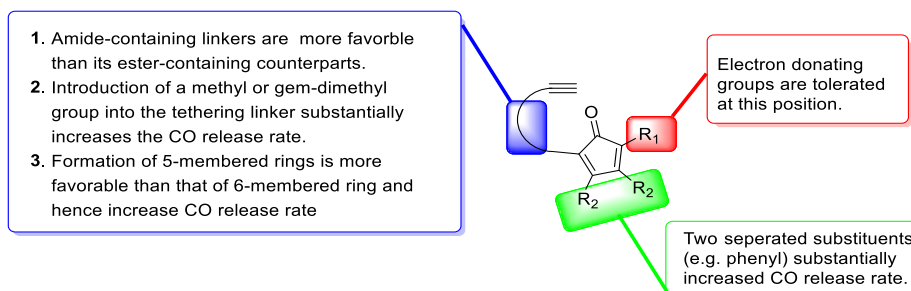


Figure 1.15 A summary of the relationship between structure and CO release rate.

1.5 Statements

The much of the results in this chapter has been published in *Chem. Eur. J.* (Pan, Z.; Chittavong, V.; Li, W.; Zhang, J.; Ji, K.; Zhu, M.; Ji, X.; Wang, B. Organic CO Prodrugs: Structure-CO-Release Rate Relationship Studies. *Chem. Eur. J.* 2017, 23, 9838-9845.). In this chapter, Wang, B conceived the initial idea, and supervised the study. I and Ji, X co-designed the CO prodrug and perform the study. Chittavong, V and Li, W conducted studies of the reaction kinetics and some of the synthesis. Zhuang, J and Ji, K conducted the in vitro biology studies. Zhu, M carried out the computational work.

2 ORGANIC CO PRODRUGS ACTIVATED BY ENDOGENOUS ROS

2.1 Introduction

Reactive oxygen species (ROS) are normal byproducts of aerobic metabolism in the process of mitochondrial oxidative phosphorylation. ROS includes free radicals such as superoxide anion (O_2^-), hydroxyl radical ($\bullet OH$), and nonradical molecules like hydrogen peroxide (H_2O_2), singlet oxygen (1O_2), and so forth.⁵⁸ When the intracellular level of ROS is higher than the level of antioxidant species, oxidative stress occurs. Oxidative stress has been reported to directly or indirectly damage nucleic acids, proteins and lipids in the progress of many diseases including carcinogenesis, neurodegeneration atherosclerosis and diabetes.⁵⁹⁻⁶¹

In the CO delivery field, there is a strong interest in controlled release, and possibly targeting.⁶²⁻⁶⁴ For example, a few triggered release mechanisms (e.g. photo,^{34, 65-70} oxidation-⁷⁰ and enzyme-triggered release,²⁸ among others) have been reported. Among CO's therapeutic indications, cancer, bacterial infection and inflammation are the most widely investigated, and CO has been firmly established as a promising therapeutic agent against these diseases. Notably, these diseases are all associated with elevated levels of ROS.^{59, 71} Therefore, it is highly desirable to devise CO prodrugs with a ROS-sensitive trigger for targeted delivery to these disease sites. However, ROS-sensitive CO delivery is a severely under-explored area, especially in ROS-triggered metal-free CO release. In this contribution, we describe a new strategy for metal-free CO prodrugs with a ROS-sensitive trigger, which release CO in response to elevated intracellular ROS levels, sensitize cancer cells to Dox treatment, and are amenable to structural modification to serve different purposes (e.g. targeting).

Previously, we have successfully developed a series of metal-free CO prodrugs using inter- and intra-molecular Diels-Alder cycloaddition to trigger CO release.^{41, 72} It was found that the

initial cycloaddition intermediate **I** (Figure 2.1) is extremely unstable, and would undergo cheletropic/retro-DA reaction to release CO spontaneously under very mild conditions. Interestingly, its structural analogue **III** with a single bond between C5 and C6 (Figure 2.1) is quite thermally stable and can be isolated without the extrusion of CO.⁷³ Therefore, we reasoned that compounds with scaffold **III** are potential CO prodrugs, provided that a double bond between C5 and C6 can be easily formed under physiological conditions. In doing so, an additional R7 group (Compound **IV**, Figure 1) has to be appended at either the C5 or C6 position for the intended elimination reaction to form compound **I** for CO release. In order to achieve selective CO release in response to an endogenous stimulus, R7 group must meet several prerequisites. First, it has to be chosen from poor leaving groups to render compound **IV** inactive for CO release, and thereby allows for the preparation and storage of such CO prodrugs without stability issues. Second, R7 has to be easily transformed into a good leaving group (LG) in the presence of an endogenous stimulus (e.g. elevated ROS) to yield compound **V**, which would elicit an elimination reaction to afford the unstable intermediate **I** for CO release.

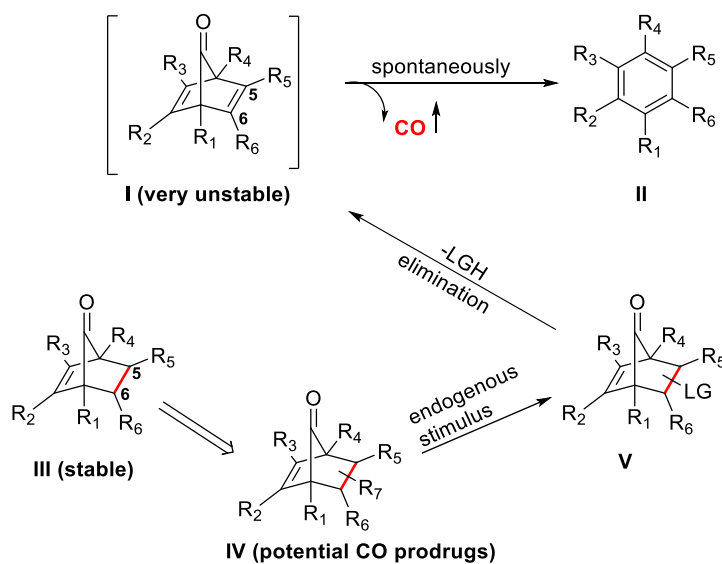
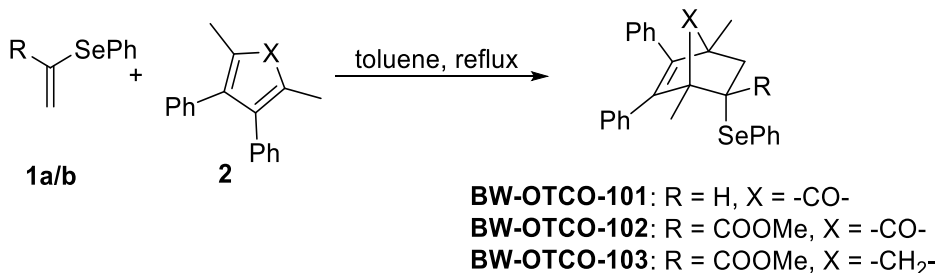


Figure 2.1 A schematic illustration of the general strategy for stimulus-triggered CO prodrugs.

2.2 Results and discussion

2.2.1 Design of reactive oxygen species (ROS) sensitive CO prodrugs

To establish the proof-of-concept, we designed and synthesized two potential CO prodrugs **BW-OTCO-101-102** with R₇ being a phenylselenenyl group for selective CO release in response to ROS (Scheme 2.1). The rationale underlying the choice of a phenylselenenyl group is three-fold. First, phenylselenenyl group is not a good leaving group, and hence **BW-OTCO-101-102** can be sufficiently stable for synthesis, purification and storage. Second, it is well-established that phenylselenenyl group is very prone to ROS oxidation⁷⁴, and the formed selenoxide analogue readily undergoes syn-elimination (selenoxide elimination)⁷⁵, leading to double bond formation between the C5 and C6 positions for the subsequent cheletropic reaction to release CO under very mild conditions. Therefore, the ligation of a phenylselenenyl group would allow for CO release to disease site with an elevated ROS level. Last, selenium is an essential trace element in mammalian system with a concentration of around 1 μM in serum of healthy adults⁷⁶. In addition, selenium containing compounds have been demonstrated to be sufficiently safe for drug development, and some have entered clinical trials.⁷⁷ In our case, the selenium containing by-product after CO release is phenylselenenic acid (Figure 2.2), which has been demonstrated to be relatively safe with a LD50 value of 1200 μmol/kg in mice.^{78, 79} Therefore, the introduction of a phenylselenenyl group would not raise additional cytotoxicity concerns. Consequently, phenylselenenyl group was chosen to achieve a balance between stability and triggered CO release.



Scheme 2.1 The synthesis of ROS sensitive CO prodrugs.

2.2.2 Synthesis of ROS sensitive CO prodrugs

As shown in Scheme 2.1, the synthesis of **BW-OTCO-101-102** was readily achieved using a one-step DA reaction between compound **1a/b** and **2**. Meanwhile, a control compound **BW-OTCO-103** (X = CH₂), which would undergo selenoxide elimination without CO release, was also prepared.

2.2.3 Kinetics study of ROS sensitive CO prodrugs

With these compounds in hand, we set out to study their CO release profiles in the absence/presence of ROS using HPLC to monitor the consumption of **BW-OTCO-101/102** and the formation of **BW-OTCP-101/102**. Initially, **BW-OTCO-102** was employed to screen its sensitivity towards various ROS. **BW-OTCO-102** is relatively more reactive toward hypochlorite (ClO⁻), singlet oxygen (¹O₂) and O₂⁻, with hypochlorite being the most reactive trigger. For example, the transformation from **BW-OTCO-102** (20 μM) to **BW-OTCP-102** completed in 30 min in the presence of hypochlorite (40 μM) at 37 °C, and no formation of **BW-OTCP-102** was observed in the absence of hypochlorite even after 48 h of incubation. Other ROS, such as hydrogen peroxide (H₂O₂, 1 mM), hydroxyl radical (HO·, 500 μM), tert-butyl hydroperoxide (TBHP, 500 μM) and tert-butoxy radical (tBuO·, 500 μM) only yield less than 5% transformation

within 30 min. CO release in the presence of hypo-chlorite was further confirmed by a widely-accepted CO-myoglobin assay.

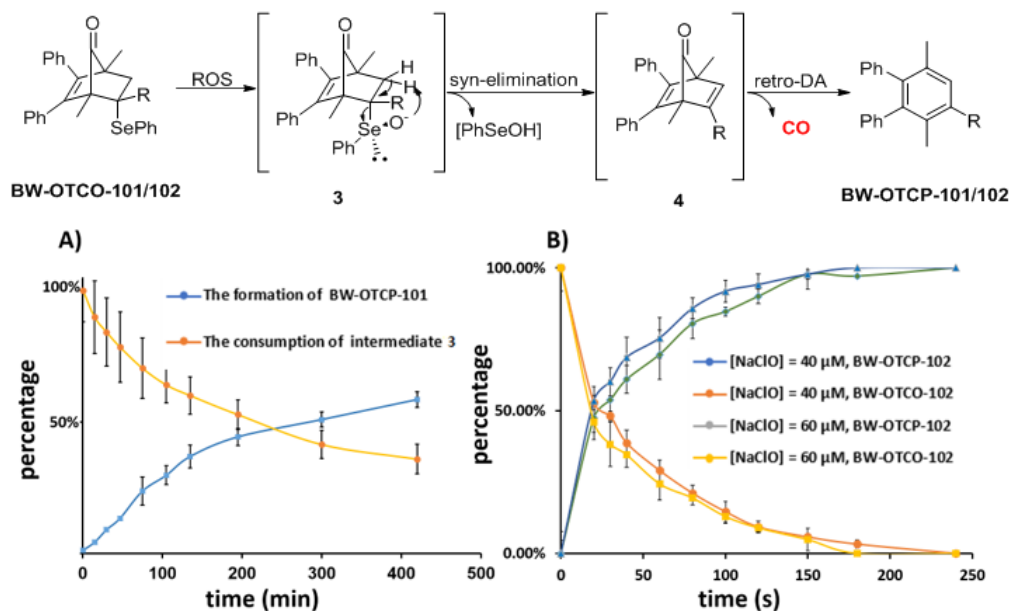


Figure 2.2 The CO release kinetics of **BW-OTCO-101** (A) and **102** (B) in response to ClO^- at 37 °C.

Hypochlorite is a major ROS species generated by immune cells in response to bacterial infection or other forms of inflammation⁸⁰, and it has also been employed as a stimulus to trigger the release of the payload from a drug delivery system.⁸¹ In our experiments, it was also the most effective in triggering CO release. Therefore, we employed hypochlorite to study the CO release kinetics of **BW-OTCO-101/102** (Figure 2.2). As shown in Figure 2.2, both **BW-OTCO-101** and **102** could undergo selenoxide elimination to form **BW-OTCP-101/102** (20 μM) for CO release in the presence of hypochlorite (40 and 60 μM) at 37 °C. In the case of **BW-OTCO-101** (Figure 2.2A), the oxidation step is quite fast (e.g. finished in 30 seconds with an initial hypochlorite concentration of 40 μM), and the accumulation of intermediate **3** (a mixture of diastereomer) was observed. However, the selenoxide elimination is quite sluggish with a half-life of around 4 h. In

contrast, the oxidation step is the rate limitation step for **BW-OTCO-102**, and intermediate **3** was not observed under the HPLC conditions used, indicating a spontaneous selenoxide elimination step. Nevertheless, **BW-OTCO-102** presented much faster CO release kinetics with a half-life of only around 30 seconds in the presence of 40 μ M hypochlorite, as compared to 4 h for **BW-OTCO-101** under the same conditions.

2.2.4 *Detection of intracellular CO release*

Having confirmed that **BW-OTCO-101/102** could specifically release CO in response to ROS in vitro, we next probed if such CO prodrugs could release CO in response to elevated intracellular ROS levels. Towards this end, **BW-OTCO-102** was tested for its intracellular CO release under various cellular conditions. Therefore, we conducted two types of comparative studies. First, it is commonly believed that cancer cells have elevated levels of ROS because of its rapid metabolism. Thus, we compared CO release in Hela (cancerous cells) and H9C2 cells (normal cells). Second, inflammatory responses are known to be associated with elevated levels of ROS. Therefore, a macrophage cell line (Raw264.7) was used with or without LPS stimulation, which is known to trigger inflammatory responses. CO production was monitored by a known fluorescent probe COP-1. As expected, Raw 264.7 cells co-treated with **BW-OTCO-102**, **COP-1** and LPS (1 μ g/mL) showed significantly enhanced green fluorescence (Figure 2.3g) compared to the control cells treated with **COP-1** and **BW-OTCO-102** without the stimulation of LPS (Figure 2.3e). Similarly, Hela cells co-treated with **BW-OTCO-102** and **COP-1** also showed much enhanced green fluorescence (Figure 2.3o) compared with H9C2 cells under the same conditions (Figure 3k). To firmly establish the connection between CO release and elevated levels of ROS, we determined the relative ROS levels in these cell lines using a widely employed ROS probe.⁸² LPS challenged Raw264.7 or Hela cells indeed possessed much higher ROS levels as compared

to Raw264.7 cells without LPS or H9C2 cells, respectively. Altogether, these results firmly established the capacity of **BW-OTCO-102** in selective delivery of CO to disease sites with elevated ROS levels.

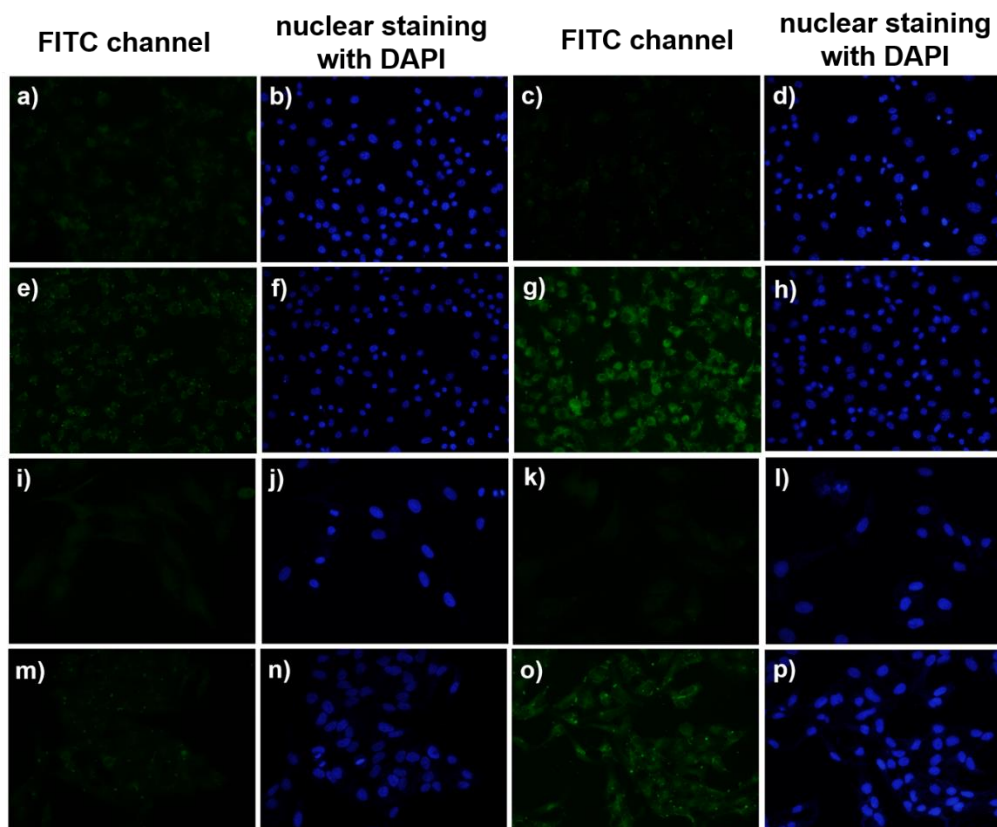


Figure 2.3 Fluorescent imaging of CO release of BW-OTCO-102 in different type of cells.

(a-h: Raw264.7 cells; i-l: H9C2 cells; m-p: HeLa cells): a) COP-1 only (1 μ M); c) LPS (1 μ g/mL) + COP-1 (1 μ M); e) BW-OTCO-102 (50 μ M) + COP-1 (1 μ M); g) BW-OTCO-102 (50 μ M) + COP-1 (1 μ M) + LPS (1 μ g/mL); i) COP-1 only (1 μ M); k) COP-1 (1 μ M) + BW-OTCO-102 (50 μ M); m) COP-1 only (1 μ M); o) COP-1 (1 μ M) + BW-OTCO-102 (50 μ M).

2.2.5 Synergistic effects of CO and doxorubicin (Dox)

Having confirmed that BW-OTCO-102 could selectively deliver CO in response to elevated intracellular ROS levels, we next set out to probe whether such CO prodrugs could recapitulate CO's synergistic effects with Dox in killing cancer cells. Towards this end, HeLa cells

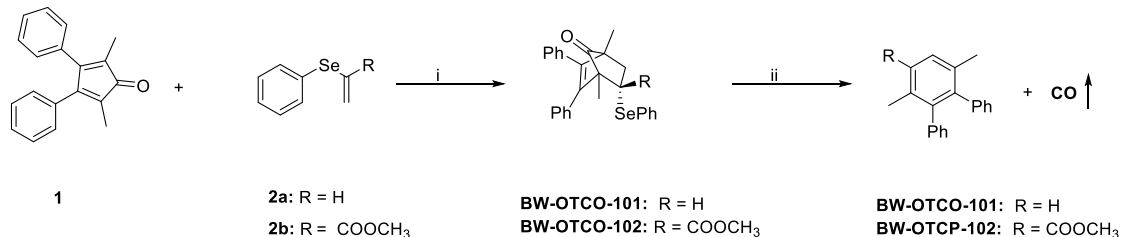
and H9C2 cells were co-treated with **BW-OTCO-102** and **Dox** for 24 h. Then the cells were subjected to the crystal violet assay for cytotoxicity evaluation. The cells treated with **BW-OTCO-102** or **Dox** only were used as controls. Additionally, the cells co-treated with Dox and compound **BW-OTCO-103/BW-OTCP-102** were employed as additional controls as well. The results are summarized in Figure 2.4. **BW-OTCO-102** inhibited the proliferation of Hela cells synergistically with Dox. For example, after 24 h of exposure with 2 μM of Dox, the cell viability only decreased to around 80%, and yet this number went down to around 20% when Dox was used in combination with **BW-OTCO-102** (12.5 μM). As controls, no decrease in cell viability was observed with the treatment of **BW-OTCO-102** only (Figure 2.4, the red and green columns in the 0- μM group). In addition, no synergistic effects were observed between Dox and the control compound **BW-OTCO-103** or the inactive compound **BW-OTCP-102** after CO release. Taken together, it can be confirmed that the observed synergistic effects were indeed attributed to the CO release from BW-OTCO-102.

2.3 Experimental Section

2.3.1 General information

All reagents and solvents were of reagent grade and were purchased from Aldrich. ^1H -NMR (400 MHz) and ^{13}C -NMR (100 MHz) spectra were recorded on a Bruker Avance 400 MHz NMR spectrometer. Mass spectral analyses were performed on an ABI API 3200 (ESI-Triple Quadruple). Compounds **2a** and **2b** were synthesized according to literature methods.^{83, 84}

2.3.2 Experimental procedure for the synthesis of ROS-activated CO prodrugs



Scheme 2.2 Synthesis of BW-OTCO-101/102 and their products

Reagents and conditions: (i) toluene, reflux, 12 h; (ii) NaClO (100 mM) in DMSO/PBS(1:5), 37 °C;

General procedure A for the synthesis of BW-OTCO-101 and 102

A solution of 2, 5-dimethyl-3, 4-diphenylcyclopenta-2, 4-dien-1-one (**1**, 1.0 mmol) and compound **2a/b** (1.0 mmol) in toluene (10 mL) was heated under reflux for 12 h. Then the reaction mixture was concentrated under vacuum, and the residue was directly purified on a silica gel column to afford the desired product.

1,4-Dimethyl-2,3-diphenyl-5-(phenylselanyl)bicyclo[2.2.1]hept-2-en-7-one (BW-OTCO-101): The title compound was synthesized according to general procedure A with compound **1** (260 mg, 2.0 mmol) and *phenyl(vinyl)selane* (**2a**, 183 mg, 1.0 mmol) in toluene (10 mL) at 110 °C for 12h. Then the reaction mixture was concentrated under vacuum, and the residue was directly purified on a silica gel column (hexane: EtOAc = 15:1) to afford the desired product **BW-OTCO-101** as yellow oil in 53% yield (235 mg). ¹H NMR (CDCl₃): δ 7.59 – 7.48 (m, 2H), 7.31 – 7.21 (m, 10H), 7.14 – 6.97 (m, 3H), 3.78 (dd, *J* = 9.3, 5.3 Hz, 1H), 2.59 (dd, *J* = 13.0, 9.3 Hz, 1H), 2.08 (dd, *J* = 13.0, 5.3 Hz, 1H), 1.32 (s, 3H), 1.28(s, 3H). ¹³C NMR (CDCl₃): δ 204.2, 144.8, 142.1, 134.6, 134.5, 134.0, 133.8, 130.6, 130.1, 129.3, 129.2, 129.1, 129.0, 128.1, 127.8, 127.5, 127.4, 127.1, 58.4, 53.2, 46.4, 41.8, 12.0, 11.8. HRMS (ESI)⁺ calcd for C₂₇H₂₄NaOSe [M+Na]⁺ 467.0885, found: 467.0899.

Methyl-1,4-dimethyl-7-oxo-5,6-diphenyl-2-(phenylselanyl)bicyclo[2.2.1]hept-5-ene-2-carboxylate (BW-OTCO-102): The title compound was synthesized according to general procedure A with compound **1** (520 mg, 2.0 mmol) and *methyl 2-(phenylselanyl)acrylate (2b*, 480 mg, 2.0 mmol) in toluene (15 mL) at 110 °C for 12h. Then the reaction mixture was concentrated under vacuum, and the residue was directly purified on a silica gel column (hexane:EtOAc = 10:1) to afford the desired product **BW-OTCO-102** as white solid in 67% yield (671 mg). ¹H NMR (CDCl₃): δ 7.58 – 7.52 (m, 2H), 7.44 – 7.37 (m, 1H), 7.34 (t, *J* = 7.3 Hz, 2H), 7.22 – 7.10 (m, 6H), 6.88-6.95 (m, 4H), 3.34 (s, 3H), 3.00 (d, *J* = 13.6 Hz, 1H), 2.11 (d, *J* = 13.6 Hz, 1H), 1.74 (s, 3H), 1.20 (s, 3H). ¹³C NMR (CDCl₃): δ 203.4, 172.7, 147.4, 139.8, 137.2, 134.2, 133.7, 129.6, 129.3, 129.2, 128.8, 128.0, 127.8, 127.5, 127.2, 60.1, 55.0, 52.2, 51.8, 43.9, 11.6, 11.3. HRMS (ESI)⁺ calcd for C₂₉H₂₆NaO₃Se [M+Na]⁺ 525.0939, found: 525.0941.

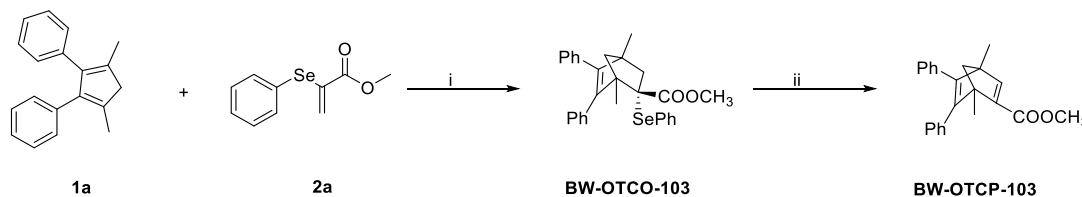
General procedure B for the synthesis of BW-OTCP-101-102

To a solution of compound **BW-OTCO-101/102** (1.0 mmol) in DMSO/PBS (10/1, 3 mL) was added an aqueous solution of NaClO (1M, 0.3 mL). The resulting solution was stirred at 37 °C until the complete consumption of the starting material as indicated by TLC. The reaction mixture was then quenched with water (20 mL) and extracted with CH₂Cl₂ (3 × 50 ml). The combined organic phase was dried over anhydrous Na₂SO₄, and concentrated under reduced pressure. The resulting residue was purified on a silica gel column to afford the title compound.

Methyl 3',6'-dimethyl-[1,1':2',1''-terphenyl]-4'-carboxylate (BW-OTCP-101): The title compound was synthesized according to general procedure B with **BW-OTCO-101** (443 mg, 1.0 mmol) and an aqueous NaClO solution (**1M**, 0.3 mL) in a solution of DMSO/PBS (10/1, 3 mL) at 37 °C for 1h. The reaction mixture was then quenched with water (20 mL) and extracted with

CH₂Cl₂ (3 × 50 ml). The combined organic phase was dried over anhydrous Na₂SO₄ and concentrated under reduced pressure. The resulting residue was purified on a silica gel column (hexane:EtOAc = 20:1) to afford the desired product **BW-OTCP-101** as white solid in 97% yield (250 mg). ¹H NMR (CDCl₃): δ 7.76 (s, 1H), 7.20 – 7.02 (m, 6H), 6.93 (t, *J* = 7.4 Hz, 4H), 3.96 (s, 3H), 2.27 (s, 3H), 2.11 (s, 3H). ¹³C NMR (CDCl₃): δ 169.0, 145.0, 143.1, 140.4, 140.2, 134.6, 133.5, 130.3, 130.1, 129.9, 129.5, 127.5, 126.2, 126.2, 52.0, 20.7, 18.7. HRMS calcd for C₂₂H₂₀O₂ [M+H]⁺ 317.1536; found 317.1541.

3',6'-Dimethyl-1,1':2',1''-terphenyl (**BW-OTCP-102**): The title compound was synthesized according to general procedure B with **BW-OTCO-102** (500 mg, 1.0 mmol) and an aqueous NaClO solution (**1M**, 0.3 mL) in a solution of DMSO/PBS (10/1, 3 mL) at 37 °C for 24 h. The reaction mixture was then quenched with water (20 mL) and extracted with CH₂Cl₂ (3 × 50 ml). The combined organic phase was dried over anhydrous Na₂SO₄ and concentrated under reduced pressure. The resulting residue was purified on a silica gel column (Hexane: EtOAc = 20:1) to afford the desired product **BW-OTCP-102** as white solid in 91% yield (288 mg). ¹H NMR (CDCl₃): δ 7.26 (s, 2H), 7.21 – 7.15 (m, 4H), 7.10-7.14 (m, 2H), 7.00-7.03 (m, 4H), 2.15 (s, 6H). ¹³C NMR (CDCl₃): δ 141.4, 140.8, 133.5, 130.0, 128.8, 127.4, 125.9, 20.9. HRMS calcd for C₂₀H₁₉ [M+H]⁺ 259.1481; found 259.1477.



*Scheme 2.3 Synthesis of **BW-OTCO-103** and **BW-OTCP-103***

Reagents and conditions: i) toluene, reflux, 12 h; ii) NaClO, DMSO/PBS, 37 °C.

Synthesis of *methyl 1,4-dimethyl-5,6-diphenyl-2-(phenylselanyl)bicyclo[2.2.1]hept-5-ene-2-carboxylate* (**BW-OTCO-103**): To a solution of *(3,5-dimethylcyclopenta-2,5-diene-1,2-diyl)dibenzene* (**1a**, 1.0 mmol, 245 mg) in toluene (10 mL), was added compound **2a** (1.0 mmol, 242 mg). The mixture was heated under reflux for 12 h, after which the reaction mixture was concentrated under vacuum, and the residue was directly purified on a silica gel column to afford the desired product as colorless oil (235 mg, yield: 48%). ¹H NMR (CDCl₃): δ 7.57 – 7.61 (m, 2H), 7.29 – 7.38 (m, 3H), 7.17 – 7.05 (m, 6H), 6.86 – 6.94 (m, 4H), 3.03 (s, 3H), 2.97 – 2.91 (m, 1H), 2.35 (d, *J* = 8.6 Hz, 1H), 2.22 (d, *J* = 13.1 Hz, 1H), 1.85 (dd, *J* = 8.6, 3.1 Hz, 1H), 1.78 (s, 3H), 1.18 (s, 3H). ¹³C NMR (CDCl₃): δ 173.6, 151.0, 142.1, 136.8, 136.3, 135.6, 130.1, 129.2, 128.9, 128.7, 128.1, 127.7, 127.4, 126.4, 62.5, 61.5, 60.1, 51.0, 50.8, 48.9, 18.2, 17.7. HRMS calcd for C₂₉H₂₉O₂Se [M+H]⁺ 489.1327; found 489.1364.

Methyl 1, 4-dimethyl-5,6-diphenylbicyclo[2.2.1]hepta-2,5-diene-2-carboxylate (**BW-OTCP-103**): The title compound was synthesized according to general procedure B with **BW-OTCO-103** (480 mg, 1.0 mmol) and an aqueous NaClO solution (**1M**, 0.2 mL) in a solution of DMSO/PBS (10/1, 2 mL) at 37 °C for 3 h. The reaction mixture was then quenched with water (20 mL) and extracted with CH₂Cl₂ (3 × 50 mL). The combined organic phase was dried over anhydrous Na₂SO₄ and concentrated under reduced pressure. The resulting residue was purified on a silica gel column (hexane:EtOAc = 20:1) to afford the desired product **BW-OTCP-103** as colorless in 93% yield (307 mg). ¹H NMR (CDCl₃): δ 7.63 (s, 1H), 7.10 – 7.25 (m, 7H), 6.96 – 6.90 (m, 2H), 3.81 (s, 3H), 2.38 (d, *J* = 6.5 Hz, 1H), 2.29 (d, *J* = 6.5 Hz, 1H), 1.60 (s, 3H), 1.41 (s, 3H). ¹³C NMR (CDCl₃): δ 165.6, 161.2, 155.1, 152.2, 150.2, 136.6, 135.8, 128.3, 128.3, 127.9,

127.8, 126.6, 126.4, 80.6, 60.5, 59.4, 51.3, 16.6, 16.2. HRMS calcd for $C_{23}H_{22}NaO_2 [M+Na]^+$ 353.1512; found 353.1522.

2.3.3 Experimental procedure for Myoglobin-CO assay

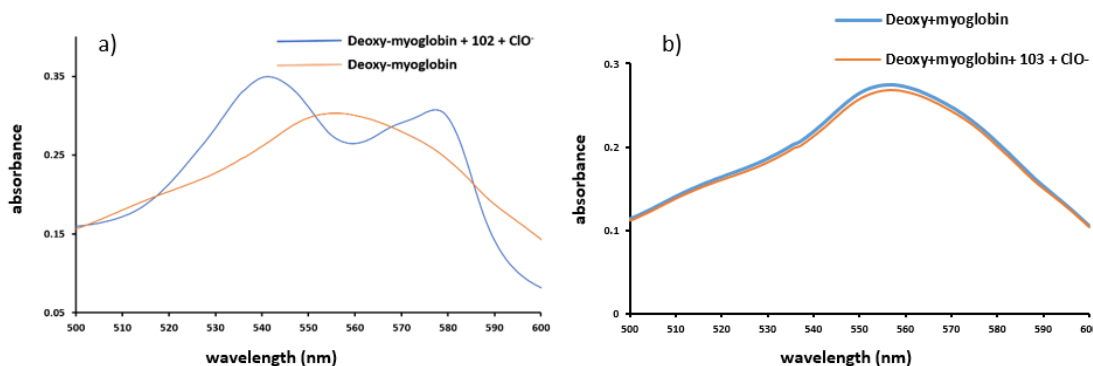


Figure 2.4 CO myoglobin assay.

Orange curve: absorbance for deoxy-Mb. Blue curve: deoxy-Mb co-treated with **BW-OTCO-102/103** and NaClO.

Our previously reported myoglobin-CO assay (two-compartment assay) was employed to confirm CO release from **BW-OTCO-102/103**.⁴¹ Specifically, a myoglobin solution in PBS (0.01 M, pH = 7.4) (1.7 mg/mL, 2.9 mL) was degassed by bubbling with nitrogen for at least 20 min and a freshly prepared solution of sodium dithionite (17 mg/mL, 300 μ L) was added to the myoglobin solution. Then the CO prodrug (3 mL, 1 mM) and NaClO (3 mL, 1 mM) were added to the inner vial. After incubation for 2 h at 37 $^{\circ}$ C, the solution was cooled in an ice bath for 10 min to increase the solubility of CO in water. Then the UV-vis absorption spectra was recorded. The maximal absorption peak of deoxy-Mb at 560 nm is converted to two maximal absorption peaks of Mb-CO at 540 and 578 nm, indicating the formation of CO bounded myoglobin when it is treated with **BW-OTCO-102** (Figure 2.4a) while there is no change of the deoxy-Mb curve after adding **BW-OTCO-103** (Figure 2.4b).

2.3.4 Experimental procedure for the study of sensitivity of BW-OTCO-102 to various ROS

Various ROS solutions were prepared according to literature procedures.⁸⁵ A solution of **BW-OTCO-102** (400 μ L, 1 mM in acetonitrile (ACN)) was added to 20 mL of PBS (pH 7.4, 10 mM). After stirring at room temperature for 5 min, the freshly prepared ROS stock solution was

added to make a final concentration of 500 μM (1 mM for H_2O_2 , 60 μM for NaClO). Additional ACN was added to maintain its final solution of 10%. The resulting mixture was incubated at 37 $^\circ\text{C}$ for 30 min. CO release was monitored by the formation of **BW-OTCP-102** using HPLC. The experiments were triplicated, and the results are reported as mean \pm SD ($n = 3$).

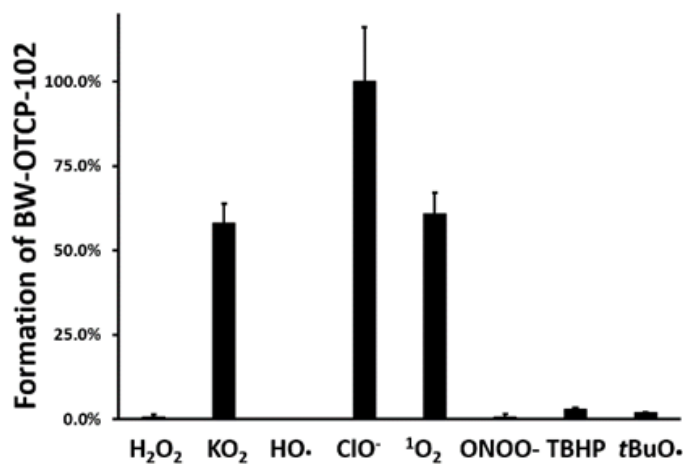


Figure 2.5 The sensitivity of **BW-OTCO-102** to various ROS at 37 $^\circ\text{C}$

2.3.5 Experimental procedure for study of stability of **BW-OTCO-101/102** in the absence of ROS

A solution of **BW-OTCO-101/102** (800 μL , 500 μM in ACN) was added to 20 mL of PBS (pH 7.4, 10 mM) in a vial. Additional ACN was added to maintain its final solution of 10%. The resulting solution was incubated at 37 $^\circ\text{C}$ for 48 h. The solution was then analyzed using HPLC. All the experiments were triplicated, and the results are reported as mean \pm SD ($n = 3$). As shown in Figure 2.6, both **BW-OTCO-101** and **BW-OTCO-102** are very stable even after 48 h's incubation in the absence of ROS.

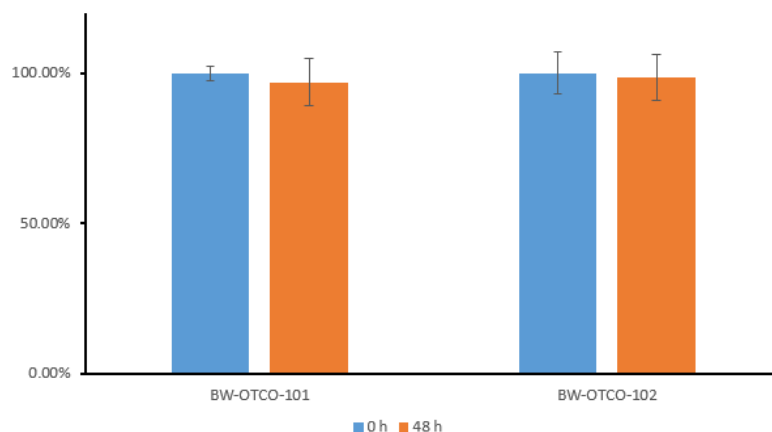


Figure 2.6 The stability of BW-OTCO-101 and BW-OTCO-102 in the absence of ROS.

2.3.6 Experimental procedure for CO release kinetics of BW-OTCO-101/102 in response to hypochlorite

A solution of **BW-OTCO-101/102** (20 μM) and NaClO (40 or 60 μM) or KO_2 (500 μM) or $^1\text{O}_2$ (500 μM) in 10% of ACN in PBS (pH = 7.4) was sealed and incubated at 37 $^\circ\text{C}$. At each defined time point, 500 μL of the reaction mixture was taken out and added into a vial containing Na_2SO_3 (100 μL , 250 mM) to quench the reaction. The resulting solution was then analyzed by HPLC (column: Waters C18 3.5 μM , 4.6 \times 100 mm, injection loop volume: 20 μL). CO release was determined by monitoring the formation of the product and the consumption of the reaction intermediate as in the case of **BW-OTCO-101** or prodrug (**BW-OTCO-102**). The mobile phase was acetonitrile ACN/ H_2O (containing 0.05% trifluoroacetic acid). Detailed conditions are summarized in Table 2.1.

Table 2.1 The HPLC condition used for analysis

	BW-OTCO-101	BW-OTCO-102
	0~5 min, 60%~80% ACN; 5~10	
Eluent	min, 80%~95% ACN; 10-13 min, 95%~	0~8 min, 30%~80%
conditions	60% ACN.	ACN; 8~15 min, 80%~95%

	ACN; 15-18 min, 95%~ 30%
	ACN.

	Prodrug: 10.9 ± 0.2 ;	
t_R	Intermediate: 4.2 ± 0.1 ; 4.9 ± 0.1 ;	Prodrug: 13.8 ± 0.1 ;
(min)	Product: 10.5 ± 0.1	Product: 13.0 ± 0.1

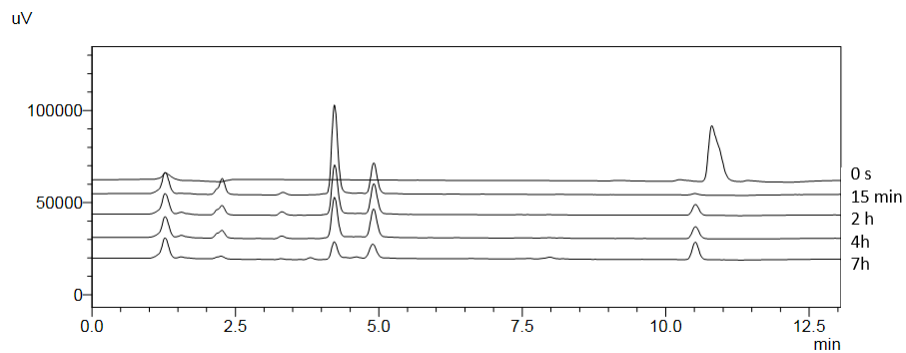


Figure 2.7 HPLC chromatogram of BW-OTCO-101 in the presence of $40 \mu\text{M ClO}^-$

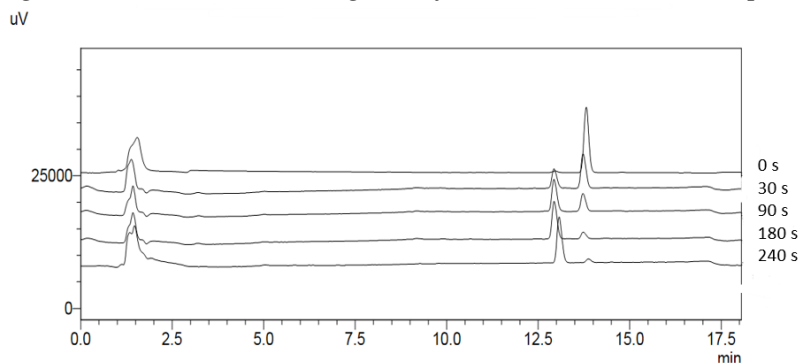


Figure 2.8 HPLC chromatogram of BW-OTCO-102 in the presence of $40 \mu\text{M ClO}^-$

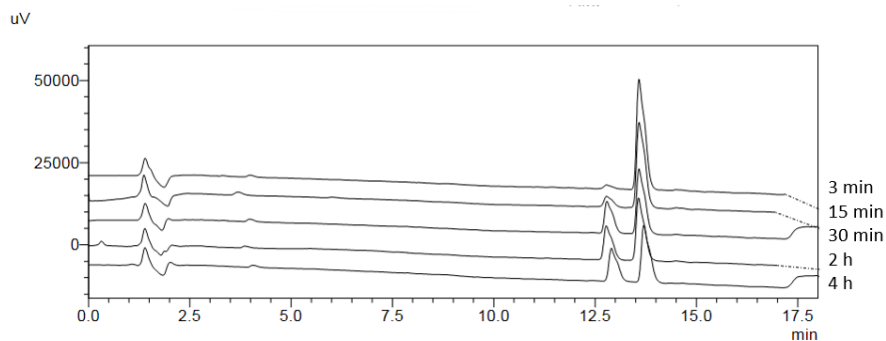


Figure 2.9 HPLC chromatogram of **BW-OTCO-102** in the presence of 500 μM O₂⁻

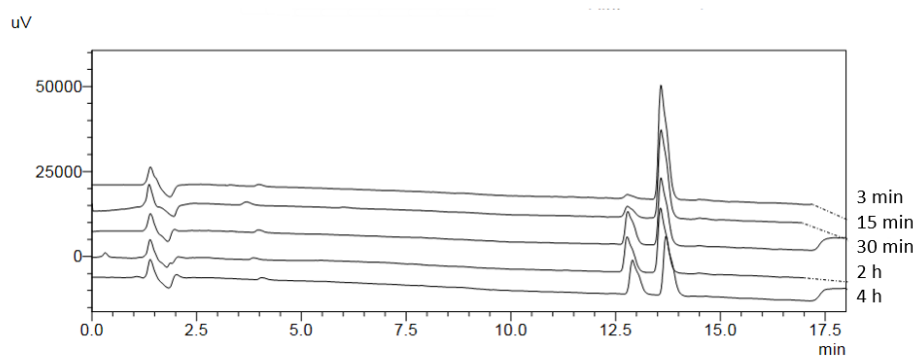


Figure 2.10 HPLC chromatogram of **BW-OTCO-102** in the presence of 500 μM ¹O₂

2.3.7 Experimental procedure for synergetic effect study of CO prodrugs with Dox in killing cancer cells

Hela cells and H9C2 cells were seeded in 96-well plates and cultured in DMEM supplemented with 10% FBS and 1% penicillin/streptomycin at 37 °C under 5% CO₂ for 24 h. The cells were either incubated with doxorubicin (1% DMSO DMEM solution, 0 to 4 μM) or a mixture of doxorubicin and indicated compounds (1% DMSO DMEM solution, 0 to 4 μM for doxorubicin) for 24 h. After removal of the medium, the plate was washed with 150 μL/well of PBS and the cell was fixed with 4% paraformaldehyde for 1 h at room temperature. The solution in the well was then removed and 100 μL of 0.5% crystal violet staining solution was added to each well. After

incubation for 15 min at room temperature, the plate was washed with 200 μL of DI water for each well twice, followed by the addition of 100 μL /well of acetic acid solution (33%) to dissolve the dye. Absorbance at 615 nm was then measured by using a Perkin Elmer 1420 multi-label counter. Cell viability was measured, and the results were normalized to the vehicle group. The experiment was triplicated, and the results are expressed as mean \pm SD ($n = 3$). The results have not shown significant difference.

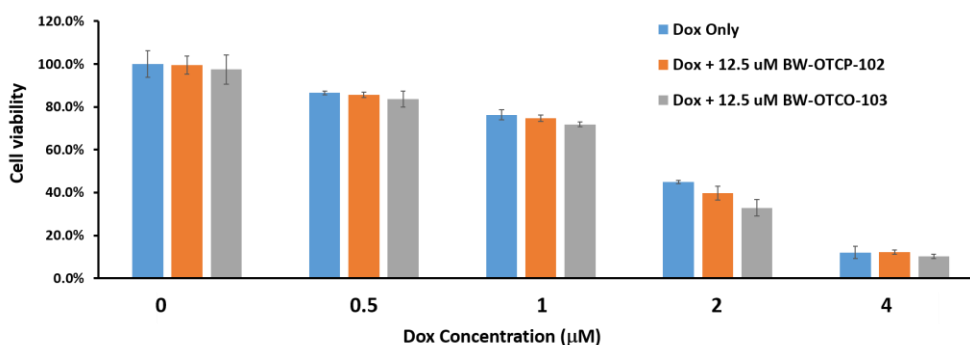


Figure 2.11 The lack of synergistic effects of control compounds with Dox

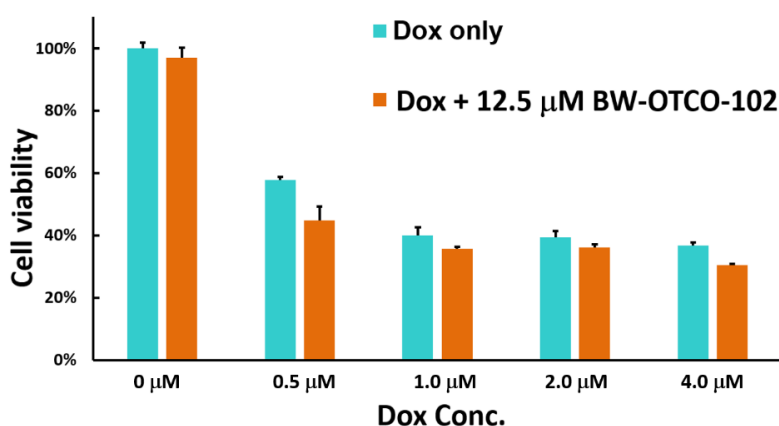


Figure 2.12 The lack of synergistic effects of BW-OTCO-102 with Dox in H9C2 cells

2.3.8 Experimental procedure for cytotoxicity study of CO prodrugs and their respective products to H9C2 cells

H9C2 cells were seeded in 96-well plates and cultured in Dulbecco's modified Eagle's medium (DMEM) supplemented with 10% fetal bovine serum (FBS) and 1% penicillin/streptomycin at 37 °C under 5% CO₂ for 24 h. H9C2 cells were incubated in DMEM containing vehicle (1% DMSO) and doxorubicin or the indicated compounds for 24 hours. After removal of the medium, the plate was washed with 150 µL/well and the cell was fixed with 4% paraformaldehyde for 1 h at room temperature. The solution in the well was then removed and 100 µL of 0.5% crystal violet staining solution was added to each well. After incubation for 15 min at room temperature, the plate was washed with 200 µL DI water for each well twice and added 100 µL/well acetic acid solution (33%) to dissolve the dye. Absorbance at 615 nm was then measured by using a Perkin Elmer 1420 multi-label counter. Cell viability was measured and the results were normalized to the vehicle group. The experiments were triplicated and the results are expressed as mean ± SD (n = 3). The result has not shown significant difference.

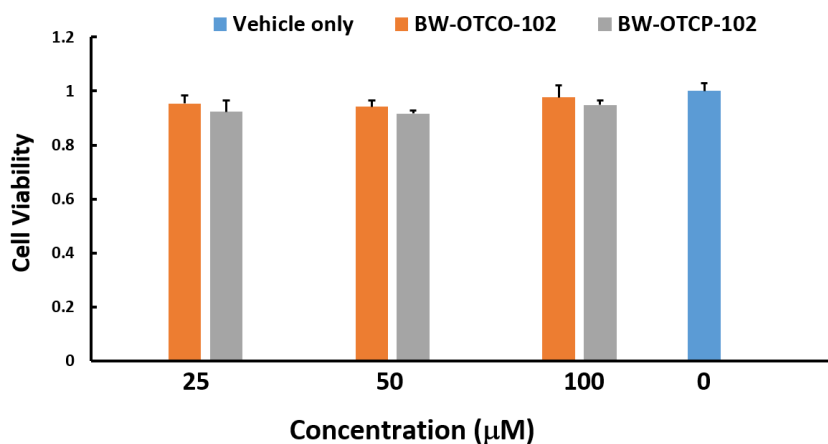


Figure 2.13 The cytotoxicity of BW-OTCO/OTCP-102 to H9C2 cells

2.4 Conclusion

In conclusion, we have successfully developed a strategy for organic CO prodrugs, which can selectively release CO in response to both exogenous and endogenous ROS. Such CO prodrugs can selectively delivery CO to cells with elevated ROS levels (e.g. cancer cells and cells with activated inflammatory responses). Additionally, such CO prodrugs also sensitized cancer cells to Dox treatment, which could potentially reduce the dosage of Dox used, and thereby alleviate Dox-related side effects. In summary, we strongly believe that the CO prodrugs described herein could serve as powerful tools for future studies of CO's various therapeutic indications.

2.5 Statements

The much of the results in this chapter has been published in *Org. Lett.* (Pan, Z; Zhang, J; Ji, K; Chittavong, V; Ji, X; Wang, B. Organic CO Prodrugs Activated by Endogenous ROS. *Org. Lett.* **2018**, *1*, 8-11.). In this chapter, Wang, B conceived the initial idea, and supervised the study. I and Ji, X co-designed the CO prodrug and I perform the study. Chittavong, V conducted studies of the reaction kinetics. Zhuang, J and Ji, K conducted the in vitro biology studies.

3 ESTERASE-SENSITIVE AND PH-CONTROLLED CARBON MONOXIDE PRODRUGS FOR TREATING SYSTEMIC INFLAMMATION

3.1 Introduction

As a well-recognized gasotransmitter, carbon monoxide imparts pleiotropic pharmacologic effects, and most of the mechanistic underpinning is at least partially associated with its strong anti-inflammatory effect.⁸⁶⁻⁹⁰ For example, CO has been shown to confer beneficial effects in mouse models of inflammation bowel diseases,⁹¹ sepsis⁹² and ischemia reperfusion⁹³, among others, partially by dampening the systemic inflammation. These results indicate CO as a very promising alternative to manage cytokine release syndrome (CRS), which can be caused by a wide range of pathological conditions including infections, organ injuries, lupus and rheumatoid arthritis, among others. It is also widely observed as an adverse effect for cancer immunotherapies.⁹⁴ Under severe conditions (i.e. cytokine storms), CRS can lead to multiple organ dysfunction and even death.⁹⁵ Current therapies in clinic largely rely on the administration of antibodies to neutralize cytokines, such as Tocilizumab.⁹⁶ However, antibody therapy as such often compromises the immune response of the host, and thereby makes the host susceptible to infections, and also is not compatible with immunotherapies. Consequently, alternative therapies with new mechanisms of action are highly desirable. The strongly anti-inflammatory effect of CO puts it in a unique position for further examination and development for CRS. However, finding an optimal method for CO delivery for eventual clinical applications has been a tortuous path.

Although inhaled CO has proven to be quite tolerable in humans at low dosage,⁹⁷ and several clinic trials using inhaled CO are on-going, gaseous CO is not an ideal way of delivery for wide-spread application due to difficulties in dosage control and in addressing individual variability, among others.⁸⁷ In order to mitigate these limitations, enormous efforts have been

devoted to the development of CO donors to trap CO in a pill, and some very exciting progresses have been achieved, including immobilized carbonyls using transition metals,^{68, 88, 98-108} commonly referred to as releasing molecules (CORMs), and photo-sensitive metal-free CORMs.^{34, 109} Our lab has been working on developing organic CO prodrugs with different triggers.^{42, 110-116} However, most of these CO prodrugs release CO either spontaneously upon dissolution or in response to a single stimulus, and very few is known to release CO with multiple triggers. In 2017, Schiller and co-workers developed the very first manganese-based CORMs controlled by an “OR” logic gate, which is sensitive to either visible light irradiation or ROS.¹¹⁷ Subsequently, the Berreau group also devised a metal-free CORMs gated by a “AND” logic triggers with visible light, thiol species and oxygen, affording more spatially specific CO release in cancerous cells.⁶⁹ Evidently, these elegant CORMs showcased the advantages of CORMs with multiple triggers over the ones with just one single trigger, and could be potentially employed for targeted delivery. For *in-vivo* applications, we are interested in CO prodrugs, which would respond to multiple endogenous triggers. Herein, we describe our efforts toward CO prodrugs with two endogenous triggers. These CO prodrugs exhibit specific CO release in a dual-response fashion to esterase and physiologic pH environment. One representative CO prodrug showed intracellular CO release and recapitulated CO-associated anti-inflammatory effects in Raw264.7 cells. Furthermore, this CO prodrug conferred significant protective effects in a LPS-induced systemic inflammation mouse model. To the best of our knowledge, this is the very first example of organic CO prodrugs that release CO in response to multiple endogenous triggers.

3.2 Results and discussion

3.2.1 Design of esterase-sensitive and pH-controlled CO prodrugs

Figure 3.1 shows the design principle of such CO prodrugs. Unlike its structural analogue C, which is known to undergo facile cheletropic reaction to extrude CO at ambient temperature or lower, compound with scaffold A is highly thermally stable. We reasoned that decorating the bicycle ring with an electron donating (EDG) and a leaving group (LG) at C5 and 6 position respectively would make compound A a potential CO prodrug, provided that the EDG can be easily biotransformed into an electron withdrawing group (EWG) under physiological conditions. In the absence of endogenous stimuli, compound A is expected to be very stable in aqueous solution. However, in the presence of an endogenous stimulus, the EDG can be transformed into an EWG to yield compound B, which can undergo beta-elimination under physiologic pH to afford intermediate C for CO release. CO prodrugs as such are dual-responsive to two endogenous triggers in a sequential manner and may yield more spatially specific CO release profiles as compared to others with no or a single trigger. Another practical advantage of such a design is sample stability during preparation of the prodrug solution for administration and stability in the stomach if administered orally.

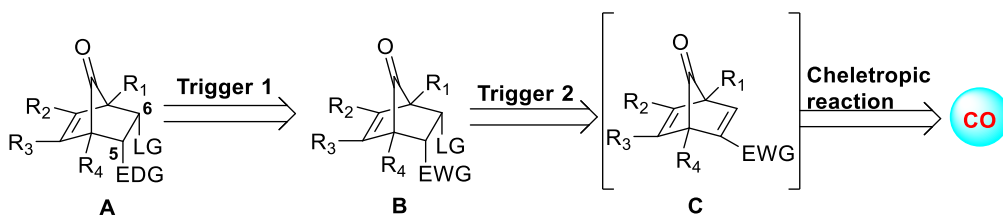
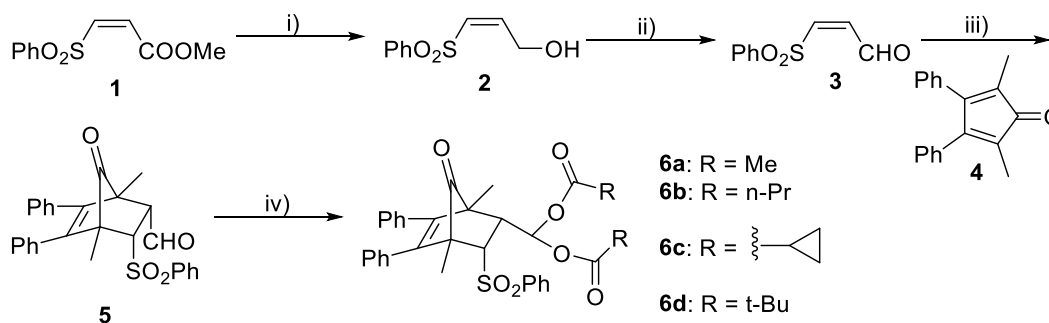


Figure 3.1 The schematic illustration of the CO prodrugs with two triggers.

3.2.2 Synthesis of esterase-sensitive and pH-controlled CO prodrugs

To establish the proof of concept, we designed and synthesized several CO prodrugs **6a-d** with the EDG and the leaving group being an acetal and sulfonyl group, respectively (Scheme 1). CO prodrugs as such are expected to be dual-responsive to esterase and physiologic pH environment. As shown in Scheme 1, compound **1**¹¹⁸ was reduced to alcohol compound **2**, which was further oxidized to aldehyde **3**. The Diels-Alder cycloaddition between compound **3** and **4** went smoothly in refluxing toluene to yield compound **5**, which was readily transformed into the CO prodrugs **6a-d** in the presence of RuCl₃.



Scheme 3.1 The synthesis of CO prodrugs.

Reagents and conditions: i) DIBAL, CH₂Cl₂, -78 °C-r.t., 70%; ii) DMP, CH₂Cl₂, 0 °C, 74%; iii) toluene, reflux, 65%; iv) (RCO)₂O, RuCl₃, r.t. 50-70%.

3.2.3 CO release kinetics study

With these compounds in hand, we tested their CO release profiles in response to an esterase and physiologic pH. Initially, we confirmed that compound **5** release CO in phosphate buffer saline (PBS) buffer (pH = 7) with a half-life of about 30 min and the CO release was validated by a CO-myoglobin assay and fully elucidating the structure of the inactive product **7** after CO release (Figure 3.2). As expected, compound **6a-c** released CO in the presence of porcine liver esterase (PLE) in PBS buffer with release half-life ranging from 30 min to 8 h. The acetal group in **6a** is so sensitive to the PLE that the prodrug is totally consumed within 2 mins with the

formation of compound **5**, which underwent beta-elimination to afford compound **7**. With the increasing steric bulk of the R group, the rate of esterase-mediated hydrolysis showed a significance decrease, eventually becoming the rate-limiting step with no build-up of compound **5** throughout the experiment. Especially for **6d**, no hydrolysis product was observed in the presence of PLE even after 36 h of incubation. Having confirmed that PLE mediated CO release from **6a-c**, compound **6a** was selected to confirm the specificity of CO release in response to PLE and physiologic pH. The results showed that no hydrolysis (formation of **5**) was observed in the absence of PLE even after 6 h of incubation either in PBS buffer (pH = 7) or simulated gastric fluid (SGF, pH = ~1). Meanwhile, incubation of **6a** in the SGF containing PLE led to the formation of **5** within 2 mins. However, no beta-elimination (formation of **7**) was observed even after 7 h of incubation at 37 °C. Collectively, these results unambiguously indicated that the CO release from compound **6a** is gated by both PLE and physiologic pH environment.

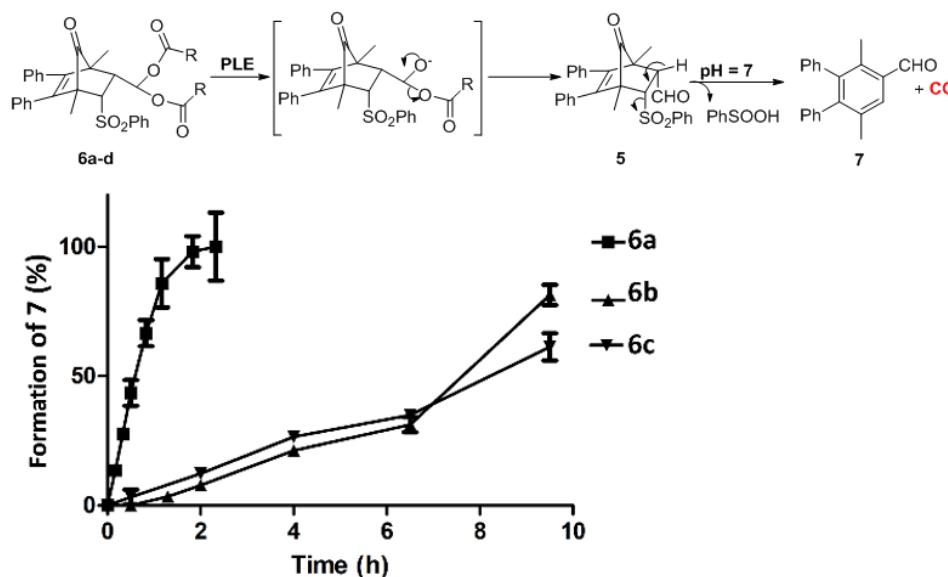


Figure 3.2 Release kinetics of CO from prodrugs **6a-c** in the presence of PLE (3 U/mL) in 5% of DMSO in PBS at 37 °C.

To further validate CO release from **6a** in response to esterase and physiologic pH, we tested the CO release profile of **6a** in mouse, rat, rabbit and human serum by using HPLC. Interestingly, the results showed that the esterase mediated hydrolysis of **6a** (formation of **5**) in rabbit, rat and mouse serum is very fast as expected with half-lives of around 30 mins, 10 mins and 3 mins respectively. However, the hydrolysis of **6a** is quite sluggish in human serum with a half-life of around 14 h. Moreover, the beta-elimination step of intermediate **5** is unexpectedly slow and is not finished even after 20 h in all the sera tested, as compared to only 3 h in PBS. This is presumably attributed to the binding of **5** to some serum proteins, which may hinder the beta-elimination. Special attention should be paid to the release kinetics difference among different species. Such information will be especially useful and important in guiding future optimization work.

3.2.4 Cell imaging study

Due to the fast release kinetics of **6a** in response to PLE and physiologic pH, it was selected for further validation in a biologic milieu. Initially, the intracellular CO release of **6a** was studied in Raw264.7 cells using a reported CO fluorescent probe COP-1. As shown in Figure 3.3, the cells treated with COP-1 and **6a** showed much enhanced green fluorescence as compared to the one treated with COP-1 only, indicating intracellular CO release from **6a**. No decrease in cell viability was observed throughout the experiment according to a WST-8 cell proliferation assay, and compound **7** did not show any cytotoxicity even at concentration up to 200 μM .

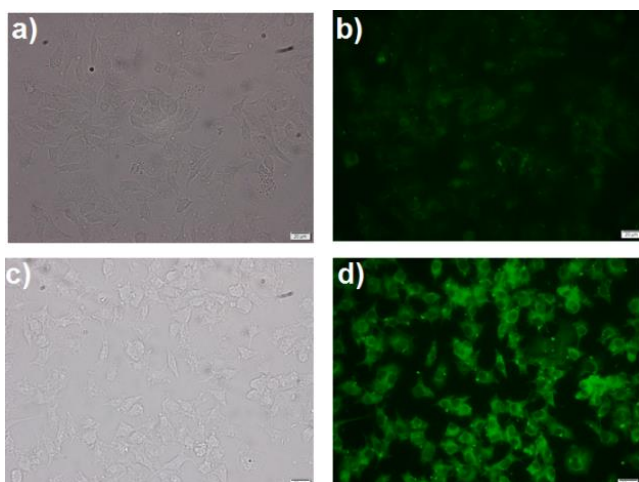


Figure 3.3 Cell imaging studies of CO release from **6a**
Cells treated with COP-1 (1 μM) only (a-b) or COP-1 and **6a** (50 μM) (c-d). Scale bar: 20 μm .

3.2.5 Anti-inflammatory study of CO prodrugs

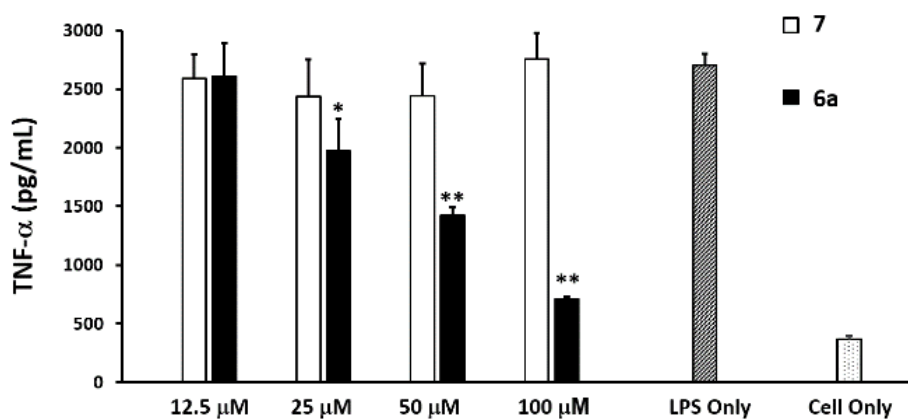


Figure 3.4 The anti-inflammatory effects of **6a** in LPS-challenged Raw264.7 cells. The mean of each concentration of **6a** and **7** treated group was compared with LPS-only group by two-sample t-test. *: $p < 0.05$; **: $p < 0.01$.

As shown in Figure 3.4, compound **6a** exhibited dose-dependent inhibition of LPS induced TNF- α secretion, while no such effects were obtained with the inactive control compound **7**, suggesting that the observed anti-inflammatory effects were attributed to the CO release from **6a**.

It is worth pointing out that the concentration needed to produce the anti-inflammatory effect is 25 μM , which seems to be less potent as compared to other CORMs. The underlying reasons are two-fold: Only one equivalent of CO is released from **6a** as compared to two or more equivalents of CO released from metal-based CORMs; the release half-life of CO prodrug also determines the real effective CO concentrations. High concentrations of CO prodrugs with slow release rate does not necessarily mean high concentration of CO.

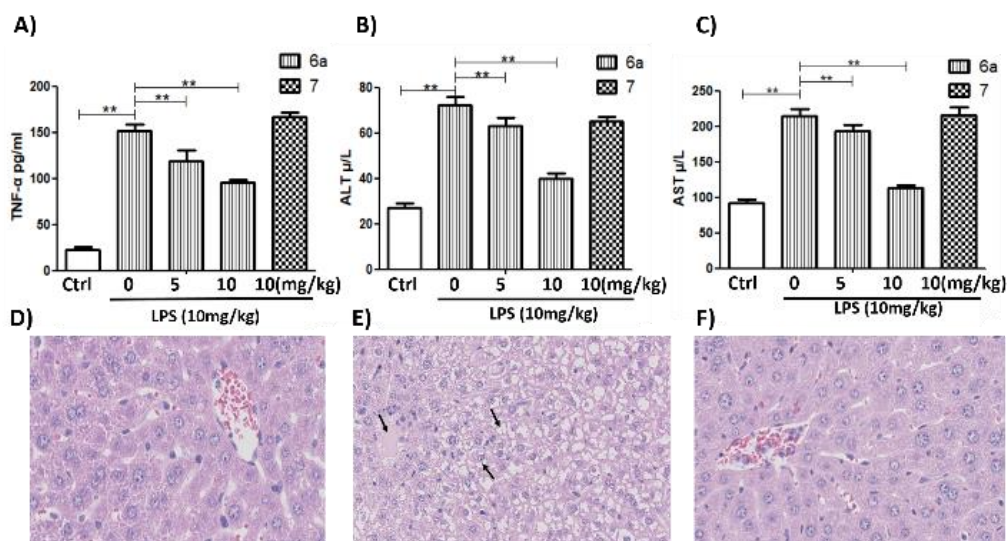


Figure 3.5 The protective effects of prodrug 6a against LPS-induced liver injuries

The effects were indicated by the suppression of TNF- α (A), ALT(B) and AST levels (C). D-E) H&E staining of liver tissue in the vehicle control (D), LPS (E), and **6a** (10mg/kg) treatment group (F). **: p<0.01.

Having confirmed that compound **6a** is able to release CO in response to intracellular esterase and physiologic pH to recapitulate CO-associated anti-inflammatory effects, we next evaluated its anti-inflammatory and liver protective effects in a LPS induced systemic inflammation mouse model.¹¹⁹ C57 mice were pre-treated with **6a**, **7** or the vehicle 30 min before LPS injection (i.p. 10 mg/kg). After 6 h, mice were sacrificed, and blood and liver were harvested for biomarker analysis including TNF- α , ALT and AST, and H&E staining, respectively. As shown in Figure 5A, treatment with **6a** dose-dependently dampened the LPS-induced systemic

inflammation as indicated by significant decreases in the serum TNF- α level. In addition, **6a** also dose-dependently alleviated LPS-induced liver injury as evidenced by the decrease in the ALT and AST levels (Figure 5B, C). The liver H&E staining results further confirmed the protective effects of **6a** (Figure 5F) against LPS-induced acute liver injury (Figure 5E). Meanwhile, no such effects were observed with the inactive control compound **7**. Collectively, these results firmly established compound **6a** as a promising CO prodrug for the treatment of sepsis or other inflammation related organ injuries.

3.3 Experimental Section

3.3.1 General information

All reagents and solvents were of reagent grade and were purchased from Aldrich. Column chromatography was carried out using flash silica gel (Sorbent 230–400 mesh) and P-2 Gel (Bio-Gel, particle size range 45- 90 μm). TLC analyses were conducted on silica gel plates (Sorbent Silica G UV254). $^1\text{H-NMR}$ (400 MHz) and $^{13}\text{C-NMR}$ (100 MHz) spectra were recorded on a Bruker Avance 400 MHz NMR spectrometer. Mass spectral analyses were performed on a Q-TOF micro (Waters Micromass) by the GSU Mass Spectrometry Facilities. Please refer to SI for the synthesis of compound **2** and **3**. The purity of all the tested compounds is over 95% as determined by HPLC.

A mouse macrophage cell line, RAW 264.7 (ATCC® TIB-71™), was used for the *in vitro* studies. RAW 264.7 cells were maintained in DMEM (Dulbecco's Modified Eagle's Medium) supplemented with 10% fetal bovine serum (MidSci; S01520HI) and 1% penicillin-streptomycin (Sigma-Aldrich; P4333) at 37 °C with 5% CO₂. The media was changed every other day. All the experiments were done within 10 passages of RAW 264.7 cells. All the tested compounds were dissolved in 100% DMSO to yield the respective stock solution.

Lipopolysaccharide (LPS) was purchased from Sigma Chemical Co.. Mouse TNF- α ELISA kits were purchased from eBioscience. Distilled water was filtered through a Milli-Q system from EMD Millipore Corporation. LPS was dissolved in saline (1mg/mL) before injection. C57BL/6 mice were purchased from Sichuan Dashuo Animal Company. The mice were maintained under controlled temperature and humidity with certified standard diet and water ad libitum and habituated to animal facilities for 1 week before the experiment. The experimental protocols were approved by Animal Use and Care Committee of Sichuan University (Approval No. 2018117A) and followed the guidelines of the Care and Use of Laboratory Animals of China Association for Laboratory Animal Science.

3.3.2 Experimental procedure for the synthesis of Esterase-sensitive and pH-controlled CO prodrugs

Synthesis of (1S,4S)-1,4-dimethyl-7-oxo-5,6-diphenyl-3-(phenylsulfonyl)bicyclo[2.2.1]hept-5-ene-2-carbaldehyde (**5**): To a solution of **4** (0.8 mmol, 208 mg) in toluene (10 mL), was added compound **3** (0.9 mmol, 177 mg). The mixture was heated under reflux for 5 h. Then, the reaction mixture was concentrated under vacuum, and the obtained residue was directly purified on a silica gel column (hexane: EtOAc = 5:1) to afford the desired product as a white solid (270 mg, yield: 60% over two steps). ^1H NMR (CDCl_3): δ 10.13 (d, J = 5.3 Hz, 1H), 7.77 – 7.71 (m, 2H), 7.67 (d, J = 7.5 Hz, 1H), 7.54 (t, J = 7.8 Hz, 2H), 7.37-7.41 (m, 2H), 7.31 – 7.20 (m, 6H), 7.10 – 7.03 (m, 2H), 4.17 (d, J = 10.3 Hz, 1H), 3.04 (dd, J = 10.3, 5.3 Hz, 1H), 1.44 (s, 3H), 1.35 (s, 3H) ppm. ^{13}C NMR (CDCl_3): δ 198.9, 196.2, 157.5, 141.9, 140.2, 139.7, 139.6, 134.5, 133.8, 133.5, 130.7, 129.8, 129.5, 128.5, 128.2, 127.9, 127.7, 70.9, 59.0, 57.6, 57.1, 12.4, 11.3 ppm. HRMS calcd for $\text{C}_{28}\text{H}_{24}\text{O}_4\text{SNa}$ $[\text{M}+\text{Na}]^+$: 479.1293; found: 479.1283.

General procedure for the synthesis of **6a-d**

To a solution of **5** (0.1 mmol, 45 mg) in the corresponding anhydride (0.1 mL) was added RuCl₃ (0.01 mmol, 2 mg) in one portion, and the mixture was stirred at room temperature for 12 h. The reaction was then quenched with water (10 mL) and extracted with ethyl acetate (3 × 20 mL). The combined organic layer was dried over anhydrous Na₂SO₄ and concentrated under reduced pressure. The obtained residue was purified on a silica gel column to afford the title compound.

((1S,4S)-1,4-dimethyl-7-oxo-5,6-diphenyl-3-(phenylsulfonyl)bicyclo[2.2.1]hept-5-en-2-yl)methylene diacetate (**6a**)

The title compound was synthesized according to the general procedure with compound **5** (0.1 mmol, 45mg) and acetic anhydride (0.1 mL). ¹H NMR (CDCl₃): δ 7.77 (d, *J* = 2.7 Hz, 1H), 7.63 (d, *J* = 8.4 Hz, 2H), 7.47 (t, *J* = 7.9 Hz, 2H), 7.34 – 7.28 (m, 7H), 7.23 – 7.17 (m, 3H), 4.12 (d, *J* = 11.0 Hz, 1H), 3.24 (dd, *J* = 11.0, 2.7 Hz, 1H), 2.13 (s, 3H), 2.05 (s, 3H), 1.47 (s, 3H), 1.02 (s, 3H) ppm. ¹³C NMR (CDCl₃): δ 196.4, 168.8, 168.6, 142.9, 141.3, 138.7, 134.7, 134.0, 134.0, 130.7, 129.3, 128.4, 127.7, 127.7, 127.5, 127.3, 88.8, 69.8, 56.8, 55.9, 50.7, 20.9, 20.9, 13.3, 13.0 ppm. HRMS calcd for C₃₂H₃₀O₇SNa [M+Na]⁺: 581.1610; found: 581.1635.

((1S,4S)-1,4-dimethyl-7-oxo-5,6-diphenyl-3-(phenylsulfonyl)bicyclo[2.2.1]hept-5-en-2-yl)methylene dibutyrate (**6b**)

The title compound was synthesized according to the general procedure with compound **5** (0.1 mmol, 45mg) and butyric anhydride (0.1 mL). ¹H NMR (CDCl₃): δ 7.70 (d, *J* = 7.7 Hz, 2H), 7.63 (t, *J* = 7.5 Hz, 1H), 7.47 (t, *J* = 7.8 Hz, 2H), 7.28 – 7.17 (m, 8H), 7.16 – 7.07 (m, 2H), 6.66 (s, 1H), 3.80 (d, *J* = 5.6 Hz, 1H), 3.14 (d, *J* = 5.1 Hz, 1H), 2.27 (t, *J* = 7.4 Hz, 2H), 2.19 (t, *J* = 7.4 Hz, 2H), 1.58-1.66 (m, 4H), 1.32 (s, 3H), 1.26 (s, 3H), 0.92-1.97 (m, 6H) ppm. ¹³C NMR (CDCl₃): δ 198.1, 171.7, 170.7, 142.8, 139.8, 139.4, 134.0, 133.9, 133.6, 130.6, 129.4, 129.3, 128.7, 128.2,

127.7, 127.6, 127.4, 88.0, 67.6, 56.2, 54.7, 47.1, 35.5, 35.5, 17.9, 17.8, 13.5, 13.4, 12.7, 10.2 ppm.

HRMS calcd for $C_{36}H_{38}O_7SNa$ $[M+Na]^+$: 637.2236; found: 637.2265.

((1S,4S)-1,4-dimethyl-7-oxo-5,6-diphenyl-3-(phenylsulfonyl)bicyclo[2.2.1]hept-5-en-2-yl)methylene dicyclopropanecarboxylate (**6c**)

The title compound was synthesized according to the general procedure with compound **5** (0.1 mmol, 45mg) and cyclopropanecarboxylic anhydride (0.1 mL). 1H NMR ($CDCl_3$): δ 7.72 (d, $J = 2.6$ Hz, 1H), 7.67 – 7.63 (m, 2H), 7.60 (t, $J = 7.5$ Hz, 1H), 7.46 (t, $J = 7.8$ Hz, 2H), 7.40 – 7.31 (m, 4H), 7.25-7.29 (m, 3H), 7.18-7.22 (m, 3H), 4.12 (d, $J = 11.0$ Hz, 1H), 3.23 (dd, $J = 11.0, 2.6$ Hz, 1H), 1.68 – 1.60 (m, 1H), 1.53 (s, 3H), 1.36-1.42 (m, 1H), 1.12 – 1.03 (m, 5H), 1.04 – 0.77 (m, 6H) ppm. ^{13}C NMR ($CDCl_3$): δ 196.8, 172.6, 172.5, 143.0, 141.4, 138.8, 134.7, 134.2, 133.9, 130.9, 130.8, 129.2, 128.3, 127.7, 127.6, 127.4, 127.3, 88.8, 69.9, 57.0, 56.0, 50.8, 13.3, 13.0, 12.8, 12.6, 9.4, 9.2, 9.1, 8.6 ppm. HRMS calcd for $C_{36}H_{34}O_7SNa$ $[M+Na]^+$: 633.1923; found: 633.1951.

((1S,4S)-1,4-dimethyl-7-oxo-5,6-diphenyl-3-(phenylsulfonyl)bicyclo[2.2.1]hept-5-en-2-yl)methylene bis(2,2-dimethylpropanoate) (**6d**)

The title compound was synthesized according to the general procedure with compound **5** (0.1 mmol, 45mg) and pivalic anhydride (0.1 mL). 1H NMR ($CDCl_3$): δ 7.78 (d, $J = 7.5$ Hz, 2H), 7.67 (t, $J = 7.5$ Hz, 1H), 7.53 (t, $J = 7.8$ Hz, 2H), 7.24-7.28 (m, 5H), 7.18-7.23 (m, 3H), 7.11-7.16 (m, 2H), 6.32 (s, 1H), 3.61 (d, $J = 6.4$ Hz, 1H), 2.98-3.04 (m, 1H), 1.44 (s, 3H), 1.30 (s, 3H), 1.18 (s, 9H), 1.16 (s, 9H) ppm. ^{13}C NMR ($CDCl_3$): δ 198.2, 176.8, 175.4, 142.8, 138.9, 134.3, 133.9, 133.6, 130.6, 129.5, 129.4, 128.7, 128.2, 127.7, 127.6, 127.4, 89.3, 67.7, 56.0, 54.5, 48.0, 39.0, 38.6, 29.7, 27.0, 26.8, 12.6, 10.9 ppm. HRMS calcd for $C_{36}H_{34}O_7SNa$ $[M+Na]^+$: 665.2549; found: 665.2545.

3.3.3 *Experimental procedure for cell imaging study*

RAW 264.7 cells were seeded on coverslips in 6-well plate at an initial density of 10,000/well one day before the imaging experiment. Compounds were dissolved in DMSO as stock solution. Final concentration of 1 μ M of COP-1 and 50 μ M of 6a were added into the cell culture. All the final samples contained 1% DMSO. After adding the compound, the cells were incubated under 37 °C for 5 h. The cell samples were then fixed with 4% paraformaldehyde. The cells were then washed with PBS again twice and the coverslips with cells were immersed in DI water. The coverslips S19 were mounted onto glass slides using the mounting media without DAPI (ProLong® Live Antifade Reagent; P36974). The fluorescent imaging was performed under FITC channel (excitation: 490 nm, emission: 525 nm) using a Zeiss fluorescent microscope (Axio Vert. A1).

3.3.4 *Experimental procedure for anti-inflammatory effects study*

RAW 264.7 cells were seeded in 96-well plates at an initial density of 10,000/well one day before the experiment. LPS was used to initiate the inflammatory response in RAW 264.7 cells. RAW 264.7 cells were pre-treated with different concentrations of 6a, 7 or sodium benzenesulfinate for 4 h. All the final samples contained 1% DMSO. Thereafter, LPS was added into the cell culture media to make a final concentration of 1 μ g/mL. The cells were then incubated at 37 °C for another 1 h, and the cell culture supernatant was collected afterwards. Cell culture without LPS treatment was used as the control. The concentrations of TNF- α in the cell culture supernatant were determined by a commercial ELISA kit (ELISA Ready-SET-Go!®-eBioscience).

3.3.5 *Experimental procedure for the study of 6a's Anti-inflammatory and liver protective effects in an LPS-simulated mouse model*

Six- to eight-week old male C57BL/6 mice weighting 22-25 g were randomly divided into five groups of eight individuals. Mice received single dose treatment of either 6a (i.p., 5, 10 and 20 mg/kg) or the vehicle (solutol : saline = 1:9) 30 min before the injection of LPS (i.p., 10mg/kg). After 6 h, the mouse serum in each group was collected by cardiac puncture after anesthesia and was centrifuged at 3000 rpm for 10 min. The supernatant was then taken for the analysis of TNF- α (Elisa), ALT and AST levels (biochemical automatic analyzer, SRL, Tokyo, Japan). After the blood sampling, the mice were sacrificed, and the liver was harvested, rinsed with saline and fixed with 10% formalin. The liver tissues were embedded with paraffin, sliced to 5 μ m sections, and stained with hematoxylin-eosin (H&E). Mouse liver histopathology images were acquired using a microscope (Zeiss AX10 imager A2/AX10 cam HRC).

3.4 Conclusion

In this work, we describe efforts toward organic CO prodrugs with dual-responsive endogenous triggers. One representative CO prodrug showed significant anti-inflammatory effects both *in vitro* and in a LPS-simulated systemic inflammation model. These results firmly establish such CO prodrugs as either research tools or candidate compounds for the treatment of systemic inflammation or inflammation related organ injuries.

3.5 Statements

The much of the results in this chapter has been published in *J. Med. Chem.* (Ji, X; Pan, Z; Li, C; Kang, T; LK De la Cruz, L; Yang, L; Yuan, Z; Ke, B; Wang, B. Esterase-sensitive and pH-controlled Carbon Monoxide Prodrugs for Treating Systemic Inflammation. *J. Med. Chem.* **2019**, *6*, 3163–3168.). In this chapter, Wang, B conceived the initial idea, and supervised the study. I and

Ji, X co-designed the CO prodrug and perform the study. LK De la Cruz, L and Yuan, Z conducted studies of the reaction kinetics and some of the synthesis. I and Ji, X conducted the in vitro biology studies. Li, C; Kang, T; and Yang, L conducted in vivo studies. Ke, B supervised and/or performed the in vivo studies, analyzed and interpreted the data.

REFERENCES

1. McCoubrey, W. K.; Huang, T. J.; Maines, M. D., Isolation and characterization of a cDNA from the rat brain that encodes hemoprotein heme oxygenase-3. *Eur. J. Biochem.* **1997**, *247* (2), 725-732.
2. Tenhunen, R.; Marver, H. S.; Schmid, R., The enzymatic catabolism of hemoglobin: stimulation of microsomal heme oxygenase by hemin. *J. Lab. Clin. Med.* **1970**, *75* (3), 410-21.
3. Ji, X. Y.; Damera, K.; Zheng, Y. Q.; Yu, B. C.; Otterbein, L. E.; Wang, B. H., Toward Carbon Monoxide-Based Therapeutics: Critical Drug Delivery and Developability Issues. *J. Pharm. Sci.* **2016**, *105* (2), 406-416.
4. Motterlini, R.; Otterbein, L. E., The therapeutic potential of carbon monoxide. *Nat. Rev. Drug. Discov.* **2010**, *9* (9), 728-43.
5. Raman, K. G.; Barbato, J. E.; Ifedigbo, E.; Ozanich, B. A.; Zenati, M. S.; Otterbein, L. E.; Tzeng, E., Inhaled carbon monoxide inhibits intimal hyperplasia and provides added benefit with nitric oxide. *J. Vasc. Surg.* **2006**, *44* (1), 151-8.
6. Otterbein, L. E.; Bach, F. H.; Alam, J.; Soares, M.; Tao, L. H.; Wysk, M.; Davis, R. J.; Flavell, R. A.; Choi, A. M., Carbon monoxide has anti-inflammatory effects involving the mitogen-activated protein kinase pathway. *Nat. Med.* **2000**, *6*, 422-8.
7. Wegiel, B.; Larsen, R.; Gallo, D.; Chin, B. Y.; Harris, C.; Mannam, P.; Kaczmarek, E.; Lee, P. J.; Zuckerbraun, B. S.; Flavell, R.; Soares, M. P.; Otterbein, L. E., Macrophages sense and kill bacteria through carbon monoxide-dependent inflammasome activation. *J. Clin. Invest.* **2014**, *124*, 4926-40.
8. Wareham, L. K.; Poole, R. K.; Tinajero-Trejo, M., CO-releasing Metal Carbonyl Compounds as Antimicrobial Agents in the Post-antibiotic Era. *J. Biol. Chem.* **2015**, *290*, 18999-19007.
9. Nagel, C.; McLean, S.; Poole, R. K.; Braunschweig, H.; Kramer, T.; Schatzschneider, U., Introducing [Mn(CO)(3)(tpa-kappa N-3)](+) as a novel photoactivatable CO-releasing molecule with well-defined iCORM intermediates - synthesis, spectroscopy, and antibacterial activity. *Dalton Trans.* **2014**, *43* (26), 9986-9997.
10. Wegiel, B.; Gallo, D.; Csizmadia, E.; Harris, C.; Belcher, J.; Vercellotti, G. M.; Penacho, N.; Seth, P.; Sukhatme, V.; Ahmed, A.; Pandolfi, P. P.; Helczynski, L.; Bjartell, A.; Persson, J. L.; Otterbein, L. E., Carbon monoxide expedites metabolic exhaustion to inhibit tumor growth. *Cancer Res.* **2013**, *73*, 7009-21.
11. Otterbein, L. E.; Mantell, L. L.; Choi, A. M. K., Carbon monoxide provides protection against hyperoxic lung injury in rats. *Am. J. Resp. Crit. Care.* **1999**, *159* (3), A218-A218.
12. Sarady, J. K.; Zuckerbraun, B. S.; Bilban, M.; Wagner, O.; Usheva, A.; Liu, F.; Ifedigbo, E.; Zamora, R.; Choi, A. M. K.; Otterbein, L. E., Carbon monoxide protection against endotoxic shock involves reciprocal effects on iNOS in the lung and liver. *Faseb J.* **2004**, *18* (3), 854-+.
13. Wegiel, B.; Gallo, D.; Csizmadia, E.; Harris, C.; Belcher, J.; Vercellotti, G. M.; Penacho, N.; Seth, P.; Sukhatme, V.; Ahmed, A.; Pandolfi, P. P.; Helczynski, L.; Bjartell, A.; Persson, J. L.; Otterbein, L. E., Carbon Monoxide Expedites Metabolic Exhaustion to Inhibit Tumor Growth. *Cancer Research* **2013**, *73* (23), 7009-7021.
14. Suliman, H. B.; Carraway, M. S.; Ali, A. S.; Reynolds, C. M.; Welty-Wolf, K. E.; Piantadosi, C. A., The CO/HO system reverses inhibition of mitochondrial biogenesis and prevents murine doxorubicin cardiomyopathy. *J. Clin. Invest.* **2007**, *117* (12), 3730-3741.

15. Pamplona, A.; Ferreira, A.; Balla, J.; Jeney, V.; Balla, G.; Epiphanio, S.; Chora, A.; Rodrigues, C. D.; Gregoire, I. P.; Cunha-Rodrigues, M.; Portugal, S.; Soares, M. P.; Mota, M. M., Heme oxygenase-1 and carbon monoxide suppress the pathogenesis of experimental cerebral malaria. *Nat. Med.* **2007**, *13* (6), 703-710.
16. Boczkowski, J.; Poderoso, J. J.; Motterlini, R., CO-metal interaction: vital signaling from a lethal gas. *Trends. Biochem. Sci.* **2006**, *31* (11), 614-621.
17. Motterlini, R.; Clark, J. E.; Foresti, R.; Sarathchandra, P.; Mann, B. E.; Green, C. J., Carbon monoxide-releasing molecules - Characterization of biochemical and vascular activities. *Circ. Res.* **2002**, *90* (2), E17-E24.
18. Clark, J. E.; Naughton, P.; Shurey, S.; Green, C. J.; Johnson, T. R.; Mann, B. E.; Foresti, R.; Motterlini, R., Cardioprotective actions by a water-soluble carbon monoxide-releasing molecule. *Circ. Res.* **2003**, *93* (2), E2-E8.
19. Motterlini, R.; Sawle, P.; Bains, S.; Hammad, J.; Alberto, R.; Foresti, R.; Green, C. J., CORM-A1: a new pharmacologically active carbon monoxide-releasing molecule. *Faseb. J.* **2004**, *18* (14), 284-+.
20. Niesel, J.; Pinto, A.; N'Dongo, H. W. P.; Merz, K.; Ott, I.; Gust, R.; Schatzschneider, U., Photoinduced CO release, cellular uptake and cytotoxicity of a tris(pyrazolyl) methane (tpm) manganese tricarbonyl complex. *Chem. Commun.* **2008**, (15), 1798-1800.
21. Bruckmann, N. E.; Wahl, M.; Reiss, G. J.; Kohns, M.; Watjen, W.; Kunz, P. C., Polymer Conjugates of Photoinducible CO-Releasing Molecules. *Eur. J. Inorg. Chem.* **2011**, (29), 4571-4577.
22. Jimenez, J.; Chakraborty, I.; Carrington, S. J.; Mascharak, P. K., Light-triggered CO delivery by a water-soluble and biocompatible manganese photoCORM. *Dalton Trans.* **2016**, *45* (33), 13204-13213.
23. Gonzales, M. A.; Mascharak, P. K., Photoactive metal carbonyl complexes as potential agents for targeted CO delivery. *J. Inorg. Biochem.* **2014**, *133*, 127-135.
24. Kawahara, B.; Moller, T.; Hu-Moore, K.; Carrington, S.; Faull, K. F.; Sen, S.; Mascharak, P. K., Attenuation of Antioxidant Capacity in Human Breast Cancer Cells by Carbon Monoxide through Inhibition of Cystathionine beta-Synthase Activity: Implications in Chemotherapeutic Drug Sensitivity. *J. Med. Chem.* **2017**, *60* (19), 8000-8010.
25. Kawahara, B.; Ramadoss, S.; Chaudhuri, G.; Janzen, C.; Sen, S.; Mascharak, P. K., Carbon monoxide sensitizes cisplatin-resistant ovarian cancer cell lines toward cisplatin via attenuation of levels of glutathione and nuclear metallothionein. *J. Inorg. Biochem.* **2019**, *191*, 29-39.
26. Romanski, S.; Kraus, B.; Schatzschneider, U.; Neudorfl, J. M.; Amslinger, S.; Schmalz, H. G., Acyloxybutadiene Iron Tricarbonyl Complexes as Enzyme-Triggered CO-Releasing Molecules (ET-CORMs). *Angew. Chem. Int. Ed.* **2011**, *50* (10), 2392-2396.
27. Stamellou, E.; Romanski, S.; Amslinger, S.; Hafner, M.; Kraemer, B. K.; Schmalz, H. G.; Yard, B. A., Enzyme-Triggered CO-Releasing Molecules (ET-CORMs): Structural Entities that Mediate Restricted Cell Specificity for CO Release. *Transplantation.* **2012**, *94* (10), 1134-1134.
28. Sitnikov, N. S.; Li, Y.; Zhang, D.; Yard, B.; Schmalz, H. G., Design, synthesis, and functional evaluation of CO-releasing molecules triggered by Penicillin G amidase as a model protease. *Angew. Chem. Int. Ed.* **2015**, *54* (42), 12314-8.

29. Hasegawa, U.; van der Vlies, A. J.; Simeoni, E.; Wandrey, C.; Hubbell, J. A., Carbon Monoxide-Releasing Micelles for Immunotherapy. *J. Am. Chem. Soc.* **2010**, *132* (51), 18273-18280.
30. Bohlender, C.; Glaser, S.; Klein, M.; Weisser, J.; Thein, S.; Neugebauer, U.; Popp, J.; Wyrwa, R.; Schiller, A., Light-triggered CO release from nanoporous non-wovens. *J. Mater. Chem. B.* **2014**, *2* (11), 1454-1463.
31. Chaves-Ferreira, M.; Albuquerque, I. S.; Matak-Vinkovic, D.; Coelho, A. C.; Carvalho, S. M.; Saraiva, L. M.; Romao, C. C.; Bernardes, G. J. L., Spontaneous CO Release from Ru-II(CO)(2)-Protein Complexes in Aqueous Solution, Cells, and Mice. *Angew. Chem. Int. Ed.* **2015**, *54* (4), 1172-1175.
32. Nagao, S.; Taguchi, K.; Miyazaki, Y.; Wakayama, T.; Chuang, V. T. G.; Yamasaki, K.; Watanabe, H.; Sakai, H.; Otagiri, M.; Maruyama, T., Evaluation of a new type of nano-sized carbon monoxide donor on treating mice with experimentally induced colitis. *J. Control. Release.* **2016**, *234*, 49-58.
33. Antony, L. A.; Slanina, T.; Sebej, P.; Solomek, T.; Klan, P., Fluorescein analogue xanthene-9-carboxylic acid: a transition-metal-free CO releasing molecule activated by green light. *Org. Lett.* **2013**, *15* (17), 4552-5.
34. Palao, E.; Slanina, T.; Muchova, L.; Solomek, T.; Vitek, L.; Klan, P., Transition-Metal-Free CO-Releasing BODIPY Derivatives Activatable by Visible to NIR Light as Promising Bioactive Molecules. *J. Am. Chem. Soc.* **2016**, *138* (1), 126-33.
35. Anderson, S. N.; Richards, J. M.; Esquer, H. J.; Benninghoff, A. D.; Arif, A. M.; Berreau, L. M., A Structurally-Tunable 3-Hydroxyflavone Motif for Visible Light-Induced Carbon Monoxide-Releasing Molecules (CORMs). *ChemistryOpen* **2015**, *4* (5), 590-4.
36. Sutton, D. A.; Popik, V. V., Sequential Photochemistry of Dibenzo[a,e]cyclopropa[c,g][8]annulene-1,6-dione: Selective Formation of Didehydrodibenzo[a,e][8]annulenes with Ultrafast SPAAC Reactivity. *Journal of Organic Chemistry* **2016**, *81* (19), 8850-8857.
37. Wang, B.; Siahaan, T.; Soltero, R., *Drug Delivery: Principles and Applications*. Wiley Ser Drug Disc: 2005; p 1-448.
38. Borchardt, R.; Kerns, E.; Lipinski, C.; Thakker, D.; Wang, B., *Pharmaceutical Profiling in Drug Discovery for Lead Selection*. John Wiley & Sons, Inc.: 2004; p 1-482.
39. Han, C.; Davis, C.; Wang, B., *Evaluation of Drug Candidates for Preclinical Development: Pharmacokinetics, Metabolism, Pharmaceutics, and Toxicology*. John Wiley & Sons, Inc.: 2009; p 1-289.
40. Wang, D. Z.; Viennois, E.; Ji, K.; Damera, K.; Draganov, A.; Zheng, Y. Q.; Dai, C. F.; Merlin, D.; Wang, B. H., A click-and-release approach to CO prodrugs. *Chem. Commun.* **2014**, *50* (100), 15890-15893.
41. Ji, X.; Zhou, C.; Ji, K.; Aghoghovbia, R. E.; Pan, Z.; Chittavong, V.; Ke, B.; Wang, B., Click and Release: A Chemical Strategy toward Developing Gasotransmitter Prodrugs by Using an Intramolecular Diels–Alder Reaction. *Angew. Chem. Int. Ed.* **2016**, *55* (51), 15846-15851.
42. Pan, Z.; Chittavong, V.; Li, W.; Zhang, J.; Ji, K.; Zhu, M.; Ji, X.; Wang, B., Organic CO Prodrugs: Structure-CO-Release Rate Relationship Studies. *Chem. Eur. J.* **2017**, *23* (41), 9838-9845.
43. Rideout, D. C.; Breslow, R., Hydrophobic acceleration of Diels-Alder reactions. *J. Am. Chem. Soc.* **1980**, *102*, 7816-7817.

44. Breslow, R.; Maitra, U.; Rideout, D., Selective diels-alder reactions in aqueous solutions and suspensions. *Tetrahedron Lett.* **1983**, *24*, 1901-1904.
45. Breslow, R., Hydrophobic effects on simple organic reactions in water. *Acc. Chem. Res.* **1991**, *24*, 159-164.
46. Otto, S.; Engberts, J. B. F. N., Diels-Alder reactions in water. *Pure. Appl. Chem.* **2000**, *72* (7), 1365-1372.
47. Palomo, J. M., Diels-Alder Cycloaddition in Protein Chemistry. *Eur. J. Org. Chem.* **2010**, (33), 6303-6314.
48. Jung, M. E.; Piizzi, G., gem-Disubstituent effect: Theoretical basis and synthetic applications. *Chem. Rev.* **2005**, *105* (5), 1735-1766.
49. Michel, B. W.; Lippert, A. R.; Chang, C. J., A reaction-based fluorescent probe for selective imaging of carbon monoxide in living cells using a palladium-mediated carbonylation. *J. Am. Chem. Soc.* **2012**, *134* (38), 15668-71.
50. Zheng, Y.; Yu, B.; Ji, K.; Pan, Z.; Chittavong, V.; Wang, B., Esterase-Sensitive Prodrugs with Tunable Release Rates and Direct Generation of Hydrogen Sulfide. *Angew Chem Int Ed Engl* **2016**, *55* (14), 4514-8.
51. Ji, X. Y.; Zhou, C.; Ji, K. L.; Aghoghovbia, R. E.; Pan, Z. X.; Chittavong, V.; Ke, B. W.; Wang, B. H., Click and Release: A Chemical Strategy toward Developing Gasotransmitter Prodrugs by Using an Intramolecular Diels-Alder Reaction. *Angewandte Chemie-International Edition* **2016**, *55* (51), 15846-15851.
52. Frisch, M. J.; Trucks, G. W.; Schlegel, H. B.; Scuseria, G. E.; Robb, M. A.; Cheeseman, J. R.; Scalmani, G.; Barone, V.; Mennucci, B.; Petersson, G. A.; Nakatsuji, H.; Caricato, M.; Li, X.; Hratchian, H. P.; Izmaylov, A. F.; Bloino, J.; Zheng, G.; Sonnenberg, J. L.; Hada, M.; Ehara, M.; Toyota, K.; Fukuda, R.; Hasegawa, J.; Ishida, M.; Nakajima, T.; Honda, Y.; Kitao, O.; Nakai, H.; Vreven, T.; Montgomery Jr., J. A.; Peralta, J. E.; Ogliaro, F.; Bearpark, M. J.; Heyd, J.; Brothers, E. N.; Kudin, K. N.; Staroverov, V. N.; Kobayashi, R.; Normand, J.; Raghavachari, K.; Rendell, A. P.; Burant, J. C.; Iyengar, S. S.; Tomasi, J.; Cossi, M.; Rega, N.; Millam, N. J.; Klene, M.; Knox, J. E.; Cross, J. B.; Bakken, V.; Adamo, C.; Jaramillo, J.; Gomperts, R.; Stratmann, R. E.; Yazyev, O.; Austin, A. J.; Cammi, R.; Pomelli, C.; Ochterski, J. W.; Martin, R. L.; Morokuma, K.; Zakrzewski, V. G.; Voth, G. A.; Salvador, P.; Dannenberg, J. J.; Dapprich, S.; Daniels, A. D.; Farkas, Ö.; Foresman, J. B.; Ortiz, J. V.; Cioslowski, J.; Fox, D. J. *Gaussian 09, Revision C.01*, Gaussian, Inc.: Wallingford, CT, USA, 2009.
53. Becke, A. D., Density - functional thermochemistry. III. The role of exact exchange. *J. Chem. Phys.* **1993**, *98* (7), 5648-5652.
54. Lee, C.; Yang, W.; Parr, R. G., Development of the Colle-Salvetti correlation-energy formula into a functional of the electron density. *Phys. Rev. B* **1988**, *37* (2), 785-789.
55. Besler, B. H.; Merz, K. M.; Kollman, P. A., Atomic charges derived from semiempirical methods. *J. Comput. Chem.* **1990**, *11* (4), 431-439.
56. Singh, U. C.; Kollman, P. A., An approach to computing electrostatic charges for molecules. *J. Comput. Chem.* **1984**, *5* (2), 129-145.
57. Sarajlic, S.; Edirisinghe, N.; Lukinov, Y.; Walters, M.; Davis, B.; Faroux, G., Orion: Discovery Environment for HPC Research and Bridging XSEDE Resources. In *Proceedings of the XSEDE16 Conference on Diversity, Big Data, and Science at Scale*, ACM: Miami, USA, 2016; pp 1-5.

58. Ray, P. D.; Huang, B. W.; Tsuji, Y., Reactive oxygen species (ROS) homeostasis and redox regulation in cellular signaling. *Cellular Signalling* **2012**, *24* (5), 981-990.
59. Trachootham, D.; Alexandre, J.; Huang, P., Targeting cancer cells by ROS-mediated mechanisms: a radical therapeutic approach? *Nat Rev Drug Discov* **2009**, *8* (7), 579-591.
60. Paravicini, T. M.; Touyz, R. M., Redox signaling in hypertension. *Cardiovasc. Res.* **2006**, *71* (2), 247-258.
61. Singh, B. K.; Kumar, A.; Ahmad, I.; Kumar, V.; Patel, D. K.; Jain, S. K.; Singh, C., Oxidative stress in zinc-induced dopaminergic neurodegeneration: Implications of superoxide dismutase and heme oxygenase-1. *Free. Radical. Res.* **2011**, *45* (10), 1207-1222.
62. Ji, X. Y.; Damera, K.; Zheng, Y. Q.; Yu, B. C.; Otterbein, L. E.; Wang, B. H., Toward Carbon Monoxide-Based Therapeutics: Critical Drug Delivery and Developability Issues. *Journal of Pharmaceutical Sciences* **2016**, *105* (2), 406-416.
63. Steiger, C.; Hermann, C.; Meinel, L., Localized delivery of carbon monoxide. *Eur. J. Pharma. Biopharma.* **2016**, DOI: doi.org/10.1016/j.ejpb.2016.11.002.
64. Marques, A. R.; Kromer, L.; Gallo, D. J.; Penacho, N.; Rodrigues, S. S.; Seixas, J. D.; Bernardes, G. J. L.; Reis, P. M.; Otterbein, S. L.; Ruggieri, R. A.; Gonçalves, A. S. G.; Gonçalves, A. M. L.; Matos, M. N. D.; Bento, I.; Otterbein, L. E.; Blättler, W. A.; Romão, C. C., Generation of carbon monoxide releasing molecules (CO-RMs) as drug candidates for the treatment of acute liver injury: targeting of CO-RMs to the liver. *Organometallics.* **2012**, *31* (16), 5810-5822.
65. Fujita, K.; Tanaka, Y.; Abe, S.; Ueno, T., A Photoactive Carbon-Monoxide-Releasing Protein Cage for Dose-Regulated Delivery in Living Cells. *Angew. Chem. Int. Ed.* **2016**, *55* (3), 1056-60.
66. Klinger-Strobel, M.; Glaser, S.; Makarewicz, O.; Wyrwa, R.; Weisser, J.; Pletz, M. W.; Schiller, A., Bactericidal Effect of a Photoresponsive Carbon Monoxide-Releasing Nonwoven against Staphylococcus aureus Biofilms. *Antimicrob. Agents Chemother.* **2016**, *60* (7), 4037-46.
67. Wright, M. A.; Wright, J. A., PhotoCORMs: CO release moves into the visible. *Dalton Trans.* **2016**, *45* (16), 6801-6811.
68. Pierri, A. E.; Pallaoro, A.; Wu, G.; Ford, P. C., A luminescent and biocompatible photoCORM. *J. Am. Chem. Soc.* **2012**, *134* (44), 18197-200.
69. Soboleva, T.; Esquer, H. J.; Benninghoff, A. D.; Berreau, L. M., Sense and Release: A Thiol-Responsive Flavonol-Based Photonically Driven Carbon Monoxide-Releasing Molecule That Operates via a Multiple-Input AND Logic Gate. *J. Am. Chem. Soc.* **2017**, *139* (28), 9435-9438.
70. G, U. R.; Axthelm, J.; Hoffmann, P.; Taye, N.; Gläser, S.; Görls, H.; Hopkins, S. L.; Plass, W.; Neugebauer, U.; Bonnet, S.; Schiller, A., Co-Registered Molecular Logic Gate with a CO-Releasing Molecule Triggered by Light and Peroxide. *J. Am. Chem. Soc.* **2017**, *139* (14), 4991-4994.
71. Bhattacharyya, A.; Chattopadhyay, R.; Mitra, S.; Crowe, S. E., Oxidative Stress: An Essential Factor in the Pathogenesis of Gastrointestinal Mucosal Diseases. *Physiol. Rev.* **2014**, *94* (2), 329-354.
72. Pan, Z.; Chittavong, V.; Li, W.; Zhang, J.; Ji, K.; Zhu, M.; Ji, X.; Wang, B., Organic CO-prodrugs: Structure CO-release rate relationship Studies. *Chem. Eur. J.* **2017**, *23*, 9838-9845.

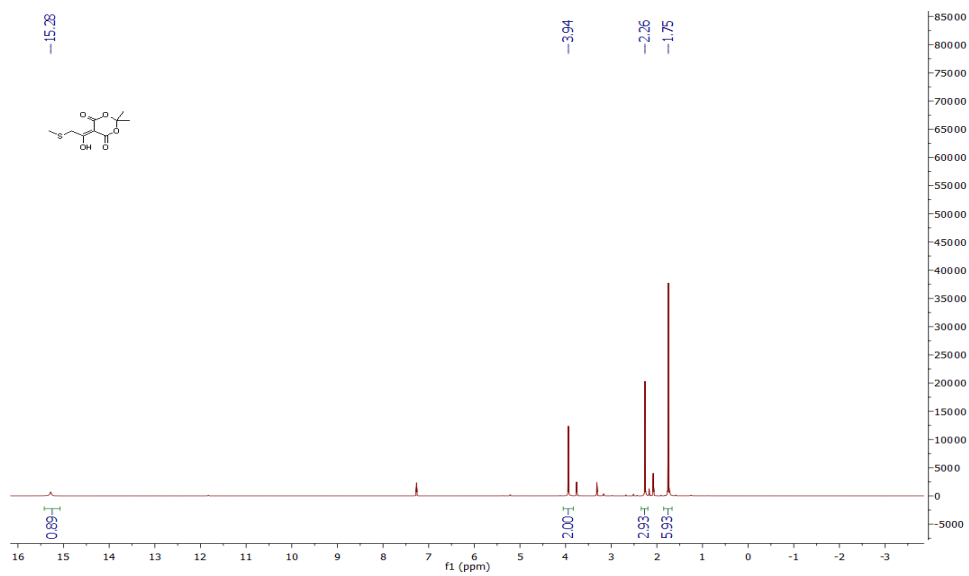
73. Eguchi, S.; Ishiura, K.; Noda, T.; Sasaki, T., Synthesis and cycloaddition reactions of homoadamantano[4,5-c]cyclopentadienones. A facile route to [4,5]-fused homoadamantanobenzene derivatives. *J. Org. Chem.* **1987**, *52* (4), 496-500.
74. Manjare, S. T.; Kim, Y.; Churchill, D. G., Selenium- and Tellurium-Containing Fluorescent Molecular Probes for the Detection of Biologically Important Analytes. *Acc. Chem. Res.* **2014**, *47* (10), 2985-2998.
75. Reich, H. J., Functional group manipulation using organoselenium reagents. *Acc. Chem. Res.* **1979**, *12* (1), 22-30.
76. Vancauwenbergh, R.; Robberecht, H.; Deelstra, H.; Picramenos, D.; Kostakopoulos, A., Selenium Concentration in Serum of Healthy Greek Adults. *J Trace Elem Electrolytes Health Dis* **1994**, *8* (2), 99-109.
77. Soriano-Garcia, M., Organoselenium compounds as potential therapeutic and chemopreventive agents: a review. *Curr. Med. Chem.* **2004**, *11* (12), 1657-69.
78. Meotti, F. C.; Borges, V. C.; Zeni, G.; Rocha, J. B.; Nogueira, C. W., Potential renal and hepatic toxicity of diphenyl diselenide, diphenyl ditelluride and Ebselen for rats and mice. *Toxicol Lett* **2003**, *143* (1), 9-16.
79. Foster, L. H.; Sumar, S., Selenium in health and disease: a review. *Crit. Rev. Food Sci. Nutr.* **1997**, *37* (3), 211-28.
80. Wyatt, A. R.; Kumita, J. R.; Mifsud, R. W.; Gooden, C. A.; Wilson, M. R.; Dobson, C. M., Hypochlorite-induced structural modifications enhance the chaperone activity of human $\alpha(2)$ -macroglobulin. *Proc. Natl. Acad. Sci. U.S.A.* **2014**, *111* (20), E2081-E2090.
81. Allen, B. L.; Johnson, J. D.; Walker, J. P., Encapsulation and Enzyme-Mediated Release of Molecular Cargo in Polysulfide Nanoparticles. *ACS Nano* **2011**, *5* (6), 5263-5272.
82. Chen, X.; Zhong, Z.; Xu, Z.; Chen, L.; Wang, Y., 2',7'-Dichlorodihydrofluorescein as a fluorescent probe for reactive oxygen species measurement: Forty years of application and controversy. *Free Radic. Res.* **2010**, *44* (6), 587-604.
83. Bagnoli, L.; Scarponi, C.; Rossi, M. G.; Testaferri, L.; Tiecco, M., Synthesis of enantiopure 1,4-dioxanes, morpholines, and piperazines from the reaction of chiral 1,2-diols, amino alcohols, and diamines with vinyl selenones. *Chemistry* **2011**, *17* (3), 993-9.
84. Huang, X.; Xu, J. F., One-Pot Facile Synthesis of Substituted Isoindolinones via an Ugi Four-Component Condensation/Diels-Alder Cycloaddition/Deselenization-Aromatization Sequence. *Journal of Organic Chemistry* **2009**, *74* (22), 8859-8861.
85. Zhao, Y.; Pluth, M. D., Hydrogen Sulfide Donors Activated by Reactive Oxygen Species. *Angewandte Chemie-International Edition* **2016**, *55* (47), 14638-14642.
86. Motterlini, R.; Otterbein, L. E., The therapeutic potential of carbon monoxide. *Nat. Rev. Drug Discov.* **2010**, *9* (9), 728-743.
87. Ji, X.; Damera, K.; Zheng, Y.; Yu, B.; Otterbein, L. E.; Wang, B., Toward carbon monoxide-based therapeutics: critical drug delivery and developability issues. *J. Pharm. Sci.* **2016**, *105* (2), 406-16.
88. Romao, C. C.; Blattler, W. A.; Seixas, J. D.; Bernardes, G. J., Developing drug molecules for therapy with carbon monoxide. *Chem. Soc. Rev.* **2012**, *41* (9), 3571-83.
89. Wu, L.; Wang, R., Carbon monoxide: endogenous production, physiological functions, and pharmacological applications. *Pharmacol Rev* **2005**, *57* (4), 585-630.
90. Otterbein, L. E., Carbon monoxide: innovative anti-inflammatory properties of an age-old gas molecule. *Antioxid Redox Signal* **2002**, *4* (2), 309-19.

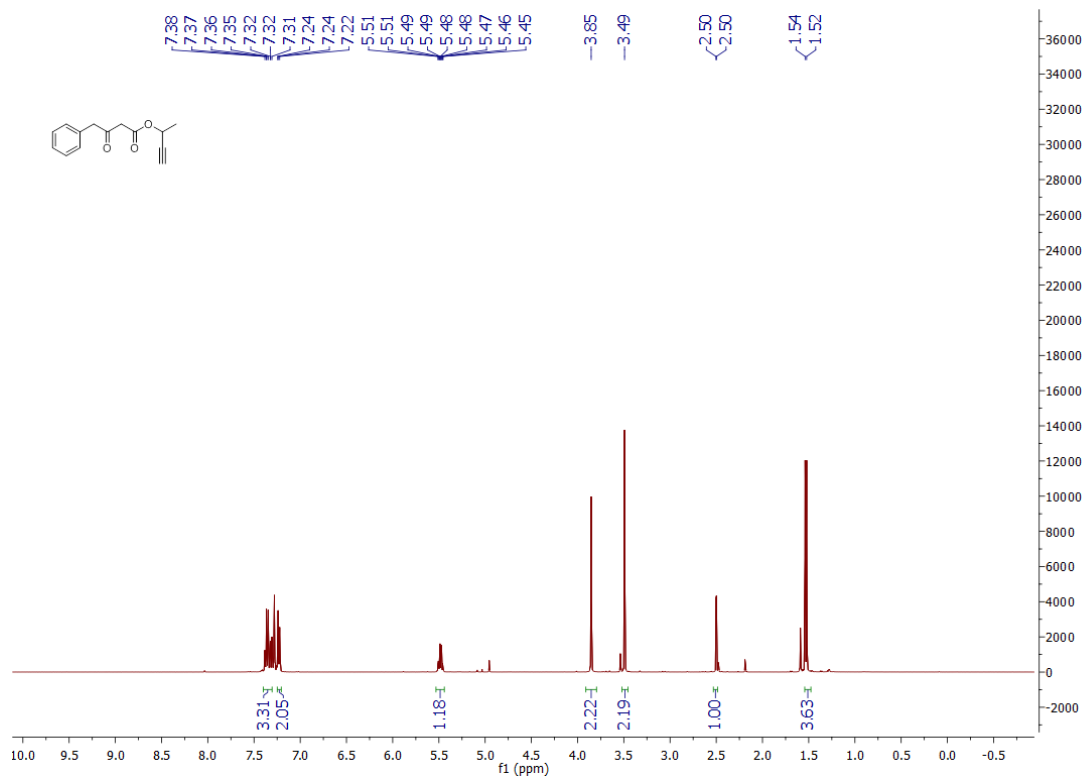
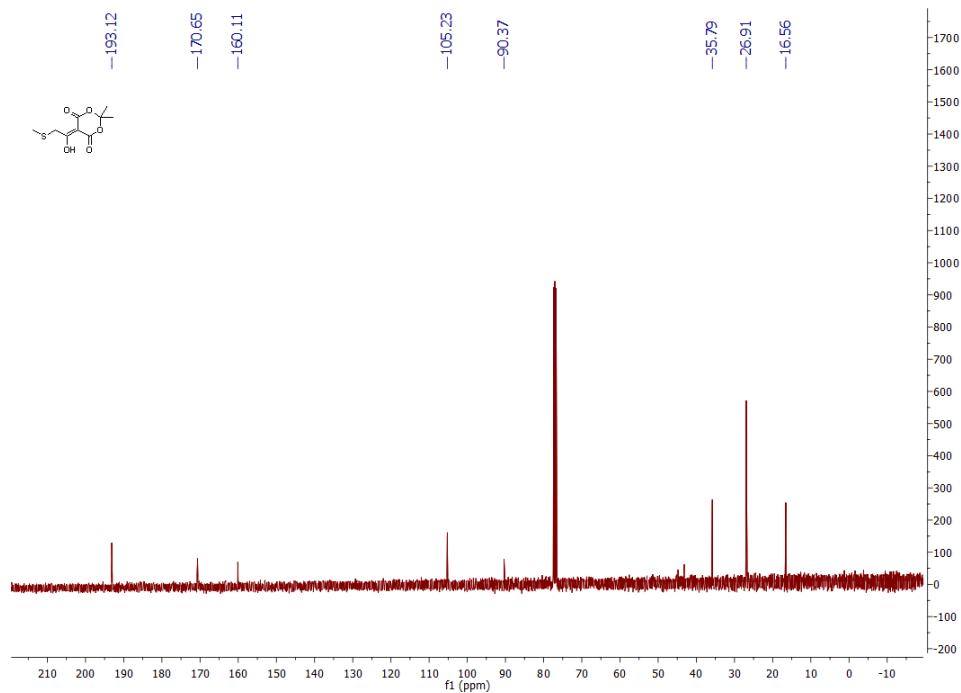
91. Takagi, T.; Uchiyama, K.; Naito, Y., The Therapeutic Potential of Carbon Monoxide for Inflammatory Bowel Disease. *Digestion* **2015**, *91* (1), 13-18.
92. Nakahira, K.; Choi, A. M., Carbon monoxide in the treatment of sepsis. *Am. J. Physiol. Lung Cell Mol. Physiol.* **2015**, *309* (12), L1387-93.
93. Ozaki, K. S.; Kimura, S.; Murase, N., Use of carbon monoxide in minimizing ischemia/reperfusion injury in transplantation. *Transplant. Rev.* **2012**, *26* (2), 125-139.
94. Kroschinsky, F.; Stölzel, F.; von Bonin, S.; Beutel, G.; Kochanek, M.; Kiehl, M.; Schellongowski, P.; Intensive Care in, H.; Oncological Patients Collaborative, G., New drugs, new toxicities: severe side effects of modern targeted and immunotherapy of cancer and their management. *Crit. care* **2017**, *21* (1), 89-89.
95. Canna, S. W.; Behrens, E. M., Making sense of the cytokine storm: a conceptual framework for understanding, diagnosing, and treating hemophagocytic syndromes. *Pediatr. Clin. North Am.* **2012**, *59* (2), 329-344.
96. Lee, D. W.; Gardner, R.; Porter, D. L.; Louis, C. U.; Ahmed, N.; Jensen, M.; Grupp, S. A.; Mackall, C. L., Current concepts in the diagnosis and management of cytokine release syndrome. *Blood* **2014**, *124* (2), 188-195.
97. Rosas, I. O.; Goldberg, H. J.; Collard, H. R.; El-Chemaly, S.; Flaherty, K.; Hunninghake, G. M.; Lasky, J. A.; Lederer, D. J.; Machado, R.; Martinez, F. J.; Maurer, R.; Teller, D.; Noth, I.; Peters, E.; Raghu, G.; Garcia, J. G. N.; Choi, A. M. K., A Phase II Clinical Trial of Low-Dose Inhaled Carbon Monoxide in Idiopathic Pulmonary Fibrosis. *Chest* **2018**, *153* (1), 94-104.
98. Garcia-Gallego, S.; Bernardes, G. J., Carbon-monoxide-releasing molecules for the delivery of therapeutic CO in vivo. *Angew. Chem. Int. Ed.* **2014**, *53* (37), 9712-21.
99. Atkin, A. J.; Williams, S.; Sawle, P.; Motterlini, R.; Lynam, J. M.; Fairlamb, I. J., Mu₂-alkyne dicobalt(0)hexacarbonyl complexes as carbon monoxide-releasing molecules (CO-RMs): probing the release mechanism. *Dalton Trans.* **2009**, (19), 3653-6.
100. Clark, J. E.; Naughton, P.; Shurey, S.; Green, C. J.; Johnson, T. R.; Mann, B. E.; Foresti, R.; Motterlini, R., Cardioprotective actions by a water-soluble carbon monoxide-releasing molecule. *Circ. Res.* **2003**, *93* (2), e2-8.
101. Henry, L.; Schneider, C.; Mutzel, B.; Simpson, P. V.; Nagel, C.; Fucke, K.; Schatzschneider, U., Amino acid bioconjugation via iClick reaction of an oxanorbornadiene-masked alkyne with a Mn(I)(bpy)(CO)₃-coordinated azide. *Chem. Commun.* **2014**, *50* (99), 15692-5.
102. Marques, A. R.; Kromer, L.; Gallo, D. J.; Penacho, N.; Rodrigues, S. S.; Seixas, J. D.; Bernardes, G. J. L.; Reis, P. M.; Otterbein, S. L.; Ruggieri, R. A.; Gonçalves, A. S. G.; Gonçalves, A. M. L.; Matos, M. N. D.; Bento, I.; Otterbein, L. E.; Blättler, W. A.; Romão, C. C., Generation of carbon monoxide releasing molecules (CO-RMs) as drug candidates for the treatment of acute liver injury: targeting of CO-RMs to the liver. *Organometallics* **2012**, *31* (16), 5810-5822.
103. Zobi, F.; Degonda, A.; Schaub, M. C.; Bogdanova, A. Y., CO releasing properties and cytoprotective effect of cis-trans- [ReII(CO)₂Br₂L₂]_n complexes. *Inorg. Chem.* **2010**, *49* (16), 7313-7322.
104. Zhang, W.-Q.; Whitwood, A. C.; Fairlamb, I. J. S.; Lynam, J. M., Group 6 carbon monoxide-releasing metal complexes with biologically-compatible leaving groups. *Inorg. Chem.* **2010**, *49* (19), 8941-8952.

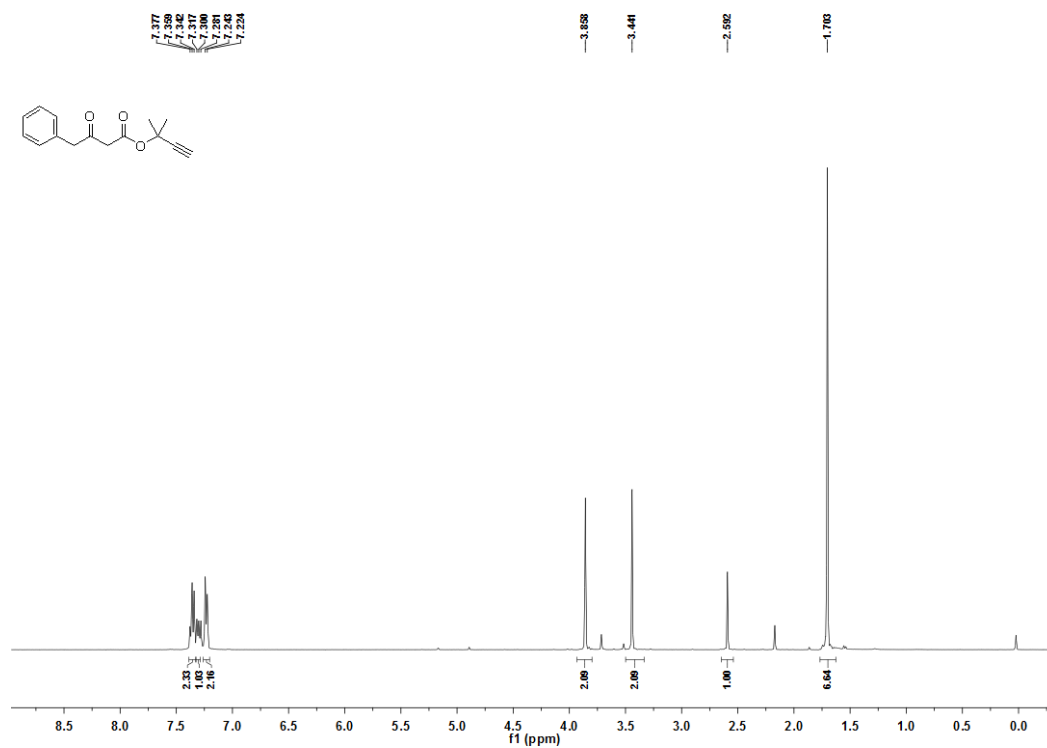
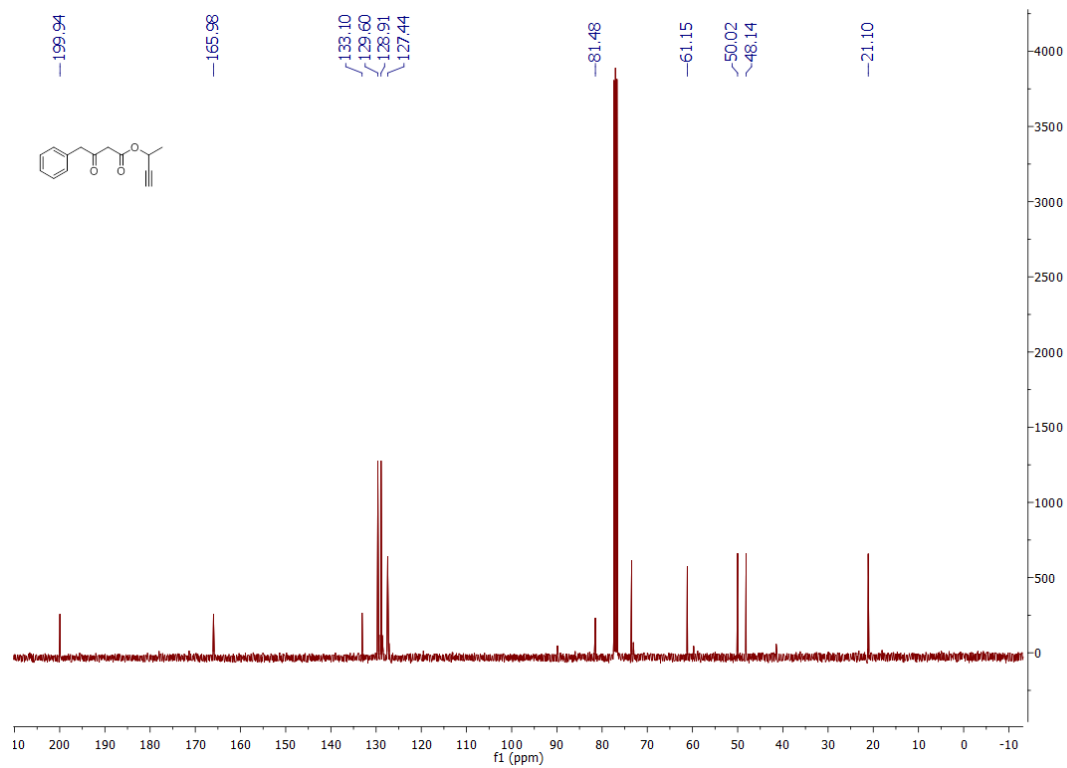
105. Schatzschneider, U., Novel lead structures and activation mechanisms for CO-releasing molecules (CORMs). *Br. J. Pharma.* **2015**, *172* (6), 1638-1650.
106. Nobre, L. S.; Jeremias, H.; Romao, C. C.; Saraiva, L. M., Examining the antimicrobial activity and toxicity to animal cells of different types of CO-releasing molecules. *Dalton Trans.* **2016**, *45* (4), 1455-1466.
107. Nakae, T.; Hirotsu, M.; Aono, S.; Nakajima, H., Visible-light-induced release of CO by thiolate iron(III) carbonyl complexes bearing N,C,S-pincer ligands. *Dalton Trans.* **2016**, *45* (41), 16153-16156.
108. Heinemann, S. H.; Hoshi, T.; Westerhausen, M.; Schiller, A., Carbon monoxide--physiology, detection and controlled release. *Chem. Commun.* **2014**, *50* (28), 3644-60.
109. Popova, M.; Soboleva, T.; Ayad, S.; Benninghoff, A. D.; Berreau, L. M., Visible-Light-Activated Quinolone Carbon-Monoxide-Releasing Molecule: Prodrug and Albumin-Assisted Delivery Enables Anticancer and Potent Anti-Inflammatory Effects. *J. Am. Chem. Soc.* **2018**, *140* (30), 9721-9729.
110. Zheng, Y.; Ji, X.; Yu, B.; Ji, K.; Gallo, D.; Csizmadia, E.; Zhu, M.; Choudhury, M. R.; De La Cruz, L. K. C.; Chittavong, V.; Pan, Z.; Yuan, Z.; Otterbein, L. E.; Wang, B., Enrichment-triggered prodrug activation demonstrated through mitochondria-targeted delivery of doxorubicin and carbon monoxide. *Nat. Chem.* **2018**, *10* (7), 787-794.
111. Ji, X.; Zhou, C.; Ji, K.; Aghoghovbia, R. E.; Pan, Z.; Chittavong, V.; Ke, B.; Wang, B., Click and Release: A Chemical Strategy toward Developing Gasotransmitter Prodrugs by Using an Intramolecular Diels–Alder Reaction. *Angew. Chem. Int. Ed.* **2016**, *55*, 15846-15851.
112. Ji, X.; Ji, K.; Chittavong, V.; Yu, B.; Pan, Z.; Wang, B., An esterase-activated click and release approach to metal-free CO-prodrugs. *Chem. Commun.* **2017**, *53* (59), 8296-8299.
113. Kueh, J. T. B.; Stanley, N. J.; Hewitt, R. J.; Woods, L. M.; Larsen, L.; Harrison, J. C.; Rennison, D.; Brimble, M. A.; Sammut, I. A.; Larsen, D. S., Norborn-2-en-7-ones as physiologically-triggered carbon monoxide-releasing prodrugs. *Chem. Sci.* **2017**, *8* (8), 5454-5459.
114. Ji, X.; De La Cruz, L. K. C.; Pan, Z.; Chittavong, V.; Wang, B., pH-Sensitive metal-free carbon monoxide prodrugs with tunable and predictable release rates. *Chem. Commun.* **2017**, *53* (69), 9628-9631.
115. De La Cruz, L. K. C.; Benoit, S.; Pan, Z.; Yu, B.; Maier, R. J.; Ji, X.; Wang, B., Click, release, and fluoresce: a cascade prodrug for co-delivery of carbon monoxide, a drug payload, and a fluorescent reporter. *Org. Lett.* **2018**, DOI: 10.1021/acs.orglett.7b03348.
116. Zheng, Y. J., X.; Yu, B.; Ji, K.; Gallo, D.; Csizmadia, E.; Zhu, M.; Roy Choudhury, M.; De La Cruz, L.; Chittavong, V.; Pan, Z.; Yuan, Z.; Otterbein, L. E.; Wang, B., Enrichment-triggered Prodrug Activation Demonstrated through Mitochondria-targeted Delivery of Doxorubicin and Carbon Monoxide. *Nat. Chem.* **2018**, Accepted manuscript.
117. Wang, W.; Ji, X.; Du, Z.; Wang, B., Sulfur dioxide prodrugs: triggered release of SO₂ via a click reaction. *Chem Commun (Camb)* **2017**, *53* (8), 1370-1373.
118. Maier, L.; Hylse, O.; Nečas, M.; Trbušek, M.; Ytre-Arne, M.; Dalhus, B.; Bjørås, M.; Paruch, K., New carbocyclic nucleosides: synthesis of carbocyclic pseudoisocytidine and its analogs. *Tetrahedron Lett.* **2014**, *55* (27), 3713-3716.
119. Wang, F.; Zhou, R.-J.; Zhao, X.; Ye, H.; Xie, M.-L., Apigenin inhibits ethanol-induced oxidative stress and LPS-induced inflammatory cytokine production in cultured rat hepatocytes. *J. Appl. Biomed.* **2018**, *16* (1), 75-80.

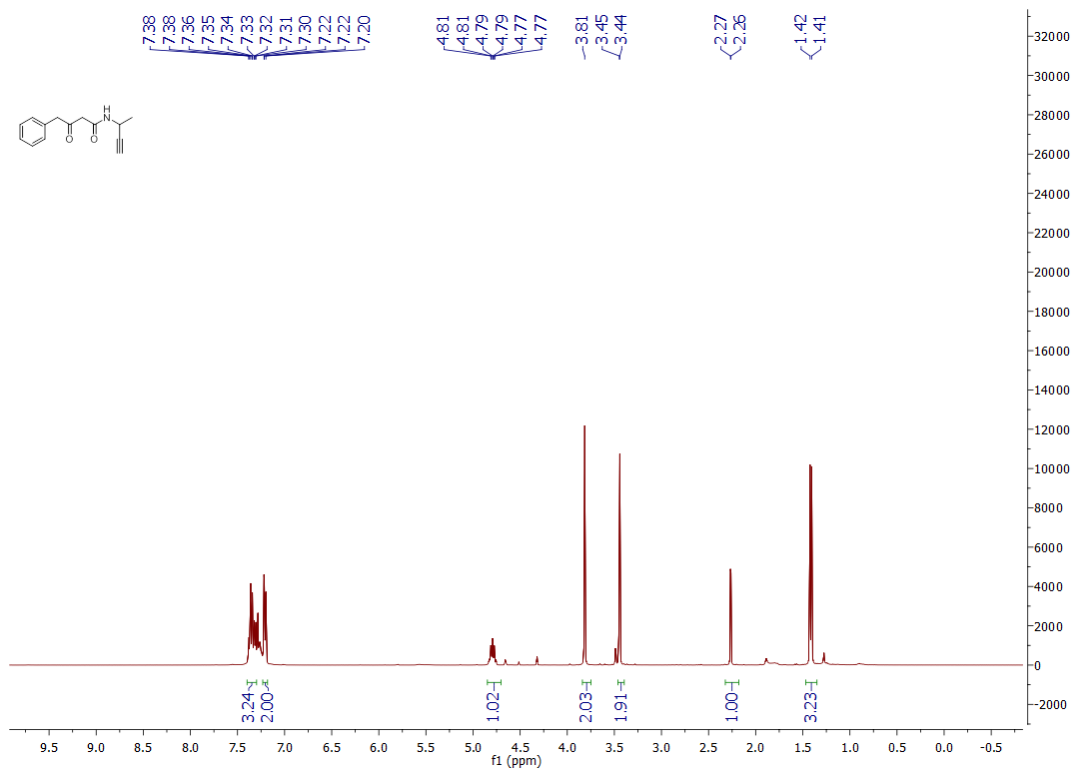
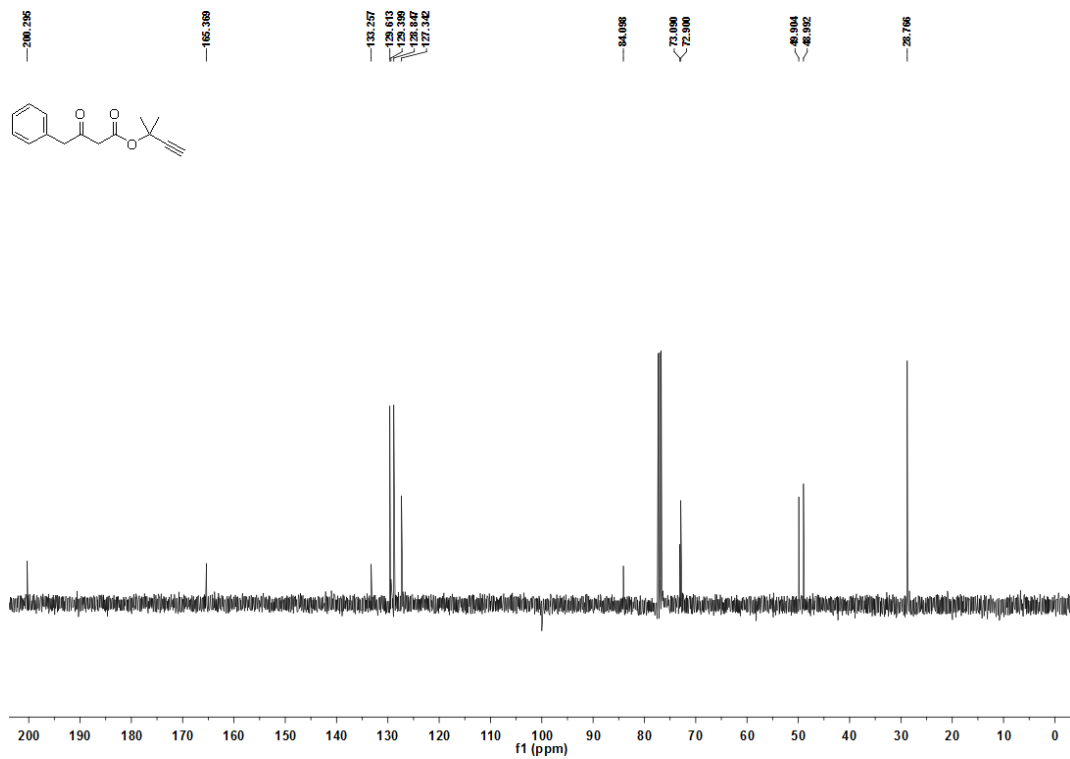
APPENDICES

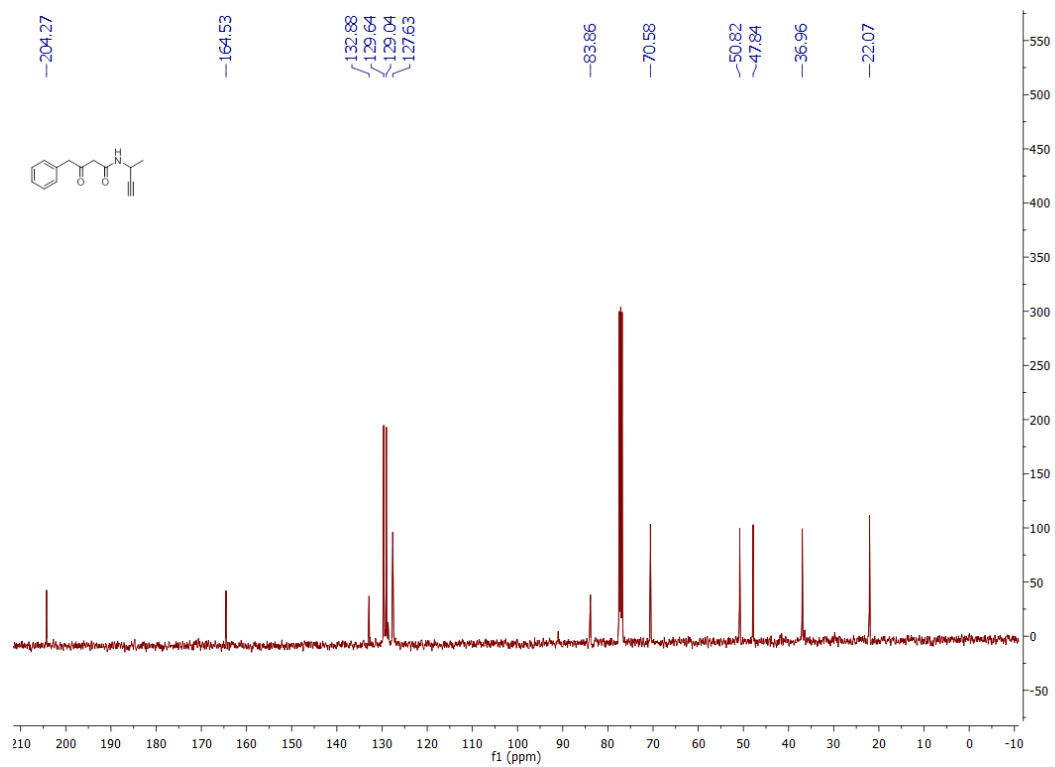
Appendix A Spectra of compounds in the study of structure CO-release rate relationship

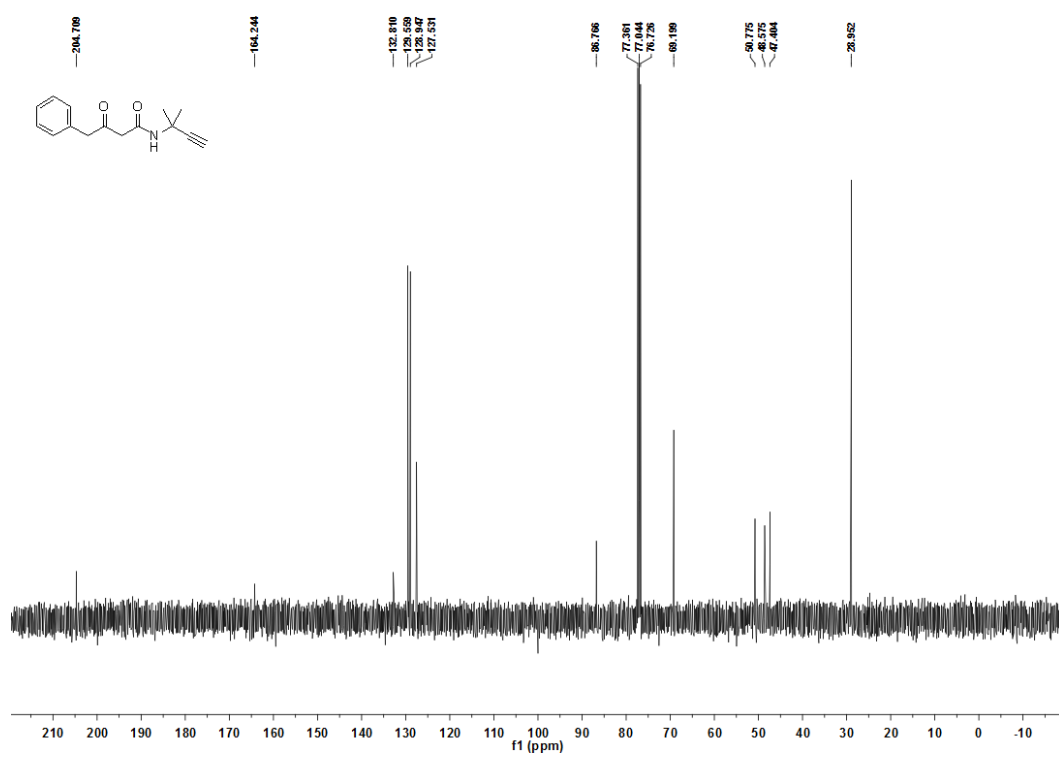
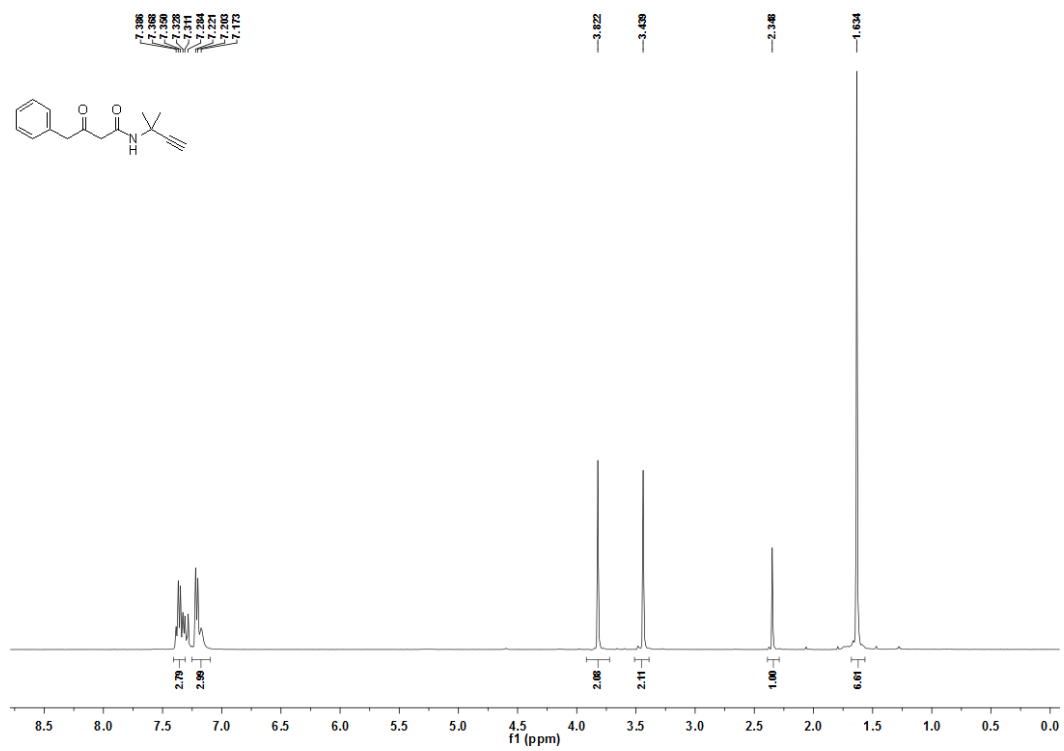


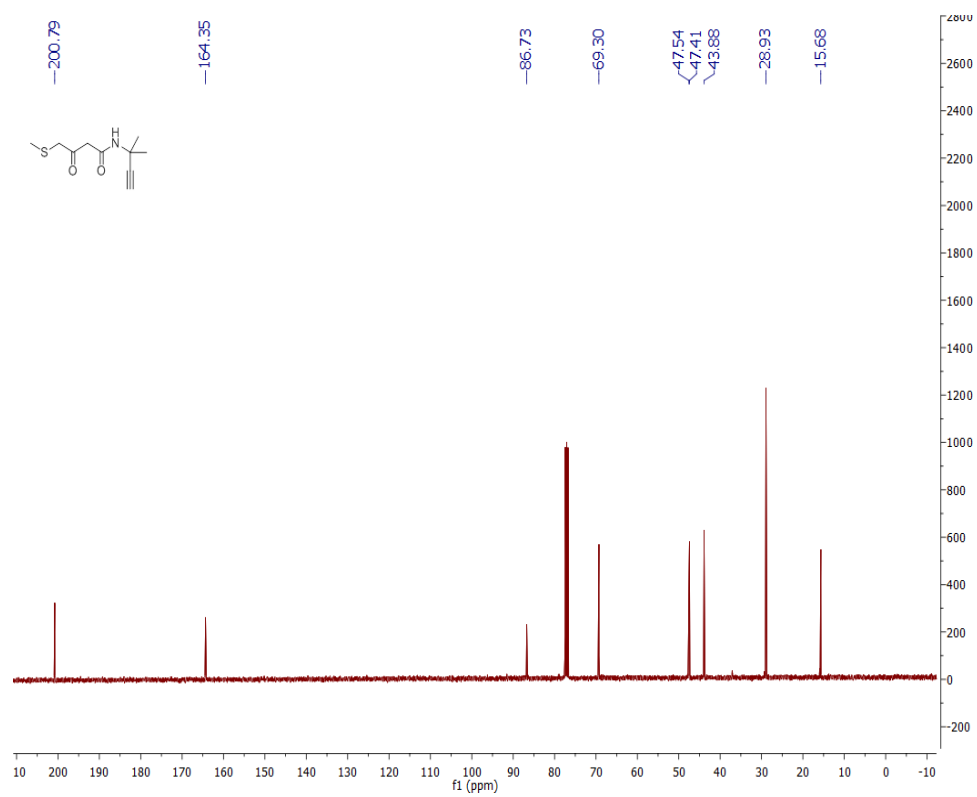
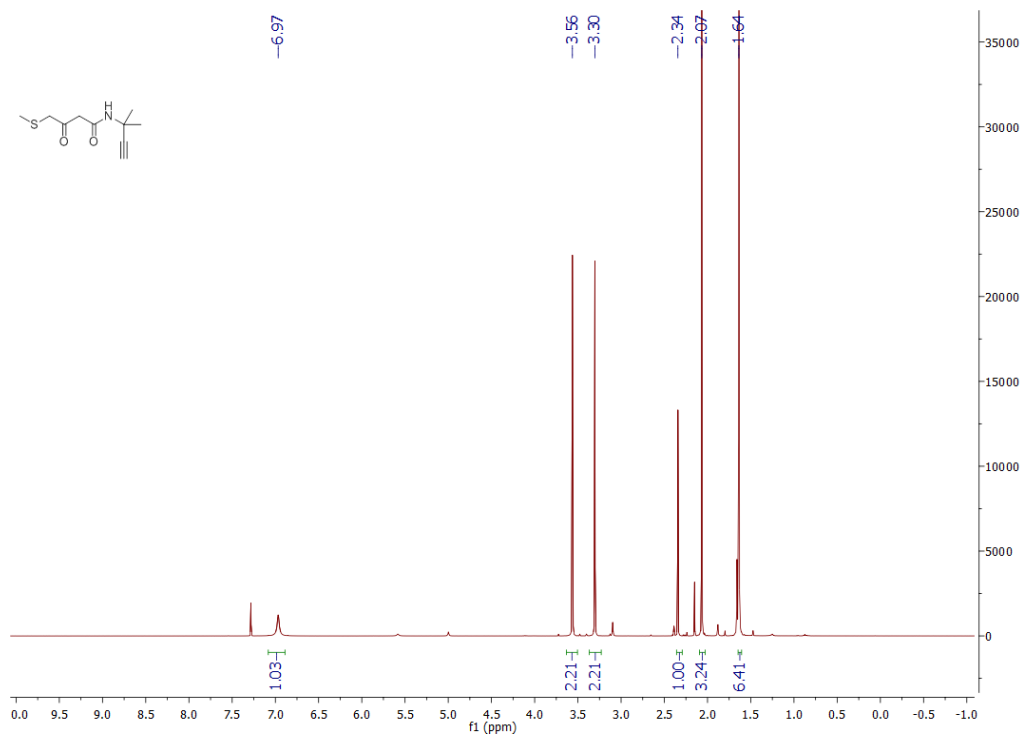


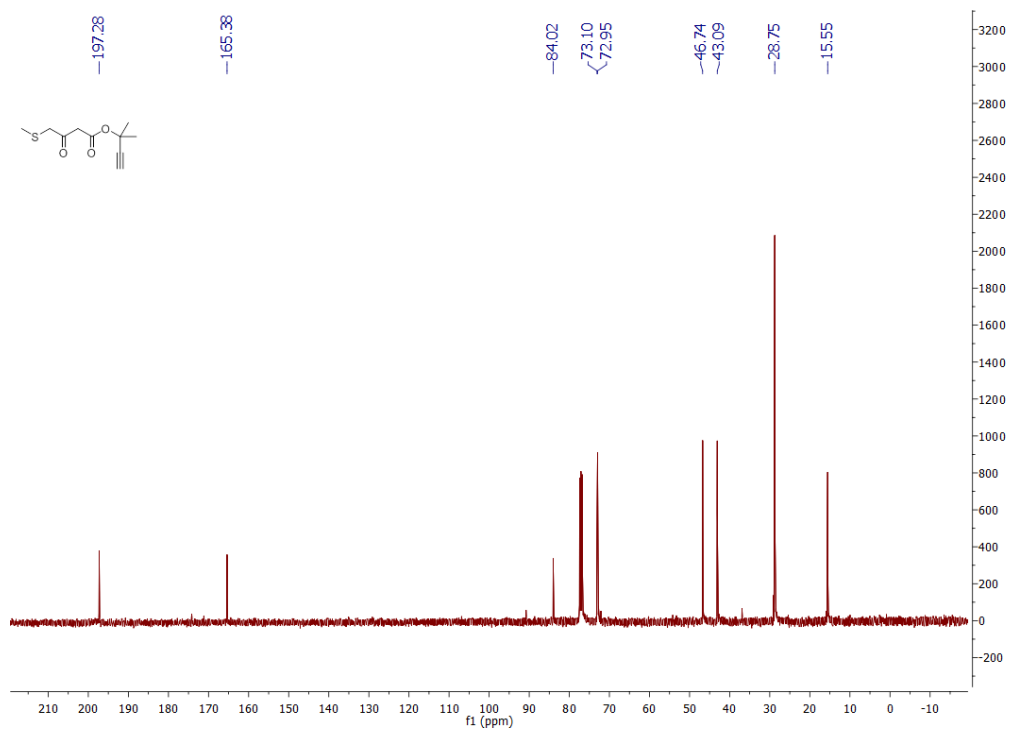
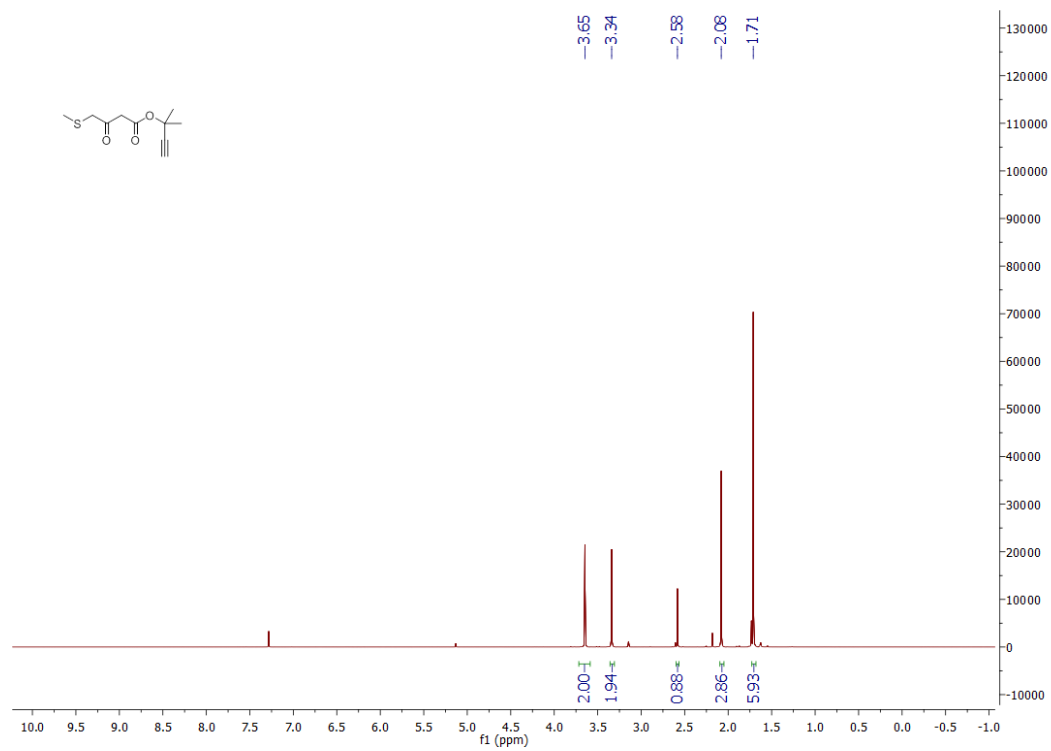


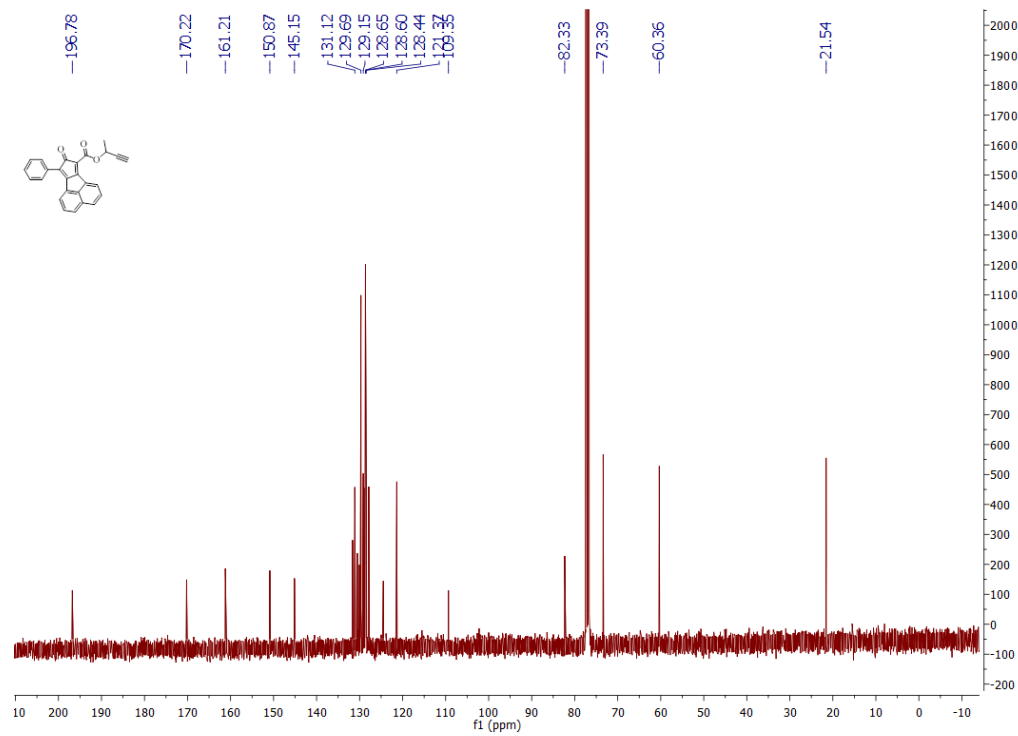
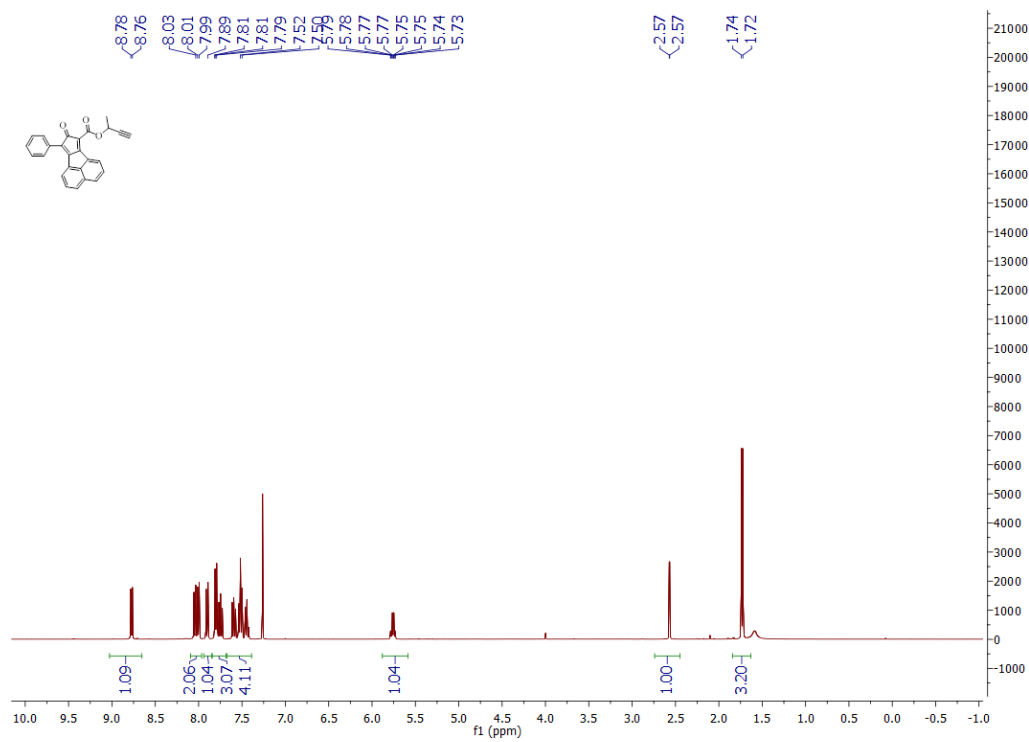


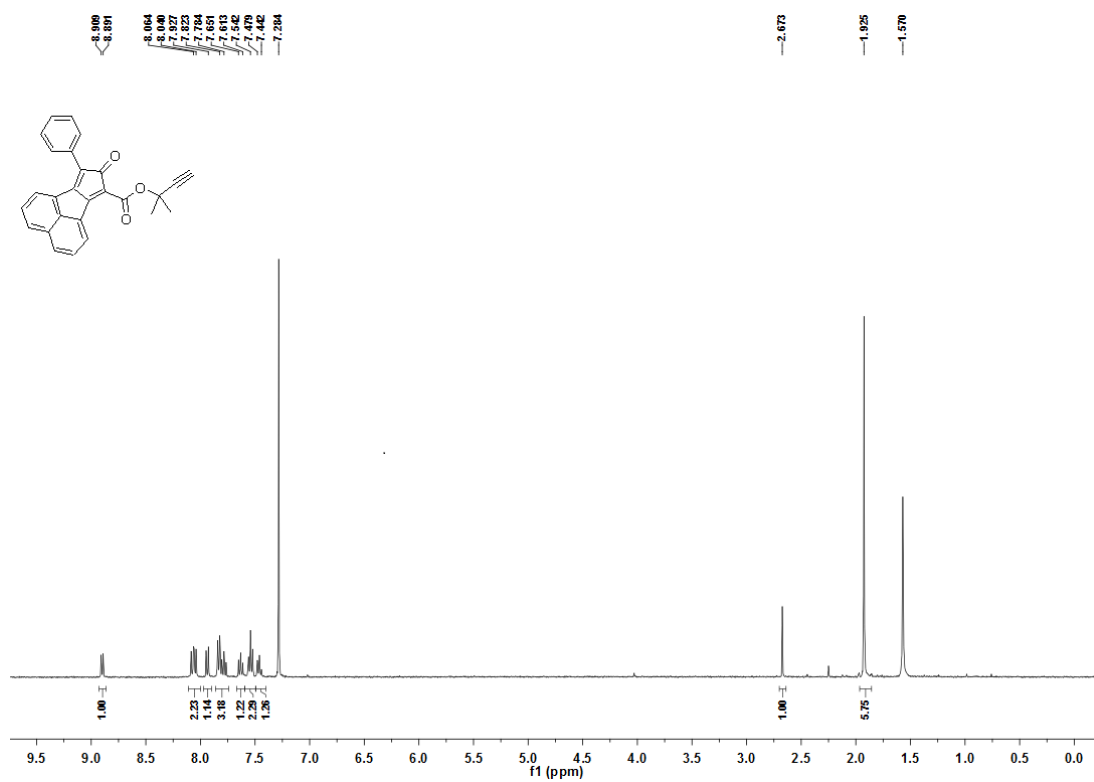
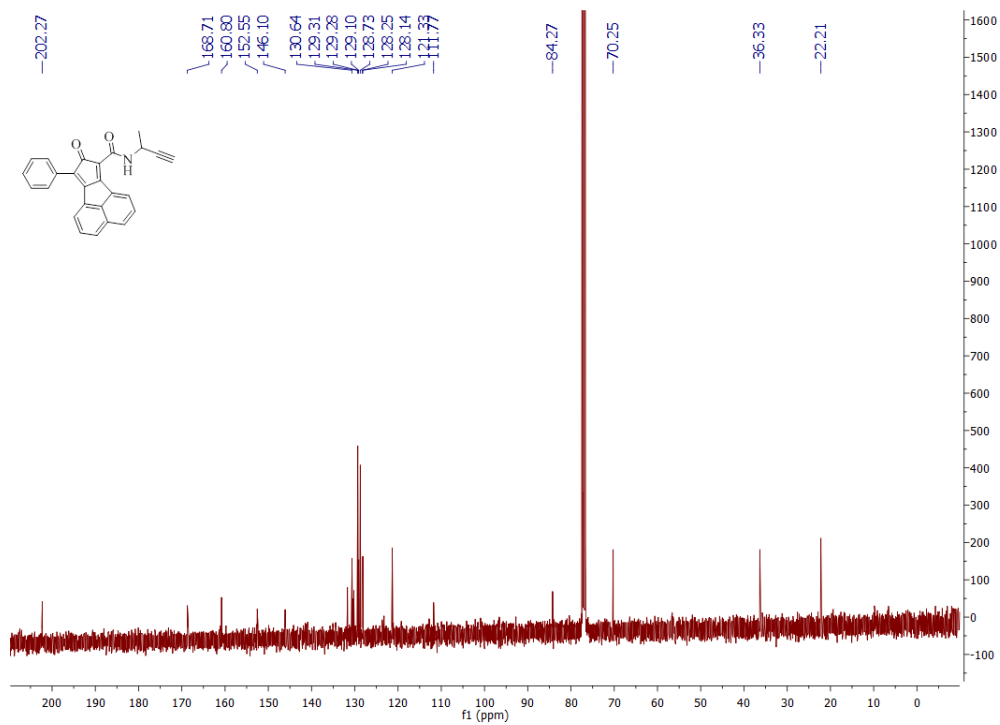


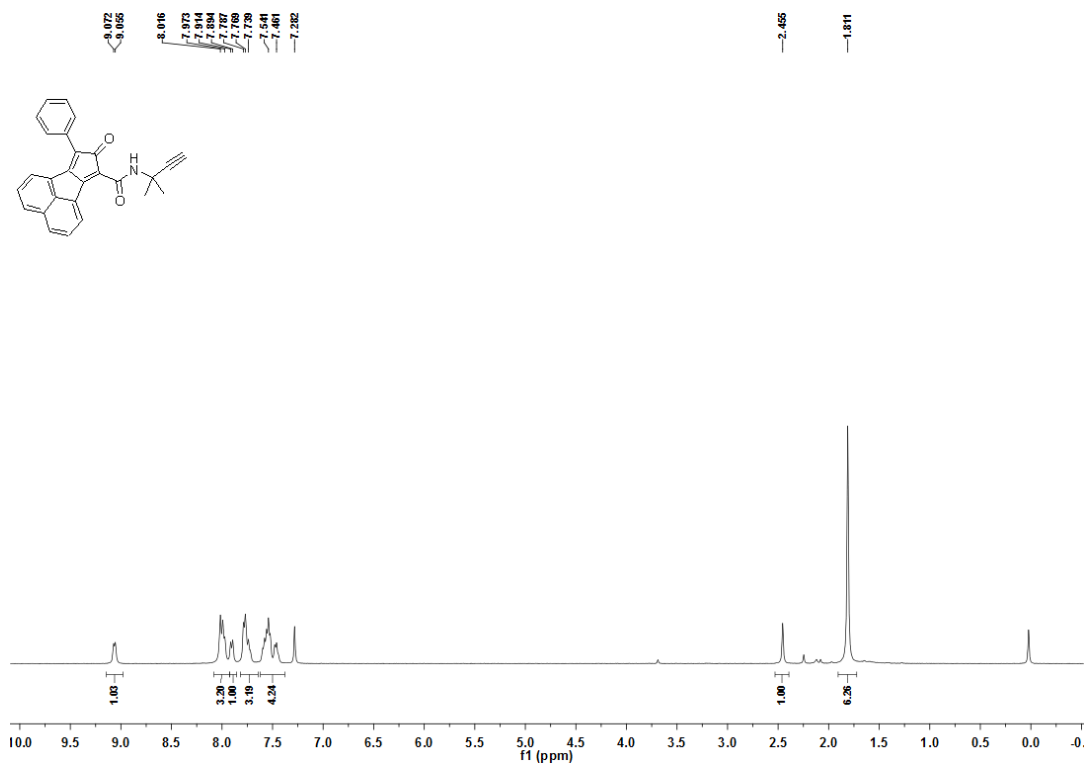
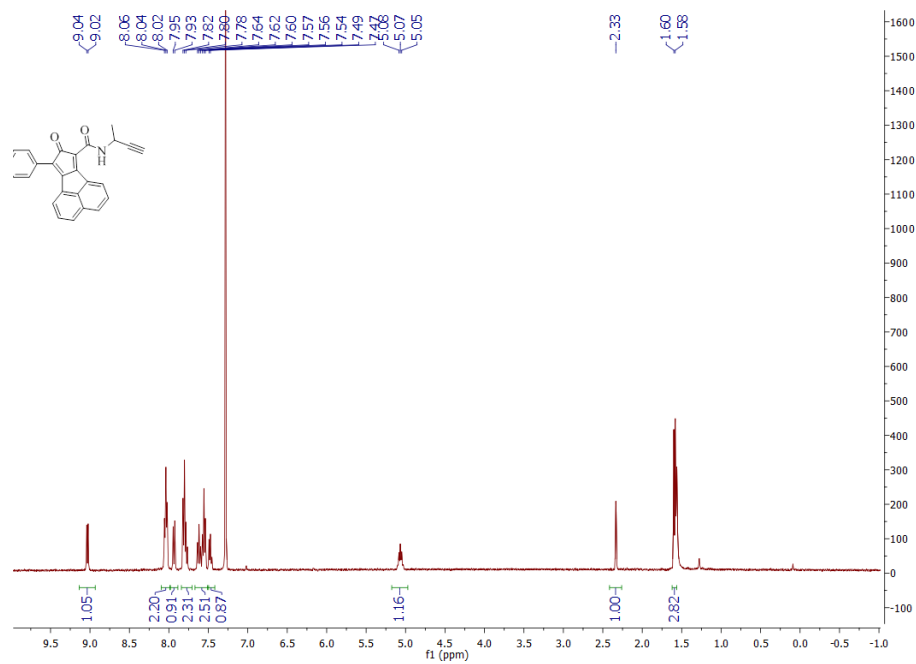


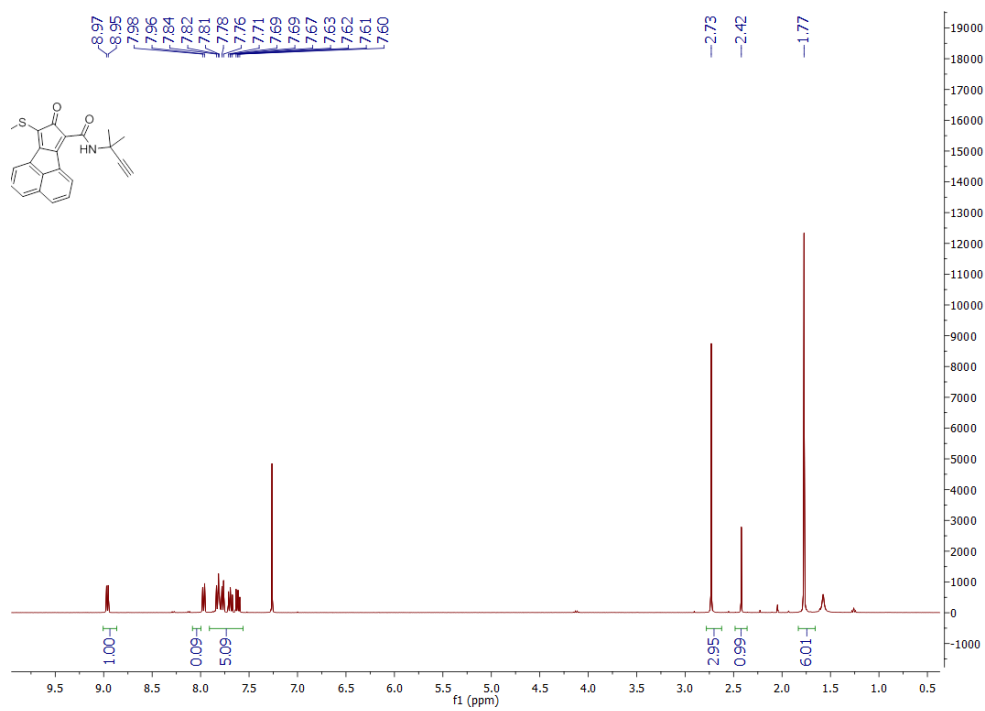
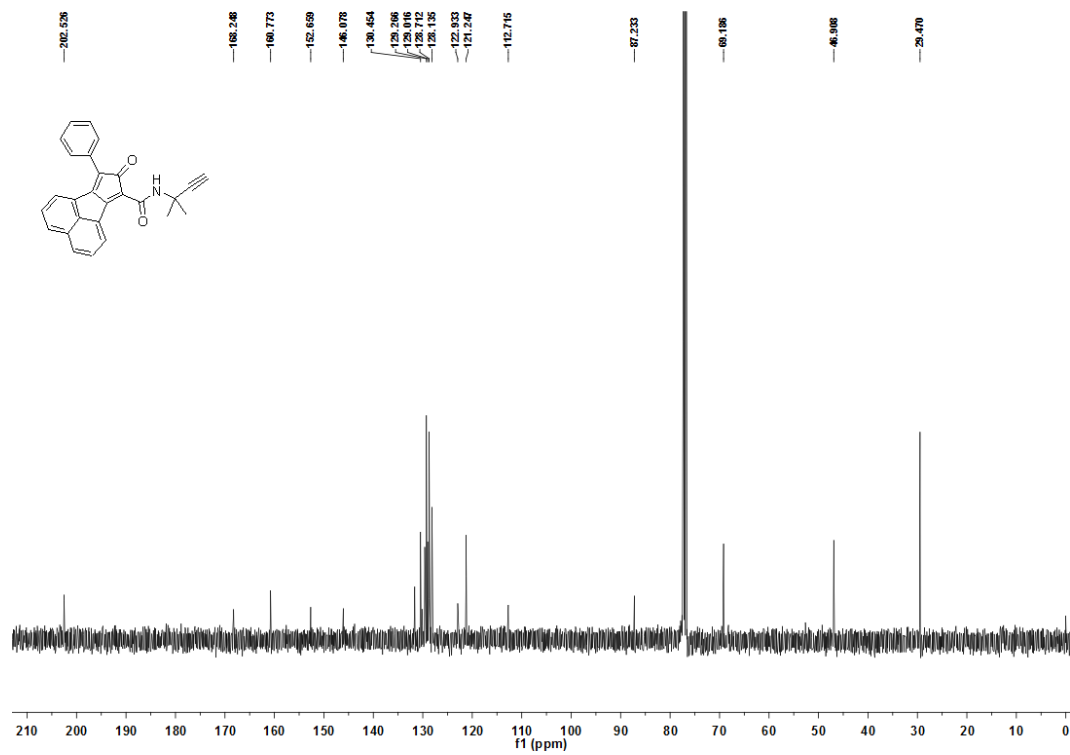


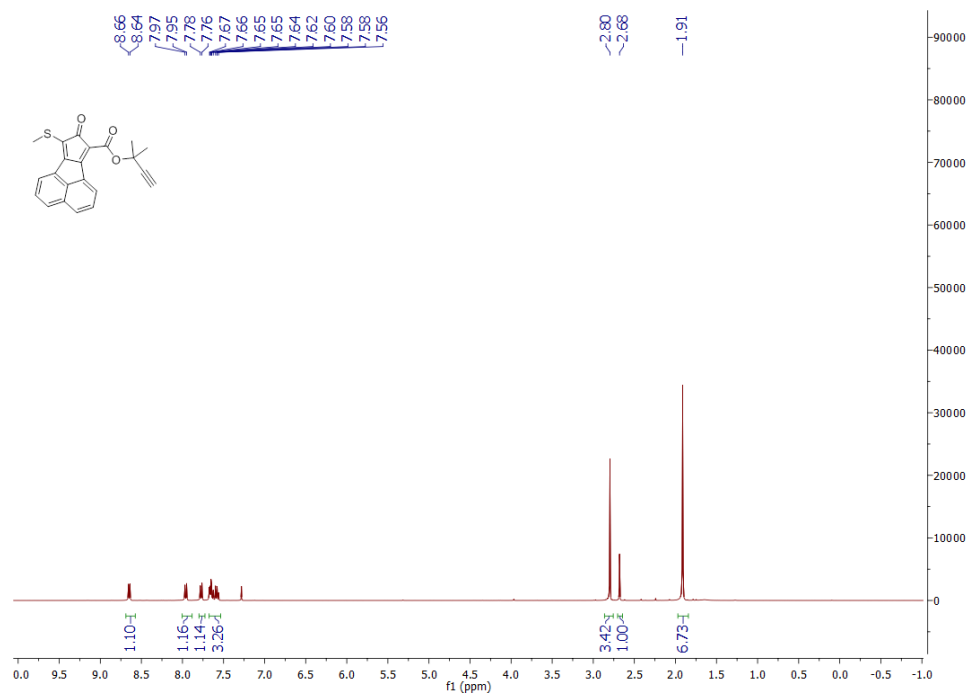
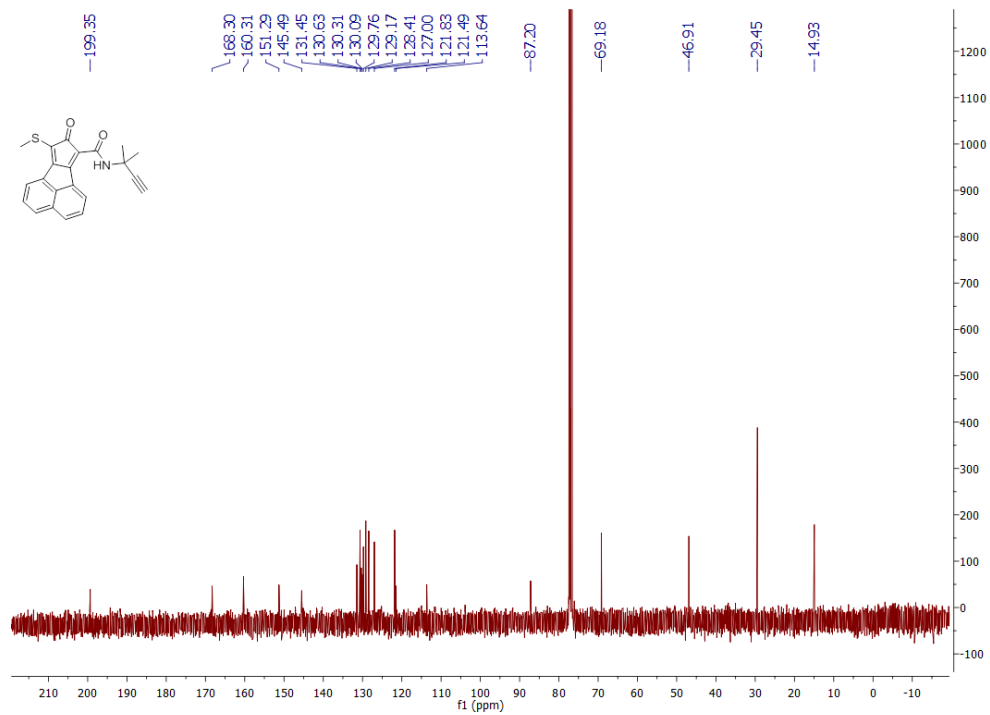


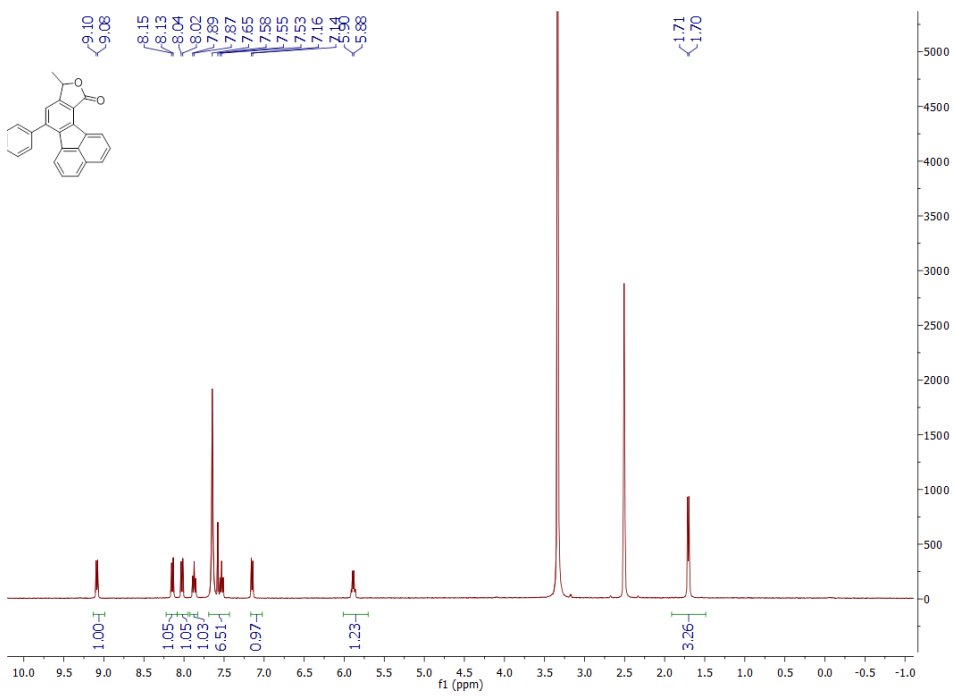
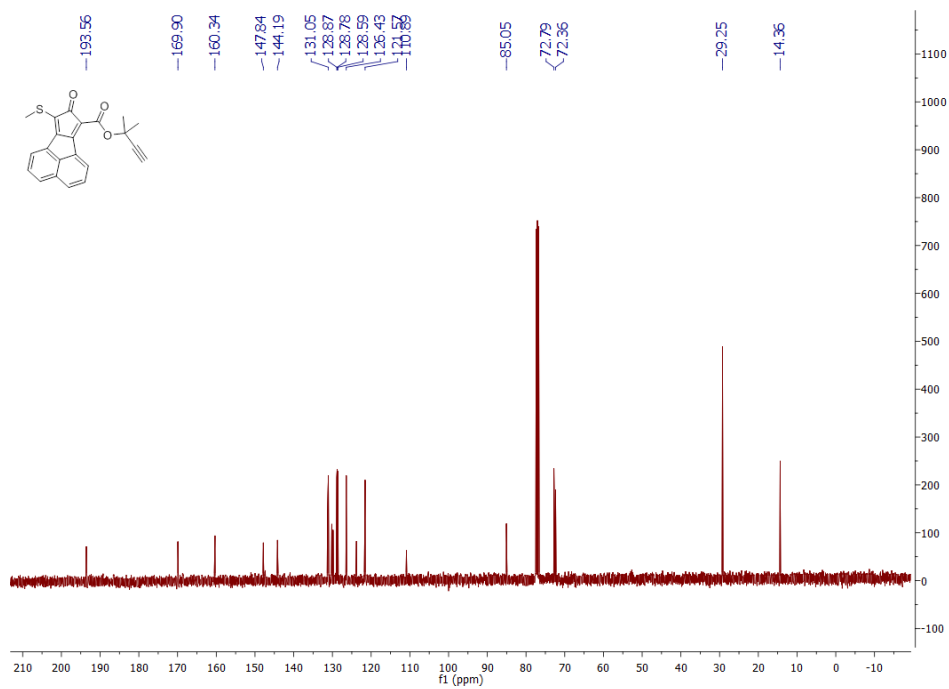


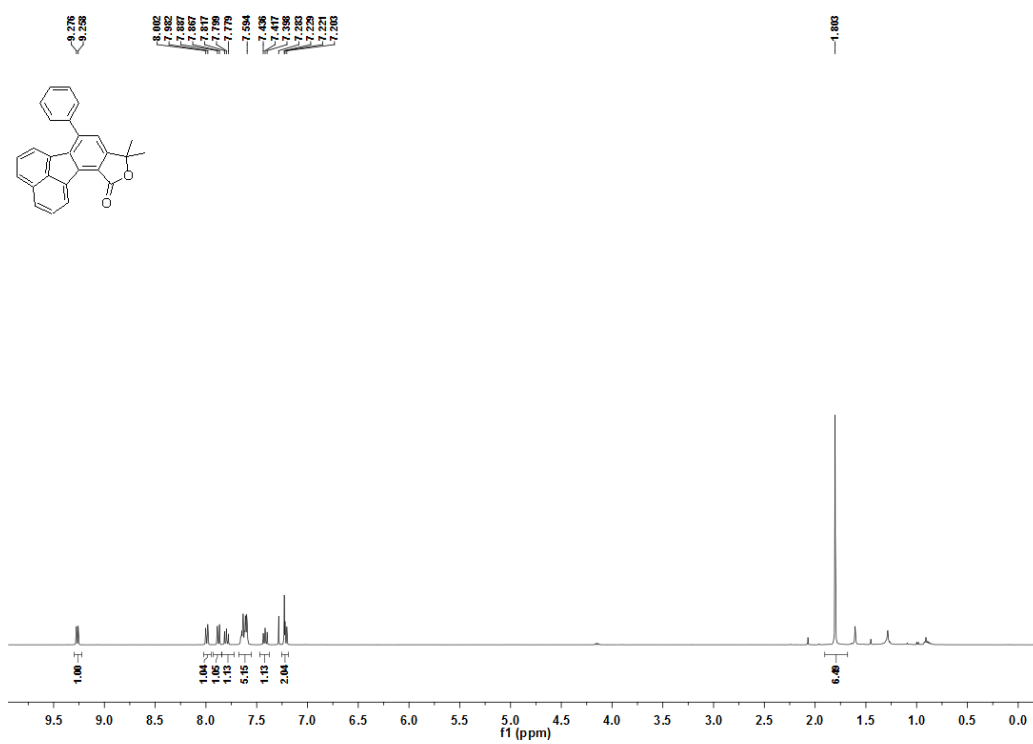
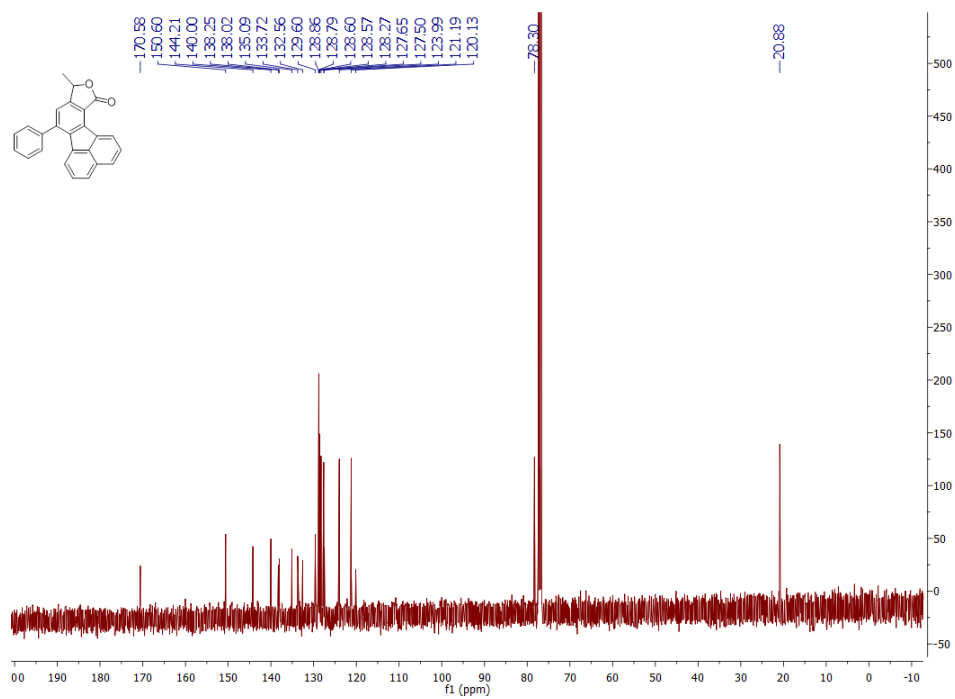


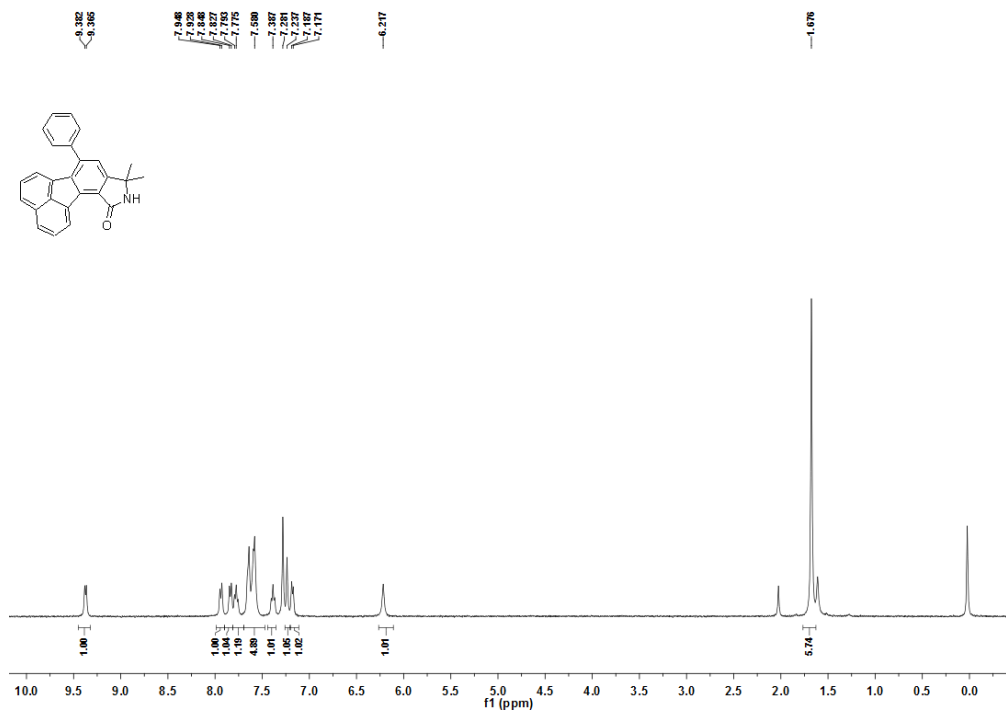
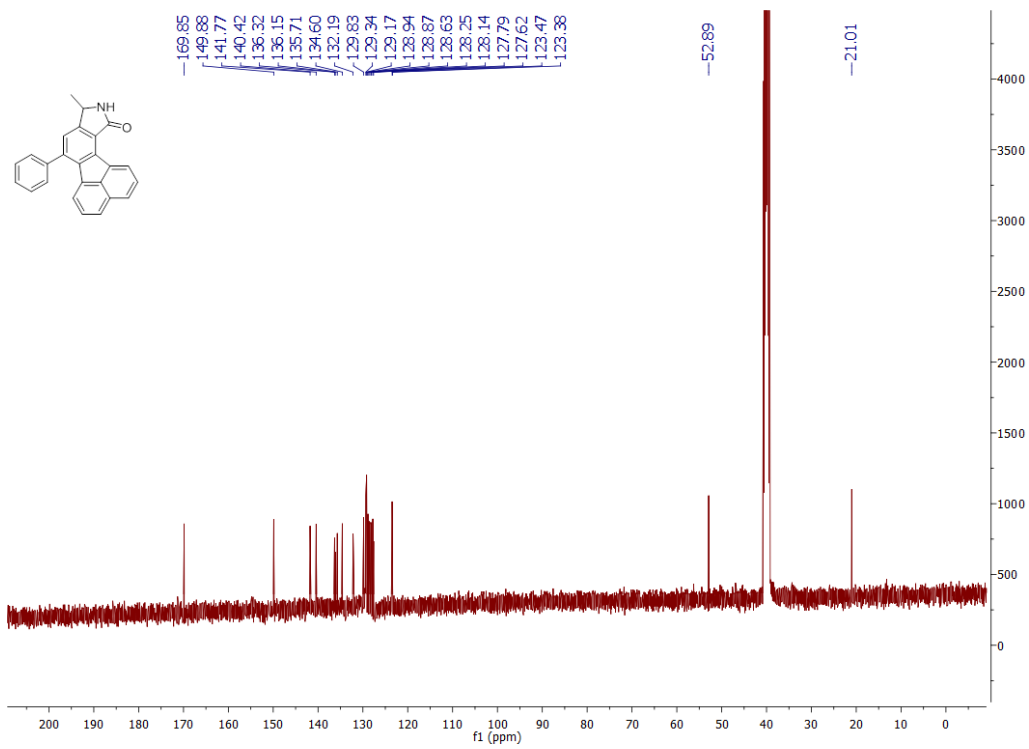


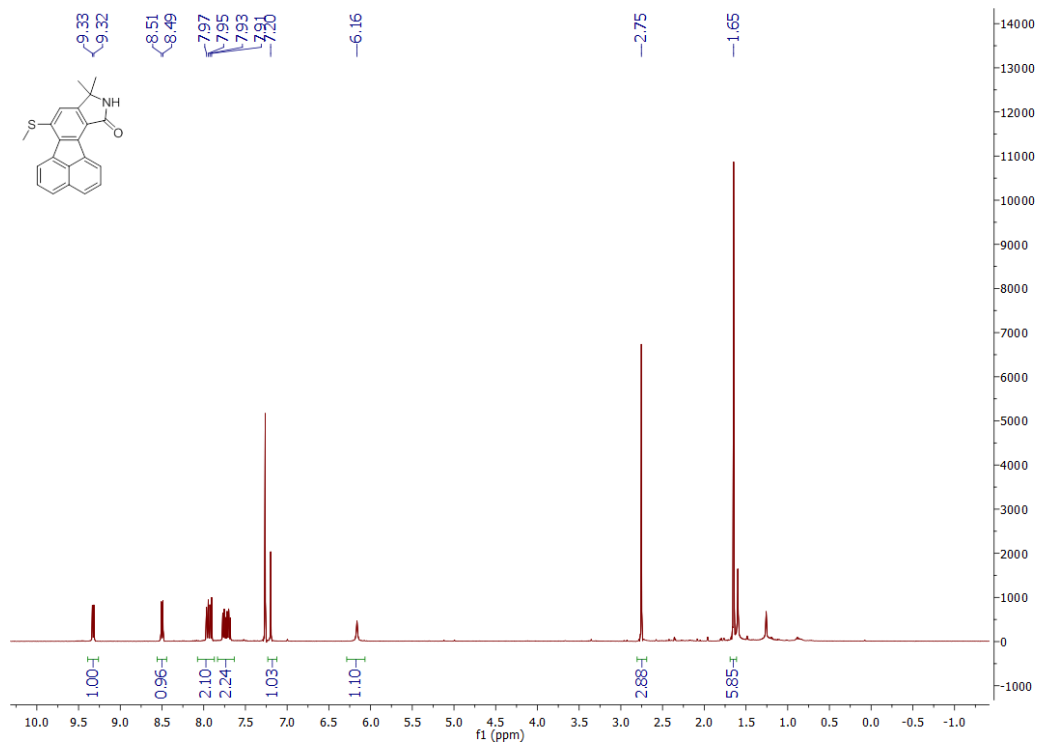
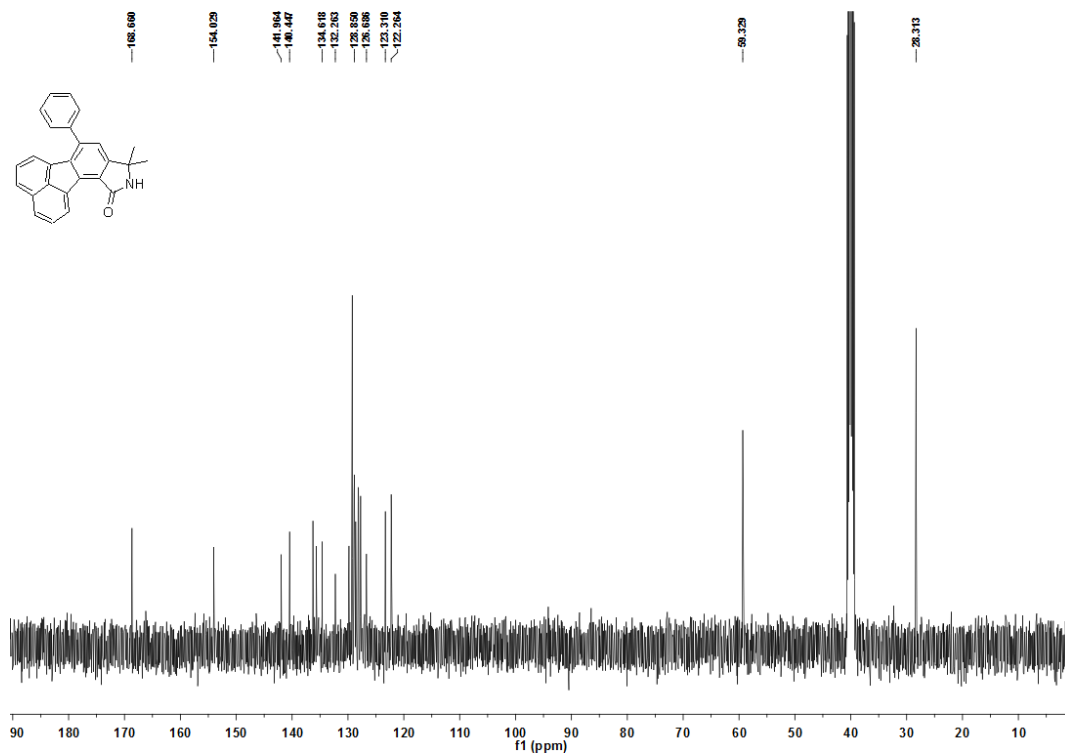


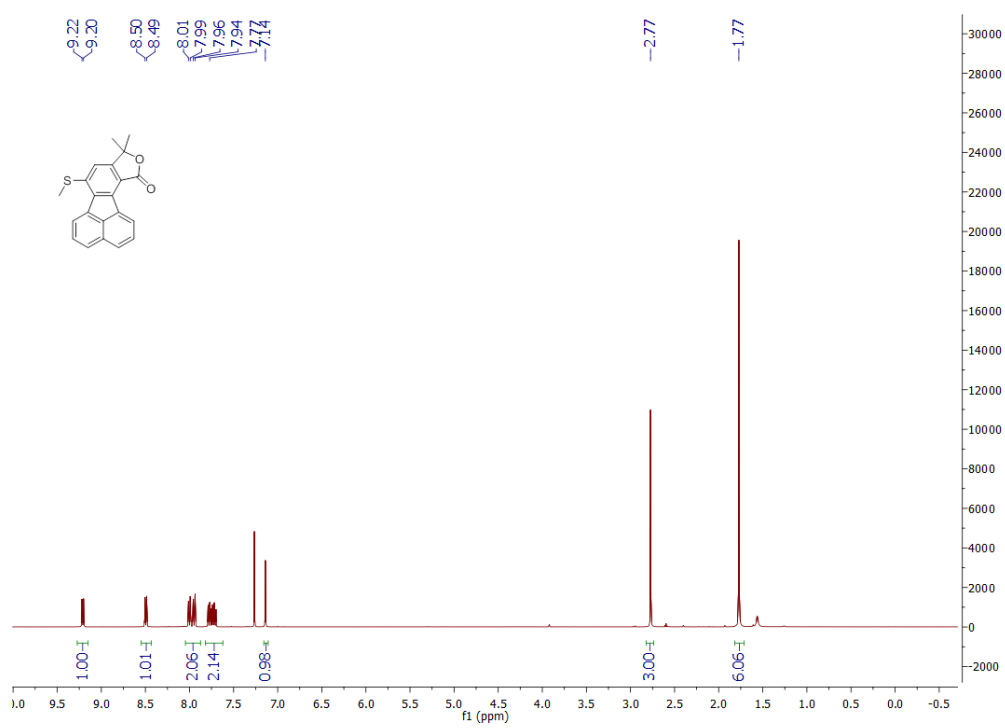
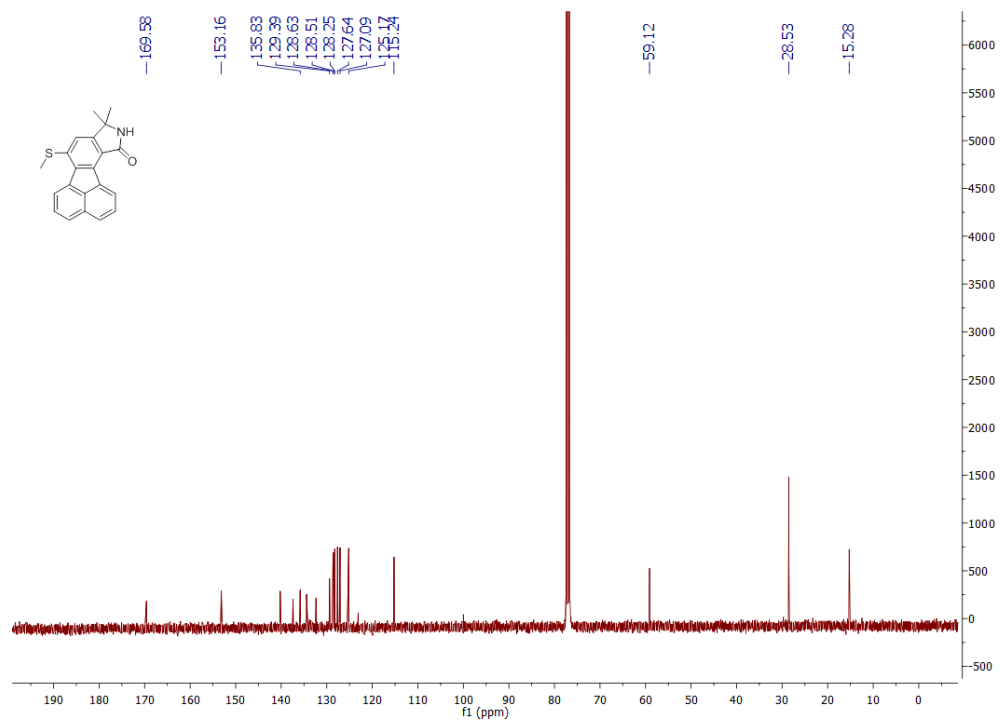


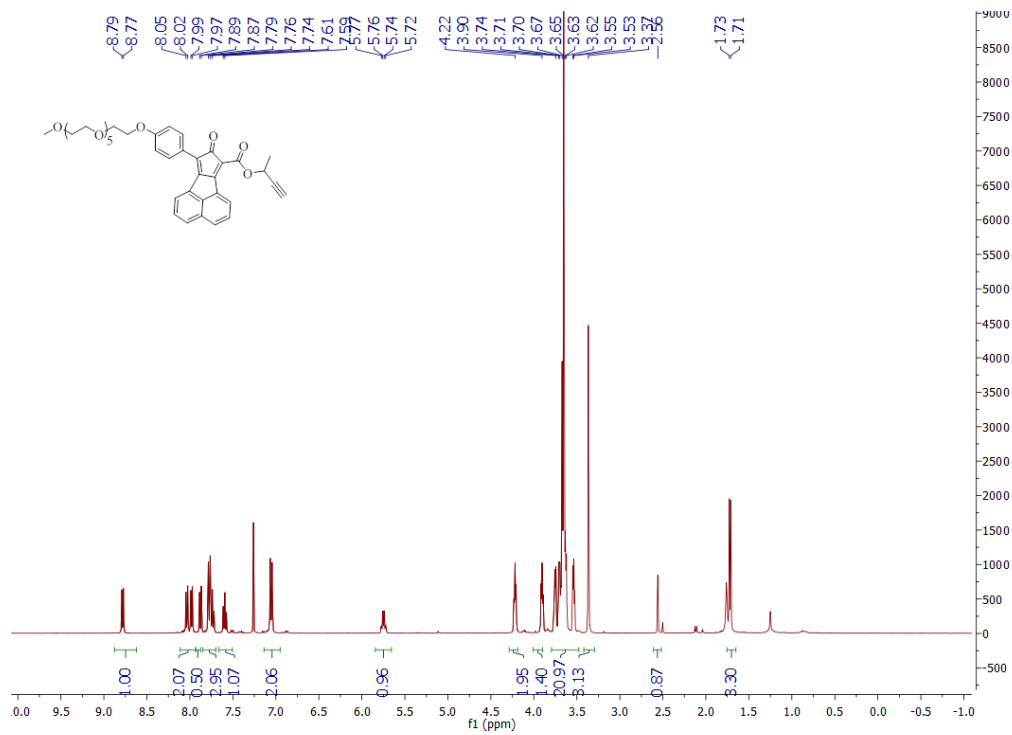
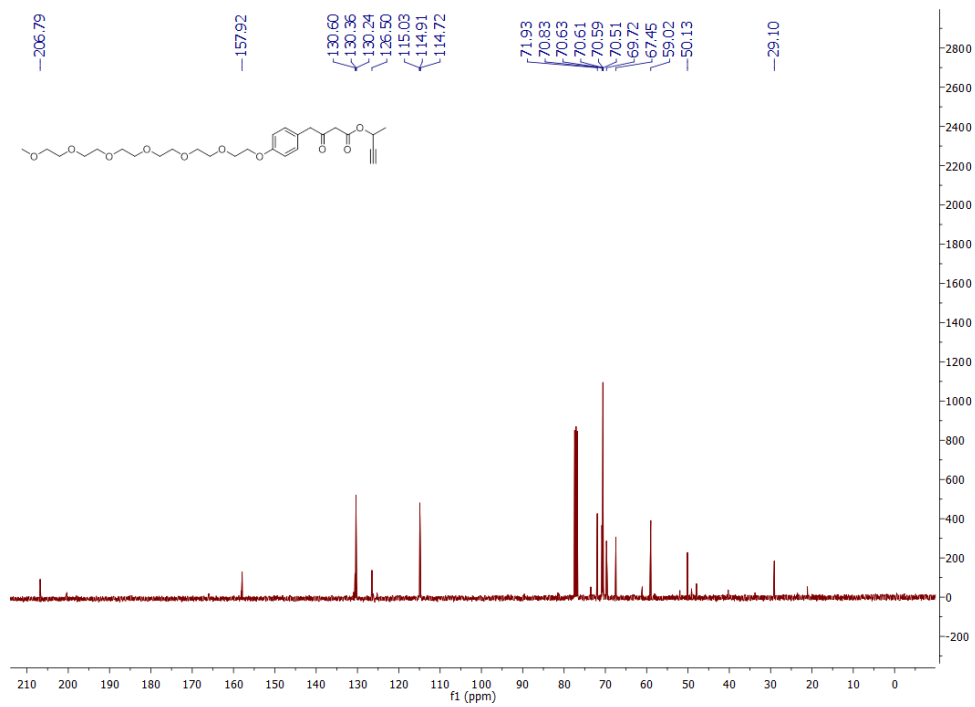


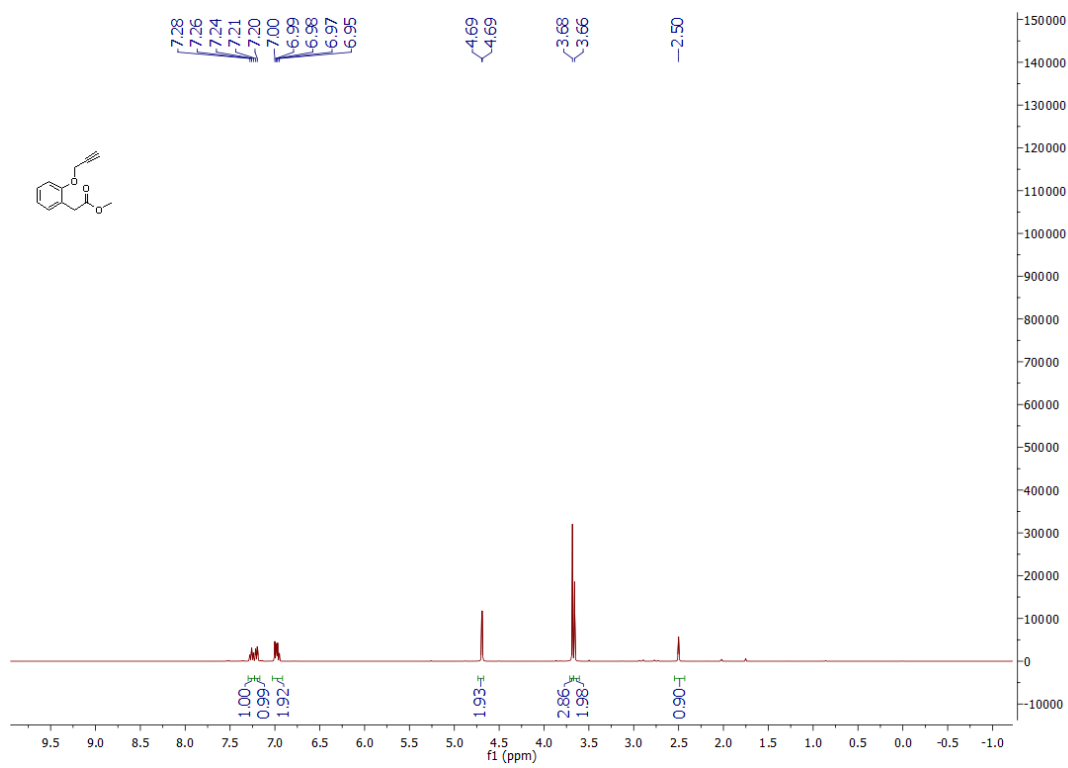
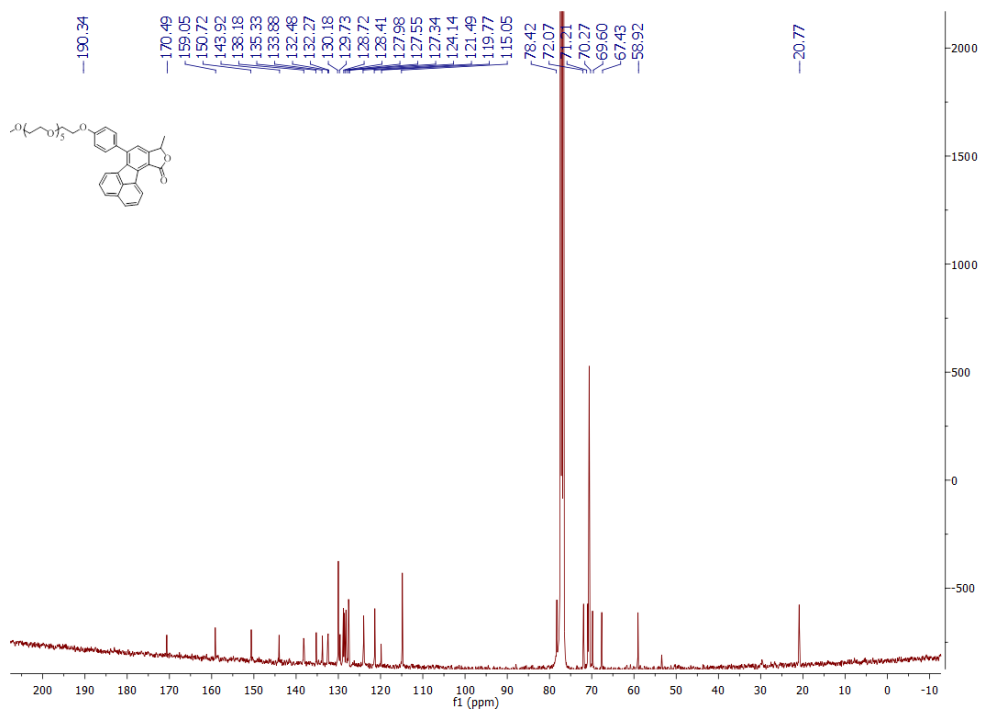


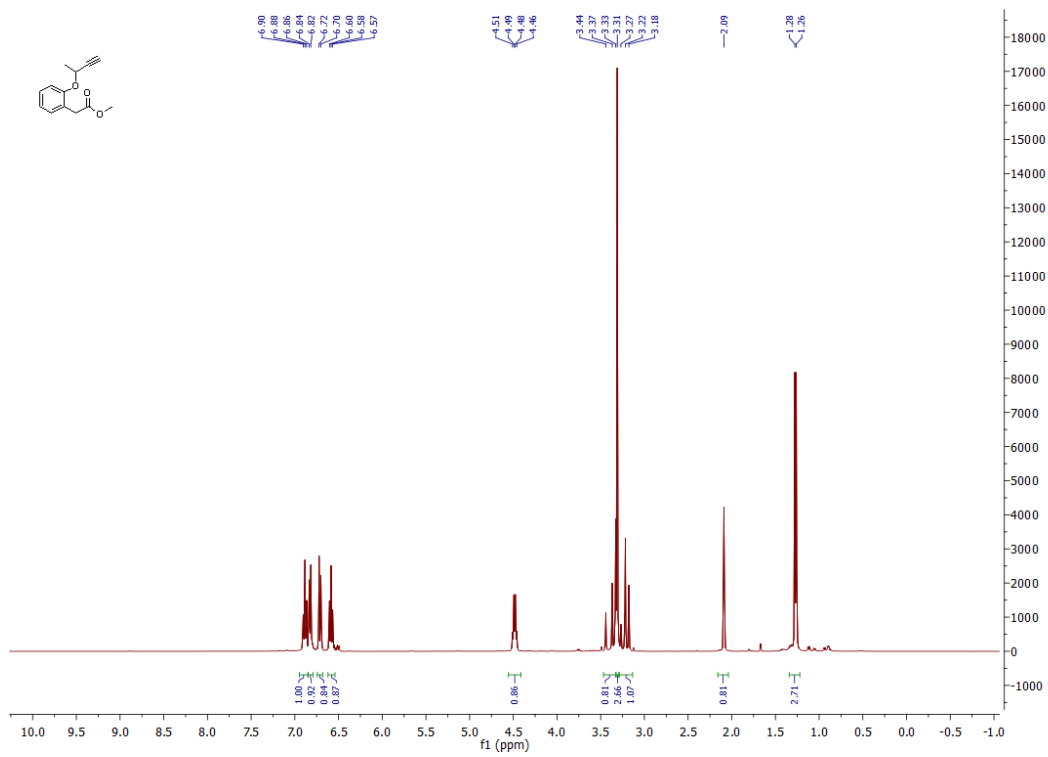
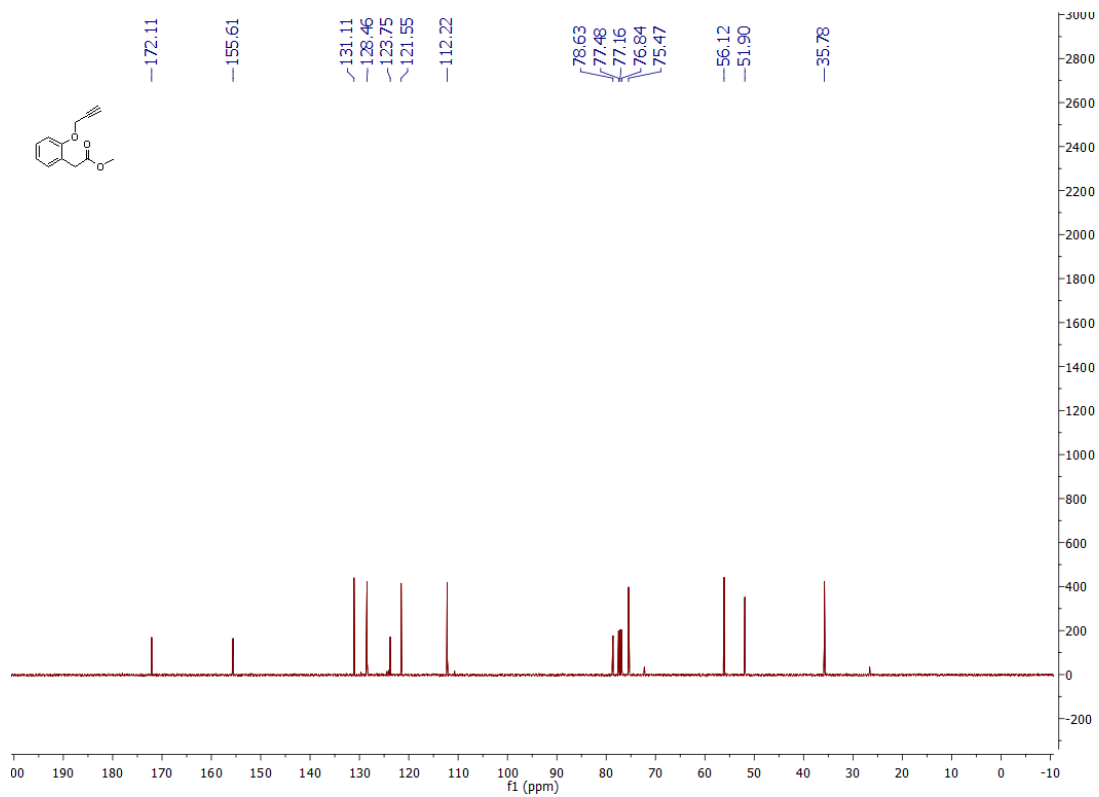


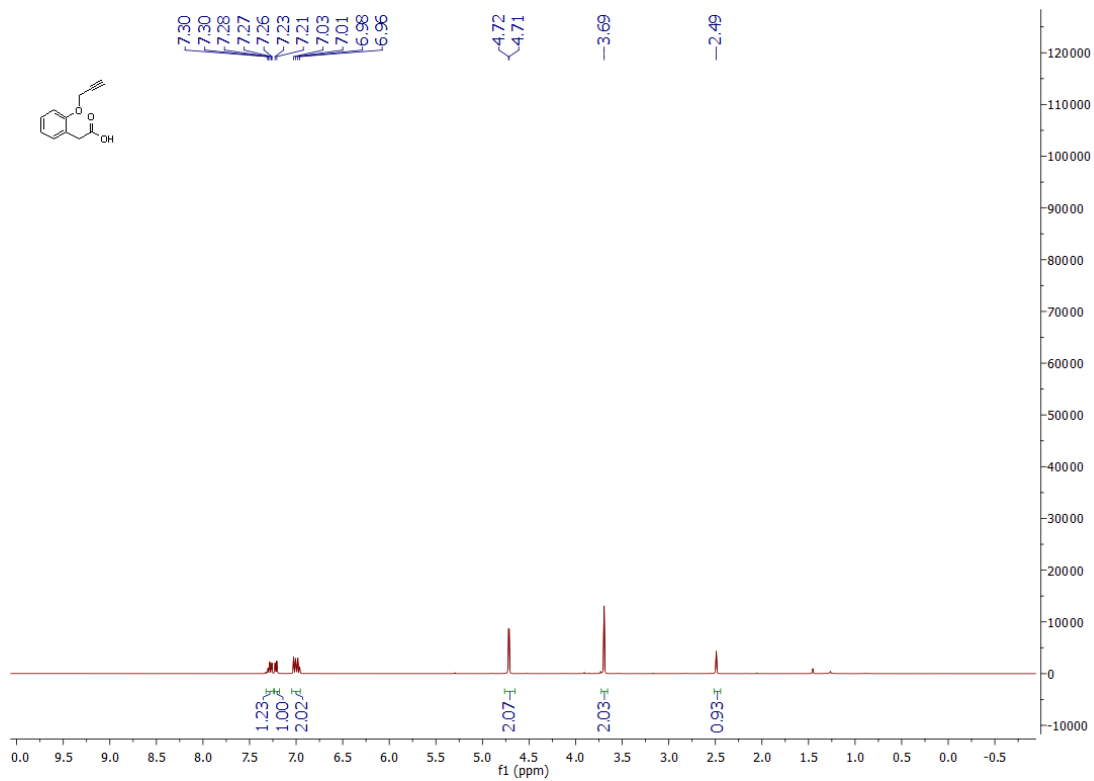
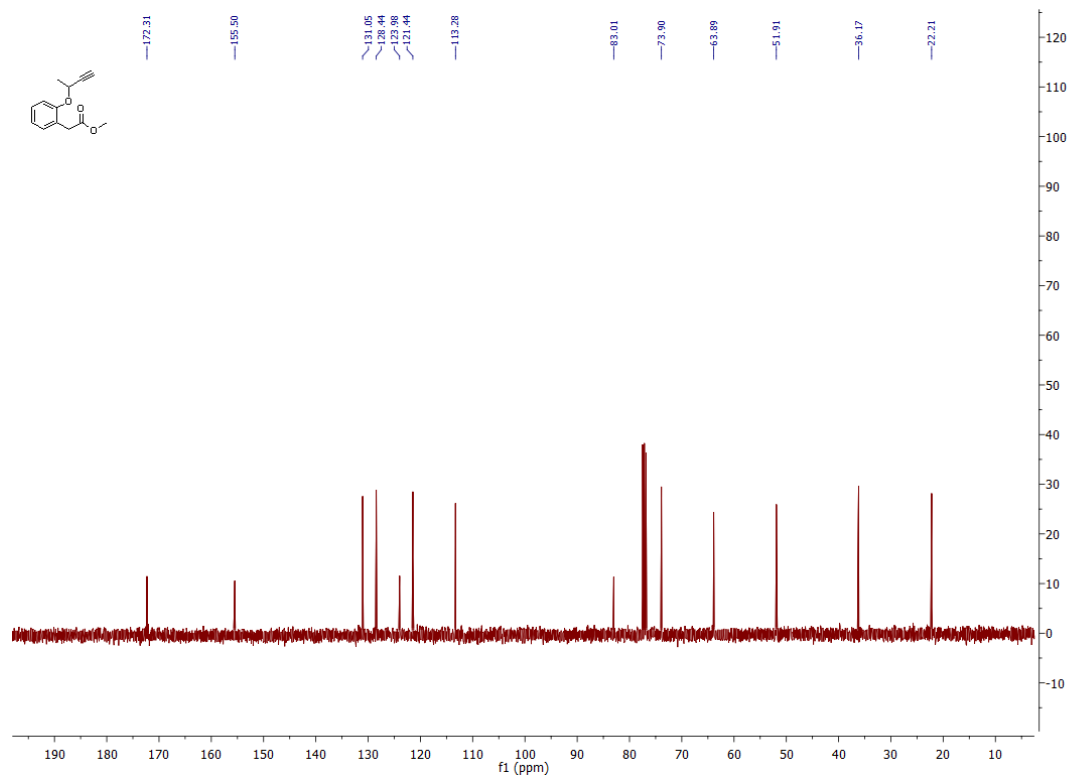


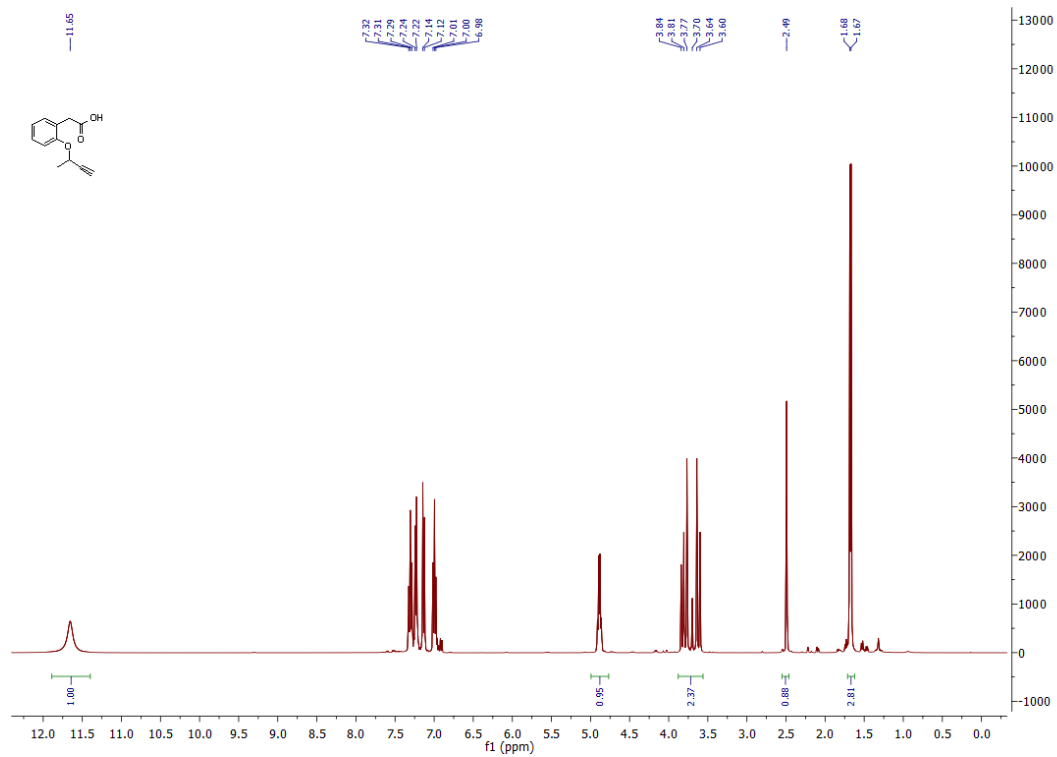
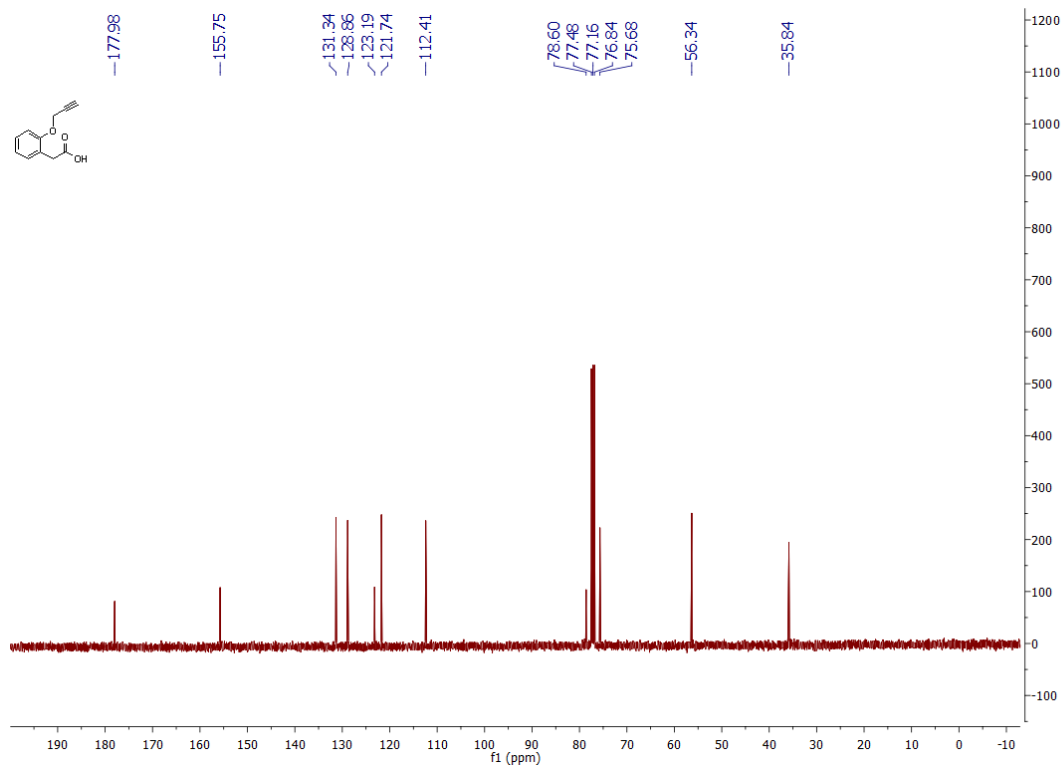


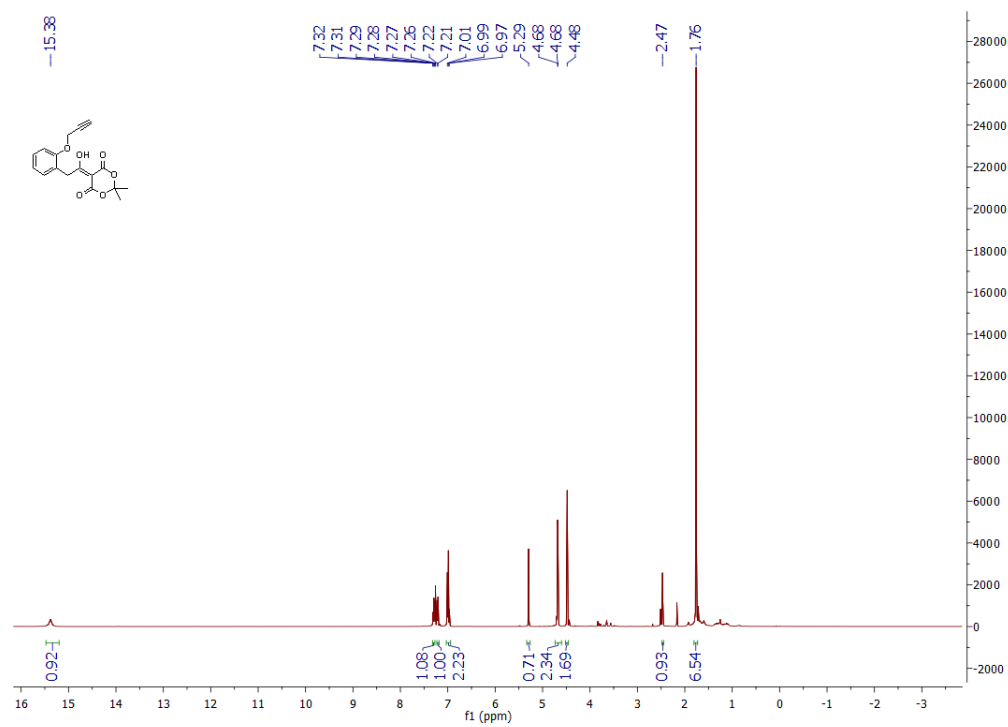
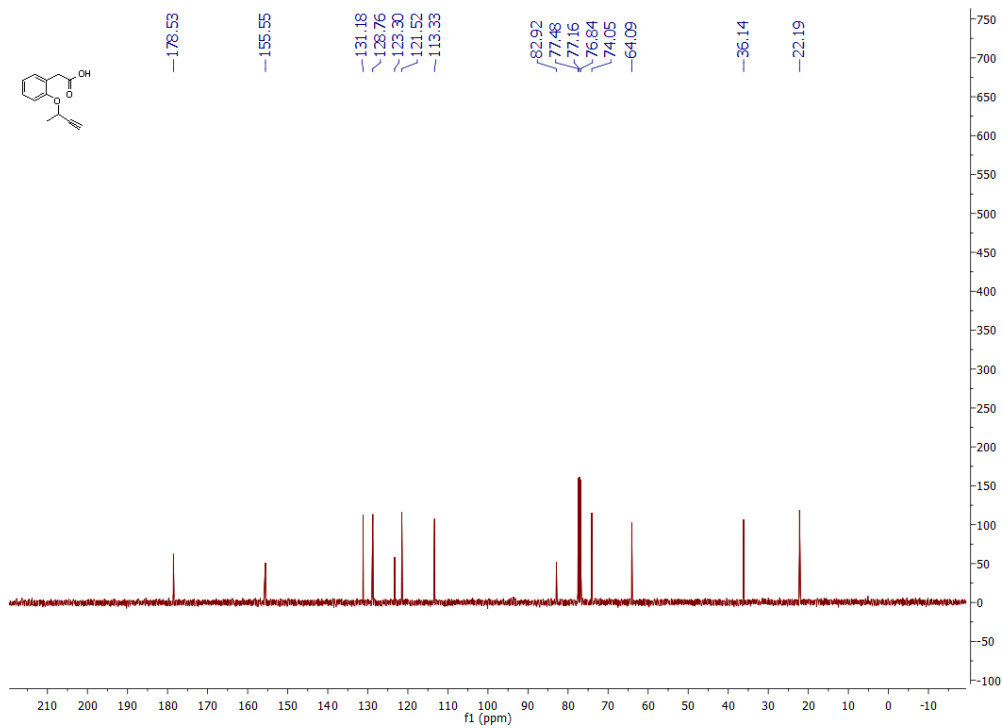


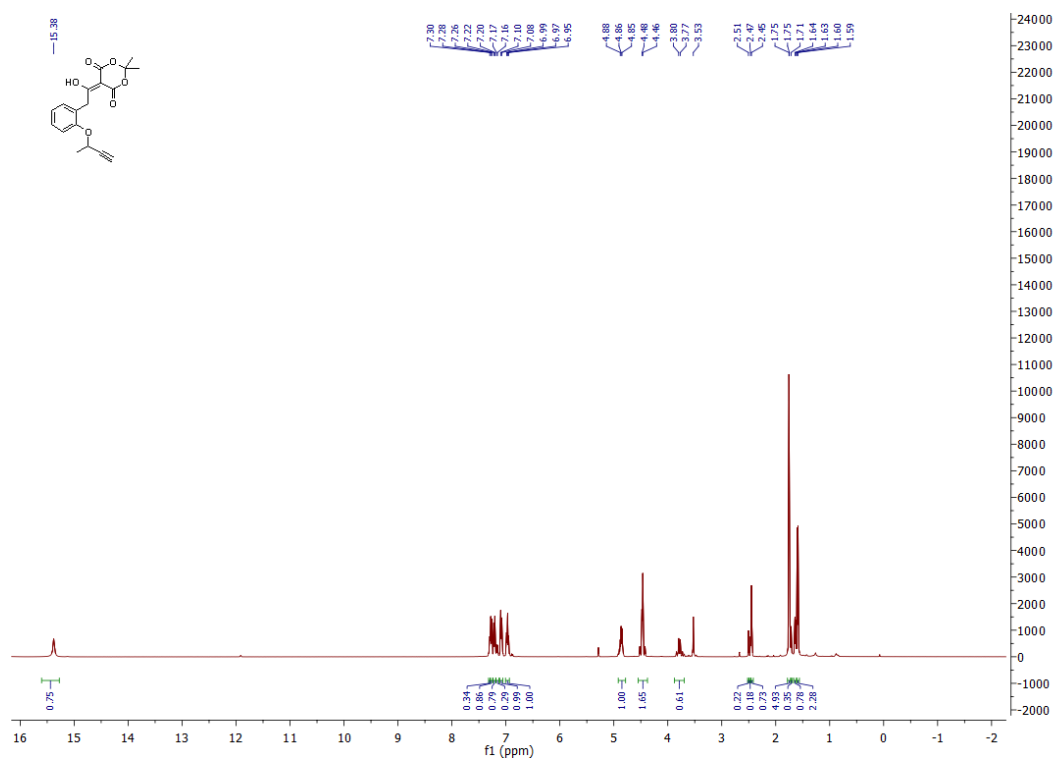
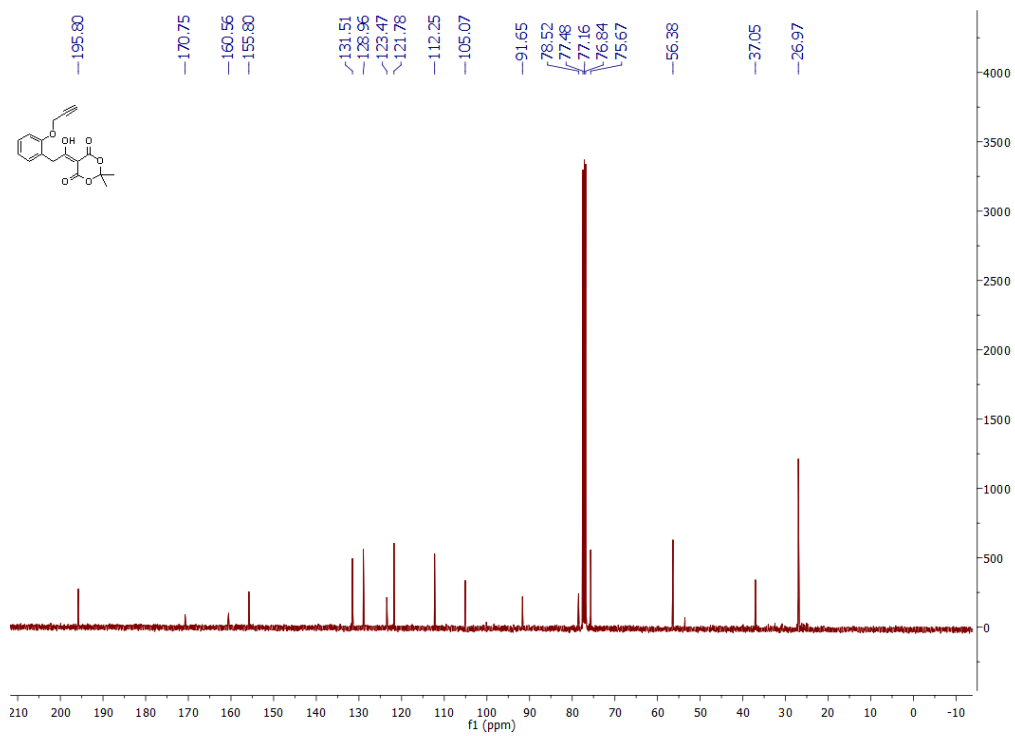


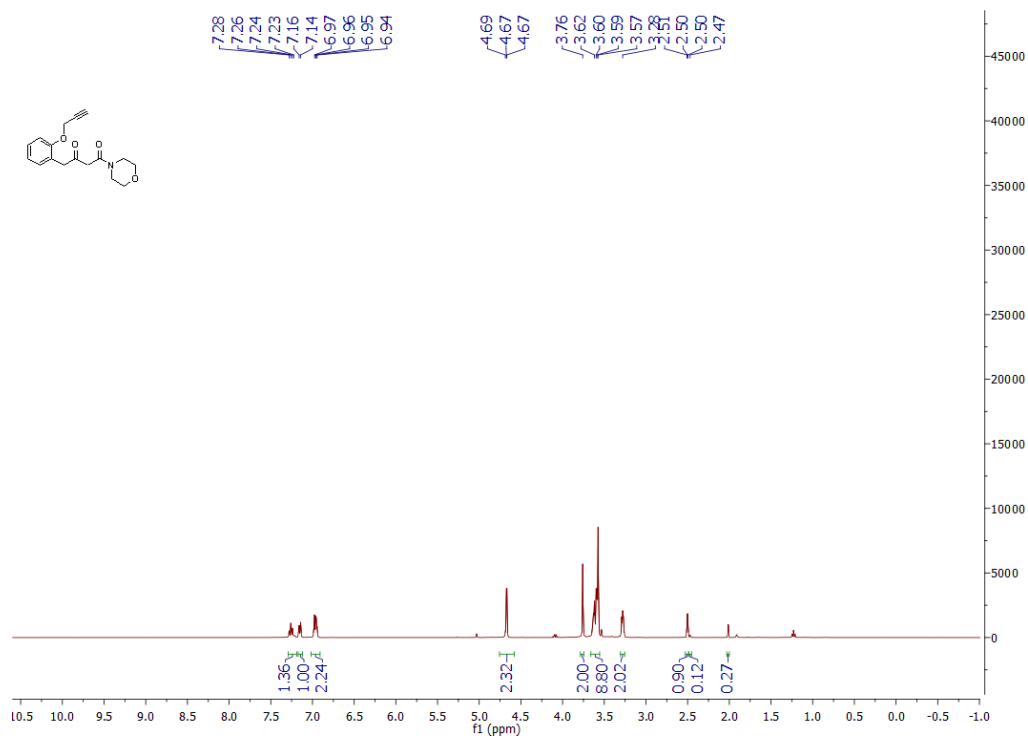
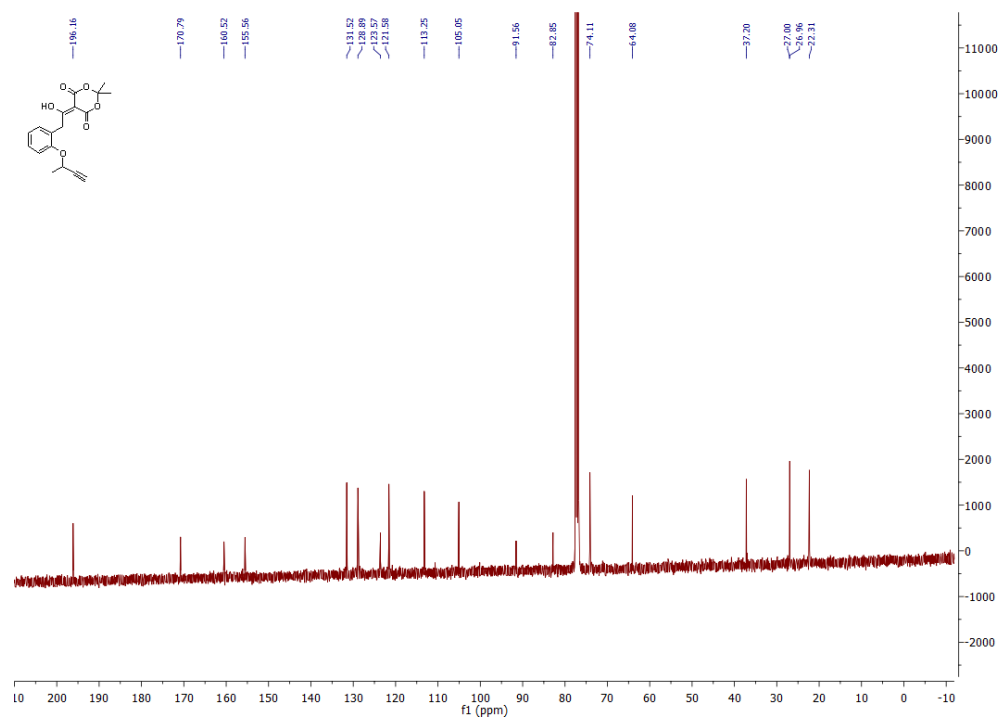


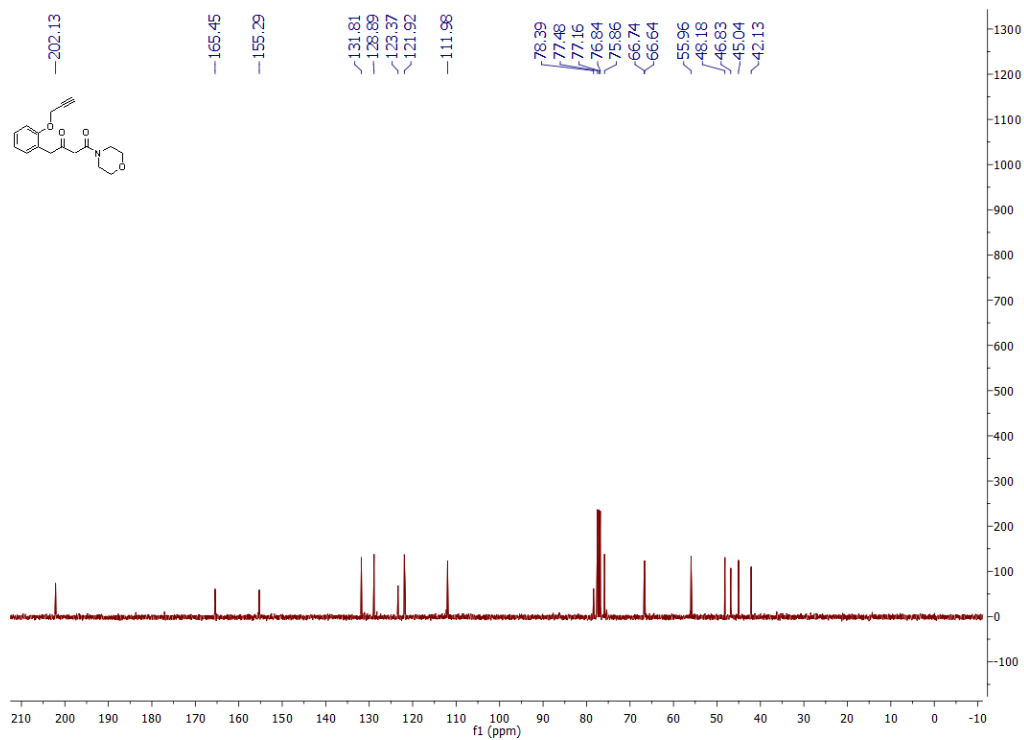
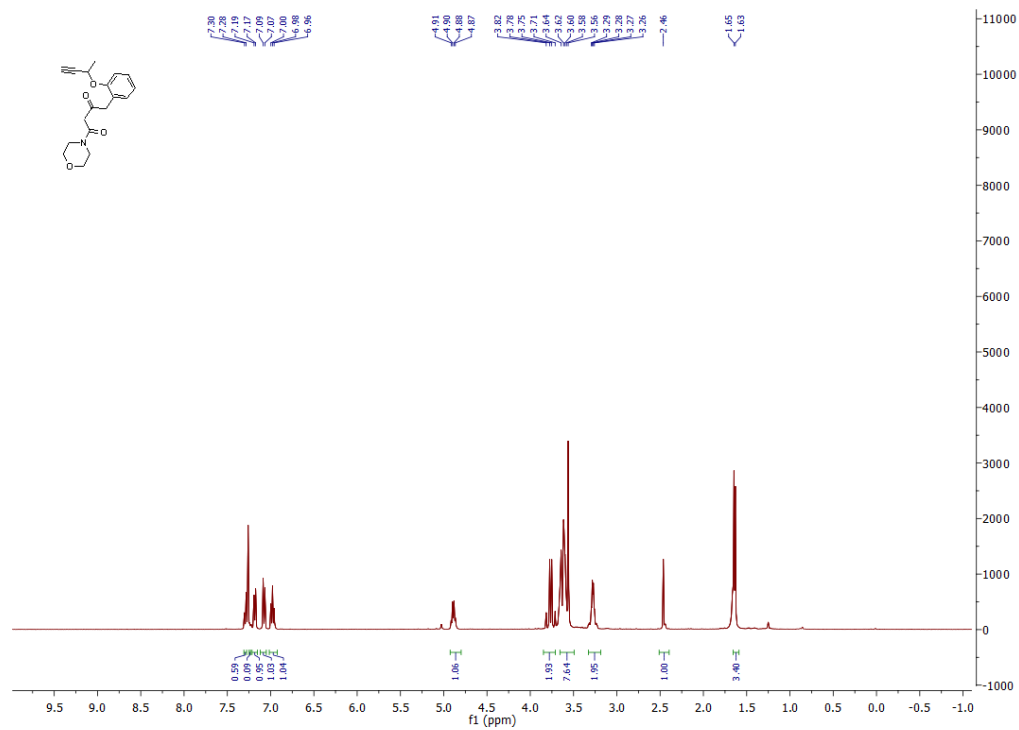


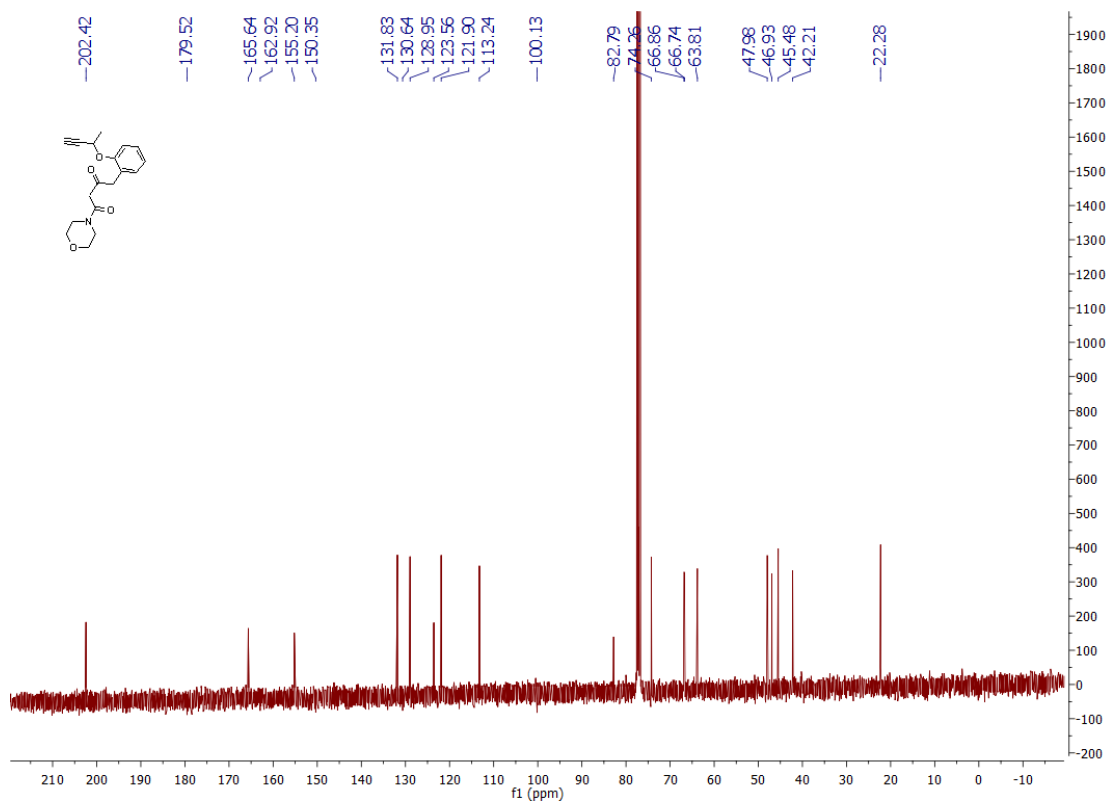
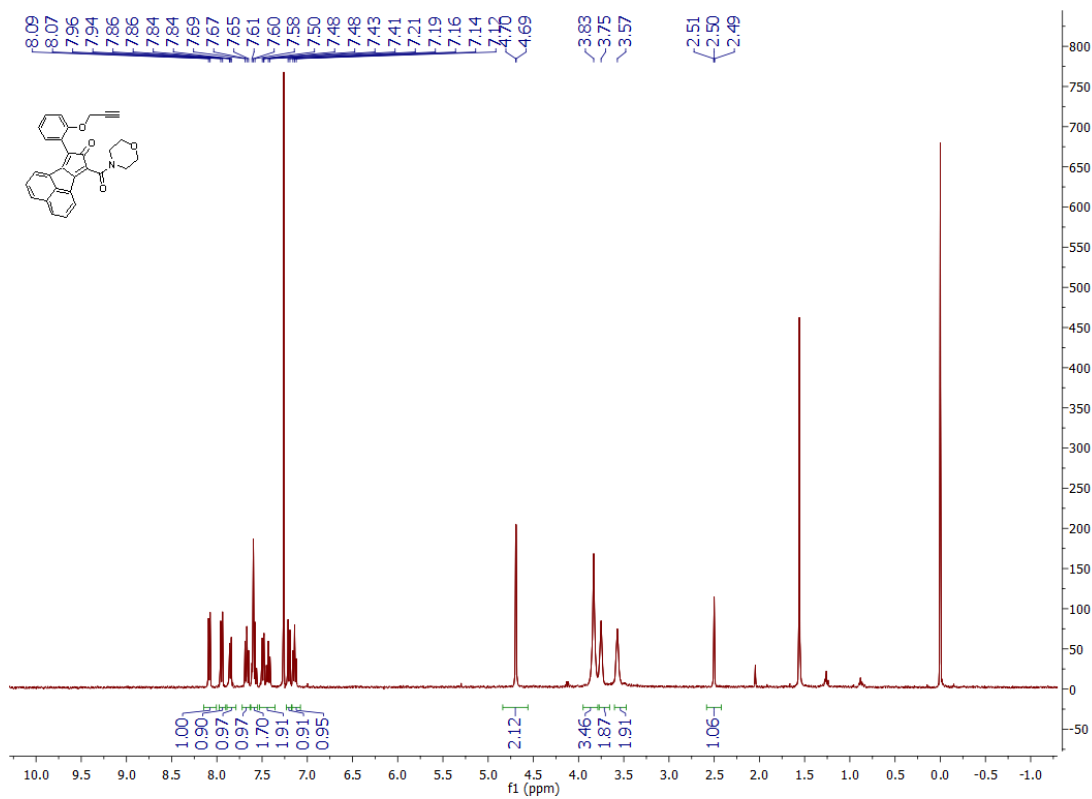


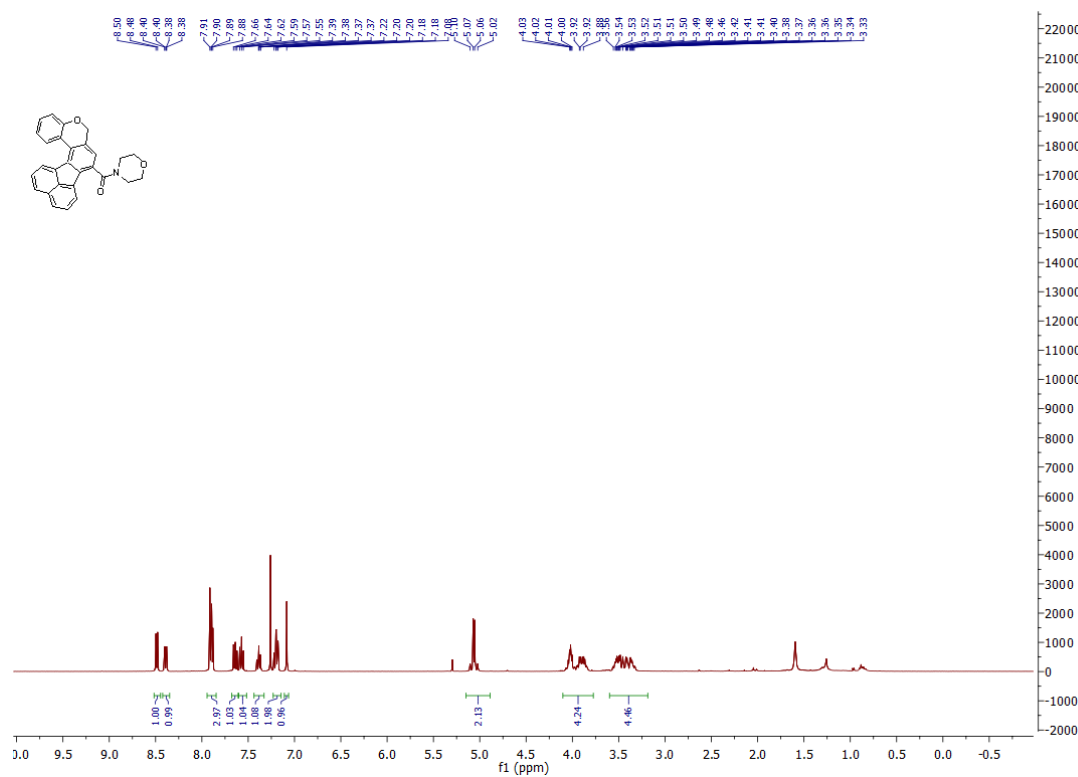
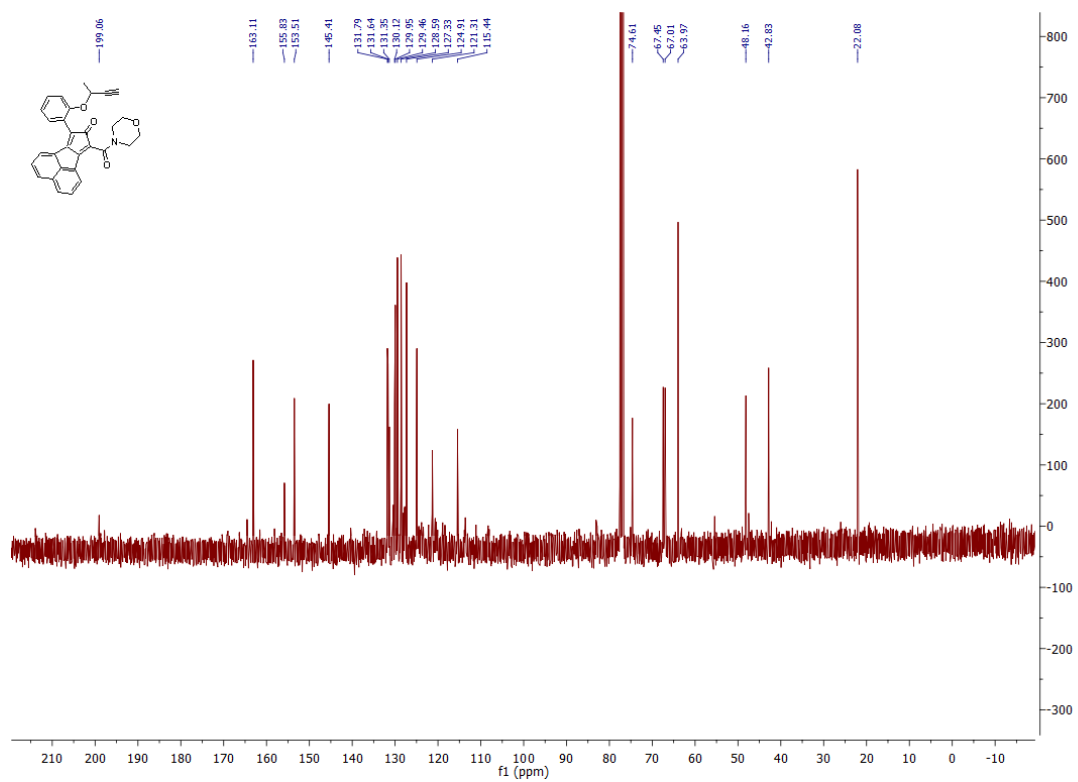


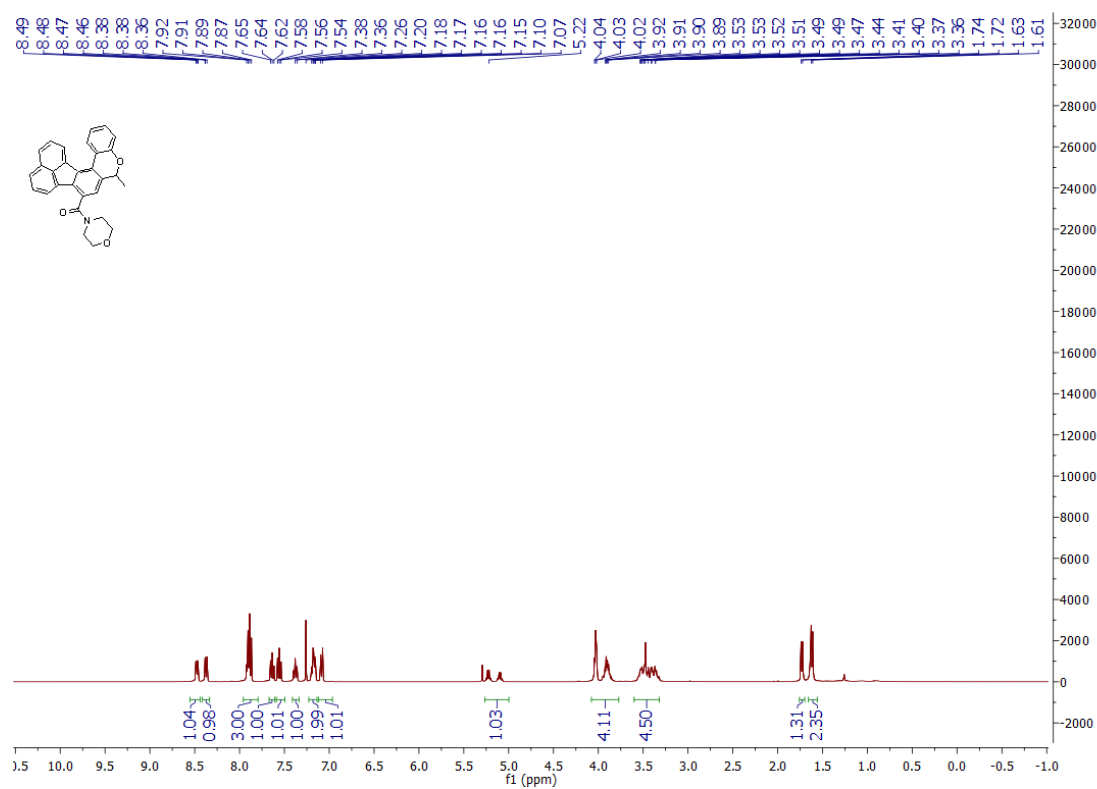
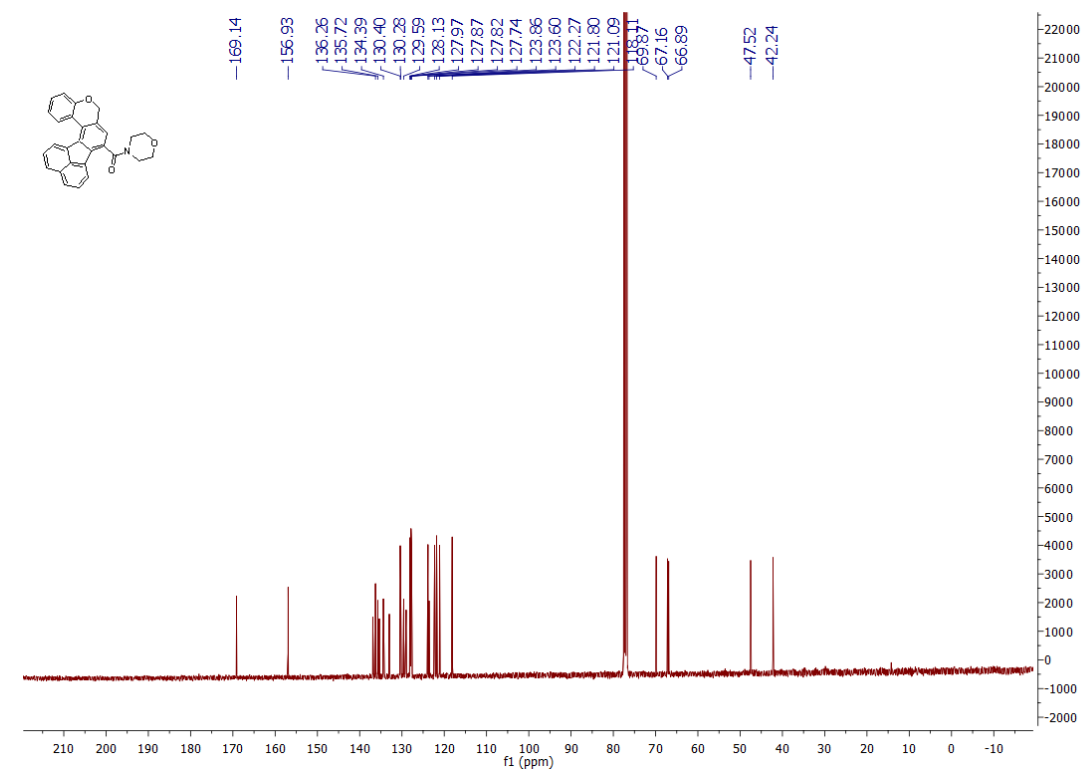


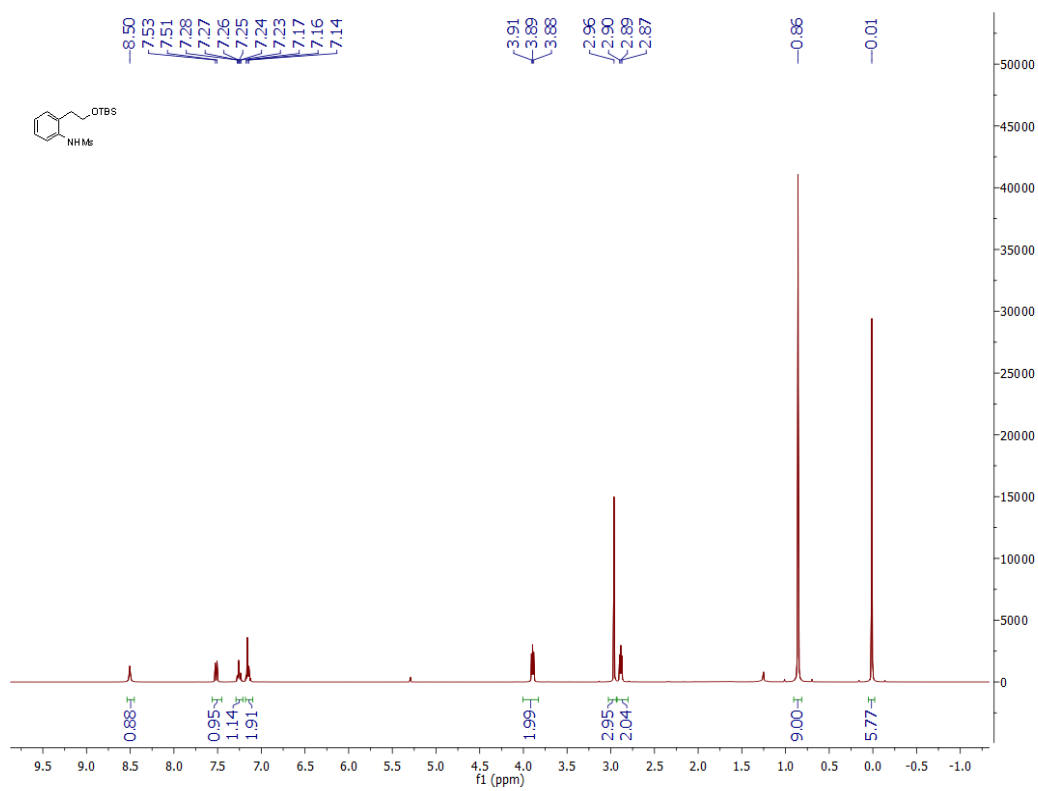
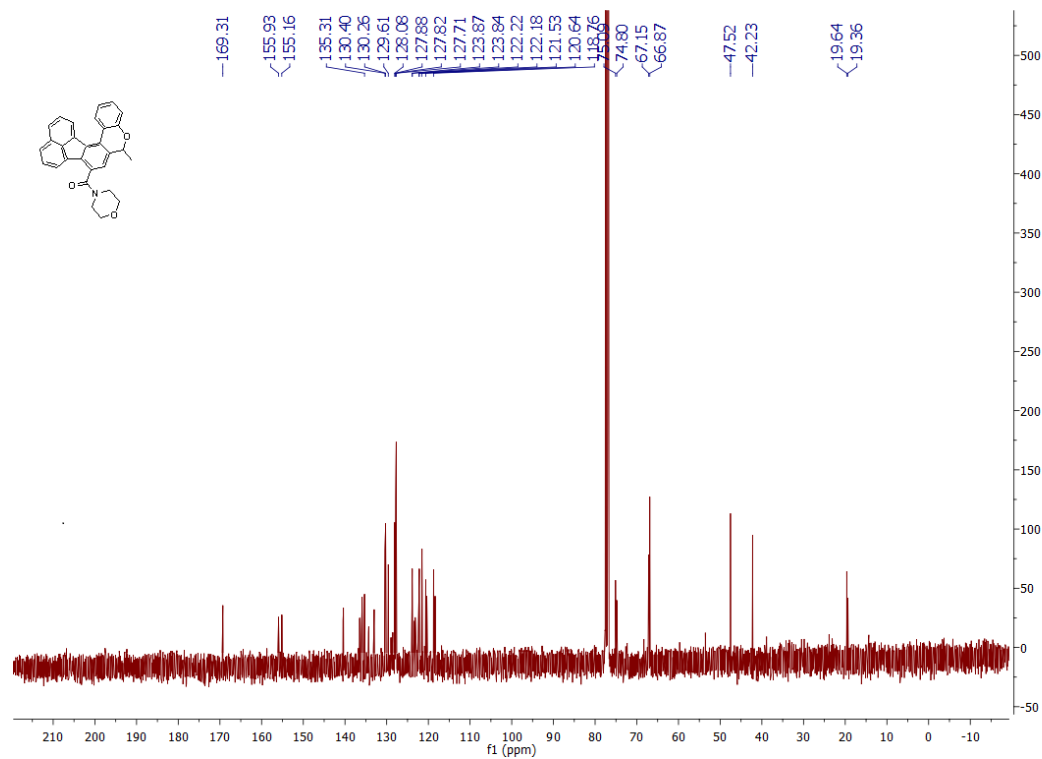


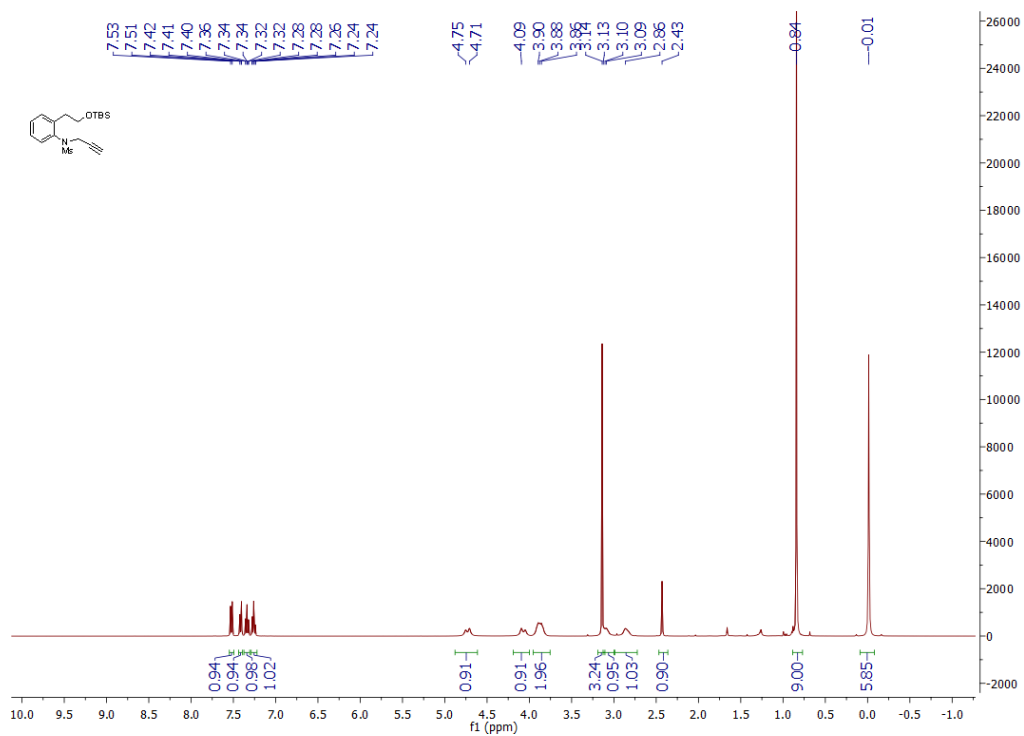
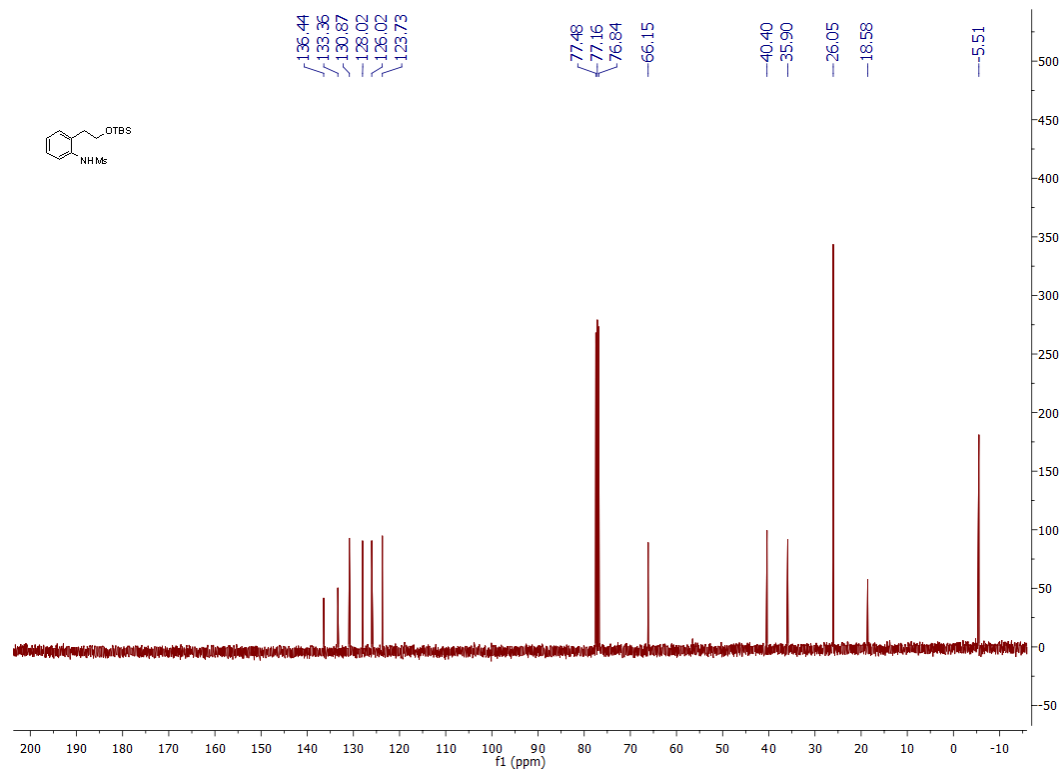


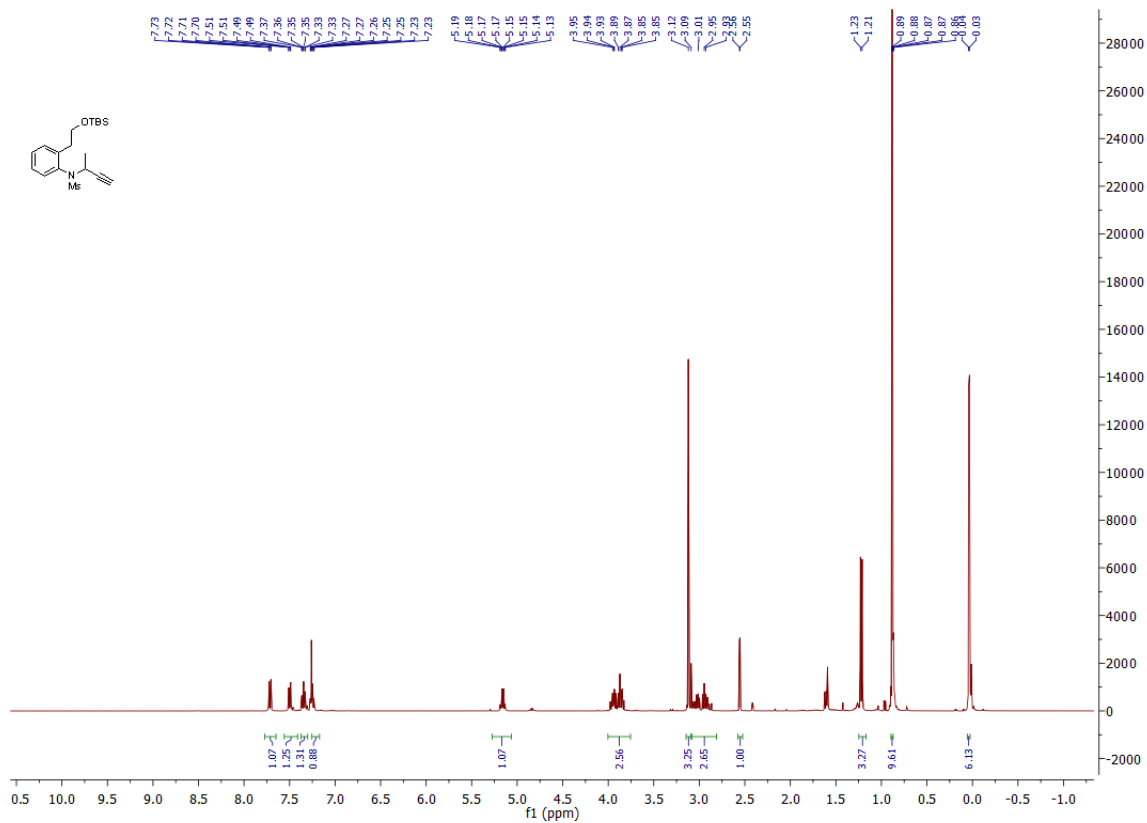
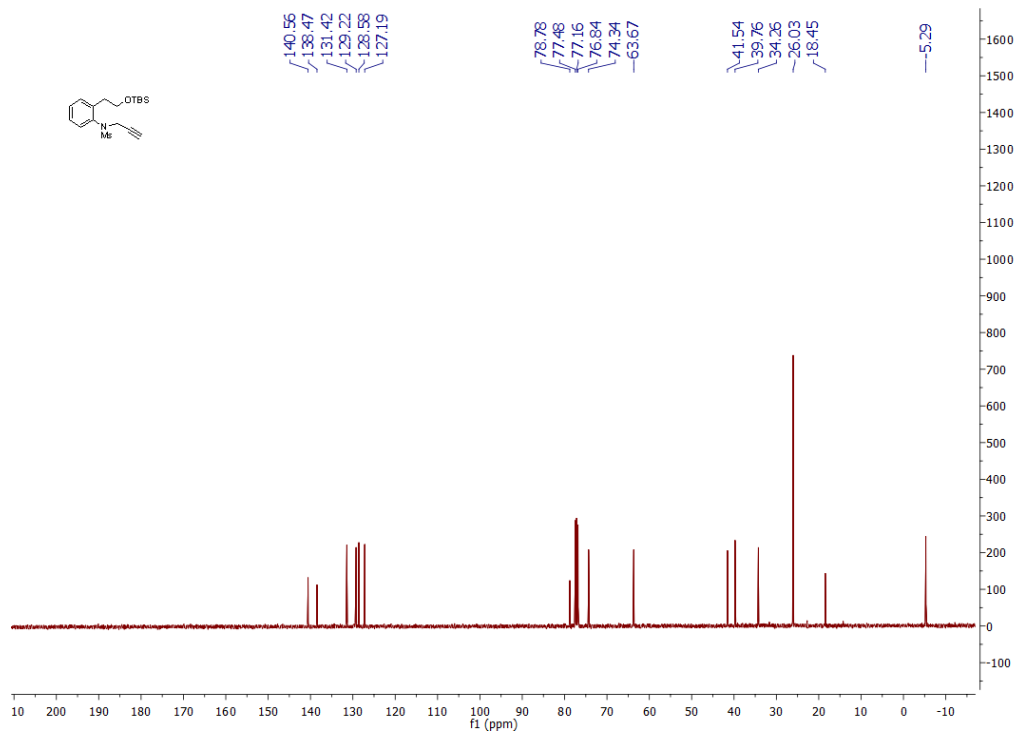


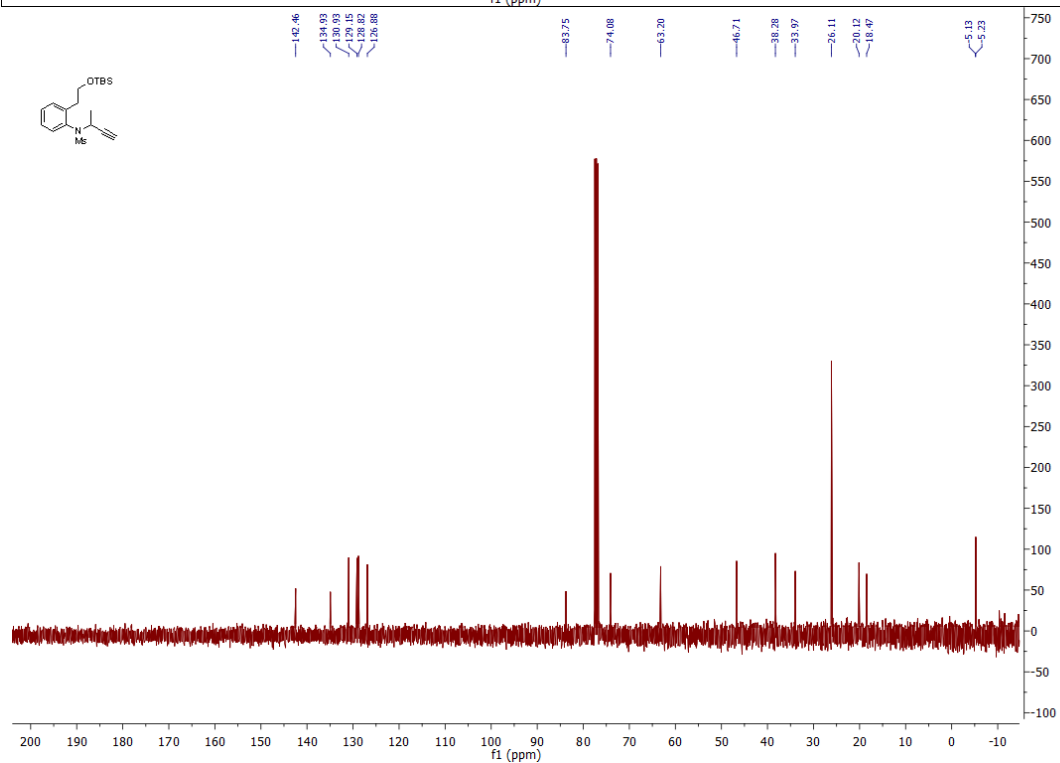
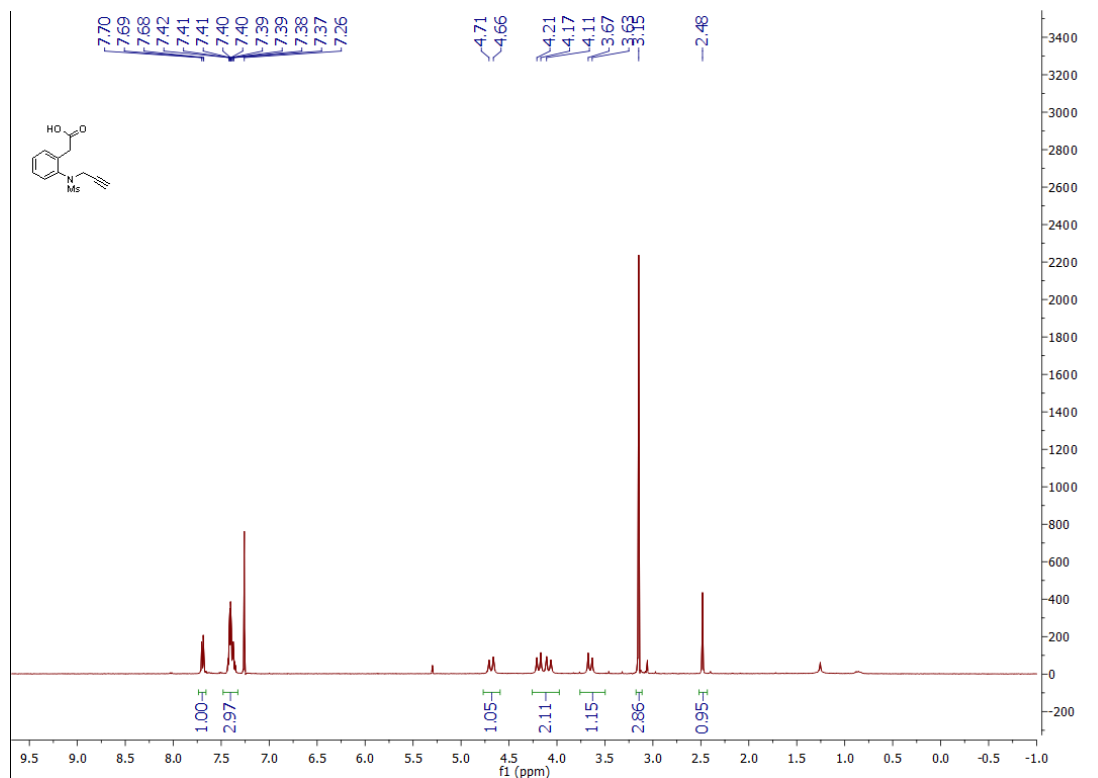


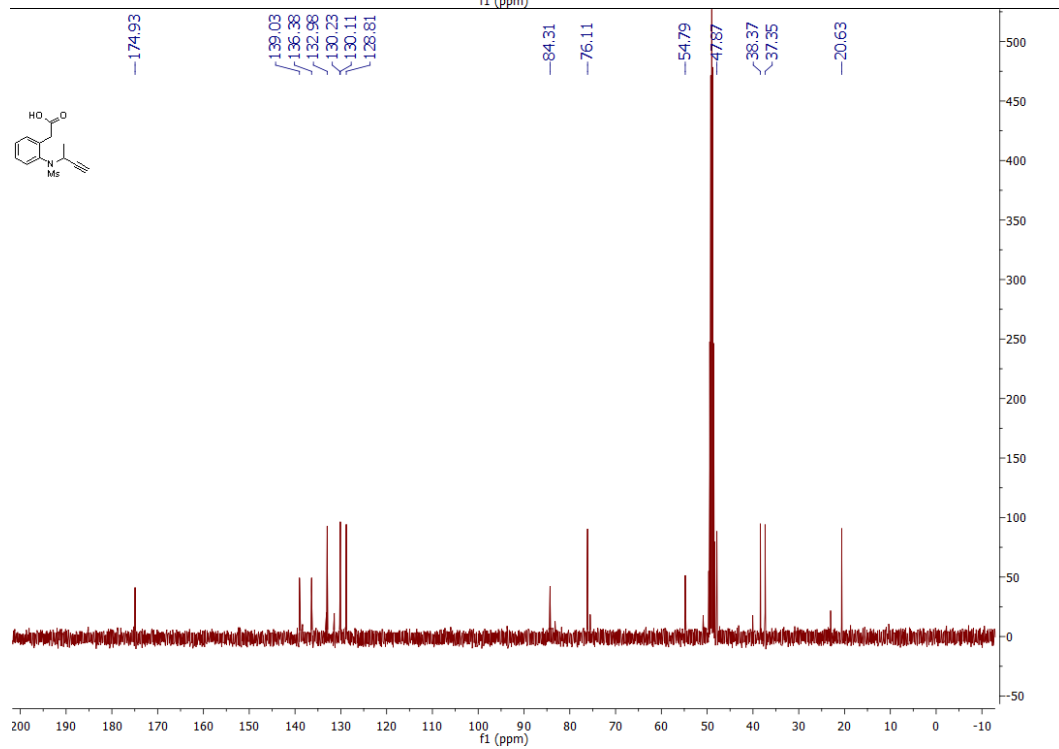
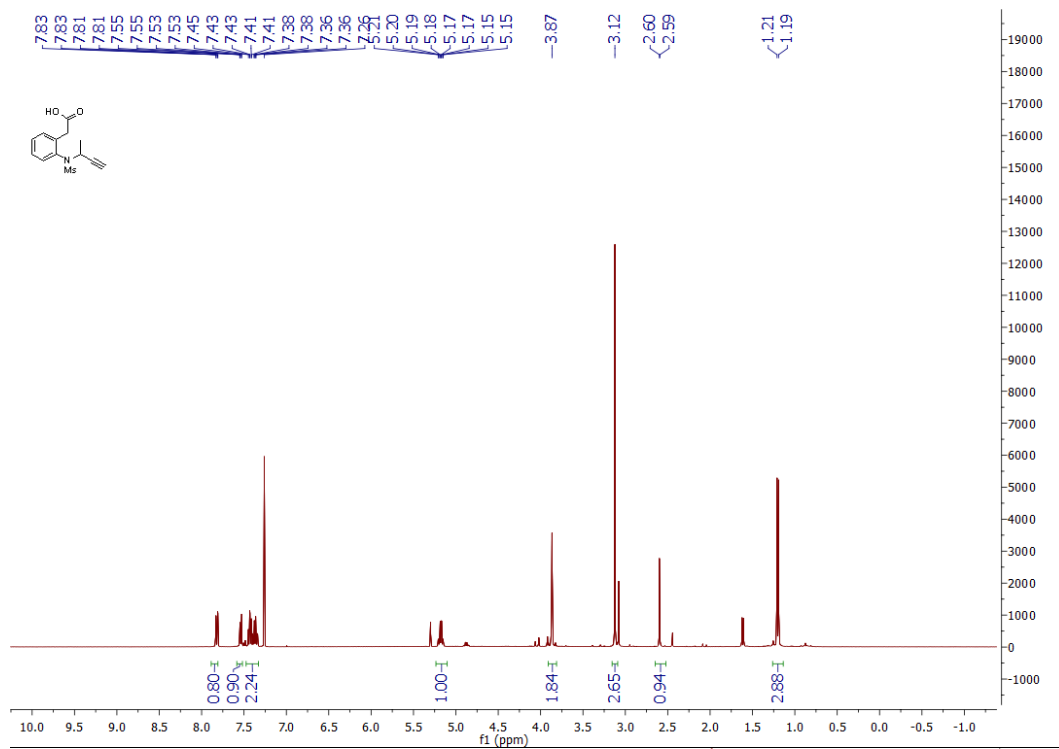


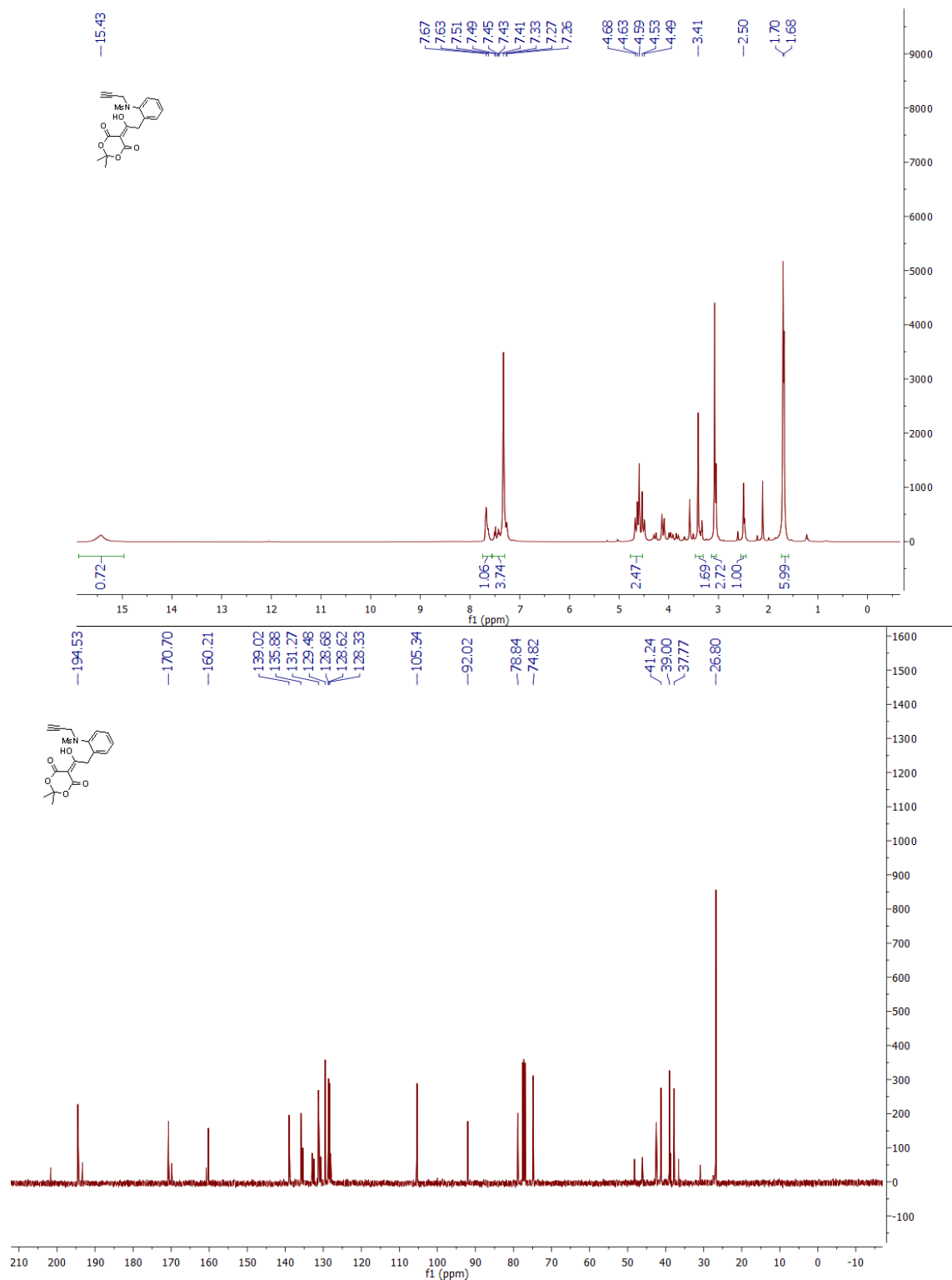


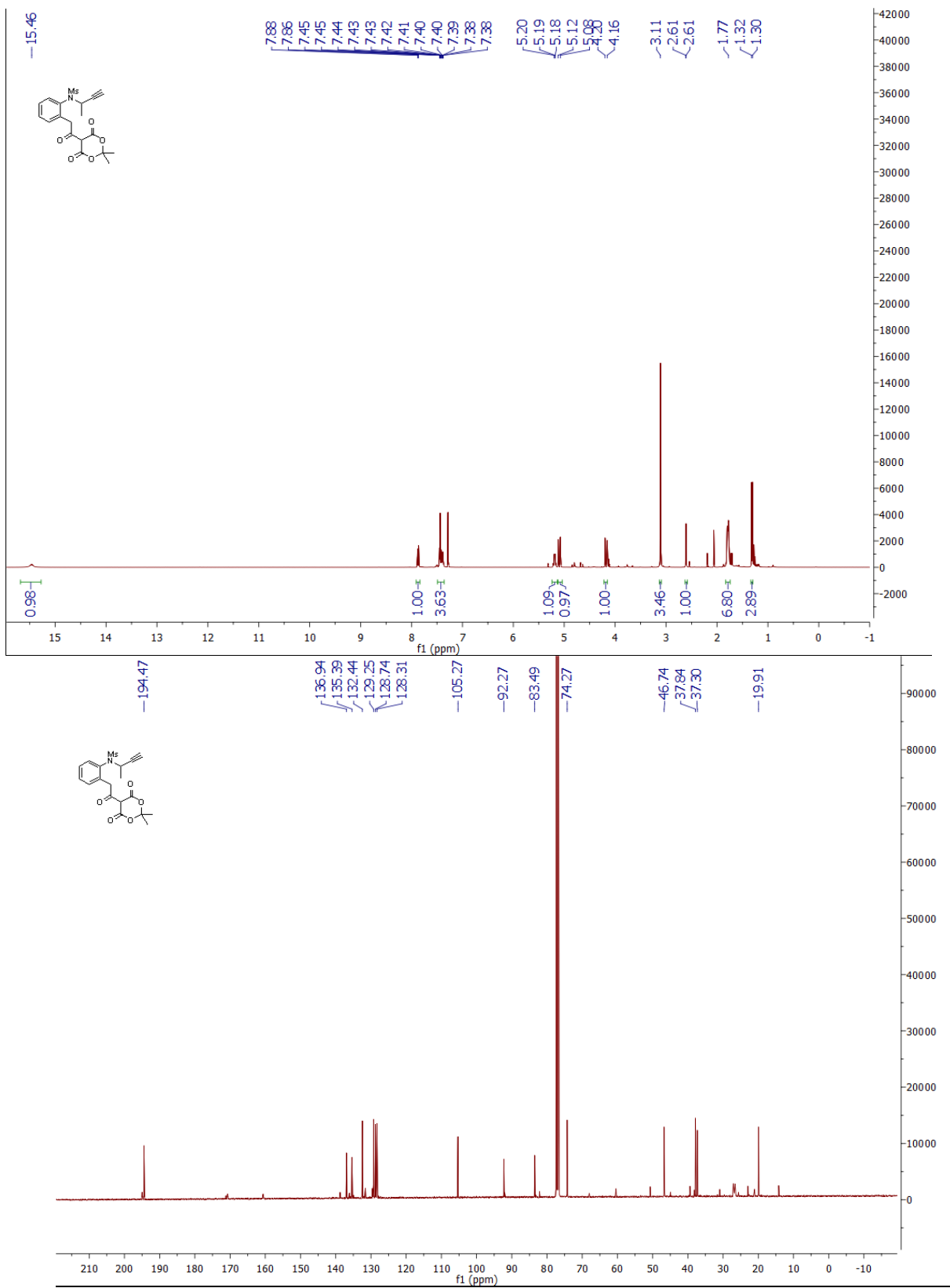


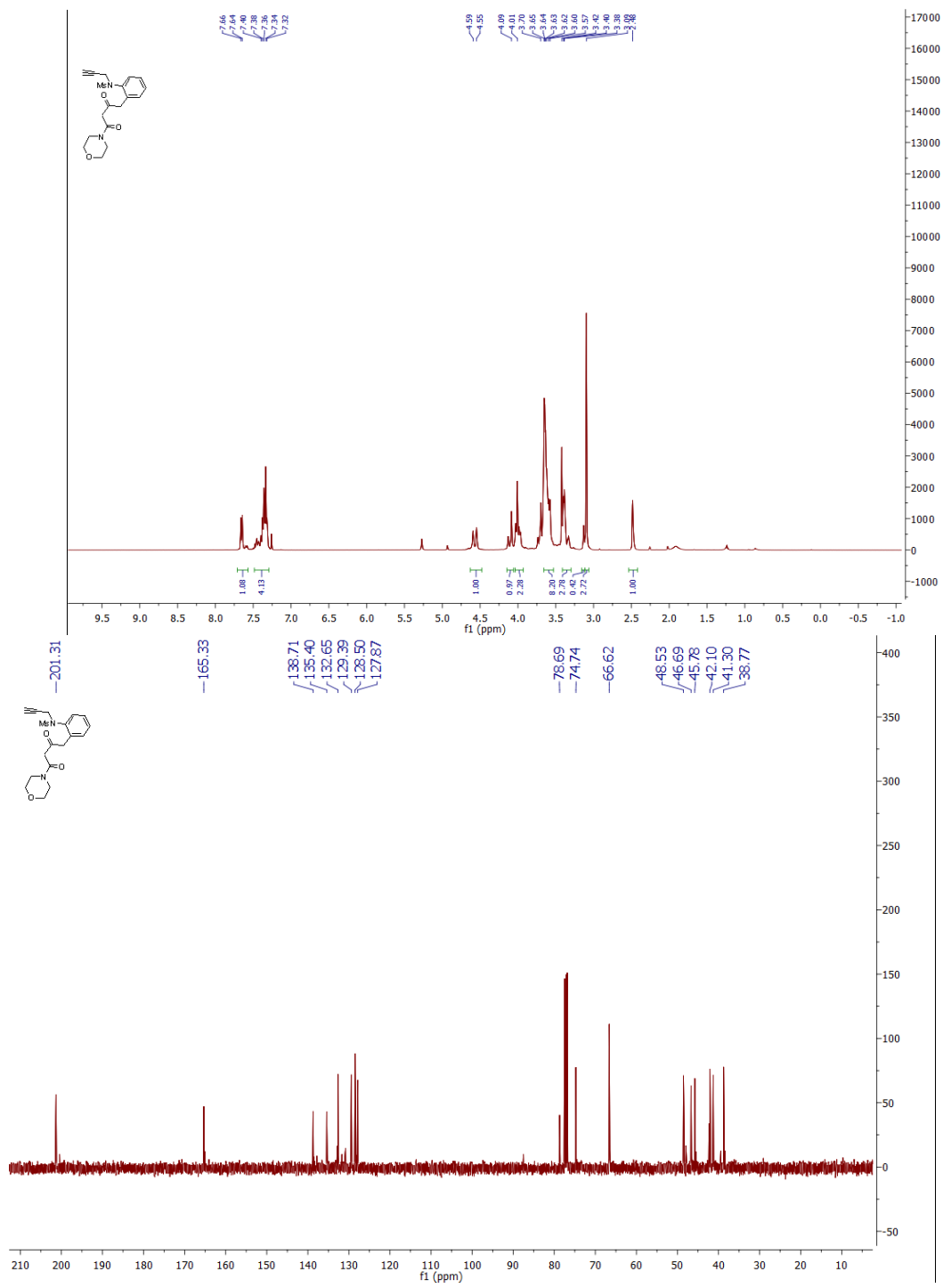


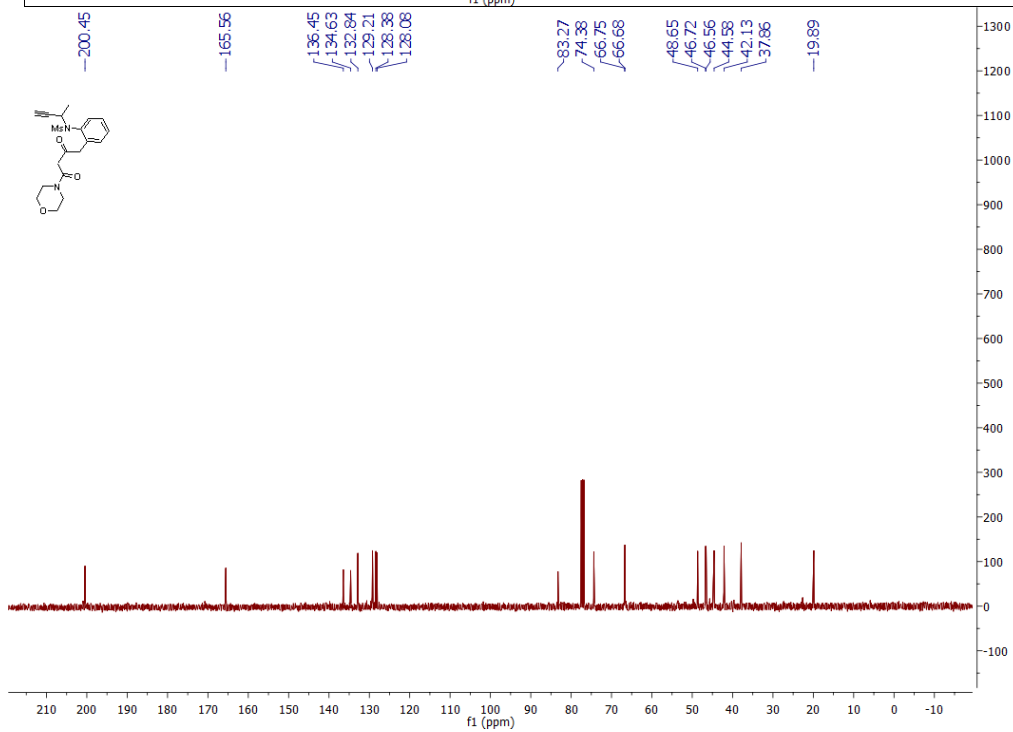
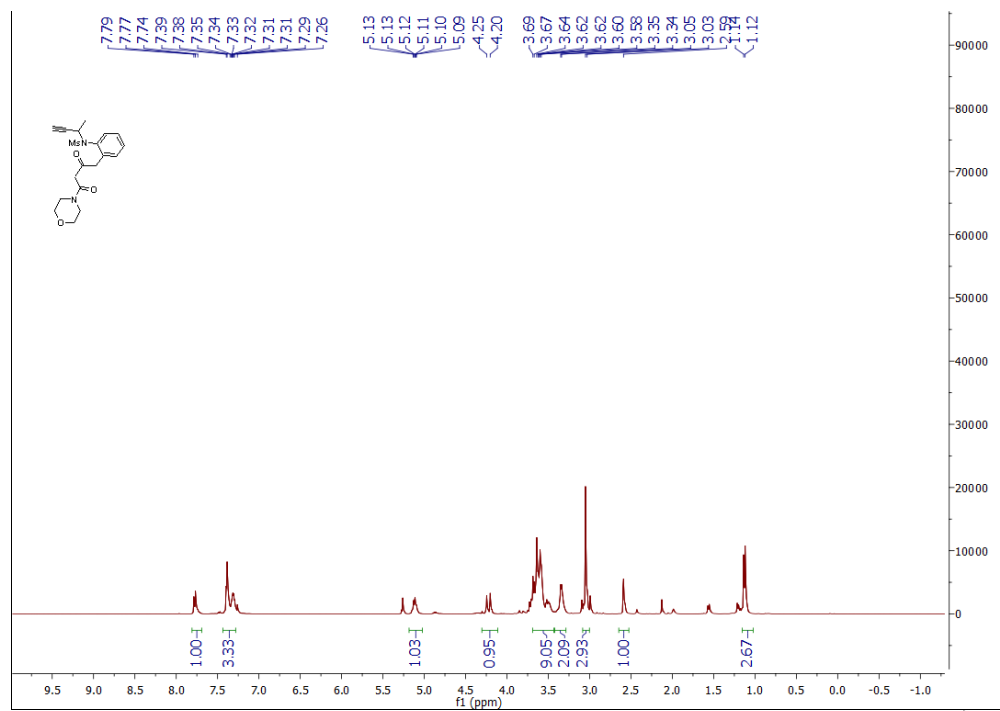


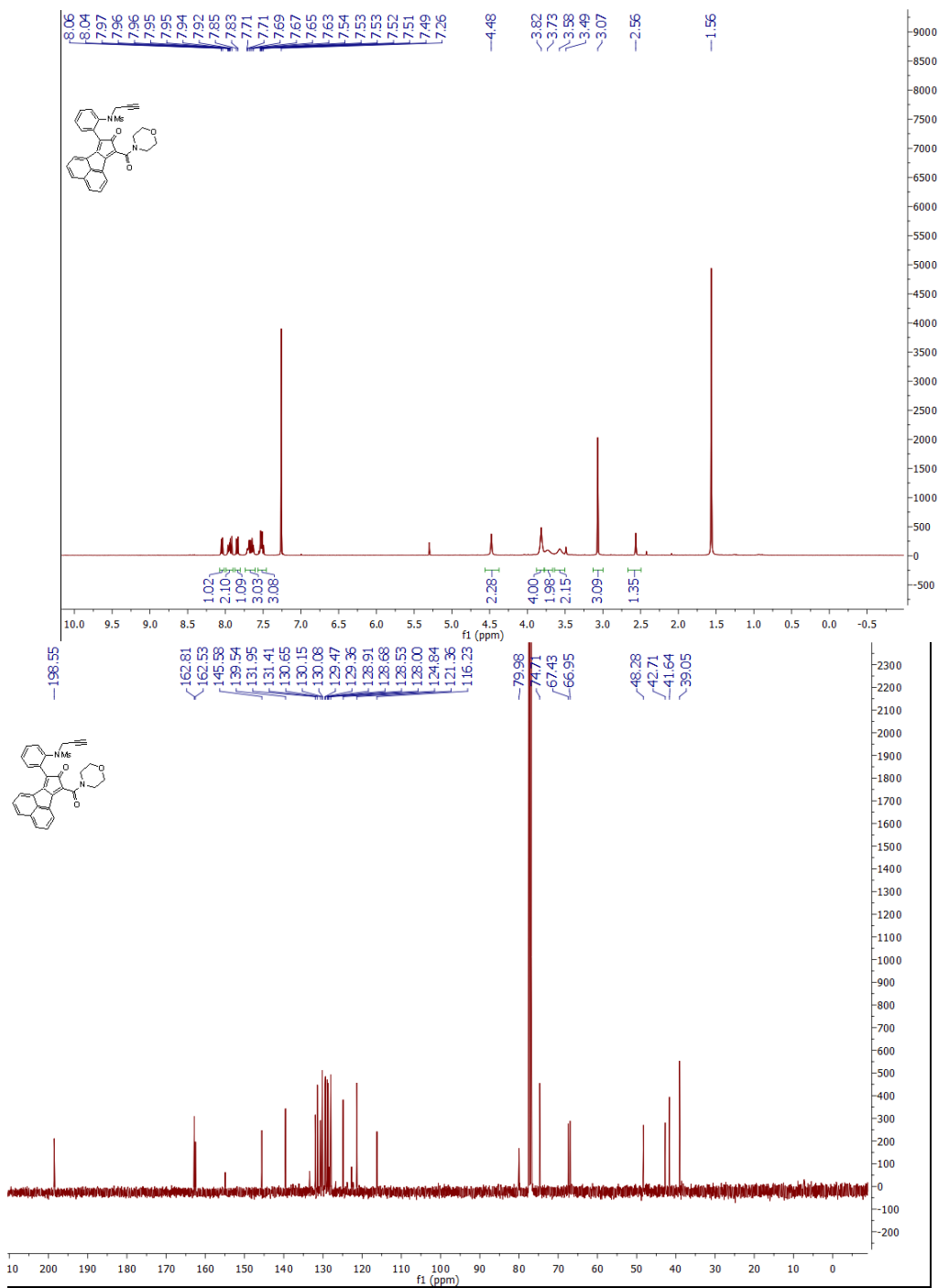


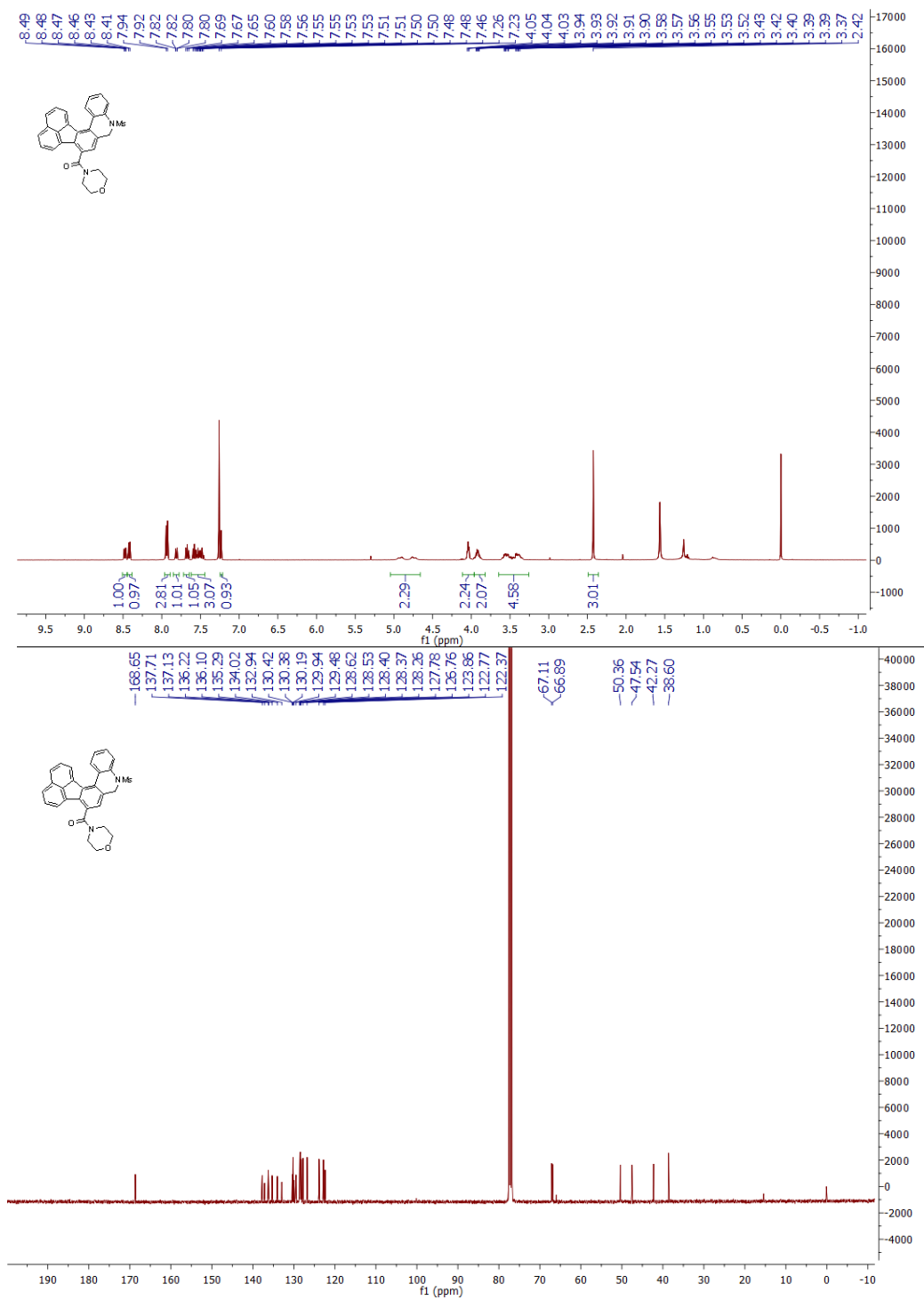


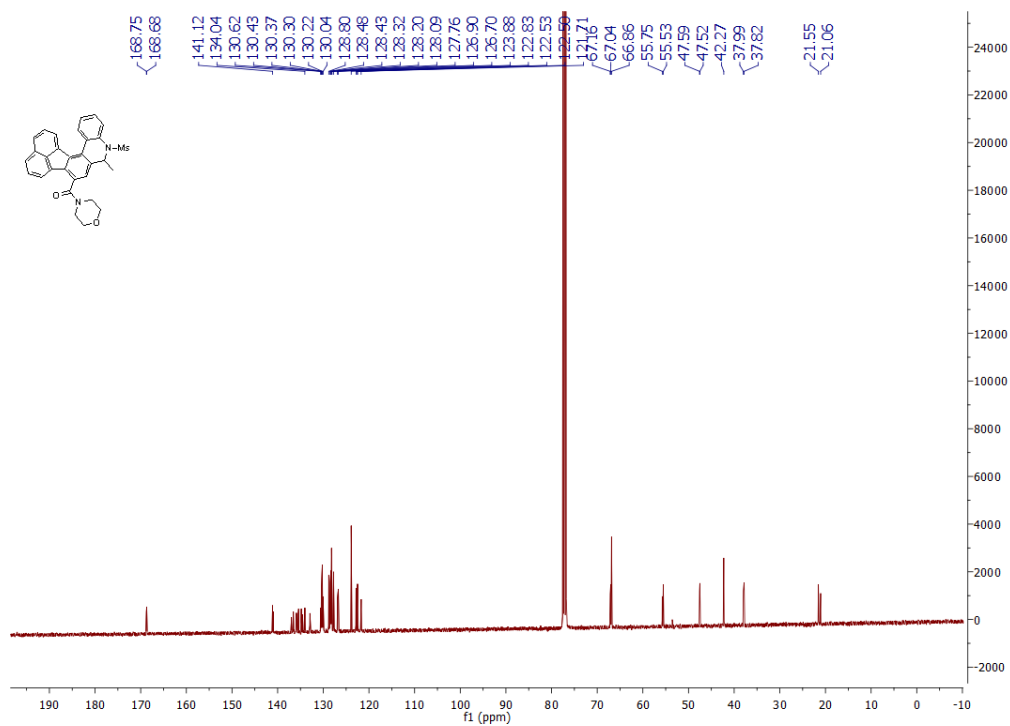
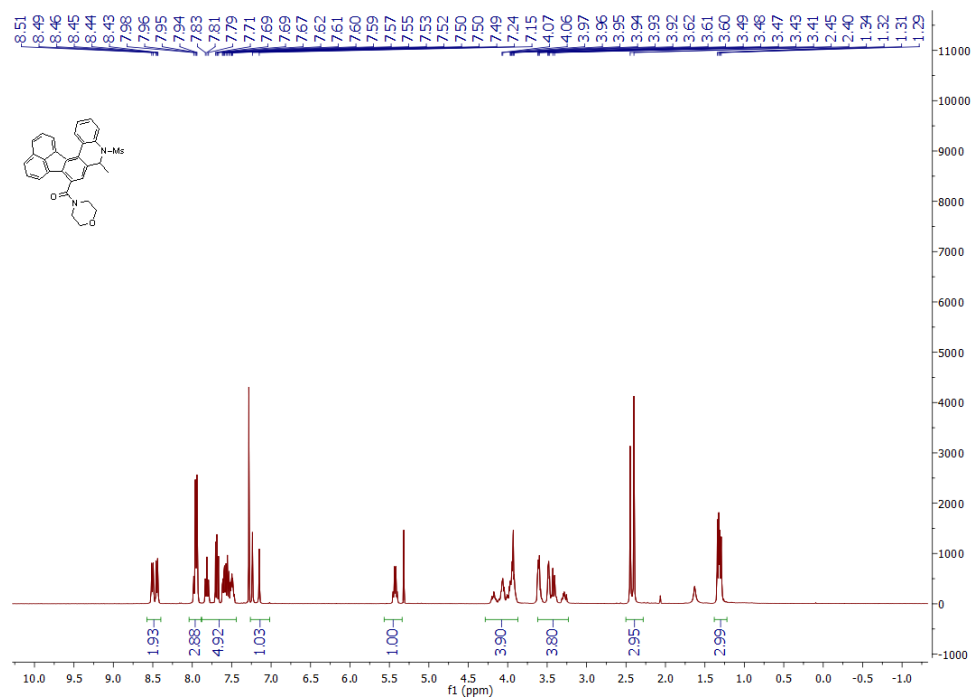


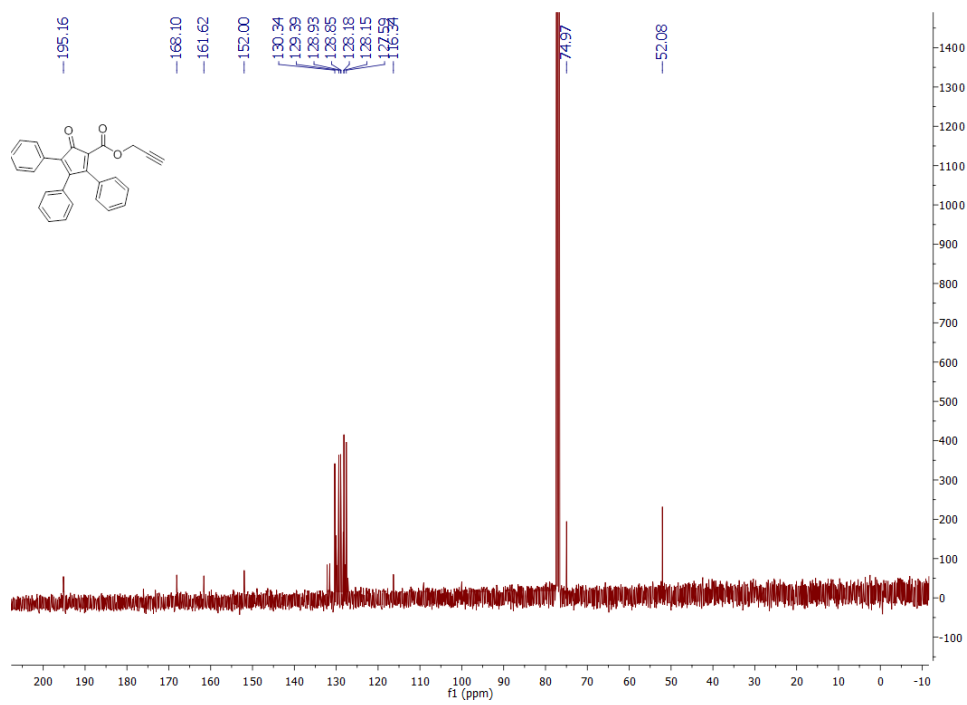
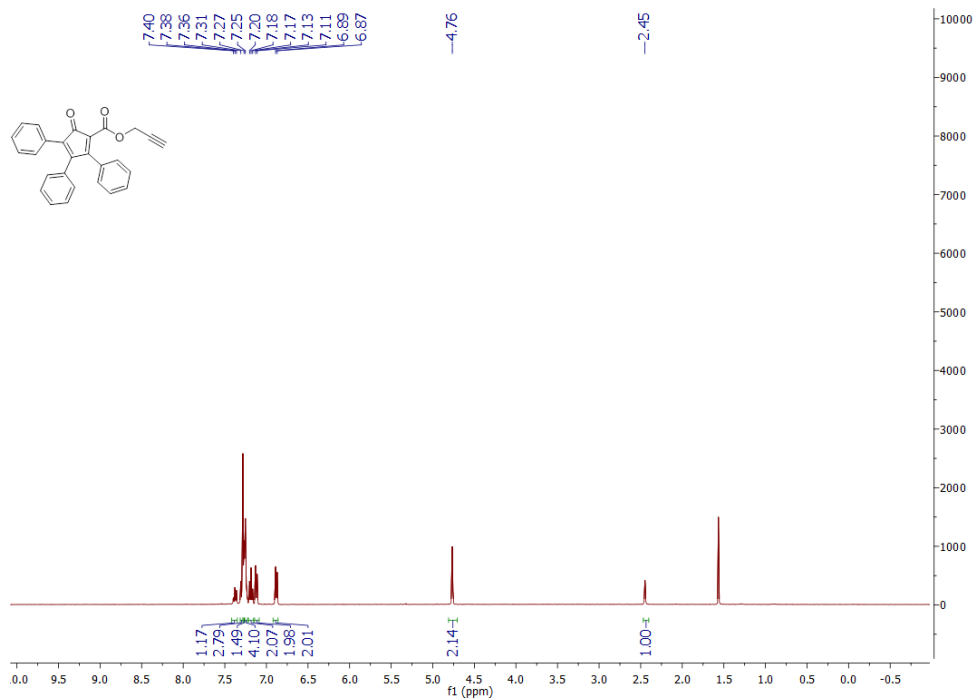


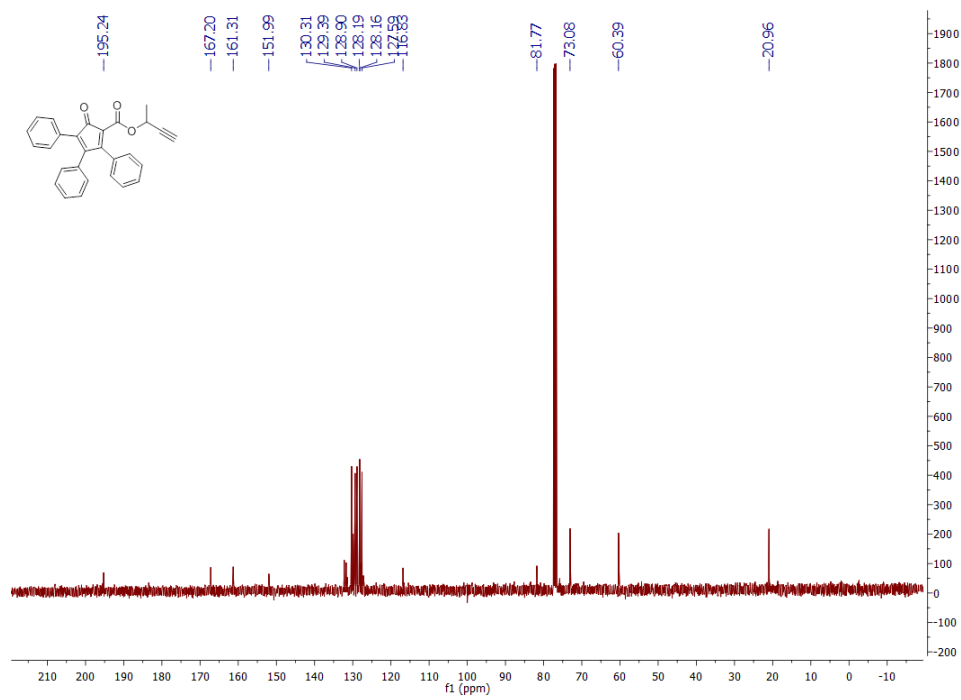
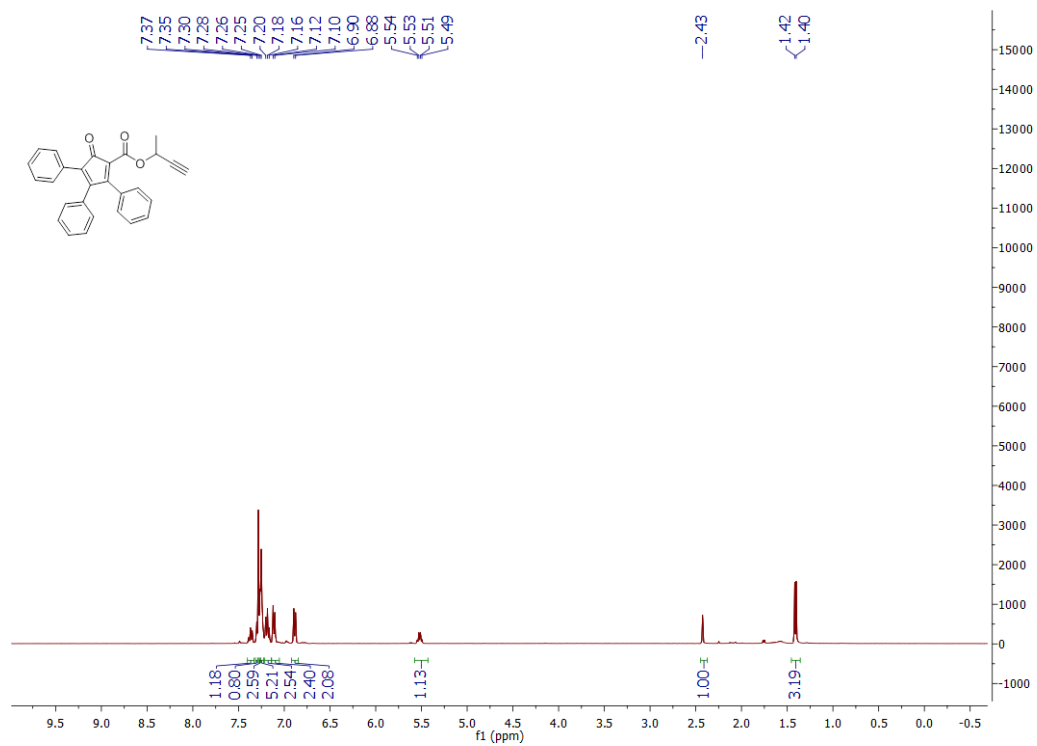


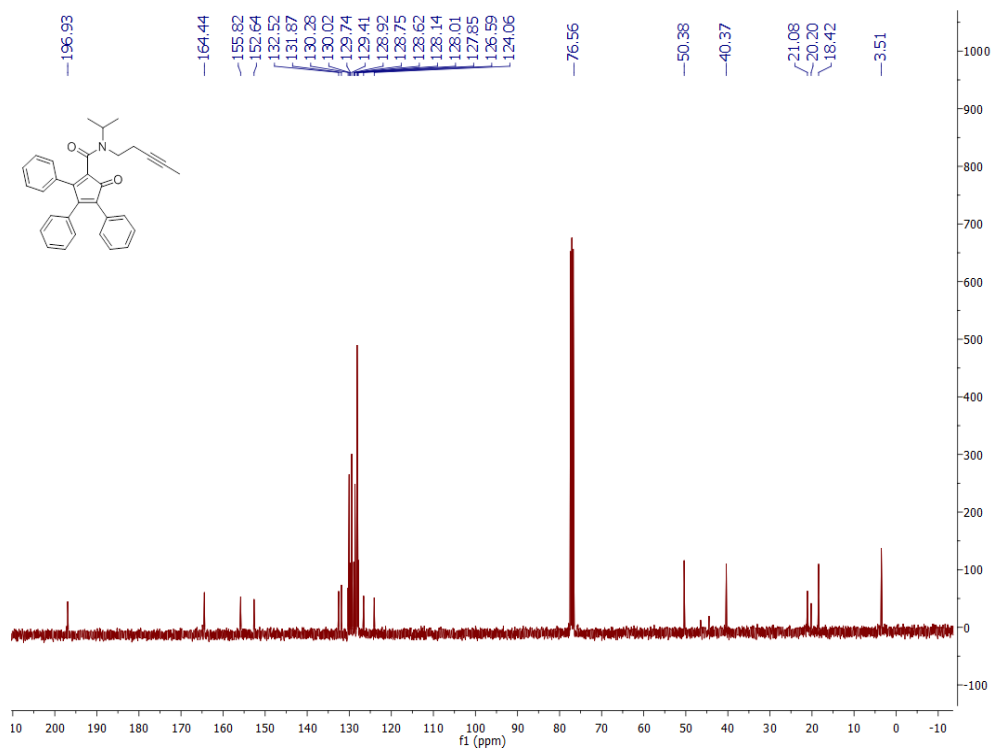
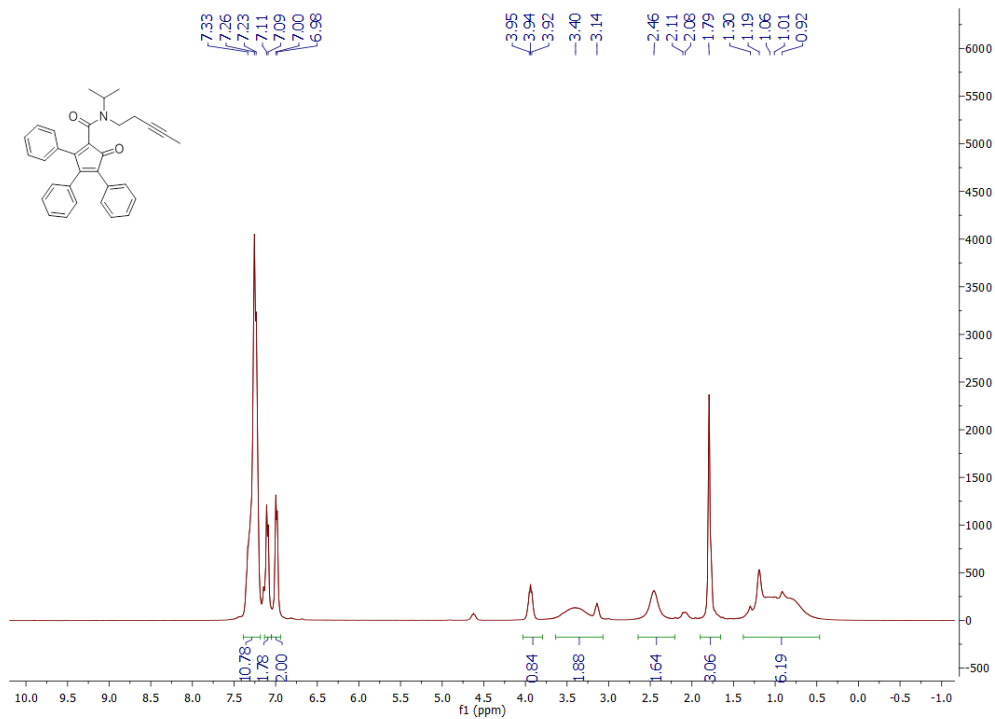


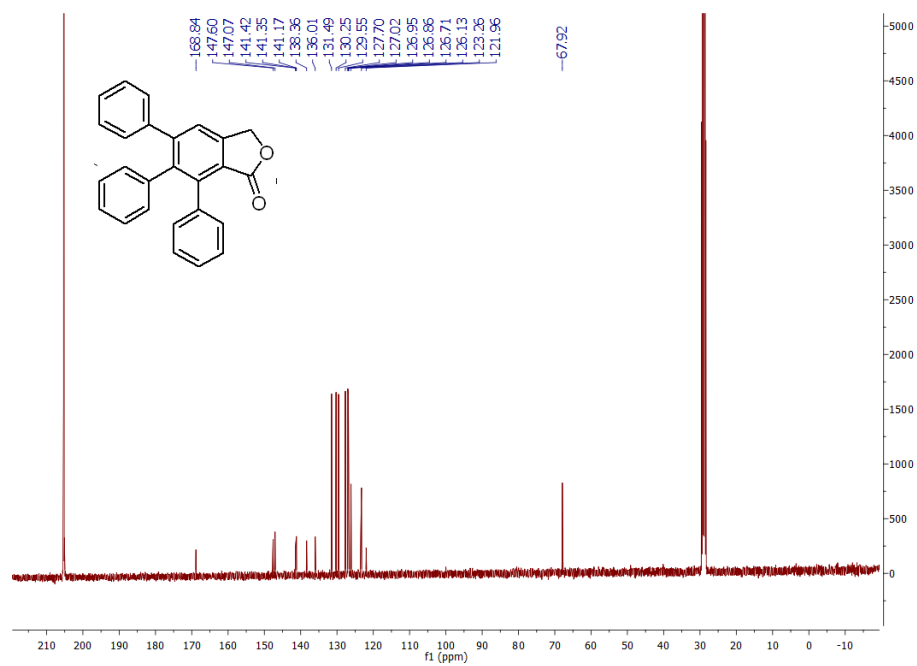
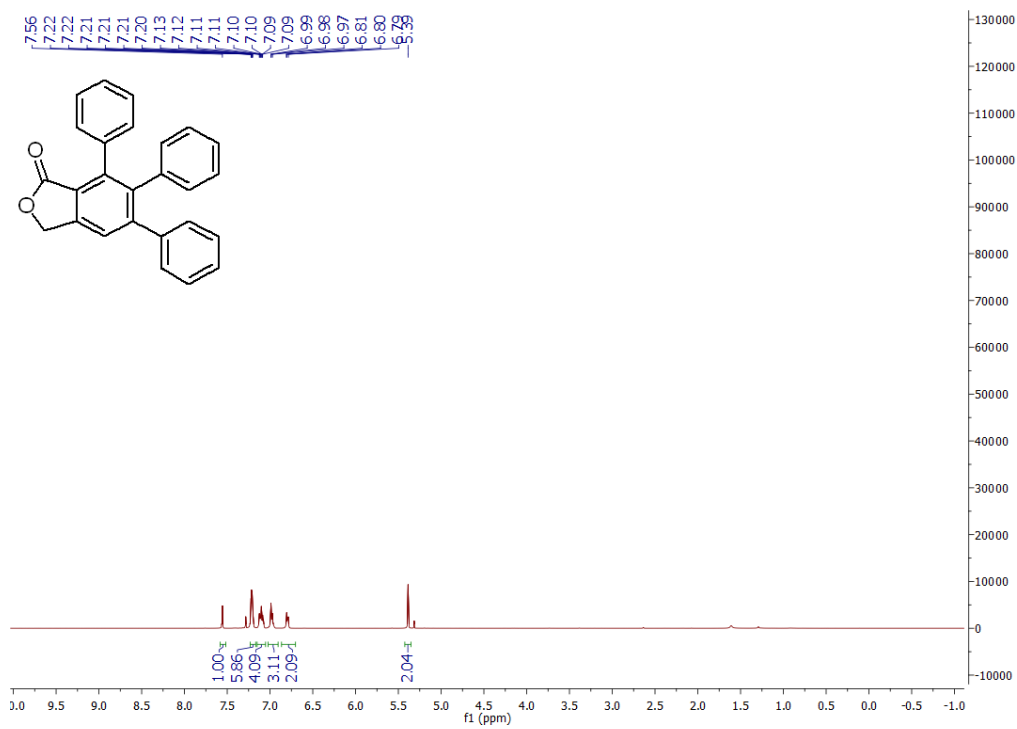


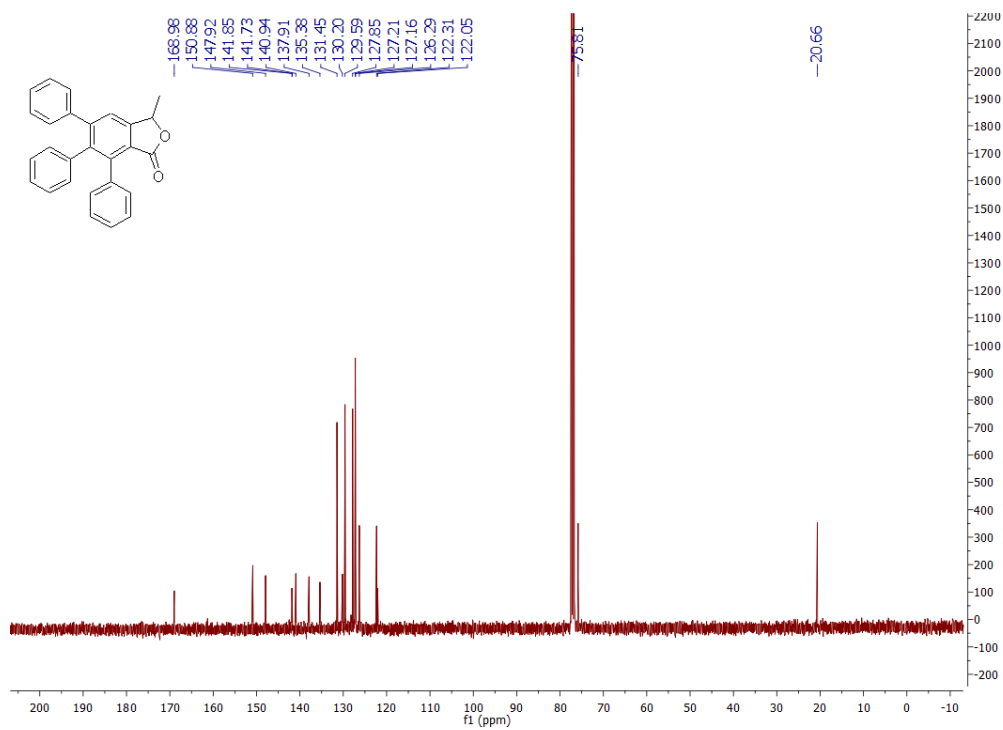
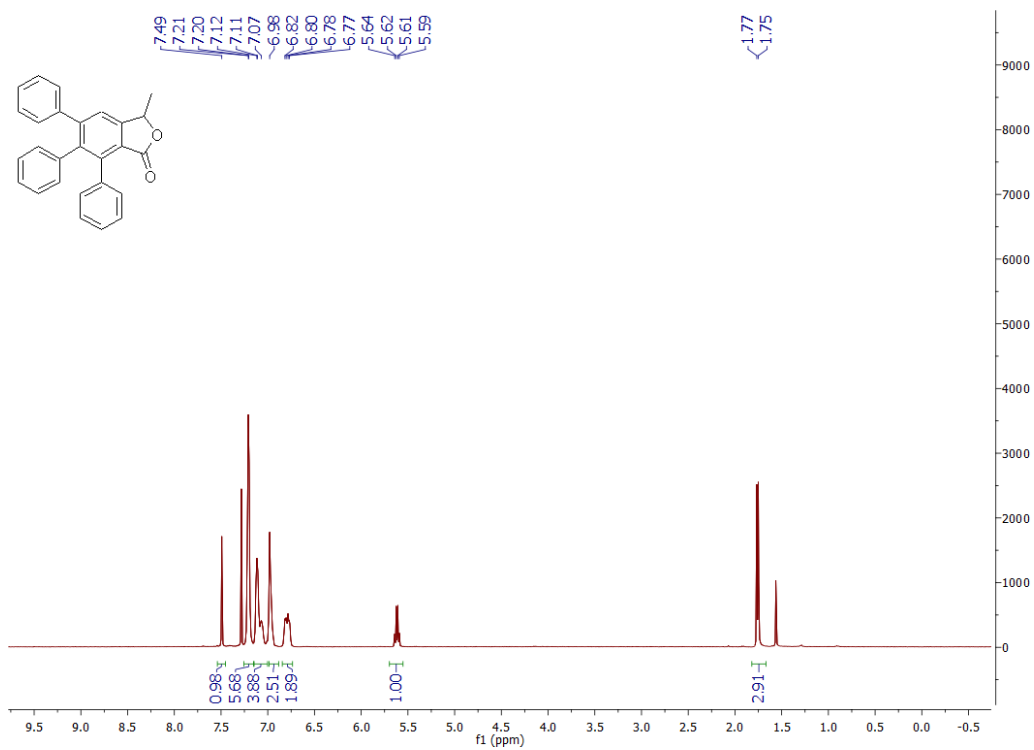


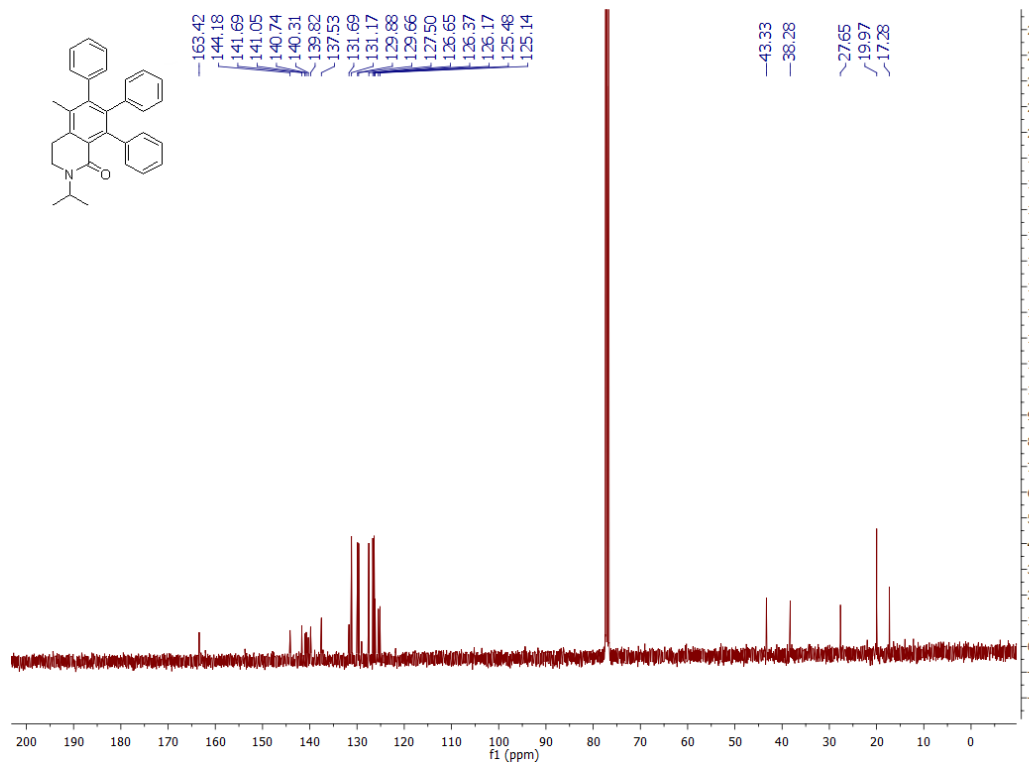
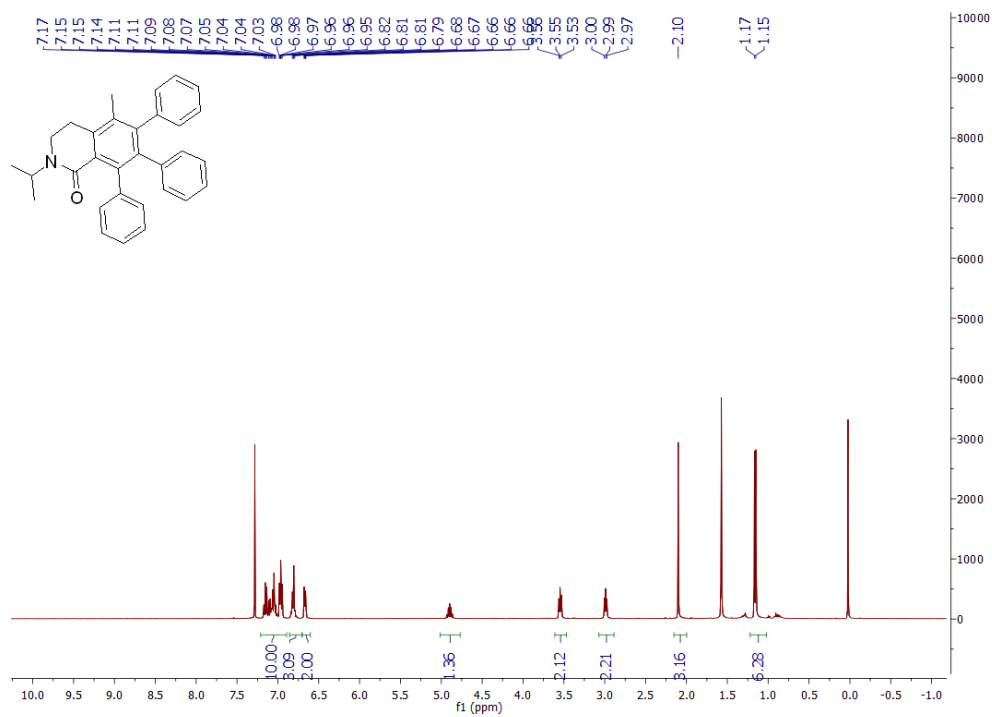




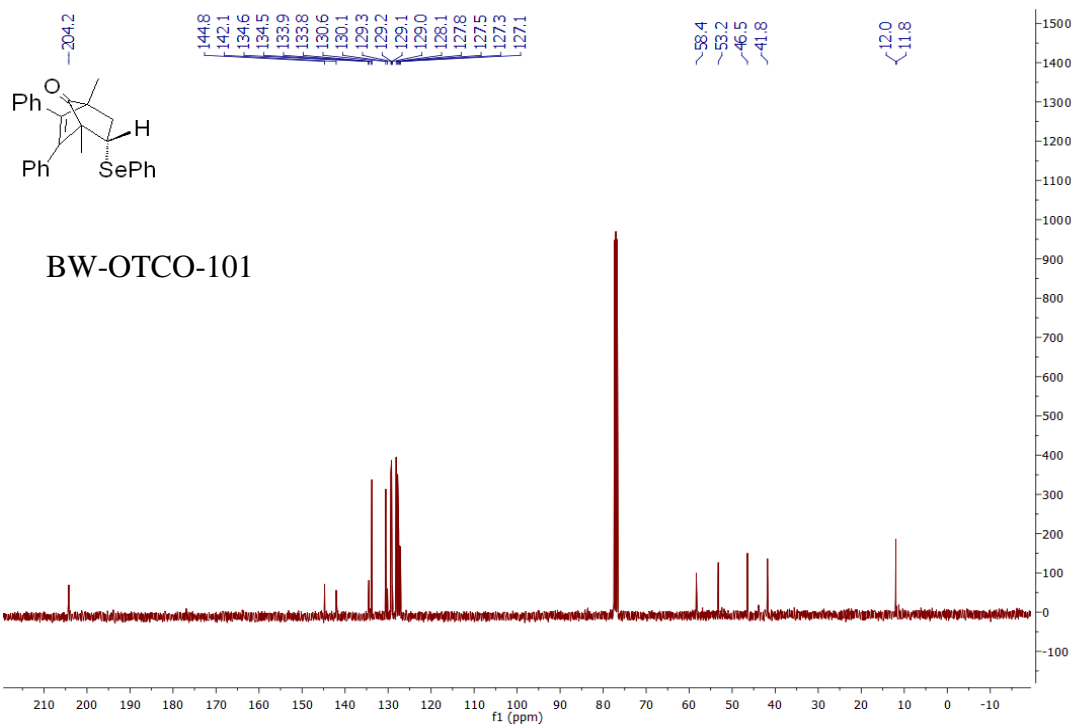
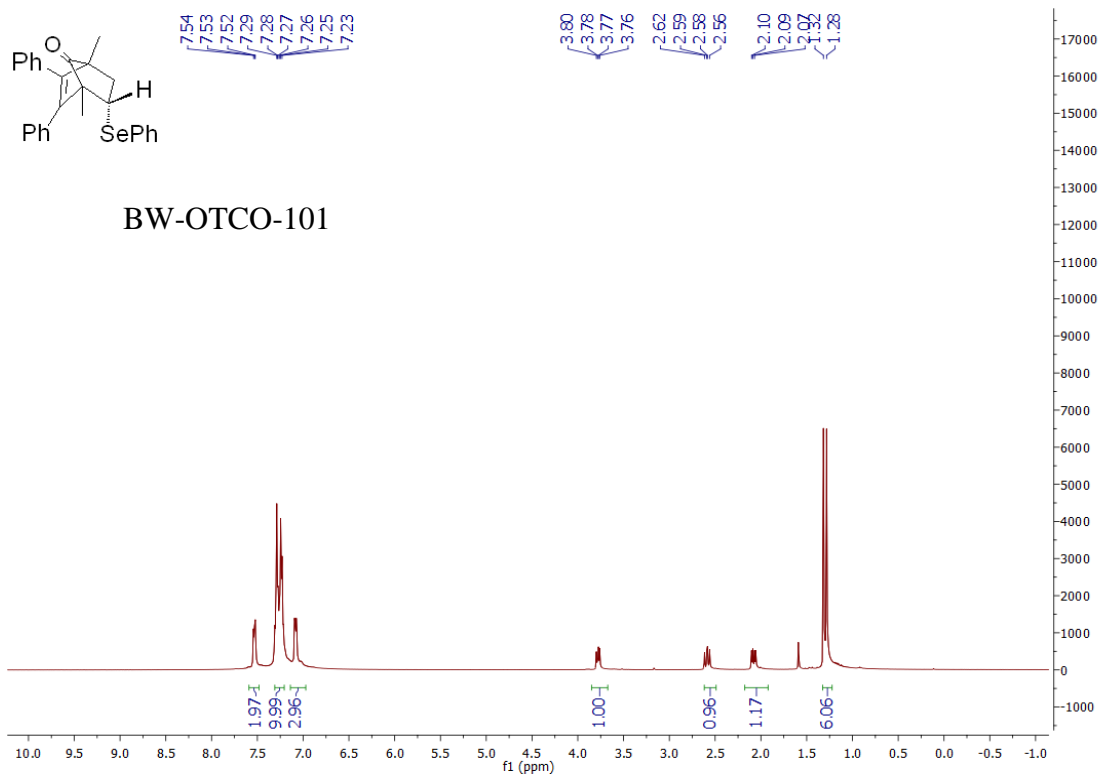


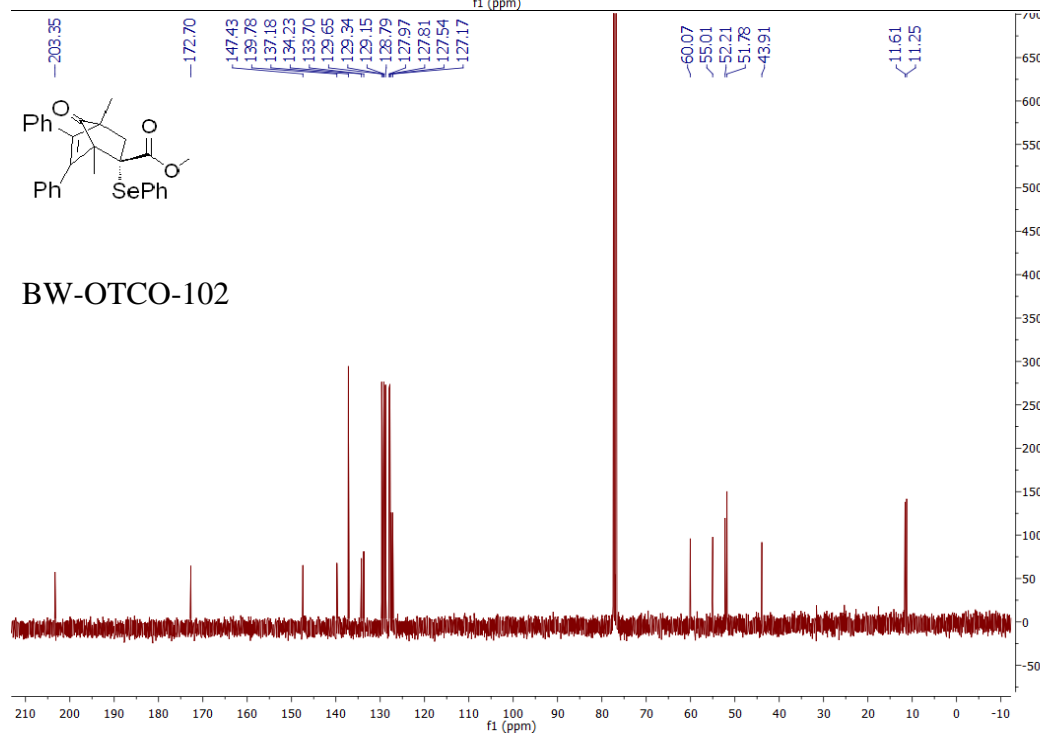
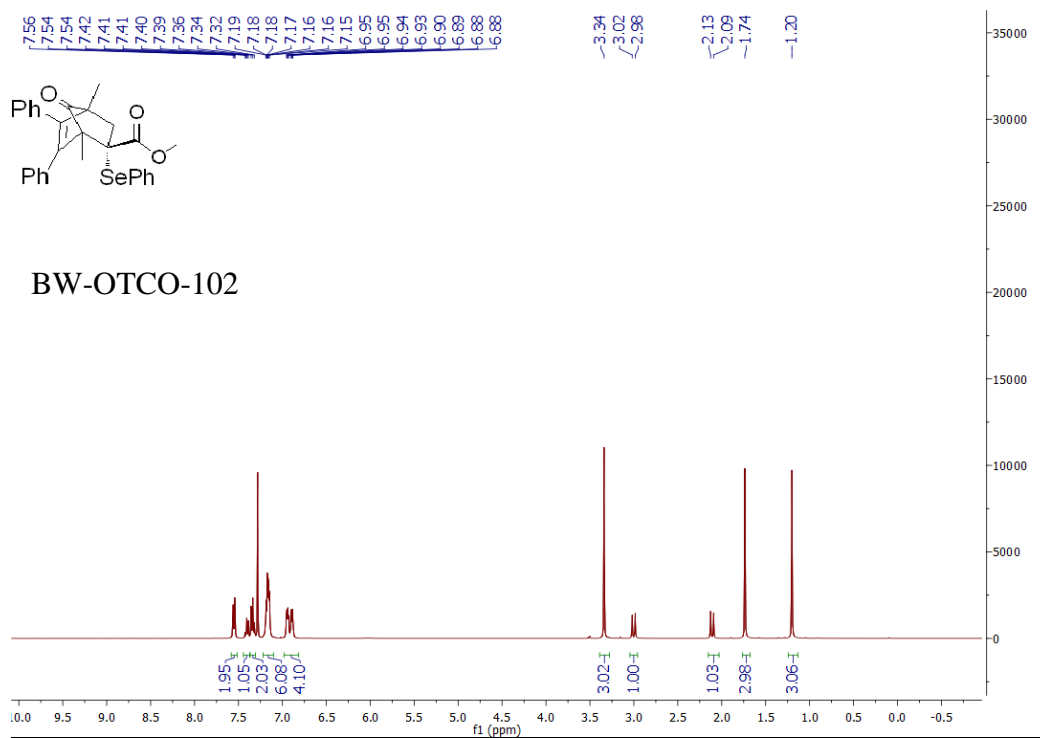


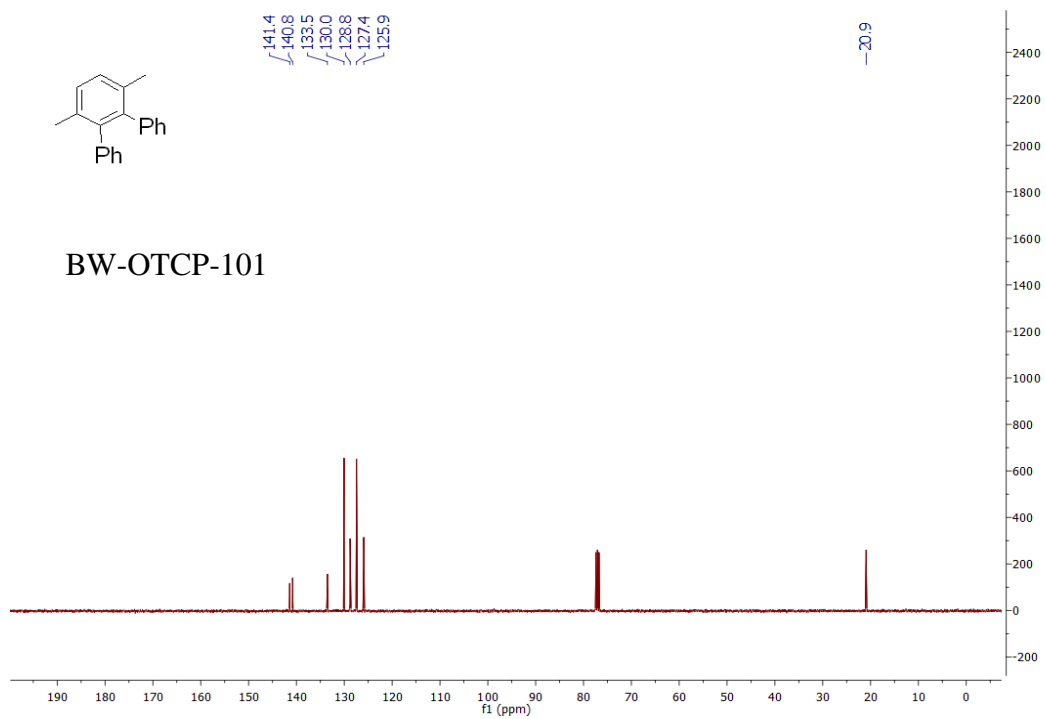
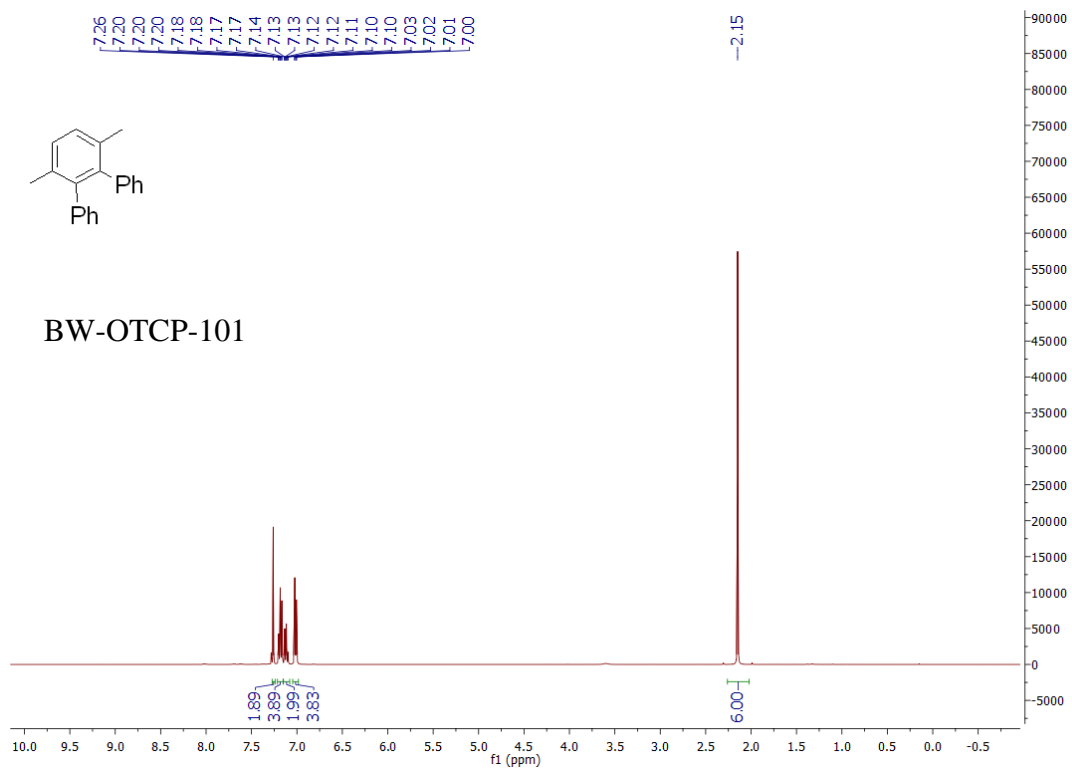


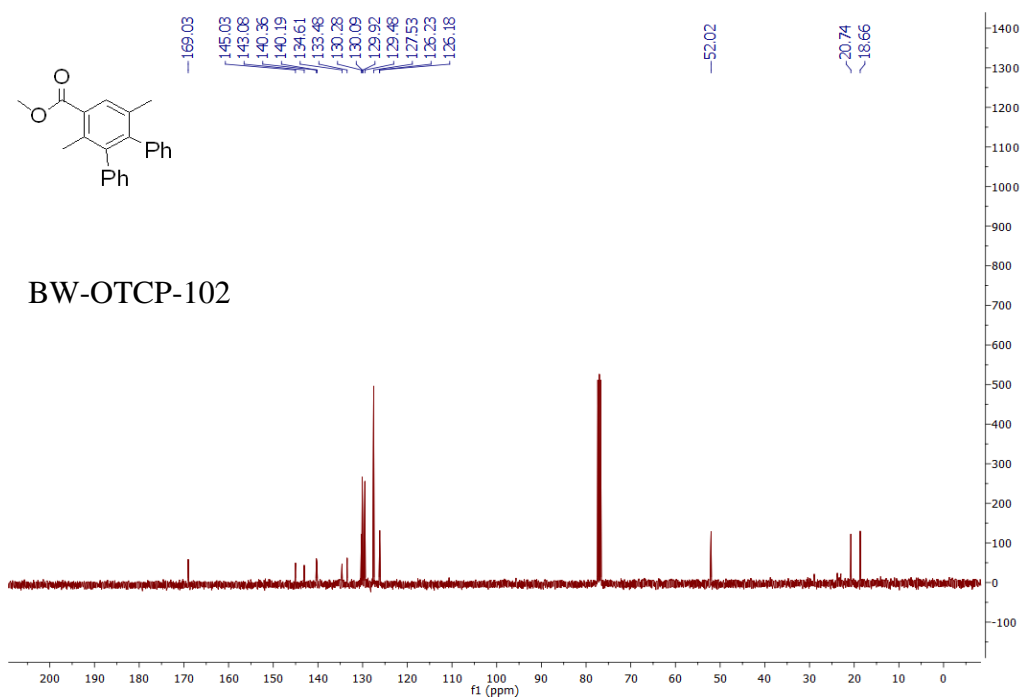
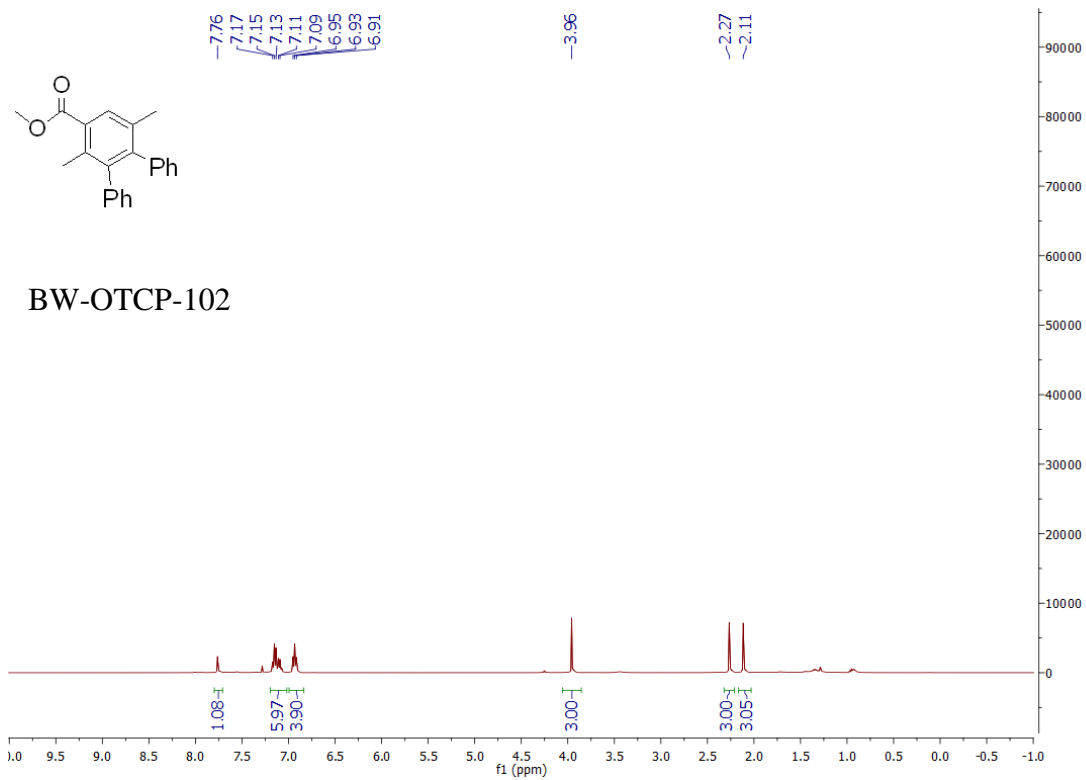


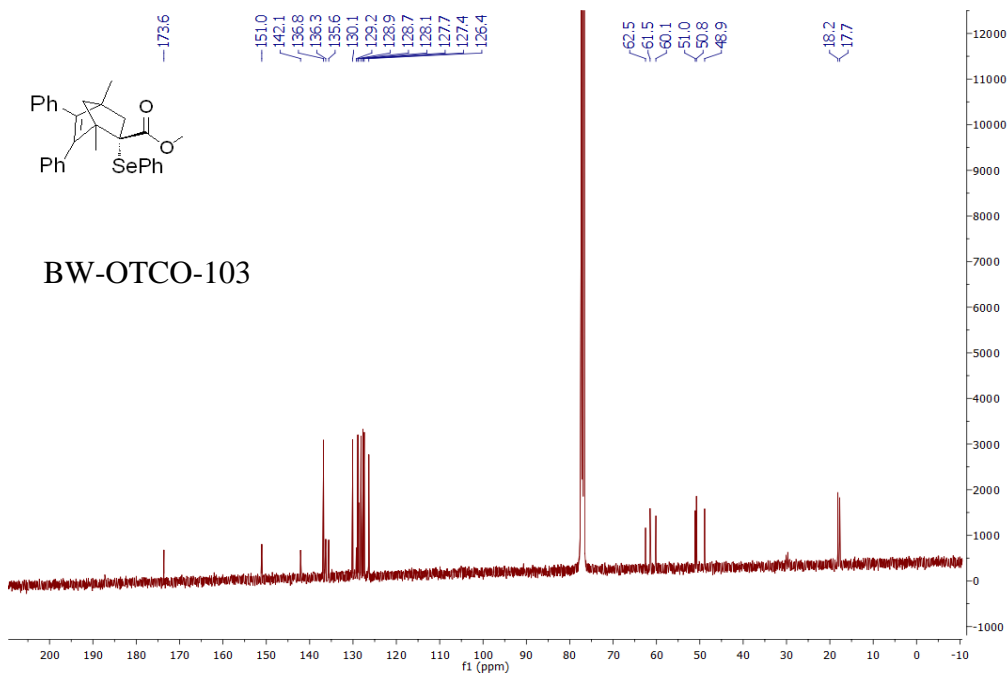
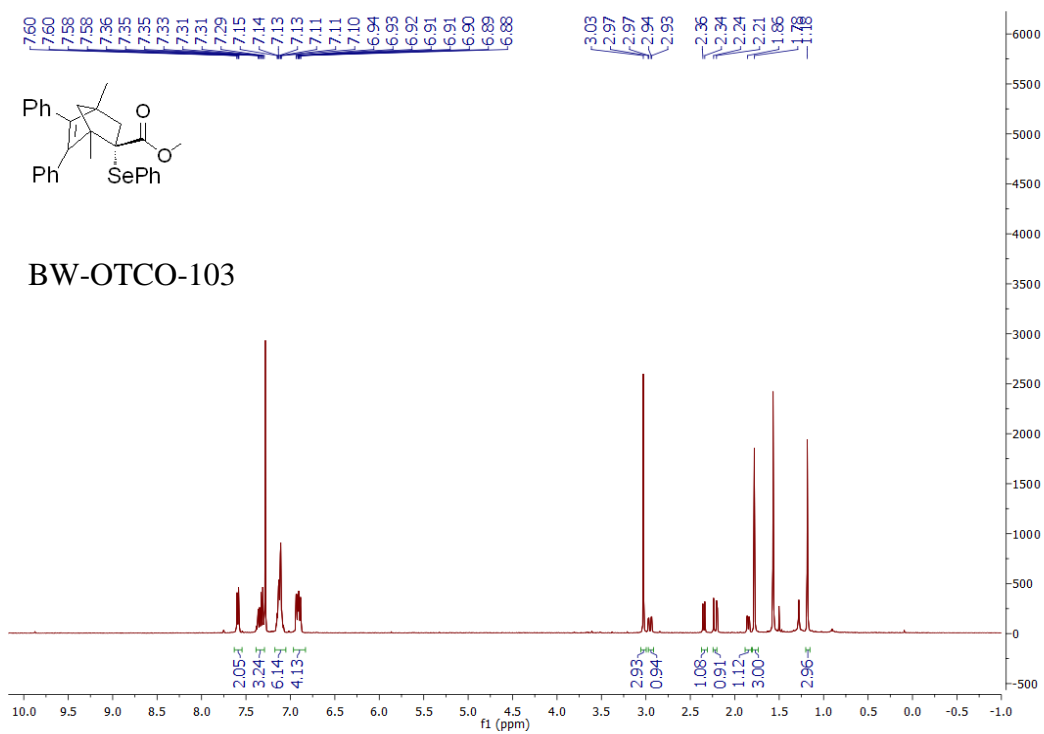
Appendix B Spectra of compounds in the study of ROS-activated CO prodrugs

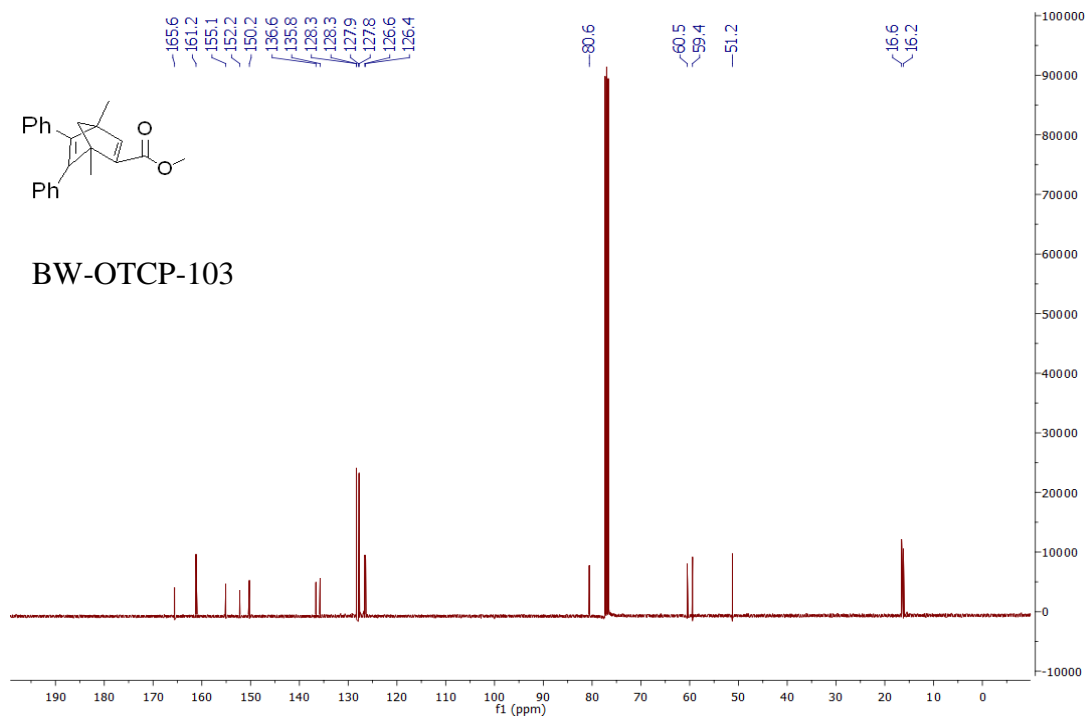
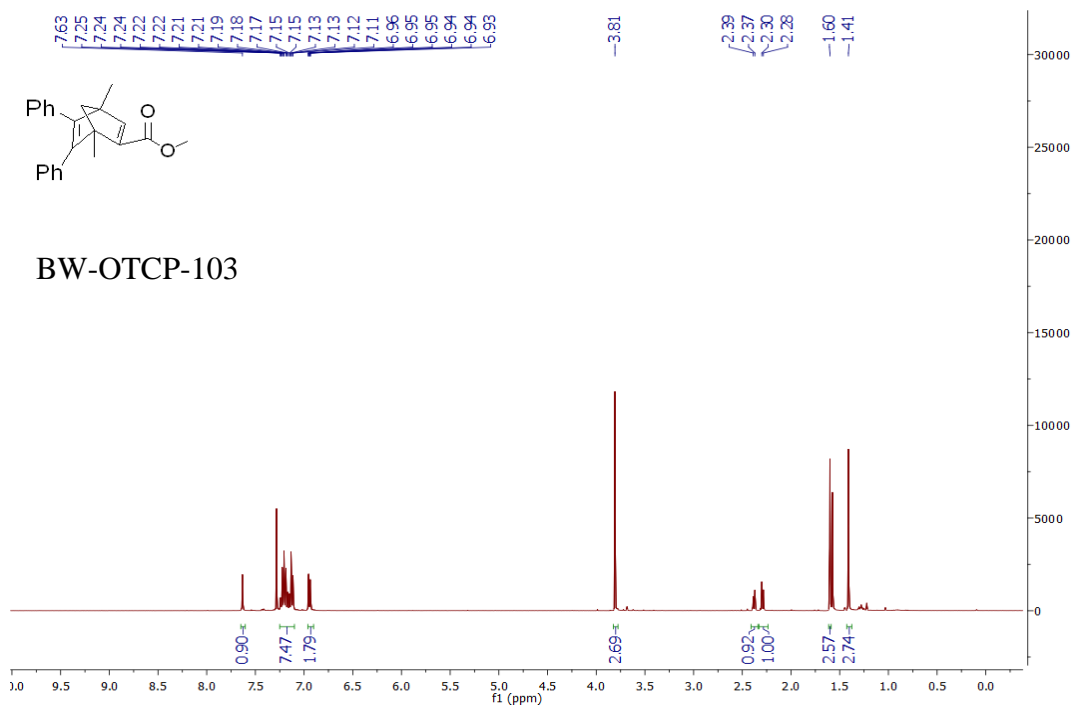












Appendix C Spectra of compounds in the study of esterase-sensitive and pH-controlled CO prodrugs

